



Contents lists available at ScienceDirect

Physics Reports

journal homepage: www.elsevier.com/locate/physrep

Networks beyond pairwise interactions: Structure and dynamics

Federico Battiston^{a,*}, Giulia Cencetti^b, Iacopo Iacopini^{c,d}, Vito Latora^{c,e,f,g},
Maxime Lucas^{h,i,j}, Alice Patania^k, Jean-Gabriel Young^l, Giovanni Petri^{m,n}

^a Department of Network and Data Science, Central European University, Budapest 1051, Hungary

^b Mobs Lab, Fondazione Bruno Kessler, Via Sommarive 18, 38123, Povo, TN, Italy

^c School of Mathematical Sciences, Queen Mary University of London, London E1 4NS, United Kingdom

^d Centre for Advanced Spatial Analysis, University College London, London, W1T 4TJ, United Kingdom

^e Dipartimento di Fisica ed Astronomia, Università di Catania and INFN, I-95123 Catania, Italy

^f The Alan Turing Institute, The British Library, London NW1 2DB, United Kingdom

^g Complexity Science Hub Vienna (CSHV), Vienna, Austria

^h Aix Marseille Univ, CNRS, CPT, Turing Center for Living Systems, Marseille, France

ⁱ Aix Marseille Univ, CNRS, IBDM, Turing Center for Living Systems, Marseille, France

^j Aix Marseille Univ, CNRS, Centrale Marseille, I2M, Turing Center for Living Systems, Marseille, France

^k Network Science Institute, Indiana University, Bloomington, IN, USA

^l Center for the Study of Complex Systems, University of Michigan, Ann Arbor, MI, 48109, USA

^m ISI Foundation, via Chisola 5, 10126 Turin, Italy

ⁿ ISI Global Science Foundation, 33 W 42nd St, 10036 New York, NY, USA

ARTICLE INFO

Article history:

Received 11 May 2020

Accepted 28 May 2020

Available online xxxx

Editor: I. Procaccia

ABSTRACT

The complexity of many biological, social and technological systems stems from the richness of the interactions among their units. Over the past decades, a variety of complex systems has been successfully described as networks whose interacting pairs of nodes are connected by links. Yet, from human communications to chemical reactions and ecological systems, interactions can often occur in groups of three or more nodes and cannot be described simply in terms of dyads. Until recently little attention has been devoted to the higher-order architecture of real complex systems. However, a mounting body of evidence is showing that taking the higher-order structure of these systems into account can enhance our modeling capacities and help us understand and predict their dynamical behavior. Here we present a complete overview of the emerging field of networks beyond pairwise interactions. We discuss how to represent higher-order interactions and introduce the different frameworks used to describe higher-order systems, highlighting the links between the existing concepts and representations. We review the measures designed to characterize the structure of these systems and the models proposed to generate synthetic structures, such as random and growing bipartite graphs, hypergraphs and simplicial complexes. We introduce the rapidly growing research on higher-order dynamical systems and dynamical topology, discussing the relations between higher-order interactions and collective behavior. We focus in particular on new emergent phenomena characterizing dynamical processes, such as diffusion, synchronization, spreading, social dynamics and games, when extended beyond pairwise interactions. We conclude with a summary of empirical applications, and an outlook on current modeling and conceptual frontiers.

© 2020 The Authors. Published by Elsevier B.V. This is an open access article under the CC BY license (<http://creativecommons.org/licenses/by/4.0/>).

* Corresponding author.

E-mail addresses: battistonf@ceu.edu (F. Battiston), v.latora@qmul.ac.uk (V. Latora), giovanni.petri@isi.it (G. Petri).

Contents

| | | |
|--------|---|----|
| 1. | Introduction..... | 3 |
| 2. | Higher-order representations of networks..... | 4 |
| 2.1. | Elementary representations of higher-order interactions..... | 4 |
| 2.1.1. | Low- versus high-order representations..... | 4 |
| 2.1.2. | Graph-based representations..... | 5 |
| 2.1.3. | Explicit higher-order representations..... | 6 |
| 2.2. | Relations and links between representations..... | 7 |
| 3. | Measures..... | 8 |
| 3.1. | Matrix representations of higher-order systems..... | 8 |
| 3.1.1. | Incidence matrix..... | 8 |
| 3.1.2. | Adjacency matrix..... | 9 |
| 3.2. | Walks, paths and centrality measures..... | 10 |
| 3.2.1. | Degree centralities..... | 10 |
| 3.2.2. | Paths and path-based centralities..... | 11 |
| 3.2.3. | Eigenvector centralities..... | 13 |
| 3.3. | Triadic closure and clustering coefficient..... | 13 |
| 3.4. | Simplicial homology..... | 14 |
| 3.4.1. | Boundary operators and homology groups..... | 14 |
| 3.4.2. | Evolving simplicial complexes..... | 14 |
| 3.4.3. | Other measures of shape in simplicial complexes..... | 15 |
| 3.5. | Higher-order Laplacian operators..... | 15 |
| 3.5.1. | Hypergraph Laplacians..... | 16 |
| 3.5.2. | Combinatorial Laplacians..... | 16 |
| 4. | Models..... | 17 |
| 4.1. | Equilibrium models..... | 18 |
| 4.1.1. | Bipartite models..... | 18 |
| 4.1.2. | Motifs models..... | 21 |
| 4.1.3. | Stochastic set models..... | 22 |
| 4.1.4. | Hypergraphs models..... | 23 |
| 4.1.5. | Simplicial complexes models..... | 25 |
| 4.2. | Out-of-equilibrium models..... | 27 |
| 4.2.1. | Bipartite models..... | 27 |
| 4.2.2. | Stochastic set models..... | 29 |
| 4.2.3. | Hypergraphs models..... | 29 |
| 4.2.4. | Simplicial complexes models..... | 30 |
| 5. | Diffusion..... | 31 |
| 5.1. | Higher-order diffusion..... | 32 |
| 5.1.1. | Edge-flows..... | 33 |
| 5.2. | Higher-order random walks..... | 34 |
| 5.2.1. | Random walks on simplicial complexes..... | 34 |
| 5.2.2. | Random walks on hypergraphs..... | 35 |
| 6. | Synchronization..... | 37 |
| 6.1. | Phase oscillators..... | 38 |
| 6.1.1. | Higher-order Kuramoto model..... | 38 |
| 6.1.2. | Higher-order interactions from phase reduction..... | 44 |
| 6.2. | Nonlinear oscillators..... | 46 |
| 6.2.1. | Chaotic oscillators..... | 46 |
| 6.2.2. | Neuron models..... | 47 |
| 6.3. | Inference of nonpairwise interactions in coupled oscillators..... | 48 |
| 7. | Spreading and social dynamics..... | 50 |
| 7.1. | Spreading in higher-order networks..... | 50 |
| 7.1.1. | Spreading on simplicial complexes..... | 51 |
| 7.1.2. | Spreading on hypergraphs..... | 52 |
| 7.2. | Opinion and cultural dynamics beyond pairwise interactions..... | 54 |
| 7.2.1. | Voter model..... | 54 |
| 7.2.2. | Majority models..... | 55 |
| 7.2.3. | Continuous models of opinion dynamics..... | 56 |
| 7.2.4. | Cultural dynamics..... | 57 |
| 8. | Evolutionary games..... | 57 |
| 8.1. | Multiplayer games on networks..... | 59 |
| 8.1.1. | Public goods game..... | 59 |

| | | |
|--------|--|----|
| 8.1.2. | Other multiplayer games..... | 60 |
| 8.2. | Games with higher-order interactions..... | 61 |
| 8.2.1. | Public goods game on bipartite networks..... | 61 |
| 8.2.2. | Public goods game on hypergraphs..... | 62 |
| 9. | Applications..... | 64 |
| 9.1. | Social systems..... | 64 |
| 9.2. | Neuroscience and brain networks..... | 67 |
| 9.3. | Ecology..... | 70 |
| 9.4. | Other biological systems..... | 74 |
| 10. | Outlook and conclusions..... | 76 |
| | Declaration of competing interest..... | 77 |
| | Acknowledgments..... | 77 |
| | References..... | 78 |

1. Introduction

Any significant understanding of a complex system must rely on system-level descriptions. Consider the following exercise: take an ecosystem, and break it into its pieces. No matter how good or accurate our knowledge at the level of the individual species is, chances are that our understanding of population dynamics—say, how the abundances of the different species change in time—will be slim at best. The same holds true when we attempt to explain epileptic seizures starting from the individual neurons of the human brain; or viral rumors spreading across societies from individual human psychology. All these approaches fail because they are missing a fundamental ingredient of any complex system, that is the rich pattern of nonlinear interactions between the system components. After many years of reductionism, science has abandoned the idea that the collective behaviors of a complex system can be simply understood and predicted by considering the units of the system in isolation [1], and now more than ever is embracing the idea of complexity as one of the principles governing the world we live in.

Within this paradigm, networks have emerged as a reference modeling tool for complex systems [2,3]. Networks are the maps that define the physical or virtual space where interactions take place [4]. Building on earlier work in mathematics, social network analysis and ecology, a handful of breakthrough papers at the turn of the millennium [5,6] attracted the interest of the scientific community, and triggered thousands of contributions over the next twenty years, culminating into the formation of the new multidisciplinary field of *Network Science*. This research community has developed an unusual mixture of graph theory [7,8] and statistical mechanics [9,10] into a flourishing discipline, with applications spanning the full range of science, from fundamental physics all the way to the social sciences. We refer the reader interested in a first approach to network science to the several early review papers [9,11–13] and textbooks [14–20] on the subject.

As exploration of real-world systems deepens, network scientists are realizing the need to further characterize and enrich the relationships captured by a network description. This, however, creates problems: networks have originally been understood as a collection of nodes, representing the elementary units of the system, and edges, describing the existence of interactions between pairs of such units. Applications to real-world systems, however, are only possible if we can describe interactions in detailed and varied ways [21], like for example: directed edges to describe the origin and destination of a message; edge weights, to highlight the intensity of an interaction; and even signs on the edges to distinguish whether a link encodes a productive or detrimental interaction among two units. More recently, a large effort has been devoted to formalize and develop the mathematical tools to analyze *temporal networks*, where interactions are not static but unfold in the temporal dimension [22]. Similarly, many works have recently considered the case of interacting systems where units can be connected by links of different nature, and which can be effectively represented in terms of *multiplex networks* or *multilayer networks* [23].

All of these extensions have contributed to better network representations. But one can reasonably ask: are networks themselves enough to provide a complete description of a complex system?

The answer is probably no. Indeed, an important limitation of networks, not addressed by these new developments, is that they capture pairwise interactions exclusively. Yet, many empirical systems seem to display group interactions. In social systems [24], neuroscience [25,26], ecology [27] and biology [28], for example, many connections and relationships do not take place between pairs of nodes, but rather are collective actions at the level of groups of nodes. Neuronal dynamics display mesoscopic behaviors that require interactions among multiple neurons to be predicted [29]. Three or more species routinely compete for food and territory in complex ecosystems [30]. The presence of a third species influences the interaction between the other two, by affecting directly the interaction (the link) rather than the species involved (the nodes). Social mechanisms, such as peer-pressure or collaborations, inherently go beyond the idea of dyadic connections [31]. Collective interactions are not an entirely new idea, and to some degree have appeared in early research on networks. Think for instance of the majority-rule model for the dynamics of opinion formation, or the public goods game in evolutionary game theory. In addition to these examples, one of the most successful streams of research in network science in recent years, complex contagion, naturally accounts for multiple simultaneous interactions [32]. However, in all cases, these applications tried to leverage the language of pairwise networks to describe interactions of

higher-order, for example by using bipartite graphs [33]. Can we instead find mathematical frameworks that can explicitly and naturally describe group interactions?

Simplicial complexes and hypergraphs are the natural candidates to provide such descriptions. And indeed, over the last few years, a wave of enthusiasm for these representations has revolutionized our vision of and ability to tackle real-world systems characterized by more than simple dyadic connections. The importance of higher-order interactions had been recognized already a long time ago [34–36], but this rejuvenated interest has brought a new, and much deeper understanding of higher-order representations. There are no doubts now that moving beyond dyadic interactions is fundamental to explain and predict collective behaviors that could not be described before.

The aim of this report is to provide a review of the state-of-the-art on the structure and dynamics of complex networks beyond pairwise interactions, as well as a reference and perspective on crucial open questions in the field. Hence, this report is organized as follows:

- The first part (Sections 2 to 4) focuses on the structure of systems with higher-order interactions. In particular, Section 2 provides an introduction to the mathematical frameworks underlying higher-order representations. Section 3 describes the most common measures and properties currently used to describe the structure of systems with many-body interactions. Finally, Section 4 reviews random models of higher-order systems and how they are used to make statistical inferences.
- The second part (Sections 5 to 8) focuses on the dynamics of systems with higher-order interactions. In more detail, Section 5 discusses models of higher-order diffusion. Section 6 describes the generalization of oscillator models and synchronization. Section 7 introduces recent models of spreading in social systems with group structure. Section 8 reports on models of competition and cooperation among multiple agents.
- Finally, Section 9 is an overview of real-world applications to systems with higher-order interactions. Our final conclusions and outlook are presented in Section 10.

Including higher-order interactions in network analysis is a simple and natural idea. Going beyond pairwise interactions might even not look harder than attaching weights or signs to the edges of a graph. Yet, in practice, moving from pairs to a more complicated interaction structure is difficult, and requires a great deal of sophistication and novel mathematical tools. This might explain why the analysis of this aspect of complex systems has been delayed compared to its weighted and signed, and even temporal and multilayer counterparts. Classical physics already knew this: while a closed-form solution is available for the two-body problem, solving for the trajectories of n interacting bodies given their positions and momenta is still an open problem!

2. Higher-order representations of networks

2.1. Elementary representations of higher-order interactions

2.1.1. Low- versus high-order representations

We begin by first defining more precisely what we consider as interactions and, as a consequence, as higher-order interactions. We define an *interaction* as a set $I = [p_0, p_1, \dots, p_{k-1}]$ containing an arbitrary number k of basic elements of the system under study, which we indicate as *nodes* or *vertices*. Such interactions can then describe different situations in real systems, e.g. the coauthors of a scientific paper, a set of genes required to perform a certain function, the coactivation of a group neurons during a specific task, etc. In a slightly counterintuitive way, we will denote the *order* (or dimension) of an interaction involving k nodes to be $k - 1$: a node interacting with itself only is a 0-order interaction, an interaction between two nodes has order 1, one among three nodes has order 2, and so on. Furthermore, we consider *higher-order interactions* to be k -interactions with $k \geq 2$. Conversely, low order interactions are those characterized by $k \leq 1$. In plain terms, low order systems are those in which only self- or pair-wise interactions take place (like edges in a graph), while *higher-order systems* (HORs, from now on) display interactions in groups of more than two elements.

The distinction between low- and high-order interactions is needed for two reasons. First, it highlights the differences between the graph-theoretic descriptions, that shaped the study of complex systems in recent decades, and the more recently (re)proposed descriptions based on genuine group interactions. Secondly, it allows us to clearly frame the connections between such descriptions, their various overlaps and reciprocal mappings. Finally, our definition explicitly leaves out other types of higher-order dependencies between the components of a system, as for example those defined by multiple link types in multilayer networks [23,37–41], or by non-Markovian paths in time-stamped interaction data [22,42–44]. While these are out of the scope of this review, the interested reader can find an extensive discussion of these topics in the references mentioned above.

We define an interacting system (V, \mathcal{I}) as the family of interactions $\mathcal{I} = \{I_0, \dots, I_n\}$ taking place on a node set V . To aid the intuition, let us make a specific example. Consider the node set $V = [a, b, c, d, e]$ and the set of interactions $\mathcal{I} = \{[a, b, c], [a, d], [d, c], [c, e]\}$ (Fig. 1A). \mathcal{I} contains three 1-interactions and one 2-interaction. While the complete information about the systems is included in the list above, the study of most interesting properties of the system requires the choice of a representation. For example, measuring the collective effects of the interactions on a specific node requires the capacity to map interactions of different orders in a way that makes them comparable to each other; asking how dense the system is, or whether one node is reachable from another, again requires being able to compare in a controlled way interactions of different order and composition.

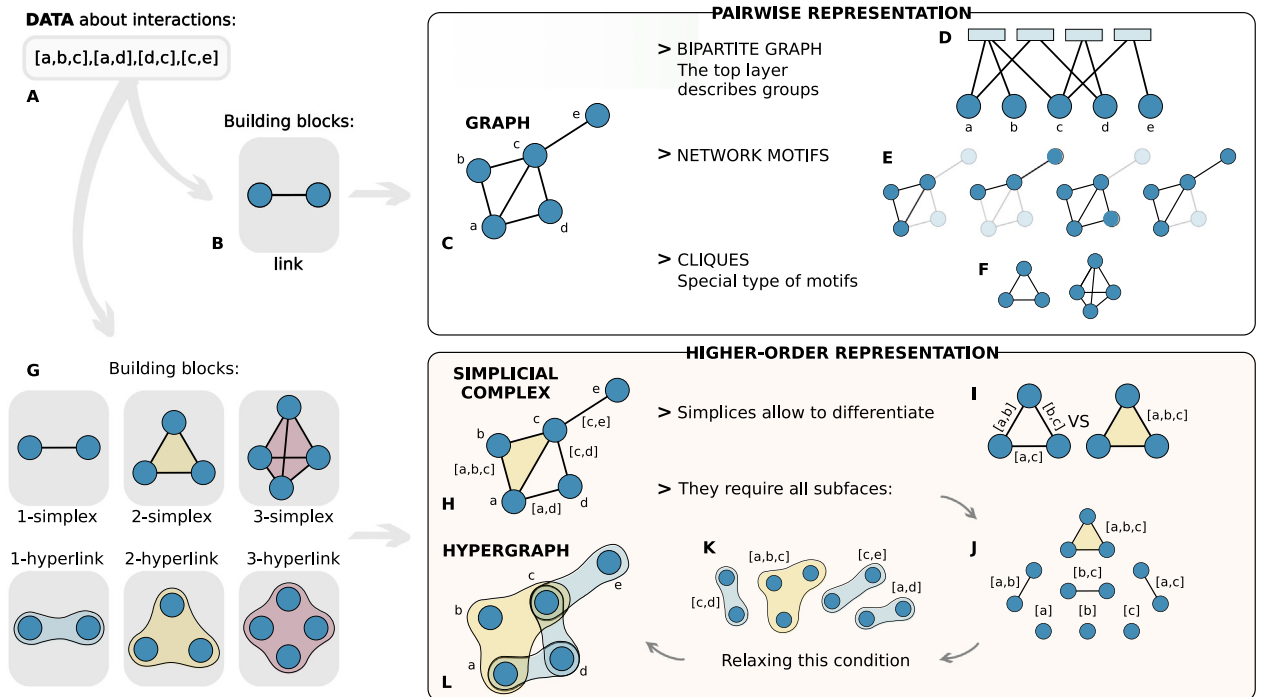


Fig. 1. Representations of higher-order interactions. A set of interactions of heterogeneous order (A) can be represented using only pairwise interactions (B). Using only low-order blocks, the set of interactions can be described in the simplest way by using a graph (C). Alternatively, interactions can be encoded as nodes in one layer of a bipartite graph, where the other layer contains the interaction vertices (D). Other examples of high-order coordinated patterns can be encoded using motifs, small subgraphs with specific connectivity structures (E). Among motifs, cliques are especially popular as they represent the densest subgraphs, akin to higher-order bricks (F). All these representations discard information that was present in the original interaction data (A). A solution is to consider explicitly higher-order building blocks, in the form of simplices and hyperedges (G). Collection of simplices form simplicial complexes (H), which allow to discriminate between genuine higher-order interactions and – even complex – sums of low-order ones (I). Unfortunately, simplicial complexes, given a simplex, require the presence of all possible subsimplices (J), which can be too strong an assumption in some systems. Relaxing this condition effectively implies moving from simplices to hyperedges (K), which are the most general—and less constrained—representation of higher-order interactions (L).

2.1.2. Graph-based representations

Graphs are the most common way to represent families of interactions (Fig. 1C). A graph $G = (V, E)$ is defined by a nodeset V with n elements, and an edgeset E whose m elements are pairs of nodes. A graph is then a collection of edges connecting pairs of nodes. In other words, the building blocks of graph representations are 1-interactions, i.e. interactions of the type $I = [i, j]$. The most natural choice is then to unfold each higher-order interaction in \mathcal{I} in terms of 1-interactions built from pairs of nodes in I . Under this assumption, our example $\mathcal{I} = \{[a, b, c], [a, d], [d, c], [c, e]\}$ maps to $\mathcal{I}_G = \{[a, b], [b, c], [c, a], [a, d], [d, c], [c, e]\}$ (Fig. 1B). This mapping makes systems amenable to be studied using tools developed in both graph theory [45] and network science [16]. Indeed, graph representations enabled the growth, depth and breadth of results on real-world complex networks in the last two decades [17–19], with applications spanning biology [46,47], ecology [27,48], social science [49,50], engineering [51,52], neuroscience [53–55], all the way to cosmology [56].

Despite the power of graph representations to capture many properties of complex interacting systems, their limits are easily identified: it is impossible to explicitly describe group interactions, or in other terms there is no direct relationship between \mathcal{I} and \mathcal{I}_G nor any way to recover the former from the latter. For example, going back to our toy example, at the description level provided by \mathcal{I}_G , it is impossible to tell (and hence to describe) whether the original interaction set contained $[a, c, d]$ or not. Naturally, in some cases networks can provide information on higher-order interactions, but these are always inferences based on the low-order interactions, obtained for example by looking for very dense subsets of nodes using community [57], clique [58] or block detection [59] techniques. However, such reconstructions are often incomplete and rife with problems [60–62].

Bipartite graph representations effectively describe group interactions. Solidly within the realms of low-order interactions, *bipartite graphs* are graphs defined by two nodesets (U, W) and an edgeset E containing only edges (u, w) such that $u \in U$ and $w \in W$. To represent higher-order interactions, one chooses U to coincide with the original nodeset V , i.e. $U = V$, and W to coincide with the set of interactions \mathcal{I} [63,64]. The links in the bipartite graph connect a node (in V) to the interactions (of arbitrary order) in which it takes part (Fig. 1D). This representation emerges naturally in many fields: it is used for example in social sciences, where it provides a way to encode the membership of individuals to groups of different dimensions [65,66]; or to describe the collaboration of actors (nodes) in movies (interactions) [67];

it is also used in ecological bipartite graphs, where species linked to a common prey represent competition for resources among more than two species [48]; in recommendation systems [68] they describe the relations between customers and purchased products, and so on.

It is easy to see that the entire information in our toy model is preserved when interactions are described as a bipartite graph. In fact, this representation is very general and can indeed well mimic most interaction structures. However, at difference with other multilayer graph formulations [23,37], in a bipartite graph the nodes of the original system do not interact directly with each other anymore. Rather, their relation is always mediated by the interaction layer, which is of a different nature from the node layer itself. This implies that any measure or dynamic process defined on the bipartite representation needs to take into account this additional complexity. The usual workaround to this problem is to consider the unipartite networks obtained by projecting the bipartite on one of the two layers. Each interaction becomes then a fully connected subgraph among the nodes belonging to the interaction, losing the group structure in the same way as in the simple graph case. In addition, it is usually impossible to translate the information contained in the standard graph operators (e.g. Laplacian) defined on a bipartite graph into the ones corresponding to the unipartite projections [69,70].

Motifs allow to extract additional information on the properties of an interaction. They are the—usually small—recurrent subgraphs of a given network, or of a class of networks of similar origin [71]. Motifs are defined as specific patterns of edges (1-interactions) between vertices that appear to be statistically significant in the network (Fig. 1E). They are considered structural signatures of the function of a network. That is, different motifs can correspond and reflect different functions or different optimization solutions to the same function [72]. Typically, the statistically validated frequencies (z-scores) with which the various motifs are observed in a network are collected into a motif profile, which can then be used for example to discriminate between different networks [24], e.g. between brain functional networks in different states [73,74] or between differently evolved biological networks [47,72,75]. Motifs also found widespread application in the study of social [76] and temporal [77,78] systems.

Motifs constitute a refinement of the bipartite representation of a system, since, in addition to a division in groups akin to that of bipartite graphs, they allow to specify the interaction pattern in which a node is involved. The drawback to this is that the number of possible motifs to investigate grows exponentially with the number of nodes involved. This unfortunately makes them quite unwieldy as a descriptive tool for large graphs and large motifs. As an example, generative models aimed to quantify randomness in networks via motif-based constraints [79] were shown to become very hard to manage, or even sample, for interactions above order 2 [80].

Because of the exponential growth in the number of motifs, a large part of the work on analyzing subgraphs focuses on a special type of motifs: *cliques* (Fig. 1F). A clique of size k is defined as a fully connected subgraph of k nodes. Here, we use size for cliques to avoid confusion, since a k -clique usually encodes an interaction of order $k - 1$. The interest in cliques is justified also by the fact that they represent the most obvious definition of group from a network point of view, because they are the densest and most uniform motif [81]. Also, they directly encode the idea that every member of the clique interacts with every other [82,83]. Due to these properties, cliques are privileged building blocks of a network and its communities [58]. However, we can incur into problems if we want to use cliques to characterize higher-order interactions. In fact, going back to our toy example, we see that both sets a, b, c and a, d, c form 3-cliques. Conversely, in \mathcal{I}_G we only had a true 2-interaction, namely $[a, b, c]$, while the fictitious interaction $[a, d, c]$ is emerging as a byproduct of the union of the 1-interactions $[a, d]$ and $[d, c]$ with the $[a, c]$ edge induced by $[a, b, c]$. We can see then that, by considering all cliques present at the graph level, we would “fill” a 2-interaction that was not included in the original interaction set. This is somewhat opposite to what happened when we considered the edges alone. In that case, we lost completely the notion of group. In the case of cliques instead, we risk “filling” too much and thus creating higher-order interactions that were not there to begin with.

2.1.3. Explicit higher-order representations

To properly describe higher-order interactions, we need to encode them explicitly. Why not encoding interactions exactly as they are in fact? *Simplices* are the simplest mathematical objects to accomplish this. The formal definition of simplices mimicks very closely the one we gave of higher-order interactions. In fact, a k -simplex σ is, in its most general form, just a set of $k + 1$ nodes $\sigma = [p_0, p_1, \dots, p_k]$ (Fig. 1G). This notation is the standard one borrowed from the literature in algebraic topology [84], where nodes are often points in a topological space. In applications where the interactions are purely combinatorial, one might want to draw attention to the interactions rather than to the underlying space. Thus, in these cases, nodes are often denominated as v_0, v_1, \dots to highlight that they are vertices of interactions, without any reference to an underlying space. The definition of dimension of a simplex coincides then with the definition of order of an interaction we gave earlier. Based on this parallel between the definitions of interactions and simplices, it is easy to see that we do not incur anymore in the problems described above. However, it is not clear how we can handle interactions of potentially different dimensions together and which are the advantages of such representations. Just like graphs are collections of edges, *simplicial complexes* are collections of simplices (Fig. 1H). At difference with graphs, they require further properties to be considered valid complexes: a collection of n simplices $K = \{\sigma_0, \sigma_1 \dots \sigma_n\}$ is a valid simplicial complex if, for every k -simplex $\sigma = [p_0, p_1, \dots, p_k] \in K$, all its subfaces of any dimensions belong to K too. For example, if the triangle $[a, b, c] \in K$, then we also require $[a]$, $[b]$, $[c]$, $[a, b]$, $[a, c]$, $[b, c]$ to belong to K . Note that if we were to extract cliques from a graph and consider them as simplices (which is the operative definition of a *clique complex*), it would be impossible to distinguish the two cases in which respectively the triangle was present or not. Using a simplicial formalism

instead this distinction is immediate, as we only need to check whether the 2-interaction $[a, b, c]$ is included in K (Fig. 11). Simplicial descriptions are very powerful because they come equipped with many nice mathematical gadgets. It is in fact straight-forward to define Laplacian operators for any dimension on simplicial complexes [85,86], they can approximate both regular manifolds and highly irregular structures [87,88], and they come naturally equipped with boundary operators stringing together simplices with different dimensions. Crucially, these operators describe the topology and shape of simplicial complexes in terms of their cycles, cavities and higher-order topological holes [89] and are naturally related to the combinatorial Laplacians [86]. In the following sections, we will describe many of these properties in greater detail, because they represent some of the most powerful tools currently available and are the foundation of recent advances in topological data analysis [90–92].

Although simplicial complexes overcome some of the problems encountered by other lower dimensional representations, they are still quite limited by the requirement on the existence of all subfaces. In some cases, this constraint is too restrictive. For instance, when studying social systems, it is important to be able to describe interactions in groups. In this case we can use simplicial complexes as it is rather safe to assume that a group interaction also implies the underlying pairwise interactions (Fig. 1J). The relative importance of pairwise versus group interactions can then be encoded in weights over the simplices.

However, in other cases, the inclusion constraint can be less easily justified: suppose for example that we are studying collaborations in scientific papers, and we observe a paper by three authors and none by the corresponding pairs of authors; or gene pathways were exactly three genes are needed to perform a function, but the subgroups are not responsible for any function on their own. Clearly, it would be useful to be able to describe also these situations (Fig. 1K).

Hypergraphs provide the most general and unconstrained description of higher-order interactions. Formally, a *hypergraph* is defined by a nodeset V and a set of hyper-edges H that specify which nodes participate in which way within an interaction. Each hyper-edge is a non-empty subset of V . It is easy to see that hypergraphs are the most appropriate description of interacting systems (V, \mathcal{I}) that we gave at the beginning of the section (Fig. 1L). Notice that a hypergraph can include the 2-interaction $[a, b, c]$ without any requirement on the existence of 1-interactions $[a, b]$, $[a, c]$ and $[b, c]$. In fact, hypergraphs are so unconstrained that it is also possible to define hyperedges that include other hyperedges, e.g. given $v, w, z \in V$ and $\gamma = [v, w] \in H$, it is possible to define a new hyperedge $\gamma' = [z, w, v; \gamma] \in H$. Such extreme flexibility comes, as expected, with an additional complexity in treating them. For example, while many graph-theoretic concepts can be extended to the case of hypergraphs, such an endeavor is often fraught with complications [93], to the point that a proper definition of Laplacian operators [94] on hypergraphs and of their properties, e.g. the spectral diameter, has only emerged in the few last years [95,96] and—to the best of our knowledge—has found few real-world applications, e.g. degree-generating models [97] and hypergraph modularity [98,99].

2.2. Relations and links between representations

Naturally, many questions emerge when discussing different representations of the same interacting system: how much overlap is there among two different representations? Is it possible to map one onto another in a canonical way? What kind of information is preserved (and lost) when moving between representations? For example, it seems obvious that a simplicial complex composed only by 1-dimensional simplices (edges) should be the same thing as a graph, right?

Well, it depends [100]. Let us illustrate the links between representations starting from simplicial complexes (Fig. 2A). There are many ways of writing down a simplicial complex, but we focus here only on two descriptions, that are equally valid yet carry very different meanings: the Hasse diagram and the facet representation.

The Hasse diagram of a simplicial complex K is the directed acyclic graph $HD(K) = (V_{HD}, E_{HD})$, whose nodeset V_{HD} contains a node for each simplex in K ($V_{HD} = \{\sigma\} \forall \sigma \in K$), while the edgeset E_{HD} contains an edge for each inclusion between simplices that differ in dimension by 1. In other terms, for two simplices $\sigma, \tau \in K$ there exists an edge $(\sigma, \tau) \in E_{HD}$ iff $\sigma \subset \tau$ and $\dim(\tau) = \dim(\sigma) + 1$. In Fig. 2B we provide an example of a Hasse Diagram for a toy simplicial complex (Fig. 2A). It is easy to see that the Hasse Diagram unfolds all the structure in the simplicial complex, by making explicit the hierarchy of simplices in the complex via its multipartite structure (one layer per dimension), and thus providing information about its internal organization. Importantly, it also gives an explicit way to walk on a simplicial complex: starting from a node (simplex), a walker can follow the links in the Hasse Diagram and explore the whole complex. It turns out that the structure of the Hasse Diagram directly relates to the generalization of the graph Laplacian to simplicial complexes and to random walks on complexes. We will describe this in detail in Sections 3 and 5, but, even without the full theory, it is already possible to understand some of the peculiarities of diffusion on simplicial complexes. The operators that link simplices that differ by ± 1 in dimension, akin to the links in the Hasse Diagram, are (co)boundary operators. For example, given a triangle (2-simplex), the boundary operator returns a combination of the three edges that form the perimeter of the triangle. Taking its boundary again, however, gives zero, because a boundary has no boundary itself (just like in standard differential geometry). It is easy to see now that any operator built on top of such boundary operators, like the combinatorial Laplacian, will only be able to describe diffusion between adjacent simplices with co-dimension 1. Similarly, it is easy to imagine that operators defined on different representations are not necessarily equivalent, as for example shown recently by Schaub and Segarra [70], that found that the Laplacian built on a graph, on its line graph and on the corresponding 1-dimensional complex are not mutually exchangeable.

On the other extreme, the facet representation of a simplicial complex is the most parsimonious in terms of number of stored simplices. A *facet* for complex K is a simplex that is not contained in any other simplex in K . In the Hasse Diagram,

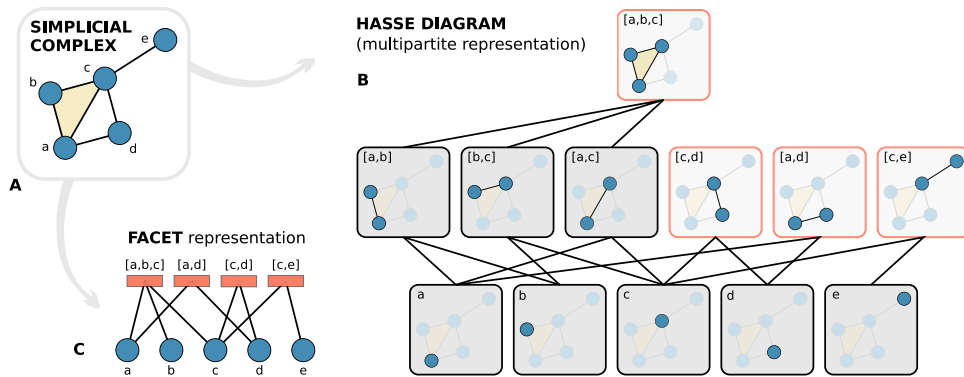


Fig. 2. Relations among representations. A simplicial complex (A) is defined by the list of simplices that compose it. The structure of the natural inclusions between simplices can be described as a graph (B), where nodes correspond to simplices and edges the inclusions (in the figure, when two simplices are linked the top one contains the bottom one). Following the chain of inclusions upward, one reaches the maximal simplices, *facets*, that are not included in any larger simplex. These facets can be used to define a bipartite (or hypergraph) representation of the simplicial complex, identifying the facets with the hyperedges (C).

facets correspond to the top nodes in Fig. 2B, that is, that are not included in any other. In Fig. 2B they are indicated as the simplices with an orange contour. In this sense, facets are akin to maximal cliques in graphs, and, just like maximal cliques, the list of facets of a complex uniquely identifies it. It is also a compressed description because it implies the existence of all the subsimplices without explicitly listing them. In truth, the facet representation is a directed bipartite graph under disguise, where facets constitute one layer, vertices the other, and directed edges represent inclusion of a node in a facet. It can also be recovered easily from the Hasse diagram, by keeping only the vertex layer and the simplices that have zero outdegree (i.e. without anything above themselves). This bipartite graph associated to the facet representation can then also be studied as a hypergraph, where facet membership defines the hyperedges (Fig. 2C). Note that the converse is generally false: a bipartite graph (or hypergraph) gives rise to a simplicial complex in the facet representation only if no set of vertex nodes linked to a facet node (hyperedge) is a subset of another set of nodes linked to another facet node (hyperedge); in short, the incident node sets of facets need to respect the non-inclusion properties of facets, or equivalently, no hyperedge can be included in another hyperedge.

3. Measures

In the previous section we have discussed the various ways and levels at which higher-order interactions can be described and represented. In this section we will focus on observables and measures that can be used to characterize and quantify the structural properties of HORs, at each level of their description. In particular, in the case of cliques, hyperedges, sets, or simplices, many common notions developed for ordinary graphs have been generalized to their higher-order counterparts. We will start by discussing how to describe interactions in terms of matrices or tensors. We will then show how standard graph-based measures have been generalized and what are the insights that can be extracted using them.

3.1. Matrix representations of higher-order systems

3.1.1. Incidence matrix

In mathematics, the incidence matrix is the classical way to describe the relationships between two classes of objects. First introduced by Kirchhoff in 1847 for applications to electrical circuits, the *incidence matrix* of a graph $G = (V, E)$ is a $n \times m$ matrix $I = \{I_{i\alpha}\}$, where n is the number of nodes and m is the number of edges. The entry $I_{i\alpha}$ in row i and column α is 1 if node i and edge α are incident, and zero otherwise. The definition can be easily extended to the case of higher-order interactions, in which case α labels the most general type of interaction (Fig. 3A). For example, in the case of hypergraphs, n is the total number of nodes while m is the number of hyperedges [35,101]. In particular, for hypergraphs allowing for a node to be represented more than once in each hyperedge, it can be useful to weight the entries of the incidence matrix. In this case then the nonzero entries of the incidence matrix would represent the number of times vertex i is present in the relative hyperedge [102]. Notice that the incidence matrix can also be seen as the adjacency matrix of a bipartite graph with two node sets one of size n and one of size m (see Section 2). In the case of simplicial complexes, the incidence matrix between nodes and simplices can be defined in the same way (Fig. 3B). In the following, we will use the language of hypergraphs whenever the definitions apply to simplicial complexes as well.

Incidence matrices come in handy when it comes to characterize the various properties of HORs. For instance, the *degree* of a node i in either a graph or a HORs can be defined as the sum of the elements of the i th-row of the incidence

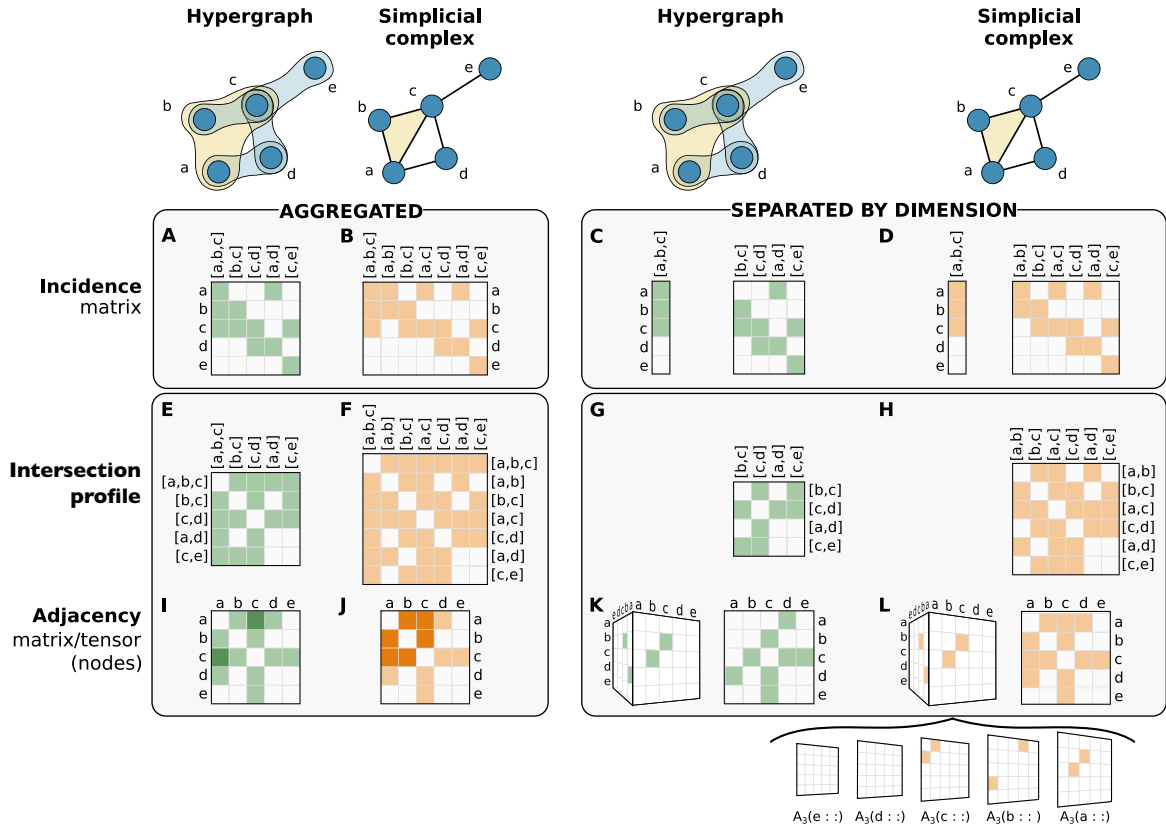


Fig. 3. Matricial and tensorial descriptions of HOrSs: Visualization of incidence matrices and adjacency matrices that can be used to represent the structure of HOrSs. There are three types of matrices: (A-D) incidence matrices relating nodes and edges, (E-H) intersection profile representing the connectivity of edges to edges via the nodes they share in common, and (I-L) adjacency matrices relating nodes to nodes via edges. Furthermore, one can consider edges aggregated by dimensions (left panels) or only subsets of edges of the same dimension, obtaining a collection of matrices, one for each of the different sizes of hyperedges present in the HOrS (right panels).

matrix. In a (simple) graph the column of an incidence matrix always sums to 2 as the relationships described are always between two nodes of the graph. In a hypergraph (simplicial complex), however, the rows of the matrix can have more than two non-zero elements as each hyperedge (simplex) can describe interactions among more than two vertices. The sum of the elements of the columns of the incidence matrix define the size sequence of the hyperedges (simplices) of the system. These two local measures, the degree of the nodes and the size of the hyperedges, are the first measures one can use to study the properties of HOrSs.

3.1.2. Adjacency matrix

From the incidence matrix of a graph we can also construct another matrix that fully encodes the connectivity of the graph, the *adjacency matrix* A . Since the matrix product $I \cdot I^T$ is a $n \times n$ matrix whose i, j element is the number of columns of the incidence matrix I that contain both vertices i and j , while i, i gives the degree of node i , the adjacency matrix of a simple graph can be defined as:

$$A = II^T - D \quad (1)$$

where D is the diagonal matrix whose diagonal entries are the nodes degrees. The adjacency matrix A is 0 along the diagonal, while for $i \neq j$ the entry $a_{ij} = 1$ iff nodes i and j are adjacent, that is, there exists an edge connecting them. We can generalize the notion of adjacency matrix to the case of HOrSs by using the same expression in Eq. (1) and considering as D the diagonal matrix whose diagonal entries are the number of hyperedges a vertex belongs to. While for simple graphs there can be at most one edge connecting a pair of nodes i and j , for HOrSs there can be more than one hyperedge α containing the two nodes. The adjacency matrix of a HOrS is then a $n \times n$ matrix whose elements a_{ij} for $i \neq j$ are the number of hyperedges that contain both i and j (Figs. 3I,J for hypergraphs and simplicial complexes respectively). When the hyperedges are weighted, the adjacency matrix of a hypergraph can be written as $A = IWI^T - D$, where I is the incidence matrix, W is the diagonal matrix with the weights of the hyperedges along the diagonal, and D is a diagonal matrix with the degrees of the nodes along the diagonal [103].

From the incidence matrix, one can also define the *intersection profile* of a HOrS as

$$P = I^T I, \quad (2)$$

which is an $m \times m$ matrix, whose elements $P_{\alpha\beta}$ count the number of vertices in common between two hyperedges α and β and m is the number of hyperedges (Fig. 3E). The intersection profile is useful in the statistical study of edge intersections in hypergraphs [104]. The same construction also applies to simplicial complexes (Fig. 3F).

The adjacency between two vertices can be defined directly, without any dependence on the definition of an incidence matrix. This approach is often used when the higher-order structures cannot be uniquely identified only by the set of nodes involved, or when there is a theoretical need for a more restrictive notion of adjacency between two hyperedges than just that they intersect in at least two vertices. For example, when studying motifs in a network, for each motif M one can construct a $n \times n$ adjacency matrix A_M , where n is again the number of nodes, and whose entries a_{ij} are the number of times i and j both belong to an instance of motif M [24]. Such adjacency matrix can also be seen as that of a weighted network built only of the instances of M . It can be useful to notice that when M is a d -clique, then $A_M = A_d$ is the adjacency matrix built from the incidence matrix containing only d -dimensional hyperedges. This same approach can be used to build incidence matrices representing the d -dimensional relationship between the nodes and HOrS (Figs. 3C,D).

The adjacency matrices $\{A_2, A_3, \dots, A_d, \dots\}$ for each d -dimensional structure in the HOrS represent the weighted networks underlying the HOrS, and can be collected in a natural way in an adjacency *tensor* of dimension d , indexed by the node labels (Figs. 3G,H). Further insights into the structure of the hypergraphs themselves [105] and into the processes taking place over them [106,107] can be obtained from studying the Laplacians of these networks and their spectra, which will be introduced in Section 3.5.

Another reason for building an adjacency tensor without relying on the incidence matrix is practicality. For example, simplicial complexes require to explicitly list all 2^k simplices included in each k -simplex and this can become very impractical. This is due to the constraint on the existence of all subsimplices of any given simplex, which in turn is fundamental for the correct construction of the useful algebraic structures that come with a simplicial complex (e.g. walks and homology, see Sections 3.2 and 3.4.1). To avoid listing all the simplices in a simplicial complex, one could only list the maximal simplices [108], as mentioned in Section 2. However, while this method effectively compresses the global structure of a simplicial complex, it does not encode the relationships between the k -simplices in the complex and the $k+1$ and $k-1$ -simplices, which are exactly the crucial ones to make the simplicial complex representation so useful and unique among the other HOrSs.

In order to avoid this problem, one can define two $m_k \times m_k$ adjacency matrices for each dimension k describing respectively an upper adjacency A_U and a lower adjacency A_L for all k -simplices. Here, m_k is the number of k -simplices. Following standard notation [109–112], two k -simplices are lower adjacent if they intersect in a $k-1$ -simplex, they are upper adjacent if they are both faces of the same $k+1$ -simplex. Then $(A_U^k)_{\alpha\beta} = 1$ only if the k -simplices α and β are lower adjacent, while $(A_L^k)_{\alpha\beta} = 1$ only if the k -simplices α and β are upper adjacent [113]. Another way of defining adjacency is to construct a single adjacency matrix A^k that isolates lower adjacent interactions that are not involved in upper ones, that is, $A_{\alpha\beta}^k = 1$ only if the k -simplices α and β are lower adjacent but not upper adjacent [86,113]. Both these definitions of adjacency will be instrumental in the study of node shortest path centrality defined on paths on k -dimensional simplices (Section 3.2).

It is also possible to define an adjacency representation which generalizes the standard one used in simple graphs, that is that an element $a_{ij} = 1$ when the edge $\{i, j\}$ is present in the graph. To generalize this idea to higher-order interactions, one needs to consider a combinatorial object A indexed by all possible permutations of α . Then, for each

order d , one defines an $\overbrace{n \times n \times \dots \times n}^d$ adjacency tensor \mathbf{A}_d so that an entry $a_{i_1, \dots, i_d} = a_\alpha$ represents d -dimensional set of nodes participating in the higher-order interaction $\alpha = \{i_1, \dots, i_d\}$. This means that $a_\alpha = 1$ if the set α is present, while $a_\alpha = 0$ otherwise. This definition was originally introduced in [114] in the context of ensembles of simplicial complexes (Fig. 3L). However, it can be easily extended to hypergraphs and other set-based HOrSs (Fig. 3K).

3.2. Walks, paths and centrality measures

Network centralities are node-related measures that quantify how “central” a node is in a network. There are many ways in which a node can be considered so: for example, it can be central if it is connected to many other nodes (degree centrality), or relatively to its connectivity to the rest of the network (path based centralities, eigenvector centrality). In the following, we review some of the most common centralities and their possible generalizations to higher-orders.

3.2.1. Degree centralities

The simplest centrality measure is the degree of a vertex, which counts how many other vertices are incident to it. The degree can easily be defined from any of the adjacency matrices defined in Section 3.2 as

$$\deg(i) = \sum_{j=1}^n a_{ij}. \quad (3)$$

Via the adjacency tensor introduced in [114], one can define a comprehensive generalized degree which incorporates not only the dependencies of nodes to their higher-order counterparts, but also for any intermediate $\delta < d$ -dimension. In terms of the adjacency tensor, the generalized degree is defined as

$$k_{d,\delta}(\alpha) = \sum_{\alpha' \supset \alpha} a_{\alpha'} \quad (4)$$

and indicates the number of d -dimensional simplices α' that are incident on the δ -dimensional simplex α . For $\delta = 0$ the generalized degree reduces to the standard node degree centrality relative to d -simplices. Finally, a coarser way to quantify node degree centrality in simplicial complexes is to just count the number of maximal simplices (or *facets*) incident on a vertex [115].

When working with weighted hypergraphs, it is slightly trickier to properly define a degree. For example, Kapoor et al. [116] illustrate how a node's degree centrality can be defined in terms of either its incident hyperedges or its adjacent nodes, where two nodes are considered adjacent if they belong to the same hyperedge. The degree centrality of a node in a hypergraph becomes then defined as the number of nodes adjacent to it, and the weighted degree centrality as the sum of weights of the ties of the node with the other nodes in the hypergraph.

How to define the weight of a tie is going to be important to identify the meaning of centrality. The weight can be in the tie between two nodes as the number of hyperedges they both belong to, or on the hyperedge itself attached as a function of its multiplicity. Kapoor et al. [116] compare degree centralities relative to five different definition of hyperedge weight: constant, frequency based, Newman's strength for collaboration networks, Gao's weights for the email dataset, the probability of a contact between the two nodes over ℓ interactions in a group of size k .

Degrees in HORs can also be defined on hyperedges or simplices. In fact, for each hyperedge or simplex α we can define the $\deg(\alpha)$ as the number of hyperedges that are adjacent to α in some of the ways introduced earlier. In particular, we can define a lower and upper adjacency degree in simplicial complexes [113,117] as the number of simplices that are either lower or upper adjacent to α , or the number of simplices that are lower adjacent but not upper adjacent to α . Moreover, these adjacency definitions can be combined as done by Serrano and Gómez in [112], where they introduce the maximal simplicial degree $\deg(\alpha) = \deg_L(\alpha) + \deg_U(\alpha)$, that counts the number of upper adjacent simplices to α and the number of lower adjacent simplices that are not upper adjacent. Degree based centralities can be defined building on any of the above definitions and generalizing on the graph based formulas. The interested reader can find an exhaustive review of centrality measures for HORs in [113,118].

3.2.2. Paths and path-based centralities

To define a centrality relative to the entire network, we need to define an acceptable way in which one can traverse a HOR by defining walks along its connections. A walk in a simple graph is a sequence of vertices $[v_1, v_2, \dots, v_\ell]$ such that two consecutive vertices v_i, v_{i+1} are adjacent to each other. A walk where a vertex is present only once is called a path.

After having introduced the concept of walks on HORs, then centralities can be defined using the classical definitions as either the number of paths that go through node v_i (betweenness centrality), or the average length of shortest path between a vertex and all vertices in the graph (closeness centrality), the number of closed walks of different lengths starting and ending at the same vertex (subgraph centrality). In the case of HORs, when defining paths, it is easier to consider walks connecting two hyperedges (simplices) than walks connecting two vertices. This is because any pair of nodes present in the two extremal hyperedges (simplices) of the path will be connected by exactly the same walk.

The easiest way to define a walk in a hypergraph is as a sequence of hyperedges with at least 1 vertex in common [103,119]. This definition follows from the notion of adjacency induced by the incidence matrix. Then, the sub-hypergraph centrality of vertex v_i is the number of closed walks of different lengths in the network starting and ending at vertex v_i [101,120], which can be expressed as

$$C_{sh}(v_i) = \sum_{v_j} u_{ij}^2 e_{\lambda_j}$$

where u_{ij} is the i th component of the j th eigenvector of the adjacency matrix.

This definition can be generalized to k -walks between hyperedges as a sequence of hyperedges such that each pair of successive hyperedges is adjacent and they intersect in at least k vertices [110,121]. This in turn requires that all hyperedges in the walk have dimension s at least $s = k + 1$, but poses no constraints on their maximum dimension s . Examples of two simple walks for regular hypergraphs, one 1-walk and two different 2-walks, are shown in Fig. 4. The corresponding closeness centrality is then the reciprocal of the average length of the shortest path between the node and all other nodes in the HOR [121].

The hypergraph definition of a k -walk also applies to simplicial complexes [118] and can be used to define other measures of betweenness and closeness centrality. However, in simplicial complexes, it is more appropriate to define a k -walk only comprised of k -simplices that are lower adjacent i.e. have in common k vertices (remember, a k simplex contains $(k + 1)$ vertices) [113]. Just as before, the simplicial closeness of a k -simplex is then the reciprocal of the sum of its k -shortest path distance to all other k -simplices. The simplicial harmonic closeness centrality of a k -simplex is instead the sum of reciprocal s -shortest path distance to all other k -simplices.

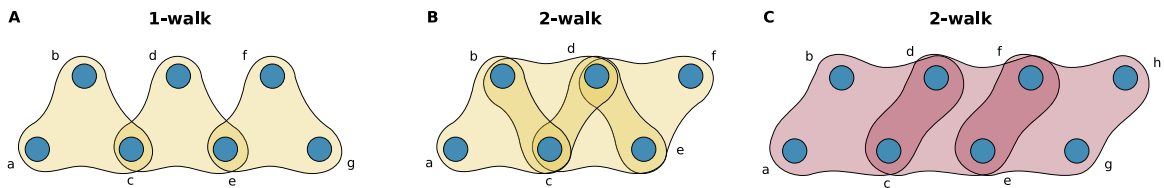


Fig. 4. Example of k -walks on hyperedges. The simplest walk, a 1-walk, is the one where hyperedges share only one vertex (A) similarly to how walks are defined on graphs. Such walks can be generalized to larger intersections (k -walks), for example 2-walks (B and C). Note that the size of the intersection poses no upper bound on the size of hyperedges along the walk, for example B and C and composed hyperedges of different size while still being 2-walks.

Source: Figures adapted from Ref. [119].

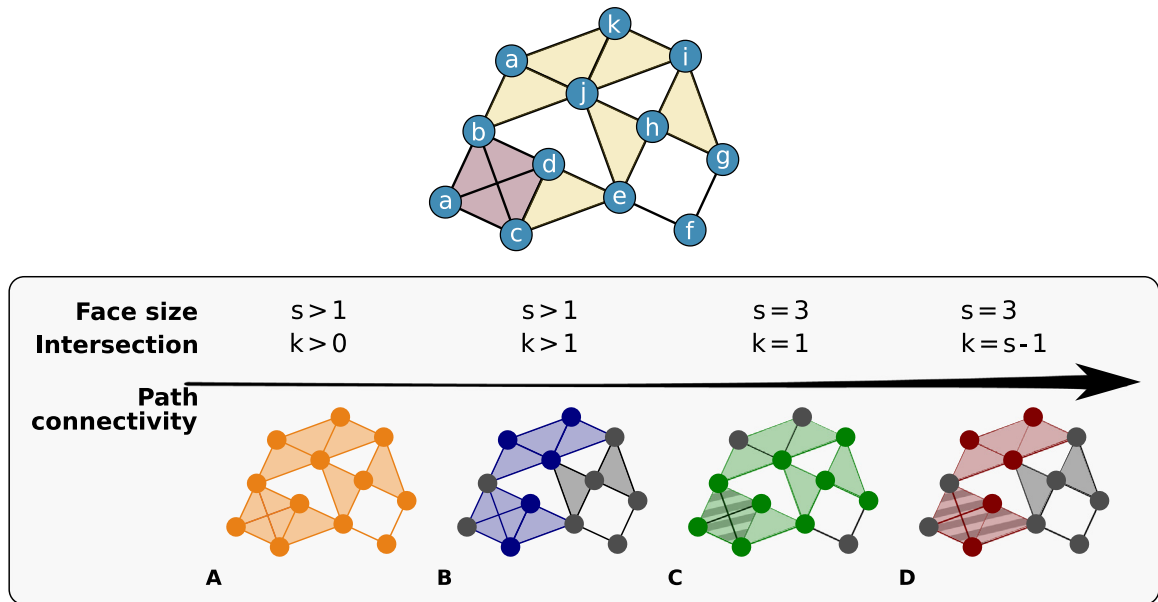


Fig. 5. Walks in HORs. Visualization of the different definitions of walks on a toy example of higher-order network. From left to right, the definition of the walk gets more restrictive. For each restriction on the defining variable of a walk (what elements are allowed to be considered for a walk and how much do they need to overlap in order to be adjacent), we color what parts of the HORs are reachable by at least a walk of length greater than one, and in gray what parts do not allow any walk to pass through them. In (C,D), some parts of the HORs are connected only if the HORs is a simplicial complex, and we visualize those with a striped pattern. We can see how the less restrictive walk (A), which can pass through two edges that have at least one vertex in common, yields the same connectivity as its underlying graph. Restricting the intersection between two adjacent edges to have at least 2 vertices in common, example (B), already highlights different mesoscale connectivity patterns in the HORs, which can be further studied introducing a further restriction on the size of the edges, examples (C) and (D).

In Fig. 5 we provide examples of how different configurations on k and s can yield different connectivity structures for the same HORs. If we allow any hyperedge or simplex dimension ($s > 1$) and any size of the intersection between them ($k > 0$), then we find that all paths are valid and the whole toy HORs is connected. In fact, we recover the simple graph connectedness (Fig. 5A).

If we instead require that interactions share at least two vertices ($k > 1$), some paths are not allowed. For example, the triangle [2, 10, 12] is not connected to any of the triangles in the tetrahedron [1, 2, 3, 4], because the only intersection is 2.

Note also at this point that whether the HORs is a hypergraph or a simplicial complex can make a difference. In Fig. 5C, if we consider the HORs to be a simplicial complex, the presence of the tetrahedron [1, 2, 3, 4] implies also the presence of all the subfaces. Combining this with the requirement $k = 1$, this also implies that some paths will not be walkable, e.g. all the triangles inside the tetrahedron share an edge with each other. Hence one cannot walk from one triangle to the other (shown as the black edges). However, there exist other paths that make the HORs connected, for example, [1, 2, 4] is connected to [3, 4, 5]. Similar considerations also apply to Fig. 5D, which shows an example of the simplicial k -walk described earlier in this section, that is, a walk limited to jumps between lower adjacent simplices.

3.2.3. Eigenvector centralities

In some applications, it is important to quantify the influence of a node on the entire network, rather than its centrality relative to possible paths. First introduced in a sociological context by Bonacich [122], the eigenvector centrality tries to capture this effect using an iterative definition. In fact, the eigenvector centrality of a node depends on the centrality of its neighbors [123]. In the graph case, it can be written as

$$x_v = \frac{1}{\lambda} \sum_{t \sim v} x_t = \frac{1}{\lambda} \sum_{t \in G} a_{vt} x_t \quad (5)$$

where x_v is the eigenvector centrality of node v and a_{vt} the adjacency matrix of the graph. Note that again the generalization to higher order interactions relies only on the definition of connectivity and walks. This measure has become widely used in a variety of situations ranging from Google's PageRank [124] to neuron's firing rate [125]. Interestingly, Bonacich [122] also showed that, if association is defined in terms of walks, a family of centralities can be defined based on the length of walk considered. Degree centrality counts walks of length one, while eigenvalue centrality counts walks of length infinity. Alternative definitions of association are also reasonable. Alpha centrality allows vertices to have an external source of influence, while Estrada's subgraph centrality proposes only counting closed walks (triangles, squares, etc.) [113,120].

Bonacich [126] generalized eigenvector centrality to the case of bipartite graphs using their adjacency matrix. A feature of this definition is that one can compute centrality score for the same eigenvalue for both node sets. Using the same technique, one can compute eigenvalue centrality scores from incidence matrices for both hypergraphs, which will give an eigencentality score for both vertices and hyperedges. A two-mode analysis of an incidence matrix then enables to identify central hyperedges in addition to nodes [127].

For motifs, it is possible to use the spectral features of the weighted motif adjacency matrix A_M defined in 3.1. For example, the clique motif eigenvector centrality score of node i is given by the i th component of the largest real eigenvector of W [128].

To incorporate non-linearities, we can make it so that the contribution of the centralities of two nodes in a 3-node hyperedge is multiplicative for the third. To do so, one can define the centrality using the eigenvector of the tensor A_k , where k labels the considered dimensions. There are several other types of tensor eigenvectors [129], and for this reason Benson [128] use Z - and H -eigenvectors which are arguably the most well-understood and commonly used tensor eigenvectors. The Z -eigenvector centrality vector is then defined as any positive vector c satisfying

$$Tc^{m-1} = \lambda c^m \quad \|c\|_1 = 1 \quad (6)$$

for some eigenvalue $\lambda > 0$ of the adjacency tensor $T = A_k$, and respectively the H -eigenvector centrality vector as the positive real vector c satisfying

$$Tc^{m-1} = \lambda c^m. \quad (7)$$

As we have seen before, for hypergraphs and simplicial complexes, adjacency can be defined not only at the vertex level, but also between hyperedges. It is possible to introduce notions of centralities for simplices and hyperedges through the components of the principal eigenvector of A_k [113]. The simplicial eigenvector centrality of the k -simplex α is given by the α component of the principal eigenvector of A_k , and its simplicial Katz centrality as $K_{k,\alpha} = [\sum_{p=0}^{\infty} x^p A_k^p]_{\alpha}$ where $0 < x < \frac{1}{\lambda_1(A_k)}$.

3.3. Triadic closure and clustering coefficient

A key concept in network analysis for going beyond node-related measures is triadic closure. It is a concept that comes from sociology [130], which argues that a strong social tie between two persons can only occur if it is part of a triangle. In other terms, my closest friends are the ones I share friends with. In a graph structure, triadic closure is represented as the paths of length 2 that are closed by an third edge. The fraction of pairs of neighboring nodes that are themselves linked by an edge defines the node's clustering coefficient. The clustering coefficient is an important network measure, which informs on the density of a node's neighborhood. This coefficient can also be computed globally as the total percentage of paths that are closed by an edge, i.e. are part of triangles.

This concept does not generalize well to bipartite graphs, because triangles – as any other odd cycle – do not exist in bipartite graphs. The global clustering coefficient can however be defined through its one-mode projections, as the number of paths of length 4 in the bipartite graph that are part of a cycle of length 6 [131,132].

Other attempts to generalize the concept of clustering coefficient beyond pairwise relations focused on keeping its close relation to the notion of triadic closure. One possibility is to define a local clustering coefficient from the new definitions of neighborhood that a node can have in a HOrS [133]. For example, in a simplicial complex, a neighborhood can also be defined at the maximal simplex level, and can also be defined for higher order simplices, not only for nodes [118].

Another possibility is to redefine the notion of walks [101] as sequence of vertices (v_1, \dots, v_ℓ) such that two adjacent vertices v_i, v_{i+1} both belong to the same hyperedge e_i . Then, the clustering coefficient follows from its pairwise definition as the ratio of 2-paths that are closed by an edge. In a HOrS, walks can also be defined as sequence of k -cliques, or $k-1$ -simplices (e_1, \dots, e_ℓ) such that two adjacent cliques e_i, e_{i+1} have $k-1$ nodes in common, which we will call k -paths as

they are formed of k -cliques. In this case too, the clustering coefficient is then defined as the fraction of k -paths of length k that are part of a $k + 1$ -clique [134].

In simplicial complexes, we can distinguish between a closed k -path of length $k + 1$ and a k -simplex. Hence, the clustering coefficient can be defined as the ratio of closed k -paths of length $k + 1$ that are closed by a k -simplex. In particular, when considering triangles, this definition of the clustering coefficient can be used to verify the sociological intuition behind the diadic triadic closure idea [115], that is, it is possible to count how many actual “full” triangles (2-simplices) among the possible “empty” triangles constructed from three edges (a closed path of three 1-simplices). Finally, this higher-order clustering coefficient can be further generalized to motifs in weighted or growing HORs [31].

3.4. Simplicial homology

One of the main reasons to use simplicial complexes as representations for higher-order datasets is an algebraic toolset that studies the topology of the HORs in a unique way: simplicial homology. Homology is an algebraic topological concept that enables us to study the structure of a simplicial complex at different dimensional scales.

Before we can introduce homology, we need to define an algebraic structure on our simplicial complex. This requires imposing an orientation on each simplex in the complex, formalized as the ordering of the vertices. The orientation can be arbitrarily chosen, just like the choice of node labels in a network, and it is only needed in order to coherently perform the computations. An orientation is an equivalence class on the vertex orderings, where two orderings are equivalent if they differ by an even permutation [84,135]. The orientation issue does not exist in a 0-simplex, since the nodes are not oriented, and only arises when we deal with higher order graphs. For simplicity, and with no loss of generality, we choose the orientation induced by the ordering of the vertex labels.

3.4.1. Boundary operators and homology groups

We can combine these oriented simplices in k -dimensional chains $c = r_1\sigma_1 + r_2\sigma_2 + \dots$ where σ_i are k -dimensional simplices and $r_i \in \mathbb{F}$ are coefficients in a field \mathbb{F} . The collection of all possible k -chains in the simplicial complex X is the vector space $C_k = \{r_1\sigma_1 + r_2\sigma_2 + \dots | r_i \in \mathbb{F}, \sigma_i \in X_k\}$ where X_k is the set of k -simplices in X .

We can also define the dual space of C_k , denoted as the *co-chain space* C^k , as the linear space of all alternating functions $f : C_k \rightarrow \mathbb{R}$. Chain and co-chain space are just two sides of the same coin, as they encode the same information. For instance, C^1 can be interpreted as the space of edge-flow vectors and each of its elements f assigns a scalar to an edge, representing the intensity of flow along that edge with a sign which represent the agreement or not with the chosen orientation of the edge.

We can relate the k -chain space C_k to the $k - 1$ chain space using the boundary operator, which maps each k -simplex to its $k - 1$ -dimensional faces $\partial_k : C_k \rightarrow C_{k-1}$. When applied on a simplex $\alpha = [v_0, \dots, v_k]$, it gives:

$$\partial_k([v_0, \dots, v_k]) = \sum_{i=0}^k (-1)^i [v_0, \dots, v_{i-1}, v_{i+1}, \dots, v_k]. \quad (8)$$

Basically, in each term of the linear combination, we remove a vertex from the original simplex. In this way, we obtain its boundary as an alternate sum of the $(k - 1)$ -order simplices. In a triangle $[v_0, v_1, v_2]$, for instance, we get the alternate sum of the three edges $([v_1, v_2] - [v_0, v_2] + [v_0, v_1])$. The image of the boundary map, $im(\partial_k)$, coincides with the space of $(k - 1)$ -boundaries. The kernel $ker(\partial_k)$ is instead the space of k -cycles, as it is easy to prove that for every cyclic chain c whose starting point coincides with the ending point $\partial_k c = 0$. Moreover, $\partial_k \circ \partial_{k+1} = 0$, which implies that $im(\partial_{k+1}) \subseteq ker(\partial_k)$. The elements of $ker(\partial_k)$ which are not included in $im(\partial_{k+1})$ can be denoted with the quotient space

$$\mathcal{H}_k \equiv \frac{ker(\partial_k)}{im(\partial_{k+1})} \quad (9)$$

which takes the name of *kth homology group*. The elements of \mathcal{H}_k correspond to the k -cycles that are not induced by a k -boundary, namely the k -dimensional *holes* of our complex [84,135].

The dimension of the homology group \mathcal{H}_k is called the *kth Betti number* and it represents a way to classify the k -dimensional topology of a HORs. Specifically, the 0th Betti number represents the number of connected component in the simplicial complex, the 1st Betti number is the number of cycles, the 2nd the number of voids enclosed by 2-dimensional simplices, the 3rd the number of 4-dimensional voids etc.

3.4.2. Evolving simplicial complexes

Homology is a century old concept in algebra and is one the key tools for the study and classification of shapes in mathematics [135]. Recently the concept has been extended to weighted and growing simplicial complexes [136]. Inspired by 90s shape theory [137], in the early 2000s persistent homology was invented in different research groups around the globe [90,138,139] giving birth to the field of Topological Data Analysis [91]. *Persistent homology* is a way of computing the homology of a growing simplicial complex and to follow how its homological features evolve along the filtration [140]. The filtration is a sequence of simplicial complexes that provide progressively finer approximations of the data space under investigation. The persistence of certain homological features through the multiple scales explored in

the filtration is related to their relevance for the data space, with the typical assumption that more persistent features are more important, although the exact interpretation of the persistence of a homological feature depends crucially on how the filtration is constructed (see for example [141]). In the last 20 years the field has been vastly developed, and new methods for tracking homological features have been introduced for cases when simplicial complexes can also lose simplices along the filtration, *zig-zag homology* [142], or for when the growth of the simplicial complex can be described through more than one parameter, *multi-persistent homology* [143]. The interested reader can find a good introduction to the theory and practice of persistent homology in [144,145]. A large fraction of the work on HORs in real datasets requires some version of persistent homology. In Section 9 we provide some examples of its use.

3.4.3. Other measures of shape in simplicial complexes

Homology in all its variants (persistence, zigzag, multiparameter) is a powerful tool to classify structure according to key mesoscale features. However, it is important to notice that it depends on the choice of coefficient field \mathbb{F} used to compute the homology. Moreover, homological invariants are not exhaustive in general, as they pertain to homological equivalence classes, thus they compress some information away. This is rooted in the invariance of topological properties to deformations, the classical example being the topological equivalence between a mug and a donut. Indeed, there are no complete topological classification known, and one can find examples of simplicial complexes homologically indistinguishable from a 3-sphere (a sphere in 4-dimensions) that are not spheres at all [146]. Nonetheless, the homological invariants give unique insights in the dynamics that can exist in data spaces and as mentioned above have found widespread application (see Section 9 for relevant examples).

In addition to the full homological description, other invariants have been used in applications [147,148]. Two commonly used ones are the Euler characteristic and the Laplacian spectral entropy.

For any simplicial complex Σ , the Euler characteristic is defined as the alternating sum $\chi = \sum_{k=0}^D (-1)^k f_k$, where f_k is the number of simplices of dimension k present in the simplicial complex, and D is the maximal dimension of a simplex in Σ [146].

The spectral entropy, first introduced by [149] for simplicial complexes, provides a measure of the degree of the overlap between simplices in the complex via the study of the eigenvalues of the L_k combinatorial laplacian. The spectral entropy is then

$$H_k = -\frac{1}{\log(f_k)} \sum_{i=1}^{f_k} p(\lambda_k^i) \log(p(\lambda_k^i)) \quad (10)$$

where $p(\lambda_k^i) = \frac{\lambda_k^i}{\sum_i \lambda_k^i}$ is the contribution of the eigenvalue λ_k^i to the eigenspectrum of the k th combinatorial Laplacian L_k , and f_k the number of simplices of dimension k present in the simplicial complex. The most general framework for non k -uniform hypergraphs requires a deeper analysis and the problem of generalizing a Laplacian for these structures has been addressed by many scientists [86,109,150,150–152].

3.5. Higher-order Laplacian operators

The Laplacian is an operator that plays a key role in information processing of relational data, and has analogies with the Laplace-Beltrami operator in differential geometry. Similarly to the adjacency matrix, there is no unique way to generalize the Laplacian to HORs. However, as networks can be thought of as a special subset of the larger family of HORs, the graph Laplacian is a special case belonging to the more general family of Hodge Laplacians. The intuition here in the construction of higher order Laplacians, either for hypergraphs or for simplicial complexes, is that the role played by the nodes in the graph Laplacian is, at higher orders, played by links, triangles, tetrahedra and higher dimension analogues.

In analogy with the standard construction in graphs, a straightforward way to introduce a higher-order Laplacian is to define a Laplacian matrix L from one of the adjacency matrices introduced in Section 3.1. We can thus write:

$$L = D - A \quad (11)$$

where A is the chosen adjacency matrix, and D is the diagonal matrix with the degree sequence of the nodes along the diagonal [153,154]. However, this approach yields a matrix L that is equivalent to the Laplacian of the weighted graph associated to the adjacency matrix A [155].

The graph Laplacian can be interpreted as a particular case of the discrete Laplace operator representing the flux density of the gradient flow of a function defined on the vertices of a graph. For hypergraphs and simplicial complexes, because of their richer structure, there are multiple ways one can define Laplacians that are compatible with the corresponding differential geometry operator. In particular, for k -uniform hypergraphs and k -regular simplicial complexes we can define a unique adjacency tensor \mathbf{A}_k that represents the HOR. Then, one introduces a Laplacian tensor which is the discretization of the higher-order Laplace-Beltrami operator in differential geometry [156,157].

This theoretical connection to the continuous operator opens the possibility to use the spectrum of this tensor to study the diffusion properties of the HOR. For example, in recent years, many authors have defined a Laplacian operator on hypergraphs for specific diffusion processes [94–96,158]. Another higher-order Laplacian, designed in the context of

synchronization in systems with higher-order interactions between oscillators placed on the nodes, and introduced in Ref. [159], is discussed in Section 6.1. In the following subsections we provide explicit definitions for Laplacian operators on hypergraphs and simplicial complexes. In Section 5 instead we discuss in detail their mathematical properties and their link to diffusion.

3.5.1. Hypergraph Laplacians

Historically, the first attempt to generalize the Laplacian operator to hypergraphs along these lines is due to Chung [154], who considered a simplified type of hypergraphs, the s -uniform hypergraphs, where all the hyperedges have the same size s . Given an s -uniform hypergraph H with N nodes and edge set E , for each $(s-1)$ -subset of nodes, x , we can define the degree $d(x)$ as the number of edges involving vertices in x , and the diagonal matrix D such that $D(x, x) = d(x)$. The adjacency matrix A used in this case is a binary matrix such that $A(x, y) = 1$ if subsets x and y are connected $(s-1)$ -subsets that share $s-2$ nodes. Formally, that corresponds to $A(x, y) = 1$ if $x = [x_1, x_2, \dots, x_{s-1}]$ and $y = [y_1, x_2, \dots, x_{s-1}]$ and $x \cup y \in E$, and 0 otherwise. The Laplacian can then be defined as:

$$L = D - A + \rho(K + (s-1)I) \quad (12)$$

where $\rho = d/N$, d is the average degree, and K is the matrix of the complete graph, such that $K(x, y) = 1$ if $x = [x_1, x_2, \dots, x_{s-1}]$ and $y = [y_1, x_2, \dots, x_{s-1}]$, and 0 otherwise.

Another possibility to define a hypergraph Laplacian is to derive the Laplacian from the transition matrix of a random walk. For instance, Lu and Peng [119] considered *random k -walks* ($k < s$) on s -uniform hypergraphs. These are k -walks generated as follows (Fig. 4). The walker starts from the sequence of k visited vertices at the initial step x_0 edge. At each time step, let S be the set of last s vertices in the sequence of visited vertices in the hypergraph $H = (V, E)$. A random $(s-k)$ -set T is chosen from the neighborhood $\Gamma(S)$ of S uniformly; here $\Gamma(S)$ is given by $\{T | S \cap T = \emptyset \text{ and } S \cup T \in E(H)\}$; the vertices in T are added into the sequence one by one in an arbitrary order. The definition of Laplacian is split in two cases:

- For $1 \leq k \leq s/2$ the k th Laplacian is defined as the Laplacian of a weighted undirected graph $G^{(k)}$ built such that a random k -walk on H is essentially a random walk on $G^{(k)}$.
- For $s/2 \leq k \leq s-1$ the k th Laplacian is defined as the Laplacian of an Eulerian directed graph $D^{(k)}$ and the random k -walk on H is in one-to-one correspondence to the random walk on $D^{(k)}$.

Lu and Peng [119] also introduced α -lazy random k -walks, with $0 \leq \alpha \leq 1$, which are modified random k -walks where with probability α the walker stays at the current edge and with probability $1 - \alpha$ it moves by appending $s - k$ vertices to the sequence.

3.5.2. Combinatorial Laplacians

For general simplicial complexes, a higher-order Laplacian can be defined for each dimension k via two matrices that encode respectively the roles of upper and lower adjacencies in dimension k :

$$L_k = L_U^k + L_L^k \quad (13)$$

where L_U^k and L_L^k are called the upper and lower adjacency Laplacians. The full Laplacian L_k is usually referred to as combinatorial, and each k -order Laplacian encodes the relationships of k -simplices with their adjacent $(k+1)$ - (upper adjacency) and $(k-1)$ -simplices (lower adjacency).

The link between L_k and the simplices of dimension k with those of dimension $k+1$ and $k-1$ can be readily understood from the definition of $L_{U/L}^k$. The linear boundary operators ∂_k described in Section 3.4.1 can be represented as a matrix B_k , whose columns represent all the k -dimensional simplices in the complex, and the rows the $(k-1)$ -dimensional simplices. Element β, α of $B_k, (B_k)_{\beta\alpha}$, is non-zero if the $k-1$ -simplex β is a face of k -simplex α , and can be $+1$ or -1 according to the orientation induced on β by α , that is the coefficient that β has in the alternating sum $\partial_k(\alpha)$. For each boundary operator, there exists also a *co-boundary operator* $\partial_k^* : C_k \rightarrow C_{k+1}$, that is, the adjoint of the boundary operator. In matricial form, this can be represented by the transpose conjugate matrix of B_k, B_k^T . These boundary matrices define L_U^k and L_L^k as:

$$L_U^k = B_{k+1} B_{k+1}^T \quad L_L^k = B_k^T B_k \quad (14)$$

The higher-order combinatorial Laplacian L_k becomes then:

$$L_k = B_k^T B_k + B_{k+1} B_{k+1}^T \quad (15)$$

Fig. 6 shows the explicit construction of the combinatorial Laplacian for the simplicial complex in Fig. 3. We first need to choose an orientation for the simplices in the simplicial complex. Here for simplicity we choose the orientation to follow the lexicographic ordering on the nodes' labels (Fig. 6A). Once fixed this, it is possible to compute the two boundary matrices that we need in this case B_1 and B_2 , corresponding respectively to the boundary matrix mapping chains of edges into chains of nodes (Fig. 6B), and to the boundary matrix mapping chains of triangles into chains of edges (Fig. 6C). We can then easily compute the corresponding combinatorial Laplacians from Eq. (15), obtaining the matrices in Figs. 6D-F. Note that for L_0 and L_2 there is only one contribution to the sum, because the simplicial complex does not contain k -simplices of order k respectively less than 0 and larger than 1, hence one of the two terms in the sum vanishes.

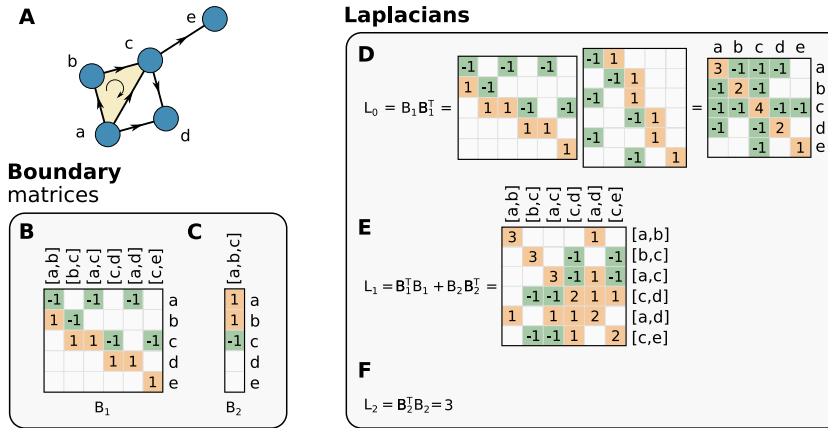


Fig. 6. Construction of combinatorial Laplacian. The first step required to define boundary operators is to endow a simplicial complex with an orientation. Here we choose to orient our toy simplicial complex with a simple lexicographic orientation (A). Once the orientation is fixed, it is possible to define boundary matrices; since there are only simplices with order ≤ 2 , we have two non trivial boundary matrices B_1 (B) and B_2 (C). Following Eq. (15), we can build the combinatorial Laplacians corresponding to the three different dimensions of simplices in the simplicial complex: L_0 defined on nodes, and identical to the standard graph Laplacian (D); L_1 defined on the edges (E); and L_2 which is a scalar in this case because the simplicial complex contains only one 2-simplex (F).

Since $L_{U/L}^k$ describe the relatedness between upper and lower adjacent simplices, they should be related to the upper and lower adjacency matrices $A_{U/L}^k$ described in Section 3.1.2. It is possible to rewrite L_k as [86]:

$$L_k = D_U^k - A_U^k + (k+1)I_{n_k} + A_L^k \quad (16)$$

where D_U^k is a diagonal matrix with on the upper degree of simplices computed from A_U^k , and n_k is the number of k -simplices. Setting $k = 0$, one recovers the standard graph Laplacian of Eq. (12). In terms of boundary operators, it is easy to see also how the combinatorial Laplacian is related to the Hasse Diagram (see Section 2) of the simplicial complex. The first term on the sum of Eq. (15) corresponds to moving from k -simplices down to $(k-1)$ -simplices and then back up to k -simplices, while the second term does the opposite, first up to $(k+1)$ -simplices and then back down to k -simplices.

The Laplacian is a crucial operator in the definition of diffusion processes on simplicial complexes [86,149] which will be discussed thoroughly in Section 5. In particular, following from the Combinatorial Hodge theorem [84], the combinatorial Laplacian decomposes the k -chain space C_k into three subspaces: $C_k = \text{im}(B_d) \oplus \ker(L_k) \oplus \text{im}(B_{d+1}^T)$. These three subspaces represent the globally acyclic, the cyclic and locally acyclic components of the flow defined on the combinatorial structure [149], which can be used to decompose and study the evolution of dynamical processes on simplicial complexes [70]. Another interesting consequence comes from the fact that the kernel of the Laplacian $\ker(L_k) = \ker(B_d^T) \cap \ker(B_{d+1})$ is isomorphic to the k -homology group H_k . This in turn implies that the number of (homological) k -holes is the same as the dimension of the kernel of L_k , establishing a direct link between the homological and spectral representations of a complex's topology. We leave to the interested reader to check that L_1 in Fig. 6E has indeed a one-dimensional kernel corresponding to the one-dimensional hole in the simplicial complex in Fig. 6A. Finally, we list a few additional spectral properties of L_k , which can be easily checked considering subcomplexes of the toy complex in Fig. 6A:

- If the simplicial complex consists of disconnected simplicial complexes, then the spectrum of L_k is equal to the union of spectra of each component's k th Laplacian.
- If the simplicial complex is formed by gluing two simplicial complexes along a k -face, then the L_k spectrum is the union of the two spectra.
- If the simplicial complex only consists of one simplex of dimension q , then the Laplacian spectrum only has one eigenvalue, $\mu = q$ with multiplicity $q!/[(q-1-k)!(k+1)!]$ [149].

4. Models

Models of HORs aim to reproduce, explain, and predict the structure of systems best described with interactions that involve two or more elements of the systems. To allow for variability in their outputs, these models are often specified as collections of random rules, i.e., as stochastic processes. Hence, they define implicit or explicit distributions over sets of HORs.

To better delineate the similarities and differences between models, we have organized them in two broad categories based on the type of stochastic process used. In the first subsection (Section 4.1), we review *equilibrium models* defined

as static distributions over HOrSs. In the second subsection (Section 4.2), we review *out-of-equilibrium models*, given as sequences of distributions over HOrSs. Although the separation is not formally perfect [160], for instance when sequences converge to equilibrium distributions, these models tend to be quite different in practice, which makes this classification a natural one. Our choice is motivated also by the fact that the philosophy underlying these models are somewhat at odd [161]. On the one hand, *equilibrium models* are usually simple and straightforward to analyze; they typically make use of independence assumptions, which lead to distributions over HOrSs that can be written down analytically. They are therefore well suited to making statistical inference and to acting as substrate for dynamical processes taking place on HOrSs. On the other hand, *out-of-equilibrium models* typically lead to complicated outcomes despite their simple specifications; this makes them ideal for explaining how the qualitative properties of real systems can emerge from simple rules.

Under these two principal headings, we have also organized models by the representation in which they are expressed (see Section 2 for an overview). We have found this separation useful because different threads of the literature have historically favored a single representation, such that models given in the same representation tend to both rest on similar assumptions, and have similar modeling objectives. At the same time, we recognize that from a strictly mathematical point of view, the choice of representation is again superficial due to the formal correspondence between HOrS representations [121]. Hence, we highlight formal equivalences whenever they exist.

On a final introductory note, we have limited the scope of this review by focusing on models where higher-order interactions appear as “first-class citizen”. As a result, we have excluded network models that happen to generate higher-order interactions as a byproduct, such as models of non-trivial clustering [162,163] or cliques [164] in networks.

4.1. Equilibrium models

4.1.1. Bipartite models

We begin our review of equilibrium models with the bipartite configuration model (bipartite CM). It is perhaps the best-known example of an equilibrium model described in the bipartite network representation. The bipartite CM generates HOrSs where both the size of the interactions and the number of interactions per element can be controlled, allowing one to investigate the impact of these quantities on the higher-order structure.

There are a number of variations on the theme of the bipartite CM [165]. In general, it is defined as some form of maximally random distribution over all bipartite networks that have a fixed degree sequence or distribution (either on average or exactly). For example, in one the version of the model, the degrees are fixed exactly: one provides two sequences of degrees $\mathbf{k}^{(A)} = (k_1^{(A)}, \dots, k_m^{(A)})$ and $\mathbf{k}^{(B)} = (k_1^{(B)}, \dots, k_n^{(B)})$, one for the m nodes in set A and one for the n nodes in set B . The probability of a bipartite graph G , according to this model, is then

$$P(G) = \frac{1}{|\Omega(\mathbf{k}^{(A)}, \mathbf{k}^{(B)})|} \quad (17)$$

for all bipartite networks G in the set $\Omega(\mathbf{k}^{(A)}, \mathbf{k}^{(B)})$ of bipartite networks with these degree sequences, and it is 0 for networks outside of this set. This version is sometimes called the microcanonical bipartite CM, or bipartite CM with hard constraints [161]. The canonical (or soft constraint) version of the model only fixes the *expected* degree of nodes [33]; see Fosdick et al. [165] for a rigorous discussion of the various versions of the model.

Early references to the bipartite configuration model first appeared in ecology [166,167]. Mathematically equivalent objects—contingency table with fixed row and column sums—were also studied in statistics around the same time [168,169]. Network science and physics innovations in this area have included thus far: the use of probability generating function to calculate properties of the model [33]; the introduction of statistical mechanics tools (grand-canonical ensembles) to analyze the model [170,171]; hidden variable formalisms [172]; and the addition of fixed degree-degree correlations to the model [173]. Direct generalizations of the bipartite configuration model have also been proposed, focusing on networks that have more than two “parts”. Although it is typically not their explicit goal, these generalizations allow one to model $k - 1$ simultaneous *types* of higher-order interactions, where k is the number of parts [174,175] (see also Boccaletti et al. [23] for a review). They collapse back to the bipartite case when $k = 2$.

The bipartite configuration model offers a paradigmatic example of how models of HOrSs are used to test hypotheses, via a technique known as “null modeling”. The general idea behind null modeling is to generate maximally random HOrSs with a few fixed properties matching that of an observed empirical system. If one observes that some other unrelated properties are systematically reproduced in the randomized ensemble, then these properties are, in a way, “explained” by the fixed properties. Hence, null modeling can help identify connections between the property of HOrSs in empirical studies.

In the context of the bipartite CM, the fixed property is the degree sequence of the two node sets. By applying this technique to bipartite networks of species co-occurrences, for example, it has been shown that the “number of sites per species” and the “number of species per sites” determine the structure, so much so that one cannot conclude on whether natural assembly rules drive the network formation [166,167]. Similar conclusions have been reached with the same method for bipartite networks of plant and pollinators species [171]. A variation on the bipartite configuration model has also been shown to reproduce most of the properties of a network of questions and tags built from the *stackoverflow* knowledge database, again showing that degrees can “explain” many network properties [176]. We note, however, that

slightly changing the model can alter the conclusions of network significance analyses a great deal [104,165]—one should carefully consider the modeling assumptions.

The bipartite CM is a special case of a much more general set of random models, known as exponential random graphs model (ERGM), or logit models [177]. These models aim to generate networks in which one controls the relative frequency of arbitrary small subgraphs (motifs). As we have seen in Section 2, these motifs can be used to encode higher-order interactions explicitly—and indeed we discuss versions of the ERGM that use motifs for this explicit purpose in Section 4.1.2. For now, however, we only focus on those versions of the ERGM that add motifs *within* the framework of bipartite networks. In other words, we focus on ERGMs that encode higher-order interactions with two node sets, but that also use bipartite motifs to generate a richer distribution over HORs.

Formally, one defines a bipartite ERGM by choosing $Q_\mu(G)$, the number of times that motif $\mu = 1, \dots, K$ occurs in G . In the context of bipartite graphs, Q_1 could refer to the number of isolated pairs of nodes, Q_2 to the number of paths of length four, and so on. The choice of motif set is, to a large extent, arbitrary, although it is usually influenced by sampling and identifiability considerations [178]. An ERGM then assigns the probability

$$P(G|\mathbf{Q}, \boldsymbol{\lambda}) = \frac{1}{Z(\boldsymbol{\lambda})} e^{\sum_{\mu} \lambda_{\mu} Q_{\mu}(G)} \quad Z(\boldsymbol{\lambda}) = \sum_G e^{\sum_{\mu} \lambda_{\mu} Q_{\mu}(G)} \quad (18)$$

to the bipartite network G , where $\boldsymbol{\lambda} = (\lambda_1, \dots, \lambda_K)$ is a set of parameters that controls the expected number of motifs of each type in G .

It is in the *unipartite* network context that exponential random graphs first appeared [179,180] (see our discussion below in Section 4.1.2). That said, there have since been quite a few explicit treatments of the bipartite case, coming mainly from social network literature where bipartite networks are known as “two-mode data” [181]. A few early models made use of small collections of local motifs, including a model that fixes the number of connected pairs (with one node of each type at the ends) and the number of “two-stars” (number of times the pattern $v_1-w_1-v_2$ is found, where v_i is a node in part A and w_j is a node in part B) [182,183]. More complicated models controlling the distribution of short paths [184] or that add annotations [185] soon followed.

It was eventually realized that sampling from ERGMs (both in the bipartite and the unipartite network context) could be extremely challenging due to a *degeneracy problem* [186,187], where the model places a high weight on empty and fully connected networks only. This realization prompted the development of subtle physics-inspired sampling methods for some ERGMs specifications [188], and of entirely new specifications for the unipartite model [178]. Analogs to the new specifications were also proposed [189,190] for the bipartite model, leading to improved inference.

Notwithstanding these problems, ERGMs have found many inferential applications. One popular use-case is generating typical network instances that match a set of motif counts \mathbf{Q} obtained via empirical surveys [191,192]. Bipartite networks generated in this way have been used to quantify the significance of specific patterns of interactions found in political networks in the US [193], and in Russia during Brezhnev’s era [194]. Another popular use-case of ERGMs is to “invert the direction” of inference and consider $P(G|\mathbf{Q}, \boldsymbol{\lambda})$ as a *likelihood* that can be used to deduce $\boldsymbol{\lambda}$ from a fully observed network G with counts \mathbf{Q} [189]. These parameters can then inform us about the presence and strength of structural effects in the network data [191]. It should be noted, however, that the inference is not necessarily robust since the problems facing ERGMs, like degeneracy, can also affect inference [195]. Additionally, it has been recently argued that if we consider—as we probably ought to—that network data we have are usually sub-samples of a larger underlying network, then ERGMs can lead to misleading inferences [196,197].

The two sets of models above—bipartite CMs and ERGMs—reproduce *local* features like the number of neighbors of a node or the number of short loops. A different set of equilibrium models instead focuses on reproducing their *mesoscale* features [198]. These models control the frequency and organization of large patterns of connections involving many of, but not all of, the nodes in a network [199]. Examples include disjoint communities of nodes, disassortatively mixing groups [200], and separations in a core and a periphery [201].

These models are most often formulated as extensions of the well-known stochastic block model (SBM) [202] to the bipartite case [203,204]. The general idea is to split the node into two sets of K_A and K_B “blocks”—one set for each part of the network—and to then connect the nodes randomly, with probabilities ω that depend on their respective blocks.

One simple instantiation of this idea goes as follows [205]. We denote by $\mathbf{g}^{(A)} = (g_1^{(A)}, \dots, g_m^{(A)})$ and $\mathbf{g}^{(B)} = (g_1^{(B)}, \dots, g_n^{(B)})$ the blocks of the nodes in each part (where $g_i^{(A)} = \ell$ means that node i of part A belongs to block $\ell \in \{1, \dots, K_A\}$). We then write the probability of a particular graph G with incidence matrix $\mathbf{B} = [b_{ij}]$ as

$$P(G|\boldsymbol{\omega}, \mathbf{g}^{(A)}, \mathbf{g}^{(B)}) = \prod_{i \in A} \prod_{j \in B} (1 - \omega_{g_i^{(A)} g_j^{(B)}})^{1-b_{ij}} (\omega_{g_i^{(A)} g_j^{(B)}})^{b_{ij}}, \quad (19)$$

meaning that an edge is placed between i and j with probability $\omega_{g_i^{(A)} g_j^{(B)}}$. By varying the connection probability matrix $\boldsymbol{\omega}$ and the blocks, one can generate networks with arbitrary mesoscopic structure, ultimately approximating all systems to arbitrary accuracy [206].

Eq. (19) refers to a canonical or soft constraint bipartite SBM since the number of neighbors of a node is fixed only on average by $\boldsymbol{\omega}$ and the blocks. Like the bipartite CM, the bipartite SBM, too, comes in many variants. One can define a microcanonical version along the same lines [207], for example. Another variant considers that edges have

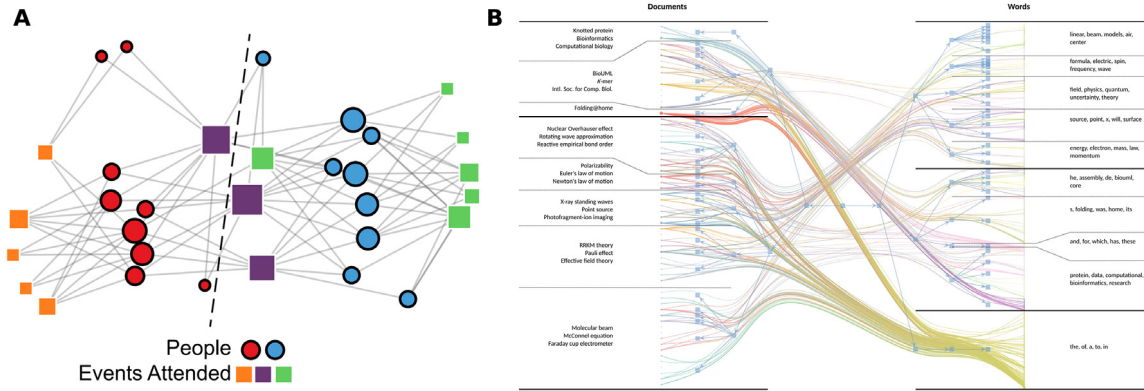


Fig. 7. Inference with the bipartite stochastic block model. (A) The data represents people (as circle) interacting through events (as squares). A variation on Eq. (19) assigns a likelihood to every joint partitions of the people and events. A high likelihood partition is shown here using colors. Simpler methods incorrectly split the network along the black line. (B) An elaborate hierarchical version of the bipartite SBM, applied to collections of words interacting via texts. This time the blocks (indicated by vertical dotted lines) are themselves regrouped in high-level blocks, hierarchically. Source: Figures reproduced from Refs. [205] and [211]

distinguishable types, e.g., in a user–movie bipartite network where edges represent ratings on a fixed scale [208]. Yet another variant jointly models the degree sequence *and* the mesoscopic structure, leading to a so-called degree-corrected bipartite SBM [209] that, unlike the classical degree-corrected SBM, makes explicit the assumptions that there are two node types [204,205,210] (Fig. 7A). Finally, it is also possible to introduce a hierarchy, with blocks that are themselves grouped into larger blocks, and so on [211] (Fig. 7B).

The many versions of the bipartite SBM are used for what is another prototypical example of a HORs inference problem: latent parameter inference. Indeed, different from the configuration models, the structure of a system does not trivially determine the SBM's parameters. In a configuration model, one calculates the degree of all the nodes of a given bipartite network to determine what is the associated randomized ensemble of networks. In contrast, the SBM assigns nodes to blocks via $(\mathbf{g}^{(A)}, \mathbf{g}^{(B)})$, a piece of information that is typically not given—unless metadata is also available [210]. This situation leads to a family of inference problems where the goal is to determine an assignment of nodes to the blocks, from a network's structure alone (see Fig. 7A). This goal has been the main driving force behind the development of sophisticated model families [205,207,210], with formal equivalence to inference problems in other fields, like topic modeling [209,211,212] or data biclustering [213].

The bipartite SBM assigns nodes to latent *discrete* categories (blocks), and adds connections to the network at random based on these categories. A somewhat related class of models instead assign continuous latent *positions* to nodes and creates connections with probabilities parametrized by the distance between nodes in the latent space. Much like the case of the bipartite CM and SBM, these models take the form of natural generalizations of simple network models to the bipartite case.

The AB random geometric graph model [214], for instance, is a direct extension of the well-known random geometric graph model [215]. In this model, two sets of nodes are first randomly embedded in a low-dimension Euclidean space. Nodes in *different sets* are then connected by edges, with a probability that depends on the distance d_{ij} separating them. The AB random geometric graph model makes use of the simplest possible connection rule: two nodes are connected if and only if $d_{ij} < r$. But we note that some unipartite models consider more complicated functional form for the connection probabilities [216] (see also the model that follows).

Another approach to latent space models builds on results coming from the network geometry literature [217]. In these models, one embed nodes in an *abstract* space of preferences (rather than a *literal* space, like what is done in the AB model). It is then possible to define general classes of models by specifying different connection rules and embedding spaces [218]. The so-called $\mathbb{S}^1 \times \mathbb{S}^1$ specification is perhaps the one that has been analyzed the most thus far [218,219]. In this version of the model, two sets of nodes are embedded uniformly at random on a circle (i.e., on the 1-sphere denoted \mathbb{S}^1). The nodes are then assigned hidden variables drawn at random from some distribution [172]—denoted ϕ_i if node i is in set A and ψ_i if it is in set B. Pairs of nodes (i, j) in different sets are finally connected with a probability that depends on their distance d_{ij} in \mathbb{S}^1 , as well as the value of their hidden variables ϕ_i and ψ_j . The specific functional form analyzed in [218,219] is

$$p_{ij} = \sigma \left(\frac{d_{ij}}{\mu \phi_i \psi_j} \right) \quad (20)$$

where $\mu > 0$ and σ is any integrable function with image in $[0, 1]$. The likelihood of the whole network is therefore $P(\mathbf{G}|\mathbf{d}, \mu, \phi, \psi) = \prod_{ij} p_{ij}^{b_{ij}} (1 - p_{ij})^{1-b_{ij}}$ where b_{ij} is an entry of the incidence matrix. The role of the hidden variable is to allow for variations in the degrees [172], while the embedding helps control the level of clustering [220].

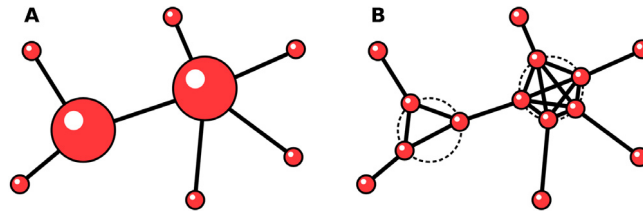


Fig. 8. Example of HORs generated by the model of Gleeson and Melnik [224]. In this model a fraction g_k of nodes of degree k of a configuration model network [33] is replaced by cliques.
Source: Figure reproduced from Ref. [224].

The main use-case for latent space models is, again, inference. With a latent space model, one can take a real bipartite network as input, and find the embedding in a latent space that best matches the network, using the likelihood $P(G|\mathbf{d}, \mu, \phi, \psi)$ to guide the search. This inference technique has been used to, for instance, infer the latent geometry of bipartite networks of metabolites and of the reactions they intervene in [219].

4.1.2. Motifs models

Motifs-based models are formulated as assembly rules for arbitrary collections of small graphs, like triangles, short-loops, or cliques. They can be viewed as higher-order models because they build systems from relationships that are not strictly pairwise, even though these models are ultimately defined as distributions over classical networks. Motifs-based models have a rich history going back to the early days of network science [221], preceded by work in sociology [222,223] and statistics [179].

The first motifs-based models of networks appeared in sociometry, motivated by the need for survey methods that would categorize and quantify patterns of interaction among small subsets of individuals of a larger directed social network [222,223]. As we have mentioned above in Section 4.1.1, Markov random graphs [179,180] and their exponential random graph model (ERGM) generalization [177] have been proposed early on to fulfill this role. In a nutshell, these models describe maximally random distributions over networks G whose properties $\mathbf{Q}(G) = (Q_1(G), \dots, Q_K(G))$ are fixed on average, in relative proportion controlled by the free parameters $\lambda = (\lambda_1, \dots, \lambda_K)$. These models are therefore quite general in what they can describe (see our discussion above and Eq. (18)).

To model higher-order interactions in the ERGM framework, one can select properties \mathbf{Q} that measure these interactions directly. An example of a set of statistics could be: the number of edges Q_1 ; the number of triangles Q_2 (a closed three-way interaction); and the number of open triangle Q_3 (an open three-way interaction).

The main inferential applications of the generic ERGM are the same as that of the bipartite ERGM: null modeling, and the construction of whole network description from local surveys [191]. There is also at least one further application of ERGMs specific to unipartite networks: quantifying the significance of motifs. The idea here is to fix the distribution of all small motifs, and compare the number of *larger* motifs to the expected motifs counts in the ensemble [71,75]. This method identifies motifs that are either under- or over-represented in a graph, based on what we expect from smaller connection patterns. This method has been used to argue that some small motifs are “significant subunits” that determine the function of the modeled system [71].

Another type of model of networks with motifs comes from the physics literature on spreading processes occurring on clustered networks. These models tend to be very flexible and to reproduce quite a few structural characteristics of real systems. They have been first and foremost used to study how structural changes affect the outcome of dynamical processes unfolding on these networks.

One of the earliest model in this category [224] begins with a unipartite configuration model network, i.e., a random network that follows some arbitrary degree distribution. After the initial network is constructed, one replaces a fraction g_k of the nodes of degree k with k -cliques for all $k \geq 3$ —selecting these nodes uniformly at random. The nodes of the new cliques are then attached to one of the edges of the node they replace, which in turn leads to a network with the same high-level structure as the original, but with added local clustering (Fig. 8). An earlier variant of this model also exists where one controls g_k indirectly [225].

Another set of model also uses the configuration model to generate HORs, but perhaps more directly. In the first model in this line of work, one not only specifies the degrees $\mathbf{k} = (k_1, \dots, k_n)$ that a node should have, but also the number of triangles in which it should participate $\Delta = (\Delta_1, \dots, \Delta_n)$ [226,227]. A generalization of the classical stub-matching scheme [165] is then used to create random networks respecting these sequences. Recall that in the classical stub-matching scheme, we first assign k_1, k_2, \dots, k_N “stubs”—half-edges—to nodes $1, 2, \dots, N$. We then pick a random matching of the stubs, in which all stubs are joined in pair to form full edges. The resulting random network respects the degree sequence $\mathbf{k} = (k_1, \dots, k_N)$ by construction. In the higher-order stub matching scheme, we should think of a node i as having k_i “edge stubs” and Δ_i “triangle stubs” attached to it. A network is then obtained by matching the stubs of the all nodes: 2 partial edges form an edge, and 3 partial triangles form a triangle. One variation on these models generalizes from triangles to generic cliques of size $c > 3$ [228], but enforces the constraint that nodes belong to only

one clique [224], i.e., that they have a single triangle or more generally a single clique of size $c \geq 3$ attached to them. The central quantity in that model is then $\gamma(k, c)$, the probability that a node has degree k and belongs to a clique of c nodes, with $k \geq c - 1$.

Encompassing both the triangle and the single clique model is a generalization of the configuration model that allows for generic distribution of motifs in the neighborhood of a node [229]. The model parameters are the number of times a motif is attached to a node, and in which way. This can be represented, again, by “stubs” stemming from each node, where a stub of type (μ, p) is attached to node i when it participates in motif μ in position p . The final graph is constructed by matching stubs of a same type to construct motifs. Specifically, say motif μ is comprised of n_1 nodes in role p_1 , n_2 nodes in roles p_2 , etc. Then one must pick $n_1 + n_2 + \dots$ stubs of the correct types at random and create a motif connecting the nodes from which the stubs stem. An even more general version of the above model assigns *types* (or colors) to nodes [230,231]. The expected number of stubs of each type for a node then depends on this type. Sampling algorithms for this general model are given by Ritchie et al. [232].

Inference with these general models is challenging, because it is not clear how one should select a meaningful set of motifs to describe a given graph [229]. So far, the only proposed approach aiming to make this type of inference relies on an information theoretic approach to “subgraph covers” [233].

There are a few other specifications of network models with motifs that do not fit squarely in any of the above categories.

One generalizes the notion of “graphon”, a form of latent space model in which nodes are assigned random positions \mathbf{x} on $[0, 1]$ and pairs of nodes are connected with probability parametrized by these positions. The motif generalization [234] also assigns latent positions $\{x_i\}_{i=1}^N$ to the nodes, drawn independently and identically according to some distribution on $[0, 1]$. Then, a motif μ on r nodes v_1, \dots, v_r in the collection of motifs μ is added to the network with probability

$$P(\mu|v_1, \dots, v_r) = \frac{\kappa_\mu(v_1, \dots, v_r)}{n^{r-1}} \quad (21)$$

where κ_μ is a function of the latent positions. Although these generalized graphons do not appear to have been used for inferential purposes, a few special cases of them (obtained by setting $r = 2$ and only allowing edges) found extensive use. For example, one can approximate κ_μ to identify the latent geometry likely to have generated a network [235].

A completely different motif mode known as the *dk-series* approach fixes local motifs and maximizes randomness otherwise [79,80]. Formally, for a given k , one fixes the distribution of the number of all the motifs of $k' \leq k$ nodes centered on a node. Hence with $k = 1$, for example, one fixes the degree distribution, while with $k = 2$ one fixes the joint degree distribution of pairs of nodes. The *dk-series* model crosses into higher-order specifications when $k > 2$; for example when $k = 3$, one fixes the distribution of wedges and triangles. This model finds use in quantifying the randomness of a network’s structure [80]. It fixes a null distribution where many local aspects are preserved, and helps to see whether these local constraints are enough to “explain” the observed large scale structure of a network. Actually carrying out the test for any $k \geq 3$ is difficult, however [80], since constructing a single example of graphs realizing a series with $k \geq 3$ is NP-complete [236]. We note that there is related work in the social network literature, in the form of models where one specifies the local structure—the “social neighborhood” of nodes [237]—up to a certain distance [190].

4.1.3. Stochastic set models

Collections of motifs become rapidly intractable with growing motif sizes since there are $2^{\binom{r}{2}}$ possible undirected graphs on r nodes. Many models avoid this exponential blowup by specifying the motifs *stochastically*, i.e., by assigning nodes to sets of r nodes and then specifying the actual motif connecting them at random.

A well-known family of models specified in terms of sets takes inspiration of hierarchies in social organizations, in which nodes are assigned to nested groups [221,238]. The groups are therefore proxy for higher-order interactions. The simplest example of a model in this class only allows for one set of groups [221]. In this model, a node i has a membership number $k_i^{(n)}$ (number of groups it belongs to), and a group j has a size $k_j^{(g)}$ (the number of nodes it has). The rest of the structure is randomized. Hence, in other words the node–group relationships are described by a bipartite CM [33]. Differently from the latter, however, one considers a *projection* onto the nodes (see Section 2), in which edges are placed at random based on the group assignments. Specifically, one determines whether two nodes are acquainted through a group and connects them in the projection if they are acquainted through at least one group (see Fig. 9).

Among the many possible generalizations of this model, some authors have: considered a deeper hierarchy of groups [238]; included heterogeneities by introducing a group dependent connection probability q_r [239]; introduced the possibility of forming a few ‘random’ links with nodes not in the immediate group of a node [240]; or used a mixture of groups [241].

An alternative point of view on these models comes from the mathematics literature, where they are known as *random intersection graphs* [243]. A random intersection graph is formed by assigning a set on some alphabet—say $Y = 1, \dots, m$ —to each node, and connecting two nodes if their respective sets intersect [242]. They are formally equivalent to the bipartite projection model above, since we can think of the set of a node as the higher-order interactions in which it participates, and of edges as arising because of these interactions (Fig. 9).

Many models of random intersections graph exist, but are somewhat less general than the projected bipartite CM discussed above. This is because mathematically exact results are typically the goal of the authors studying these models,

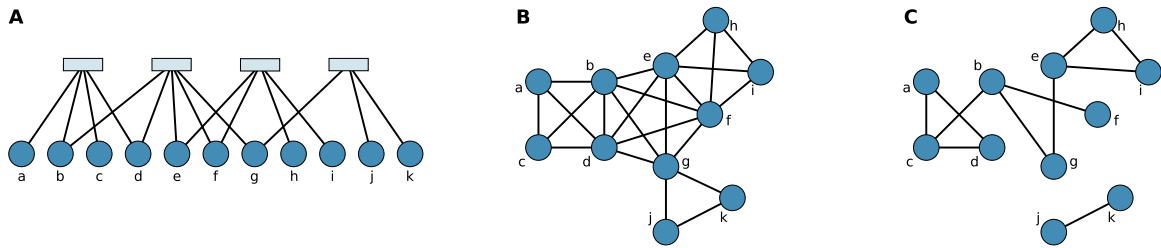


Fig. 9. Constructing random HORs by projecting a bipartite network of interactions [200]. (A) Realization of the bipartite configuration model, (B) projected as a network, where (C) some edges are removed. The construction shown in panels (A) and (B) is also known as a random intersection graph [242].

Source: Figures adapted from Ref. [200].

rather than coming up with models of “realistic” HORs. An example of one such model is dubbed $G(n, m, p)$. It defines a distribution over intersection graphs that have m sets and n nodes, and where every node is included independently in each set with probability p [242], yielding the likelihood

$$P(\mathbf{B}|m, n, p) = \prod_{i=1}^n \prod_{j=1}^m (1-p)^{B_{ij}} p^{B_{ij}}, \quad (22)$$

for the assignments \mathbf{B} of nodes to sets, where $B_{ij} = 1$ if node i is in clique j and 0 otherwise. This model is a special case of the projected bipartite model discussed above, obtained by setting the degrees of nodes to mp , the size of groups to np , and by connecting all nodes in a shared group with probability $q = 1$. The properties of these random intersection graphs have since been studied extensively, see the detailed review of Frieze and Karoński [244]. Inhomogeneous generalizations allow for some variations, such as inclusion probabilities $\mathbf{p} = (p_1, \dots, p_n)$ that are node-dependent and fixed as parameters [245,246], or where the size of the sets are drawn from a distribution and the node in it chosen at random [247].

While the sets themselves are random in all of the interaction graph models above, the *interior* of sets themselves are not random—all nodes are connected and form a clique. Other models of intersection graphs include the possibility of noise in this process [248], and are therefore formally equivalent to the noisy version of the node–group models discussed above [239]. For instance, one model assigns nodes to one or more cliques of varying sizes, and two nodes are only connected in the projection with a probability that depends on the number of shared cliques [249]. A more exotic construction assigns nodes to the cliques with probabilities p_i that are the outcome of a stochastic beta process [250].

As we have mentioned, in the mathematical literature, random intersection graphs are studied for their structural properties [242]. But they also find inferential application in the epidemiological literature as models of systems with higher-order interactions [251]. In the statistical literature, they have found application in fitting clique-cover models to real networks [250], in the same spirit as the cover models used to fit models of networks with motifs [233].

We note in passing that some models of overlapping communities lead to formalisms close to that of the stochastic set models mentioned here. However, since one seldom thinks of overlapping communities as higher-order interactions—a typical community is far too big to classify as encoding an “interaction”—we will not review them here. The interested reader can refer to the review of Xie et al. [252] for an overview of models of networks with overlapping communities.

4.1.4. Hypergraphs models

Many equilibrium models of HORs incorporate multi-body interactions more directly, by encoding them in hypergraphs. Much of the work on random hypergraphs comes from the mathematical literature, where they were introduced as immediate and natural generalizations of classical models in random graph theory.

Perhaps unsurprisingly, the earliest random model of hypergraphs was an extension of the well-known Gilbert–Erdős–Rényi (ER) model [253–255]. In the most direct generalizations of this model, every hypergraph of m hyperedges of size k on n nodes is given the same probability [256], with the ER case obtained by setting $k = 2$. The structural properties of the random hypergraphs generated in this way have been analyzed extensively, see [244] for a review. A canonical variant, in which hyperedges are created independently at random with fixed probability p , also exists [164].

All hyperedges connect precisely k nodes in the two models above. This is an arbitrary choice and not a constraint of the hypergraph formalism. Other uniform models do away with this constraint, and include many sizes $\mathcal{K} = \{k_1, k_2, \dots, k_\ell\}$ of hyperedges simultaneously (where $\mathcal{K} \subseteq \mathbb{N}$ is some choice of hyperedge sizes, with $\mathcal{K} = \{2\}$ corresponding to a graph).

One version stipulates that all hypergraphs are equiprobable, provided that they have exactly m_{k_1} hyperedges of size k_1 , m_{k_2} hyperedges edges of size k_2 , and so on for all $k \in \mathcal{K}$ (where \mathbf{m} and \mathcal{K} are chosen at deterministically [257] or at random [258]). Like in the classical ER case, hypergraphs that do not respect the constraint on the number of hyperedges are assigned a probability of zero. Yet another uniform model instead prescribes that each of the $\binom{n}{k}$ possible sets of size k on n nodes exists, with a probability λ_k that depends on the size $k \subseteq \mathcal{K}$ of the set [259].

While the specifications of these models differ from cases to cases, the underlying goal is always to study the properties of the generated hypergraphs, like their components structure, for example [257]. Even though these uniform hypergraph model are somewhat crude approximations of real HORs, they have found extensive application in technical fields like computer science, where they are used to generate the structure of idealized random decision problems (random k -sat) [260,261].

Other uniform models differ from the ones above in that they ensure that the generated hypergraphs are “ k -partite”. By k -partite, it is meant that the $n = k \times r$ nodes of the hypergraph can be separated into k disjoint subsets of r nodes, such that every hyperedge comprises of precisely one node in each subset. These k -partite hypergraphs are useful when one wants to encode interactions that *always* involve nodes of different natures, for example, when modeling a collaborative tagging system where all hyperedges connect an element, a person, and a tag [97].

One possible construction for uniform and random k -partite hypergraphs was introduced in the mathematical literature, with the goal of studying “perfect matchings” in hypergraphs, i.e., minimal subsets of hyperedges connecting every node [262,263]. The model first singles out one the subset of nodes as “special”. Then it stipulates that, for each node in this special subset, we should choose $d - 1$ neighbors uniformly at random (one per subset) to form a hyperedge, repeating the process z times per node in the special set [262]. The resulting hypergraphs are k -partite by construction, and all the nodes in the special set have precisely degree z . A more general but still uniform model of random k -partite hypergraphs, coming from the information retrieval literature, eliminates this constraint [264]. Aiming for flexibility, the model assigns a different weight to every possible hyperedge, and actually instantiates a hyperedge with probability proportional to this weight. It is shown that, within this framework, under entropy maximization constraints, one does not need all these weights: all the probabilities are identical under the so-called “uniform random data base model” [264].

Much like their graphical counterparts, the uniform hypergraph models also admit generalizations to cases where one controls the *degree* of nodes, i.e., the number of hyperedges incident on each node (see Section 3.1). This leads to configuration models (CM) for hypergraphs.

A configuration model for k -partite hypergraphs was proposed early in the network science literature, with the purpose of studying realistic *folksonomies* (tagging databases) [97]. A related model allowing for node features soon followed [265].

As for hypergraphs where no k -partite structure is enforced, there are quite a few recent generalizations, developed mostly with the goal of obtaining null models for community detection purposes. Indeed, one of the best-known community detection [57,266] methods relies on a so-called “modularity function” [267] to assign a quality to possible decompositions of a network in communities. In particular, the modularity uses a random null model to determine whether the number edges found within a community is significant enough to warrant isolating it as a separated group. In the case of graphs, the most popular baseline is the configuration model, and many models have since been proposed recently to fulfill the same role in the case of hypergraphs. For example, a recently proposed model directly generalizes the configuration model of Chung and Lu [268] to the hypergraphical case [102]. In this version of the model, the number of times a node participates in any given hyperedge is drawn from a multinomial distribution. This leads to a canonical version where the degrees of nodes are fixed on average. Microcanonical variants are also analyzed by Chodrow [104], and generalized to the case where the same node can take different roles in different edges (like broadcaster and receiver, for example), again by Chodrow et al. in [99].

Similar models have also been recently proposed in the statistics literature, where they are used for estimation purposes [269]. These models are collectively dubbed β -models, and they are treated as generalizations of the p_1 model for graphs [180] (an exponential random graph approach to the configuration model, for directed graphs). They propose several flavors of the model, all making use of node *propensities*, i.e., of a parameter $\beta_i \in \mathbb{R}$ to control how likely it is that node i will be connected to any given hyperedge. In the simplest proposed specification, the probability of a hypergraph H is given by

$$P(H|\beta) = \prod_{i_1, \dots, i_k \in C_n(k)} p_{i_1, \dots, i_k}^{a_{i_1, \dots, i_k}} (1 - p_{i_1, \dots, i_k})^{1 - a_{i_1, \dots, i_k}} \quad p_{i_1, \dots, i_k} = \frac{e^{\beta_{i_1} + \dots + \beta_{i_k}}}{1 + e^{\beta_{i_1} + \dots + \beta_{i_k}}} \quad (23)$$

where $C_n(k)$ is the set of all combinations of n indexes. They also propose a layered and general version where edges of different sizes co-exist. The common thread shared by all the specifications of the β -model is that, the larger the parameters β , the more likely we are to see the hyperedge a_{i_1, \dots, i_k} in the final hypergraph H .

The stochastic block model (SBM) is another network model that has been generalized to hypergraph extensively, motivated by the search for random processes able to produce hypergraphs with non-trivial mesoscopic patterns. The earliest reference to the hypergraphical SBM opts for a natural generalization from the network case [270], by parameterizing the probability of hyperedges of size k with a symmetric tensor \mathbf{Q} of dimension k , whose “rows” correspond to communities. More precisely, in this SBM the probability that an edge exists between nodes i_1, \dots, i_k assigned to communities $\sigma(i_1) \dots \sigma(i_k)$ is given by $q_{\sigma(i_1) \dots \sigma(i_k)} \in [0, 1]$. The likelihood of a hypergraph H with adjacency tensor \mathbf{A} is then straightforwardly:

$$P(H|\sigma) = \prod_{i_1, \dots, i_k \in C_n(k)} q_{\sigma(i_1) \dots \sigma(i_k)}^{a_{i_1, \dots, i_k}} (1 - q_{\sigma(i_1) \dots \sigma(i_k)})^{1 - a_{i_1, \dots, i_k}}, \quad (24)$$

where $\sigma(i)$ is the index of the block to which node i is assigned. Ke et al. [271] add degree-correction and modify the probability of the hyperedge i_1, \dots, i_k to $q_{\sigma(i_1) \dots \sigma(i_k)} \prod_{j=1}^m \beta_{i_j}$ where $\beta_i > 0$ is a propensity for node i . Ahn et al. [272] consider

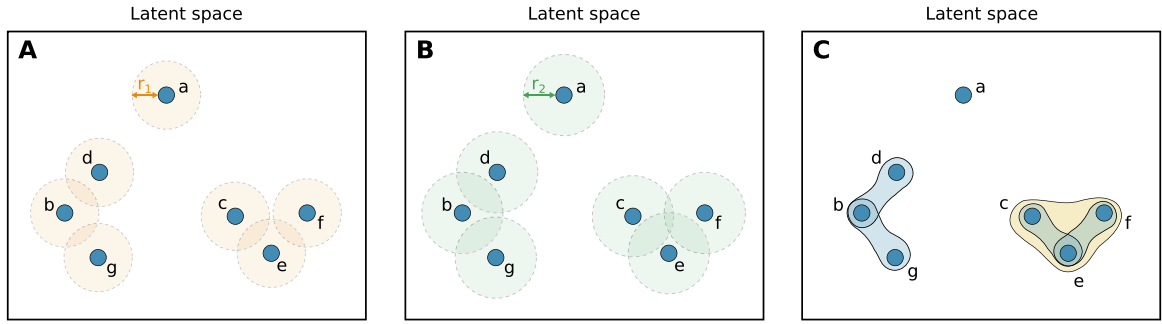


Fig. 10. Latent space hypergraphical model [274]. (A,B) Nodes embedded in \mathbb{R}^2 , with radii of length r_1 and $r_2 > r_1$ drawn around them. (C) Hypergraph obtained by connecting sets of nodes mutually at a distance of $d_{ij} < 2r_1$ and $d_{ij} < 2r_2$. Notice the multiple radii allow the model to create the hyperedge $\{c, e, f\}$, $\{c, e\}$ and $\{e, f\}$. A model with only one radius would not be able to omit $\{c, f\}$.
Source: Figures adapted from Ref. [274].

weighted edges parametrized by the communities σ . Finally, Paul et al. [273] combine the notion of communities with hyperedges of different sizes, albeit in a limited sense: the model conditions the presence of hyperedges of size 2 (edges) and 3 (triangles) on latent communities σ , but does not include interactions at any higher orders. In all cases, the models are introduced as a benchmark, to test whether partitioning methods—say spectral methods—can reliably recover the partition σ from hypergraph generated by the model.

A recent approach to hypergraph modeling uses an abstract embedding space to create realistic HOrSs [274], paralleling similar development in the network context (see Section 4.1.1 above). The idea is again that if *groups* of nodes are close-by in the latent space, then they should tend to be connected. The specific construction considered by Turnbull et al. [274] embeds nodes randomly in \mathbb{R}^d , and adds hyperedges by connecting all set of nodes at a distance $d_{ij} < r_\ell$ from one another, for a few random choices of distances r_ℓ (see Fig. 10). This construction allows the model to create hyperedges included within others, such as the hyperedges $\{c, e\}$ and $\{c, e, f\}$ in Fig. 10. A last step is added whereby hyperedges are flipped (non-hyperedges become hyperedges and vice versa) with a small probability ϵ . This step ensures that the model assigns a non-zero probability to all hypergraphs.

The last model of hypergraphs that we review generalizes the Kronecker model [275], again first introduced in the context of networks. In the classical Kronecker graph model, one starts with a small matrix $\mathbf{P}^{(0)}$, and repeatedly takes the Kronecker product of the matrix with itself to generate increasingly large matrices $\mathbf{P}^{(1)}, \mathbf{P}^{(2)}, \dots, \mathbf{P}^{(f)}$. For example, supposing that $\mathbf{P}^{(0)}$ is a 2×2 matrix we have:

$$\mathbf{P}^{(1)} = \mathbf{P}^{(0)} \otimes \mathbf{P}^{(0)} = \begin{bmatrix} p_{11}\mathbf{P}^{(0)} & p_{12}\mathbf{P}^{(0)} \\ p_{21}\mathbf{P}^{(0)} & p_{22}\mathbf{P}^{(0)} \end{bmatrix} = \begin{bmatrix} p_{11}p_{11} & p_{11}p_{12} & p_{12}p_{11} & p_{12}p_{12} \\ p_{11}p_{21} & p_{11}p_{22} & p_{12}p_{21} & p_{12}p_{22} \\ p_{21}p_{11} & p_{21}p_{12} & p_{22}p_{11} & p_{22}p_{12} \\ p_{21}p_{21} & p_{21}p_{22} & p_{22}p_{21} & p_{22}p_{22} \end{bmatrix} \quad (25)$$

Then, once the matrix attains dimension $n \times n$, it is used to generate a graph on n nodes in which edge (i, j) exists with probability $p_{ij}^{(f)}$. The hypergraph generalization, called HyperKron [276], works essentially in the same way: one starts with a small k dimensional tensor $\mathbf{P}^{(0)}$ and obtains a large final tensor of dimension k and of $n \times n \times \dots \times n$ components. One can then use the tensor to generate a random hypergraph, with hyperedges of size k . The model has found application in generating large realistic graphs and hypergraphs.

4.1.5. Simplicial complexes models

We complete our overview of equilibrium models with approaches formulated in the simplicial complex representation. The theoretical study of models of simplicial complexes is still in its infancy [277]. Save for some early work in the social sciences [34], the abstract simplicial complex representation has seen little applications until recent years. As a result, the literature is so far limited, and mostly comes from mathematics and physics.

Before we review these models, a word of warning is in order: many authors blur the line between models of simplicial complexes and of hypergraphs. Recall that in an abstract simplicial complex, when a *facet* encodes an interaction between k nodes, then implied is the existence of the k *faces* of $k-1$ nodes, $k(k-1)$ faces of $k-2$ nodes, and so on. This inclusion property means that all models of simplicial complexes are specified in terms of their distribution over *facets* (the top-level interactions). Many authors define facets as higher-order interactions, with no attention to the inclusion property. This omission has no consequence when all interactions have the same size, but can lead to different results when they do not [121]. In the interest of avoiding confusion, we have modified the nomenclature favored by the authors where necessary.

The study of random simplicial complexes first started, perhaps unsurprisingly, with generalizations of the Erdős–Rényi (ER) model. The earliest model of random simplicial complexes, known as the Linial–Meshulam model, is arguably the

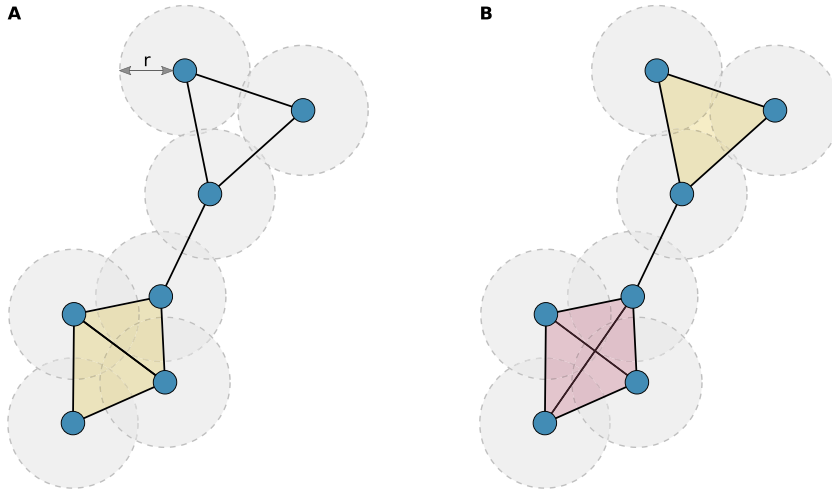


Fig. 11. Simplicial complexes from point clouds. Two popular constructions are the (A) Čech and (B) Vietoris-Rips complexes. These two constructions generate simplicial complexes based on the distance between nodes in an embedding space. See text for details. Source: Figures adapted from Ref. [286].

simplest higher-order version of the ER model one can define. In this model, one begins with a connected graph on n nodes, to which some number m of triangles are added to form facets of 3 nodes [278]. The resulting object is a prototypical example of the approach favored by mathematical literature in this topic, whose focus is to find simple random objects with non-trivial *homology* (see Section 3.4). There has since been many generalization and analysis of this model, see the survey of Kahle [279] for a summary of recent results. Of particular interest is the natural generalization in which one begins with a complete simplicial complex of dimension k on n nodes and adds $k + 1$ facets at random [280] (with the Linial–Meshulam model recovered by setting $k = 1$).

A different form of ER-like models of simplicial complexes relies on the idea of *flag complexes* (also known as clique complexes). A flag complex is obtained by replacing all the maximal cliques of a graph by facets. Another equivalent definition is that a flag complex is completely defined by its 1-skeleton (the underlying graph). In the model analyzed by Kahle [281], one first creates a classical ER network G , and then uses it to generate the associated flag complex. The construction is related to much earlier work in graph theory [164], where the distribution of cliques in networks drawn from the ER model was analyzed. However, in the case of Kahle [281], the focus is instead on the homology and homotopy of the resulting simplicial complexes.

To organize the rapidly growing family of models of random simplicial complexes, a model known as the “ Δ -ensemble” has been proposed in by Kahle [279]. In this model, one first connects the pair of nodes of a graph with probability p_1 . Then, all the (edge-only) triangles created in this first step are closed by a face (2-simplex), independently, with probability p_2 . All the empty pyramids created as a result of closing triangles are then replaced by a 3-dimensional face with probability p_3 , and so on. One recovers the classical ER model by setting $p_1 = p$ and all other p_d to 0; the model of Linial–Meshulam by setting $p_1 = 1$, $p_2 = p$ and all other p_d to 0; and the model of Kahle with $p_1 = p$, $p_d = 1$ for all $d > 1$. Fowler [282] and Costa and Farber [87] studied the homology of the simplicial complexes generated by this ensemble independently. A closely related model, also introduced by Costa and Farber [87], does not define the process recursively. It instead fixes the average number of faces in all dimensions as well as the number of external faces, i.e., the way in which faces of different dimensions interact. Restricted versions of these models have been used to generate simplicial complexes on which spreading process occurs [283] (see Section 7.1), to predict higher-order interactions in streaming data [31], and to study polymers [284].

The Δ -ensemble is not the only general model able to encompass many models as special cases. Indeed, a different specification, in the spirit of exponential random graph discussed above, has also been introduced recently by Zuev et al. [285]. In this model, one defines a series of functions $Q_\mu(S)$ on simplicial complexes for $\mu = 1, \dots, K$. These functions can be, for example, the number of 2-facets, or much more exotic functions, like the number of homological cycles of some dimension. The *exponential random simplicial complex model* then assigns a probability

$$P(S|\mathbf{Q}, \boldsymbol{\lambda}) = \frac{1}{Z(\boldsymbol{\lambda})} e^{\sum_{\mu} \lambda_{\mu} Q_{\mu}(S)} \quad Z(\boldsymbol{\lambda}) = \sum_S e^{\sum_{\mu} \lambda_{\mu} Q_{\mu}(S)} \quad (26)$$

to simplicial complex S and where $\boldsymbol{\lambda}$ is a vector of parameters controlling the relative importance of the functions \mathbf{Q} in the ensemble. Much like the Δ -ensemble, special choices of parameters and function can be made to reproduce known models like that of Linial–Meshulam, Kahle, or even the Δ -ensemble itself [285].

Another rich line of inquiry focuses on random *geometric* simplicial complexes. These models build on a long lineage of work in topological data analysis [115], whose focus is the recovery of topological information, such as the number of holes in a surface, from noisy objects on geometric objects embedded in space as point clouds.

In these models, one first places nodes in some metric space, e.g. \mathbb{R}^d , by drawing from a random point process. Nodes are then connected based on their distance, generating a simplicial complex. There are two canonical ways in which this last step can be done (see Fig. 11). In random Čech complexes [287], one places a ball of radius r around every node; whenever the intersection of k balls is non-empty, one adds a $(k - 1)$ -face between these nodes. In random Vietoris-Rips complexes [277,287], instead, one connects every node at a distance at most $2r$ from one another, and then replace cliques by facets, effectively taking the flag complex of the underlying geometrical graph. The resulting objects have been studied for their connectivity properties and homological properties, among other things (see the thorough survey of Bobrowski and Kahle [288] for more details). A fundamental result in this context concerns the limiting behavior of random geometric complexes. In particular, three regimes exist that display starkly different properties as a function of the parameter $\Lambda = nr^d$, where n is the average number of points in a ball of radius r in d -dimensional space. The three regimes correspond to different limits for Λ : for vanishing Λ , the simplicial complexes are sparse, highly disconnected and dust-like; for constant Λ (also called thermodynamic regime), the homology of the complexes reaches its peak growth; and for diverging Λ , higher homology displays two phase transitions, one where the homology first appears and a second where it disappears, as cycles are progressively filled in. Finally, Fasy et al. [289] also found statistical application in the calculation of confidence interval on the results of persistent homology calculations.

In the physics literature, the focus thus far has been to develop models similar to the configuration model (CM), with the goal of introducing heterogeneities and realistic properties in the generated random simplicial complexes. By analogy with the case of graphs, these configuration models fix the degree of nodes, defined as the number of *facets* incident on them. All other properties are randomized. Courtney and Bianconi [114] considered a model where every facet is of size k and the degree of nodes is fixed exactly or on average; Kamiński et al. [102] have later proposed a hypergraphical CM that formally equivalent to the previous one. A different specification fixes the degrees *exactly*, and lets the facets have different dimensions while forbidding inclusions [108]. The resulting models have been studied for their structural properties [114] (like the projected degree or the entropy), and have found application as a null model for the homology of real systems [108]. A recent approach to random simplicial complex [290,291] follows the interpretation of the (classical) configuration model as a random branching tree [33]. In this model of random branching simplicial complexes [291], one starts with a single edge and attaches m faces of dimension k to each edge of the faces created in previous iterations. Crucially, k is treated as a random variable such that the dimension of every new face is random, leading to a simplicial analog to the configuration model. This model was introduced to study the percolation properties of the resulting “simplicial tree”.

4.2. Out-of-equilibrium models

All of the models we have seen thus far define distributions over static HORs. In other words, these models viewed HORs not as dynamical, evolving objects, but instead as static systems, drawn from some fixed distribution. We now turn to a different approach, mainly developed in the physics and network science literature, that adopts a dynamical point of view of HORs.

Since there are several similarities between many of these out-of-equilibrium models, even across different choices of representations (see Section 2), it is worth going over some general notions before we delve in. The modeling goal motivating these models is almost always the same: finding minimal rule sets such that the typical HORs produced by the model reproduces the structural characteristics of empirically observed bipartite networks [63]. The rules are often chosen to allow for analytical calculations of properties of interest. But the authors of these model also often try to find rules that can be motivated mechanistically i.e., that could explain *why* a HORs evolves the way it does [292].

An overwhelming majority of the out-of-equilibrium models focuses on *growing* systems, in which nodes and edges are added as time unfolds, but never removed. This is perhaps due to the influence of foundational work in network science, where growing models were put center stage early on [6]. Hence, with very few exceptions, these out-of-equilibrium are *growth models*. Furthermore, with few exceptions like the activity-driven models [293], time is measured in discrete steps $t = 1, 2, \dots, T$, where each step is associated with an event. Events typically involve the creation of a new node, or edge, or both. Echoing work on the preferential attachment model for classical networks [6], many of the growth events somehow favor existing nodes. As we will see, this is often achieved by selecting the nodes that receive new edges from a categorical distribution, with probabilities proportional to some growing function of the degree of the nodes already in the HOR.

4.2.1. Bipartite models

A prototypical example of out-of-equilibrium bipartite model is the model of G. Ergün, whose goal was to reproduce the evolution of sexual contact networks in a heteronormative society [294]. Recall that there are two sets of nodes (which we have called A and B) in a bipartite network. The model of Ergün [294] postulates that the evolution of the network can be explained with 3 types of events, occurring with probabilities p , q and r summing to 1. At each time step, a new node arrives in set A (with probability p), or in set B (with probability q); or a new edge appears between sets A and

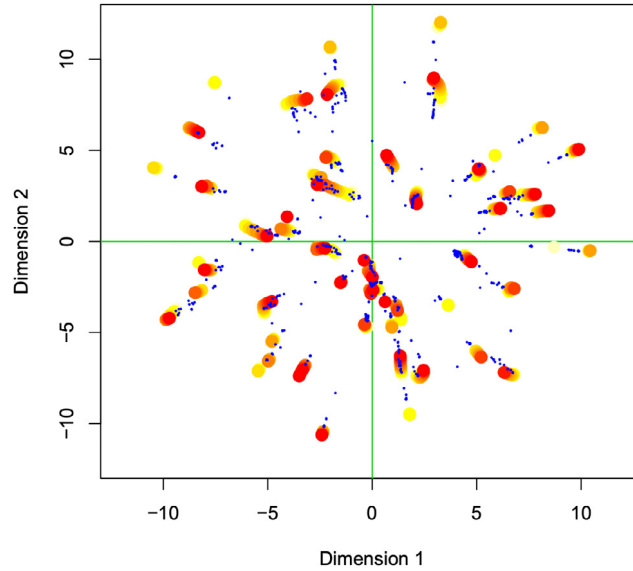


Fig. 12. Boards and directors moving about a latent space. Board are represented as large colored dots, going from 2003 in yellow to 2013 in red. Directors are shown as small blue dots. Edges are not shown.

Source: Figure reproduced from Ref. [299].

B (with probability $r = 1 - p - q$). To avoid nodes of degree 0, all new incoming nodes are initially attached to one node in the opposite set, selected at random. Building on the well-known preferential attachment model [6], all of the choices are made *preferentially*. That is, whenever one or two nodes must be selected to form an edge, they are selected with probability proportional to their current degree (plus some offset specific to the set, called *charisma* in the original model [294]). Thus, the probability that a node $i \in A$ is chosen at time t is calculated as

$$p_i(t) = \frac{k_i(t) + c_A}{\sum_{j \in A} (k_j(t) + c_A)} \quad (27)$$

where $k_i(t)$ is the degree of node i at time t , and c_A is the offset parameter.

Many variations on this theme have since been proposed. For instance, a related—and this time system-agnostic—model of evolving bipartite networks [63,64] proceeds by adding new nodes to set A only. Different from the sexual network model, the degree of the incoming node is chosen from a fixed degree distribution. For each of its k edges, the new node chooses to attach to an existing node of B , with probability $\lambda \in [0, 1]$, or to a new one otherwise. Hence new nodes appear in set B only through their connection with incoming nodes in set A . Again choices are made preferentially, using Eq. (27) with $c_A = 0$. Ramasco et al. [295] make use of two distributions instead. After drawing the degree k of the new node in A , a second number $\ell \leq k$ is drawn from a second distribution, determining the number of target nodes in B . These nodes are again chosen preferentially, while the $k - \ell$ remaining degrees are attributed to new nodes in B . Beguerisse Díaz et al. [296] instead consider node sets whose evolution is independent of node creations. In this case, time is measured in terms of edge creation events, connecting the two sets. Different from the models above, it mixes the preferential attachment probabilities appearing in Eq. (27) with *uniform attachment*, in which nodes are chosen uniformly from the node set, i.e.,

$$p_i(t) = \frac{1}{N(t)} \quad (28)$$

where $N(t)$ is the size of the target set [296].

In all of the models above, the modeling goal is to reproduce the structure of empirically bipartite systems, be it sexual [294], collaborative [295] or competitive [296]. Connections tend to be concentrated in these human systems, and preferential probabilities like the one appearing in Eq. (27) are used to induce such a skewed distributions of degrees [6]. Uniform probabilities like the one appearing in Eq. (28), on the other hand, favor more equitable distributions, which can also be found in some bipartite systems [63,296].

Not all out-of-equilibrium models of HORsS can be modeled with straightforward growth models like the one above. For instance, in one model [297] that is closer to the literature of self-organized criticality [298], nodes re-arrange their edges following connection events, and replicate the behavior of nodes to which they are connected. As another example, a different approach by Friel et al. [299] relies on a dynamical formulation of latent space models, in which nodes in the two sets A and B move in a latent space, and in which edges and edges/non-edges tend to perpetuate themselves (Fig. 12).

Other out-of-equilibrium models focus on *rewiring*, a process by which the edges of a bipartite network are reorganized, all the while preserving the node set. For example, Evans [300] starts from some configuration where the nodes in one of the sets A have exactly one neighbor in the other. At each time step, a node in set A is chosen using an arbitrary selection process, and the edge connecting it to its sole neighbor in B is disconnected. A new target in B is then chosen, again arbitrarily, and a new edge is formed. It turns out that the sequence of generated bipartite networks can be described exactly at all times [300], and that the model allows for a number of useful generalizations, including a version of the models where the choices are driven by a superimposed unipartite network or node types [301]. We note that for some choices of rewiring mechanism, averages over the rewiring process can be thought of as averages over a static ensemble of bipartite networks, such that these rewiring processes straddle the boundary between out-of-equilibrium and equilibrium models [165].

4.2.2. Stochastic set models

A different category of out-of-equilibrium models focuses on how the membership of nodes to sets evolves through time. There has been relatively little work in this representation, since models that reproduce the evolution of set memberships are ironically most often couched in the language of bipartite networks [299], hypergraphs [223], or simplicial complexes [302]. That said, a few models have made explicit use of the set representation, because it turns out to be a natural choice for higher-order interaction of limited scope, and for two-mode data [36].

These set-based models again build on the observation that the distribution of the number of sets per node and of the number of nodes per set are often heavy-tailed [63]. Hence, the evolution of these sets can be plausibly reproduced with a process in which rich-get-richer [2], an observation that has been supported by the empirical analysis of evolving sets [303]. Zhou et al. [304] harness these observations to create a model of evolving networks with communities overlain, in which nodes join communities based on their size and create connections with nodes chosen preferentially in large communities. A simpler model, known as the structural preferential attachment (SPA) model [305–307], incorporates the rich-get-richer mechanism without any explicit need for a network; it instead models the evolution of the sets directly. In this particular model, every time step consists of a node joining a set, with both the node and set being either new or old (such that there are $2 \times 2 = 4$ possible outcomes). The particular type of event is determined from a categorical distribution, and every choice of nodes and sets is made preferentially with respect to the set size/membership numbers of the nodes, see Eq. (27). A hierarchical extension of the model exists [308], where sets themselves belong to larger overlapping sets, and preferential attachment is applied at all levels.

The SPA model is closely related to the Chinese restaurant process [309] and the related Indian Buffet Process [310], both developed to create distributions over set membership relationships, in the statistics and machine learning literature. In the Chinese restaurant process, for instance, a new element (node) is created at each time step, and either join an existing set with probability $1 - 1/(t + 1)$ or create a new set by itself with probability $1/t$. The specific set to which the incoming element is attributed is chosen preferentially. The Indian Buffet Process is defined in similar terms but allows for multiple set memberships. These process have found wide statistical applications because they satisfy an exchangeability property. Here, exchangeability means that the probability of an observed collection of sets is independent of the order in which the “growth” events actually occurred. This property greatly simplifies, for instance, the calculation of expectations over the process.

4.2.3. Hypergraphs models

There has been some work on out-of-equilibrium models of HORs in the hypergraph representation as well, mostly confined to the physics literature. In this literature, the evolving hypergraphs are often called *hypernetworks*, but the underlying concepts are nonetheless the same.

One of the earliest out-of-equilibrium model of hypergraphs considers the very same type of hypergraphs that were analyzed in the first *equilibrium* models of hypergraphs, in the physics literature: k -partite hypergraphs [97], used as models of folksonomies in which users tag items. In the model in question [311], users have intrinsic *activities*, corresponding to the likelihood that they will be the next user to tag an item. At each time step, one picks a random user proportionally to this activity, and then decides on both the type of tag to apply and the item to tag. The specific ways in which the choices are implemented allow for a rich-get-richer phenomenon, and the creation of new items.

This particular model is somewhat unique in that most models of evolving hypergraphs focus on more general hypergraphs that need not be k -partite. Work on these general out-of-equilibrium-models of hypergraph was initiated by Wang et al. [312], who proposed a prototypical model of growing hypergraphs. The model takes motivation in the study of how co-authorship systems evolve (with nodes being authors and hyperedges being papers). In this model, k new nodes are added at every time step, and they form a hyperedge with precisely 1 node present in the extant hypergraph, chosen with probability proportional to its degree (the number of hyperedge incident on nodes, see Section 3.1). By construction, the model generates hypergraphs in which every hyperedge has size k .

There have since been countless variations on these rules, all leading to slightly different models. For instance, Liu et al. [313] allow the sizes of the hyperedges to vary by specifying these sizes as input (the sequence can be generated at random or deterministically). Hu et al. explore alternatives where both the size and the composition of new hyperedges vary at random [314]. Guang-Yong and Jian-Guo [315] introduce the notion of a “local world”, by forming the new hyperedges with nodes selected in a small subset of nodes that is itself selected at random. In Wu et al. [316], choices are not made

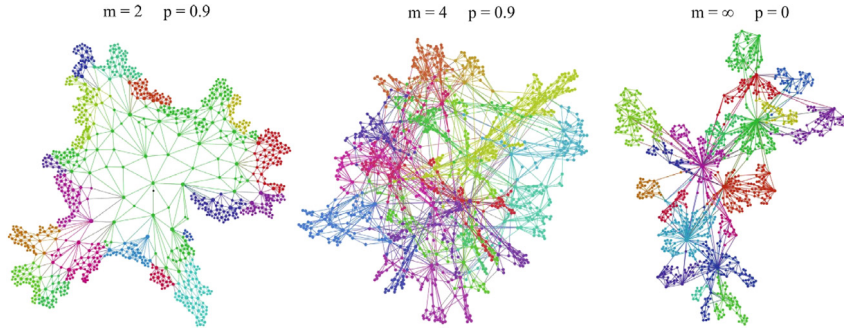


Fig. 13. Different growing geometrical HORs produced by the simple model of Wu et al. The parameter m controls the maximal number of triangles per edge, and p controls the amount of closed triangles.
Source: Figure reproduced from Ref. [302].

preferentially but instead proportionally to the “joint degree” of nodes, i.e., the number of hyperedges they share with the hyperedges that are already in the set. Finally, yet another model uses a complicated choice function to decide which nodes should be involved in new hyperedges [317], namely

$$p_i(t) = \frac{f(k_i(t))}{\sum_j f(k_j(t))} \quad (29)$$

where $k_i(t)$ is the degree of node i at time t , and $f(k_i(t)) = (k_i(t) + c)^\gamma$ include both an offset c and a non-linear exponent γ in the spirit of the classical model of Krapivsky et al. [318]. See also [319] for a version of the function that allows for node-dependent offsets and includes a node-dependent multiplicative term.

Paralleling the bipartite case (see Section 4.2.1), these models have all been introduced to reproduce some set of characteristics of empirical systems, e.g. collaboration hypergraphs. We note, however, that the analysis of these models has so far been limited to reproducing the degree distribution of the nodes, with matching numerical simulations.

4.2.4. Simplicial complexes models

The last set of out-of-equilibrium models that we review are specified in the simplicial complex representations. Similar to the equilibrium models of simplicial complexes, some of these models can be interchangeably thought of as hypergraphs models, when they do not make use of the inclusion property explicitly. Hence, we have again altered the nomenclature favored by the authors when most appropriate.

There are a few approaches to dynamical models of simplicial complexes. The first work that uses simplicial complexes to model hyperbolic network geometry comes from the physics literature, where it is studied under the name of “Complex Quantum Network Manifolds” [302]. These models are motivated by geometric considerations [320], the modeling goal being to specify models of how a wide variety of discrete spaces, represented as simplicial complexes, may arise. The first model in this line of work tracks the evolution of a growing simplicial complex, made exclusively of triangles [302]. At each step, a new node comes in and forms a triangle with two existing nodes, chosen uniformly from the set of all connected nodes that have less than m triangles together, where m is called the saturation bound. At each time step, with probability $p \in [0, 1]$, one also closes a triangle, a process that is implemented by choosing an edge uniformly from the set of unsaturated edges, and choosing an unsaturated edge at random in the neighborhood of e_1 . With this simple model, one can create many quantitatively different outcomes, for example: planar graphs for low m , or complex geometries in the limit $m \rightarrow \infty$, see Fig. 13.

Many variations on this model followed [321,322], culminating into a general model of “Network Geometry with Flavor (NGF)” [88], in which facets have all the same dimension, but are not necessarily triangles anymore. The existing facets have a latent (quenched) energy ε that is a function of the nodes they connect to, and incoming k facets are connected to an existing $k - 1$ facet α , chosen with probability

$$p_\alpha(t) = \frac{e^{-\beta\varepsilon_\alpha}(1 + sn_\alpha)}{\sum_{\alpha'} e^{-\beta\varepsilon_{\alpha'}}(1 + sn_{\alpha'})} \quad (30)$$

where $s \in \{-1, 0, 1\}$ is called the flavor of the model, β is a temperature, and n_α is the number of facets incident on α , minus one. The models that precede the NGF model are all special cases of it. For example, the model of Bianconi and Rahmede [321] focused on the case of triangles $k = 2$, with saturation parameter $m = 2$, flavor $s = 0$, and facets that have latent energies. A later model of Bianconi et al. [322] is similar, but focuses on the flavor $s = 1$.

Some models that have followed borrow much of the mechanisms from the NGF model. For instance, the model of Courtney and Bianconi [323] functions more or less in the same way, but adds a mechanism to track the evolution of weights on the simplices, while that of Fountoulakis et al. [324] also works in fixed dimension but is otherwise very general, introducing the possibility to remove smaller facets when adding new ones.

Other out-of-equilibrium models of simplicial complexes favor approaches that are not related to the NGF model. For instance, one set of methods [325,326] by Sizemore et al. favors the flag complex approach that was also used in the context of equilibrium models by Kahle [281] (see Section 4.1.5). In these approaches, sequences of growing graphs are first generated with a series of standard network models, like for example preferential attachment [6]. Then, one takes the flag complexes of these graphs by replacing every clique with a facet, yielding a sequence of growing simplicial complexes. These models have been used to study the evolution of the topological invariants of the resulting growing simplicial complexes [325] and their sensitivity to changes in the sequence of events [326].

Another recent—and extremely general—model moves away from the “simplicial-complexes as generalized networks” metaphor, and instead focuses on the properties of the manifold they describe, like their Hausdorff and spectral dimensions [327]. Many basic mechanisms by which these complex manifold may evolve are explored and classified.

A different model, introduced by Courtney and Bianconi [328], focuses on *directed* triangular simplicial complexes. In this model, the simplices are either created or reinforced by first selecting a source node, proportionally to its out-strength (the total weight of triangles for which it is the source), with some probability that the node is new. To determine whether the event leads to the creation of a new simplex or to reinforcement, one then selects an edge at random in the simplicial complex, and reinforces the weight of the triangle this edge forms with the source, if it exists, or creates the triangle when it does not. In this case, the modeling goal is to obtain dense simplicial complexes with scale-free degree distributions.

Finally, there are some models that consider *dynamical* simplicial complexes—not simplicial complexes that merely grow. These models are event-based, focusing on what happens in a time slice of a continuous process [329]. The work of Petri and Barrat [293] is prototypical in this regard. In this model, each node i is endowed with an activity rate a_i drawn from some distribution treated as a parameter of the model. Then, when a node i fires (at rate a_i) in continuous time, a $(k - 1)$ – simplex is created with $k - 1$ other nodes chosen uniformly at random. The simplex then disappears after Δt , a parameter. In this case, the model is introduced to study the structural property of the generated simplicial complexes like the degrees aggregated over time, as well as and dynamics taking place on the simplicial complexes generated by this model (see Section 7).

5. Diffusion

In the previous sections we have focused on the structure of higher-order interactions. We have introduced HOrSs and showed their versatility in describing the structural properties of complex systems with more than pairwise couplings among their components. We will now discuss how the dynamical processes traditionally defined on networks can be extended to HOrSs. We will start in this section with diffusion, a linear process that, despite its simplicity, is of high relevance in many different contexts, and also provides an useful first approximation in the case of nonlinear dynamical systems.

Under the name of diffusion we usually indicate two distinct processes that is important to distinguish. The first one is the pure (or standard) process of *diffusion*, also known as the “fluid model”, in which the quantity of interest moves from one region to another following the gradient of concentration. The second one is the so-called *continuous-time random walk* [330]. Here, we will first discuss these two processes in the context of networks, focusing on their similarities and differences. We will then show how to implement them on HOrSs in Sections 5.1 and 5.2, respectively.

In standard diffusion on a network, a (material or immaterial) substance is allocated to the nodes of a graph and flows over each of its edges from the node with higher concentration to the node with lower concentration [331–333]. The process produces a redistribution of the substance, which finally leads to a state where all the nodes have the same concentration. This state of the system, which also takes the name of consensus [334], represents a stable equilibrium of the process, subject to detailed balance condition [335,336]. If we indicate as $x_i(t)$, with $i = 1, 2, \dots, N$, the concentration at the generic vertex v_i at time t , the time evolution of the network state is governed by the following system of N coupled linear differential equations:

$$\dot{x}_i(t) = \sum_j a_{ij}(x_j(t) - x_i(t)) = - \sum_j (k_i \delta_{ij} - a_{ij}) x_j(t) = - \sum_j (L_0^D)_{ij} x_j(t) \quad (31)$$

where $A = \{a_{ij}\}$ is the adjacency matrix of the network, which we assume here for simplicity to be a binary and symmetric matrix (although it is straightforward to extend the formalism to directed and weighted networks), and $k_i = \sum_j a_{ij}$ is the degree of node i . In the last equality, we have defined the diffusion Laplacian matrix:

$$(L_0^D)_{ij} = \begin{cases} k_i & \text{if } i = j \\ -1 & \text{if } v_i \sim v_j \\ 0 & \text{otherwise} \end{cases} \quad (32)$$

where $v_i \sim v_j$ indicates that vertices v_i and v_j are adjacent. In matricial form, we can write $L_0^D = D - A$, with D the diagonal degree matrix. Eq. (31) can then be written as $\dot{\mathbf{x}}(t) = -L_0^D \mathbf{x}(t)$, where we have defined the concentration vector $\mathbf{x} = (x_1, x_2, \dots, x_N)$. The fact that the homogeneous solution $\mathbf{x}^{(\infty)} = \mathbf{1} \sum_i x_i(0)/N$ represents a stationary equilibrium for the process is easily proven by observing that the Laplacian, by definition, is characterized by having all the rows summing to zero, $\sum_j (L_0^D)_{ij} = 0$. For undirected networks, characterized by symmetric Laplacian, this implies from Eq. (31) that the

total concentration $\sum_i x_i$ is conserved, and in particular $\dot{\mathbf{x}}^{(\infty)} = 0$. The stability of such equilibrium is governed by the spectral properties of the Laplacian matrix. In fact, the solution of Eq. (31) can be written by projecting on the Laplacian eigenvectors, which form a basis in the case of a connected network:

$$x_i(t) = \sum_{\alpha=1}^N c_{\alpha}(0) e^{-\lambda_{\alpha} t} \phi_i^{(\alpha)} = c_1(0) \phi_i^{(1)} + \sum_{\alpha=2}^N c_{\alpha}(0) e^{-\lambda_{\alpha} t} \phi_i^{(\alpha)} \quad (33)$$

where λ_{α} and $\phi^{(\alpha)}$, with $\alpha = 1, 2, \dots, N$ are the α -th eigenvalue and eigenvector of L_0^D , while the coefficients $c_{\alpha}(0)$ depend on the initial conditions. We have used the fact that one of the eigenvalues of the Laplacian is zero, because of the zero-row-sum property, which also implies that the corresponding eigenvector $\phi^{(1)}$ is homogeneous. If the network is connected the zero eigenvalue is unique, and all the other eigenvalues are positive by definition [16]. Hence, we can see from Eq. (33) that $\mathbf{x}(t)$ will always converge to the homogeneous solution for $t \rightarrow \infty$, the convergence time being given by the inverse of the smallest eigenvalue different from zero, λ_2 .

A qualitatively different class of processes arises when one considers continuous-time random walk. In this stochastic process a single walker jumps from one node to one of its neighbors on the network, and cannot divide or distribute itself over more than one node, as happens in standard diffusion. In this case, we consider various realizations of the process and we describe the state of the system by a vector $\mathbf{q}(t)$, representing the probability for each node to be occupied by the walker at a given time t . The probability that the walker moves from the generic node v_j to v_i in one step is given by the (i, j) entry of the transition matrix $\Pi = \{\pi_{ij}\}$. In an unbiased random walk this is given by $\pi_{ij} = a_{ij}/k_j$, representing the fact that the walker on node v_j can choose equally among k_j neighbors. The time evolution of the occupation probability is consequently governed by a set of differential equations:

$$\dot{q}_i(t) = \sum_j \pi_{ij} q_j(t) - \sum_j \pi_{ji} q_i(t) = - \sum_j (\delta_{ij} - \pi_{ij}) q_j(t) = - \sum_j (L_0^{\text{RW}})_{ij} q_j(t), \quad (34)$$

which is similar to that in Eq. (31). The last equality defines the random walk Laplacian L_0^{RW} , which is related to the diffusion Laplacian by $L_0^{\text{RW}} = L_0^D D^{-1}$, and for this reason is also called *normalized Laplacian*. In matricial form, Eq. (34) can be written as $\dot{\mathbf{q}}(t) = -L_0^{\text{RW}} \mathbf{q}(t)$.

As well as diffusion, a random walk process is characterized by a stationary distribution where the flows of probability in each direction equal each other, and a detailed balance is reached. In this case the stationary state $\mathbf{q}^{(\infty)}$ corresponds to a probability distribution that is proportional to the degree of nodes: $q_i^{(\infty)} = k_i/2K$, implying that, at the equilibrium, it is more likely to find the walker on the network hubs. As for standard diffusion, also the dynamics of a random walk process is intimately related to the spectral properties of its own Laplacian operator. Again, the stationary state can be found as the Laplacian eigenvector $\phi^{(1)}$ associated to the unique (if the network is connected) eigenvalue 0, which is indeed proportional to the vector of node degrees. The time dependent solution of Eq. (34) can be written analogously to Eq. (33), and it is thus clear that also in a random walk the velocity at which the stationary state is reached depends on the second eigenvalue (the smallest eigenvalue different from zero) of L_0^{RW} . Summing up, in both cases of standard diffusion and random walk, the Laplacian matrix encodes the structure of the network and its spectral properties are related to the dynamical features which ultimately govern the time evolution of the state vector [337].

When it comes to generalizing diffusive processes to higher-order structures, many authors have attempted to extend the microscopic mechanism known to underlying diffusions in pairwise networks to larger groups of nodes. Importantly, traditional diffusion is a linear process and consequently the simplest generalization to higher-order structures can always be reduced to equations involving only pairwise couplings. For instance, as shown by Neuhäuser et al. in [338], an extension of Eq. (31) to 3-body interactions can be formalized as:

$$\dot{x}_i(t) = \sum_{jk} a_{ijk}^{\Delta} [(x_j(t) - x_i(t)) + (x_k(t) - x_i(t))] \quad (35)$$

where $\mathbf{A}^{\Delta} = \{a_{ijk}^{\Delta}\}$ represents a tensor whose entry (i, j, k) is equal to 1 only if there is a triangle involving the three nodes i, j and k . It is easy to see that Eq. (35) can be rewritten in terms of a new Laplacian matrix $L^{\Delta} = \{\ell_{ij}^{\Delta}\}$ as $\dot{x}_i = -2 \sum_j \ell_{ij}^{\Delta} x_j$, where $\ell_{ij}^{\Delta} = \delta_{ij} \sum_k a_{ijk}^{\Delta} - \sum_k a_{ijk}^{\Delta}$. The system in Eq. (35) can thus be reduced to a system with pairwise interactions, where the pairwise interactions are weighted according to the organization of the HORs under study.

To see the effects of multi-body coupling we need to insert a non-linearity in the equations, see Section 7. There are many ways in which this can be done. As we have seen in Section 3.5, it is possible to introduce generalized Laplacians both for diffusion and for random walk. In the next two subsections we will see how such mathematical concepts can turn useful to talk of diffusion on HORs, when the role played by the nodes for the network Laplacian is, at higher orders, played by the edges, the triangles, the tetrahedra, etc.

5.1. Higher-order diffusion

A simplicial complex can be studied at different orders $k \geq 0$, since for each order we can define a k -Laplacian with its spectrum and consequently its own diffusive dynamics. As a consequence, the same simplicial complex can sustain

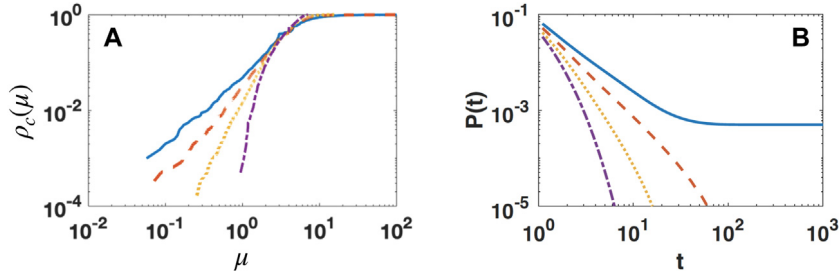


Fig. 14. Laplacian spectrum and return-probability in higher-order diffusion according to Torres and Bianconi [339]. (A) Cumulative density of the eigenvalues of the combinatorial Laplacian of order k , with $k = 0$, standard Laplacian (blue solid line), $k = 1$ (red dashed line), $k = 2$ (yellow dotted line) and $k = 3$ (purple dot-dashed line) for a symplial complex with 2000 nodes generated by means of the NGF model with $d = 3$ and flavor $s = -1$ (see Section 4.2.4). (B) Return-probability for the same system.
Source: Figures adapted from Ref. [339].

different types of diffusion, depending on the order k , or in other words, depending on the dimension of the simplices over which the diffusion is defined. The idea is to indicate as $x_\sigma(t)$ the concentration, at time t , at the generic simplex σ of order k , and to consider the following set of coupled dynamical equations:

$$\dot{x}_\sigma(t) = - \sum_{\sigma' \in X_k} (L_k^D)_{\sigma\sigma'} x_{\sigma'}(t) \quad (36)$$

where L_k^D is the combinatorial Laplacian based on the upper and lower matrices of dimension k that we have introduced in Section 3.5 [86]. Notice that we have N_k of these equations where $N_k = |X_k|$, and X_k represents the set of all simplices of dimension k in the simplicial complex under study. The system in Eq. (36) generalizes the one in Eq. (31) and reduces to the latter when $k = 0$. In this more general setting the substance that is diffusing is not bounded to live at the nodes of a network, but depending on the value of $k \geq 1$, is located at the edges (when $k = 1$), or the triangles ($k = 2$), or higher-order simplices of a HORS, respectively. In analogy with Eq. (33), the general solution to Eq. (36) can be written as [339]:

$$x_\sigma(t) = \sum_{\alpha=1}^{N_k} e^{-\mu_\alpha t} \phi_\sigma^{(\alpha)} \sum_{\sigma' \in X_k} \phi_{\sigma'}^{(\alpha)} x_{\sigma'}(0) \quad (37)$$

where μ_α and $\phi^{(\alpha)}$ are respectively the eigenvalues and eigenvectors of the Laplacian L_k^D . The authors of Ref. [86] have estimated how fast the system relaxes to equilibrium. If $\mathbf{x}(t)$ indicates the vector whose N_k entries represent the concentrations at time t at the N_k simplices of order k , the bounds they have found, when the system is started at $\mathbf{x}(0)$, read:

$$\frac{1}{\mu_2} \|L_k^D \mathbf{x}(t)\| \leq \|\mathbf{x}^{(\infty)} - \mathbf{x}(t)\| \leq N_k \exp(-\mu_2 t) \|\mathbf{x}(0)\| \quad (38)$$

where $\mathbf{x}^{(\infty)} = \lim_{t \rightarrow \infty} \mathbf{x}(t)$, μ_2 is the smallest non-zero eigenvalue of L_k^D , and $\|\cdot\|$ is the usual Euclidean norm. Torres and Bianconi [339] have studied Eq. (36) on simplicial complexes generated by the NGF model (see Section 4.2.4), and have focused on the spectral (and thus dynamical) differences between different orders k . In particular, they have generalized to HORSs the concept of spectral dimension. In a network, the spectral dimension is the dimension of the network “as seen by a diffusion process” and is defined from the exponent of the power-law scaling of the density $\rho(\mu)$ of the eigenvalues of the standard Laplacian (the network spectral density) when $\mu \ll 1$ [340,341]. Fig. 14A shows that a similar definition can be adopted for HORSs, and that the spectral dimension of simplicial complexes generated by the NGF model increases with the order k . Moreover, the authors of Ref. [339] have found an analytical relation between the spectral density and the return-time probability, reported in Fig. 14B. The latter is defined in HORSs as the probability that, starting from an initial state which is localized on a given simplex σ , the diffusion process comes back to the simplex σ at time t , averaged over all simplices σ . Such a relation strengthens the link between spectral dimensions and the dynamical behavior of high-order diffusion processes on HORSs.

5.1.1. Edge-flows

The special case $k = 1$, the so-called edge-based Laplacian, is a particularly important case of the k th order Laplacian L_k^D we have discussed above. Edge-flows turn in fact very useful in many contexts, ranging from graph-based machine learning to signal analysis.

In graph signal processing, although the basic approach is to consider the signals at the nodes of a graph, an edge-based approach becomes important when we need to analyze a flow (of mass, energy, information, traffic, etc.). In such cases,

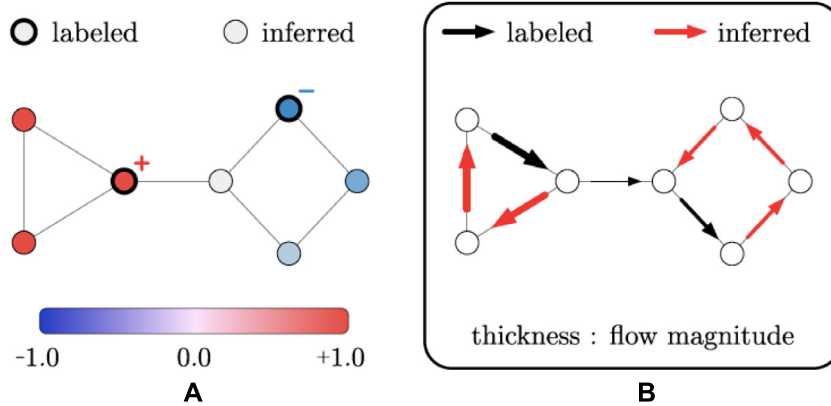


Fig. 15. Semi-supervised learning: vertex and edge perspective. (A) In the standard graph-based semi-supervised learning, the structure of data points is encoded in a similarity graph, where each node is a data sample and the edges represent the similarity between pairs of nodes. (B) In the semi-supervised learning for edge-flows proposed in Ref. [342] data points are instead assigned and inferred on the edges of a graph. Source: Figures reproduced from Ref. [342].

a vertex-based analysis cannot take into account notions like the orientation of flows, which is instead considered in the edge Laplacian by the sign of the entries. The natural generalization has been studied by Schaub and Segarra, who have used the spectrum of the combinatorial Laplacian L_1^D to decompose the space of edge-flows into harmonic and gradient flows [70]. Within this framework the authors have been able to address the problem of denoising and smoothing of flow signals by means of a series of filters that enforce approximate flow-conservation in the processed signals. They also show an application of their methods to denoise vehicular traffic flows in street networks.

The authors of Ref. [342] have instead considered the problem of semi-supervised learning (SSL) for edge-flows in networks. Given a graph $G(V, E)$ edge-flows are defined by a set of real-valued functions $f : V \times V \rightarrow \mathbb{R}$, such that:

$$f(i, j) = \begin{cases} -f(j, i) & \forall (i, j) \in E \\ 0 & \text{otherwise.} \end{cases}$$

The authors make use of the edge-Laplacian and focus on divergence-free flows (i.e. cases in which the flow is approximately conserved) in order to define a process where, given a set of labeled edge-flows it is possible to infer the unlabeled edge-flows. In particular, they study how to select the fraction of most informative edges in order to accurately infer the remaining ones. Fig. 15 illustrates the relation between a vertex-based and the edge-based SSL. An application of the method to real-world street networks proves its superiority with respect to traditional alternatives.

5.2. Higher-order random walks

5.2.1. Random walks on simplicial complexes

An example of higher-order random walk in which the walkers populate the edges instead of the nodes has been proposed by Schaub et al. [152]. The Laplacian L_1^D defined in Section 3.5 is characterized by positive and negative entries that depend on the edge orientations. Therefore, differently from the standard random walk Laplacian, the non-diagonal entries do not reflect the transition probabilities among nodes. It is however possible to define a normalized variant L_1^{RW} of the Laplacian L_1^D which can be related to an edge-based random walk process. The idea is to consider a random walk in a higher dimensional lifted state space. In other words, instead of considering L_1^D applied to an edge-flow function f of the co-chain space C^1 , Schaub et al. propose a sequence of three operations: the lifting of f into a higher dimensional space, the action of a linear operator (playing the role of L_1^{RW}) and the projection back down to the original state space. The linear transformation in the lifted space can be normalized so as to represent a random walk. This procedure allows to interpret the components of the flow in the following way: the magnitude represents the volume of the flow, while the sign indicates the orientation, which can be aligned or anti-aligned with the chosen reference orientation. The higher space where the co-chain vector is lifted up has double the size of C^1 since both possible orientations for each edge are present. The effect of the Laplacian can be split in two contributions, taking into account connections at the upper and lower order respectively. At each time step, the walker takes a step via either the upper or the lower adjacency connections, with equal probability. If the lower connection space is chosen, the walker has probability 1/2 of moving along the reference edge orientation and 1/2 of moving against. The transition probability towards a target edge is, in each case, proportional to the upper degree (or weight) of the edge. If instead the walker makes a step via the upper adjacency connections, there are two cases: if the edge has no upper adjacent faces, the walker stays at the same edge and can change orientation with probability 1/2; if instead the edge has upper adjacent faces, then the walker will transition to an upper adjacent edge with a different orientation with respect to their shared face. In other words, the walker performs a random walk with

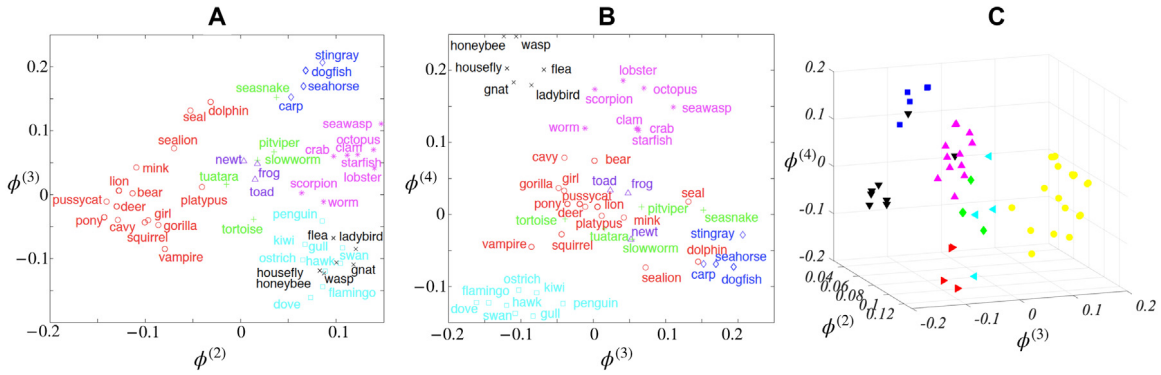


Fig. 16. Classification methods based on random walks on hypergraph. The performance of both Zhou et al. [103] and Carletti et al. [345] models of random walk on hypergraphs is tested on a classification task performed on a zoo dataset. Reported are the embeddings of the nodes of the hypergraph in a Euclidean space built from the Laplacian eigenvectors. Different symbol colors and shapes represent different animal classes. (A,B) Results obtained with eigenvectors corresponding to the 2nd and 3rd smallest eigenvalues, and the 3rd and 4th smallest eigenvalues respectively, in the model by Zhou et al. (C) Embedding based the eigenvectors corresponding to the three smallest eigenvalues in the model by Carletti et al.. Source: Figures adapted from Ref. [103] and Ref. [345].

adjacency matrix A^u , unless there is no upper adjacent connection, in which case the walker can stay put or move to the edge with reverse orientation. It is important to observe that the eigenvectors of L_1^{RW} relative to the eigenvalue $\mu = 0$ are associated to harmonic functions. Schaub et al. propose an application of their random walk trajectory embedding and simplicial PageRank [152].

A second example of a higher-order random walk in which the walkers live instead on the triangles of a HORs has been proposed by Mukherjee et al. [343]. The authors have considered a special case of a simplicial complex where every edge is contained in at most two triangles. At each time step t , a walker at a triangle σ remains still with probability $1/2$, or otherwise moves to a triangle on the other side of one of the three edges of σ . In other words, at each time step, the walker can move to a triangle that is lower adjacent to the current triangle. The transition matrix $\Pi = \{\pi_{\sigma\sigma'}\}$ of the walker reads:

$$\pi_{\sigma\sigma'} = \begin{cases} \frac{1}{2} & \text{if } \sigma = \sigma' \\ \frac{1}{6} & \text{if } \sigma \text{ and } \sigma' \text{ share an edge} \\ 0 & \text{otherwise} \end{cases} \quad (39)$$

and is possible to show that it can be expressed in terms of the higher-order Laplacian L_2^D as $\Pi = I - L_2^D/6$.

5.2.2. Random walks on hypergraphs

The hypergraph formalism is simple enough to allow to consider random walks on hypergraphs of arbitrarily large order.

A first basic model of random walk on hypergraphs has been proposed by Zhou et al. [103]. In their implementation, the walker selects one of the hyperedges of the current node, and then chooses to move to one of the nodes of the selected hyperedge with a uniform probability. In principle, hyperedges can be weighted according to different criteria. However, in their numerical experiments the authors adopt the case in which each hyperedge is assigned a weight equal to 1. Zhou et al. use their random walk model to perform a classification task. They make use of a dataset [344], in which the animals of a zoo are associated to a set of features (tail, hair, legs and so on), and build a hypergraph where each animal is a node and two or more nodes are in the same hyperedge if the corresponding animals have a common feature. The eigenvectors associated to the smallest non-zero eigenvalues μ_α of the random walk Laplacian on this hypergraph are then used in order to embed each animal in a two-dimensional Euclidean space. Figs. 16A,B show the classification performance of the method when the 2nd and 3rd smallest eigenvalues, μ_2 and μ_3 , or the 3rd and 4th smallest eigenvalues, are used respectively.

Carletti et al. have instead proposed a random walk model in which the walkers spend more time inside larger communities [345]. In practice, this is obtained by considering the basic model of Ref. [103] and assigning to each hyperedge a weight that is proportional to its size. In this way, the transition probability reflects the interplay between the walker's willing to explore the network and the attractiveness of large hyperedges. The authors of Ref. [345] have provided an analytical description of the process and of its stationary state. They make use of a different Laplacian operator suitably defined to generalize the standard random walk, and which reduces to the traditional pairwise Laplacian when all hyperedges are of size 2 and the hypergraph reduces to a graph. The results obtained for this random walk on a given hypergraph are compared with those obtained by a traditional random walk on a projected network, where the hyperedges of the original hypergraph are transformed into cliques. This is illustrated with the example reported in

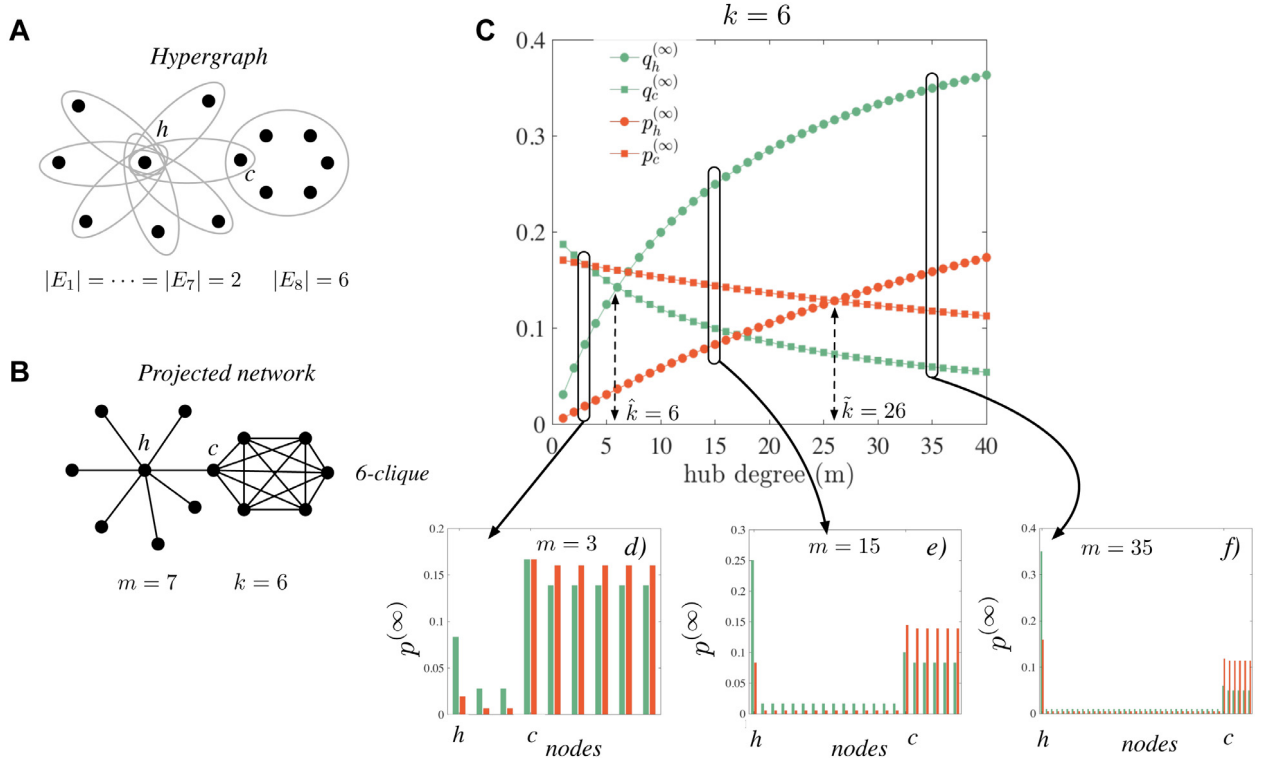


Fig. 17. Example of random walk on hypergraphs. (A) A hypergraph with $m = 7$ hyperedges of size $k = 2$ and one hyperedge of size $k = 6$, and (B) its corresponding projected network. (C) Probability of finding the walker on node h (circles) and c (squares) for a random walk on the hypergraph (red) and on the projected network (green), and for different size m of the hub.
Source: Figure reproduced from Ref. [345].

Fig. 17. The hypergraph in Fig. 17A is composed of one hyperedge of size k , where one of the nodes, denoted as c , is also connected to a hub node, h , which is at the center of m hyperedges of size 2. The corresponding projected network is shown in Fig. 17B. The difference between the HOrS and its projection clearly emerges from the node rankings based on the stationary probability distribution of the walkers in the two cases. In the case of the projected network, the equilibrium distribution $q^{(\infty)}$ is proportional to the degree of the nodes. This means that $q_h^{(\infty)} \propto m$ and $q_c^{(\infty)} \propto k$, which implies that the hub node h is the top node in the ranking when $m > k$. The stationary distribution of the random walk on the hypergraph, denoted as $p^{(\infty)}$, gives instead $p_h^{(\infty)} \sim m$ and $p_c^{(\infty)} \sim 1 + (k-1)^2$ [345]. Consequently, the hub node h becomes the node with the highest occupation probability only when $m > 1 + (k-1)^2$. In general, at fixed hyperedge order k , the two processes provide the same ranking for $m < k + 1$ or $m > 1 + (k-1)^2$. Conversely, at intermediate values of m , the hub h is the top node in the projected network, while node c is ranking first in the hypergraph. The inversion is graphically shown in Figs. 17C-F. The authors of Ref. [345] have proposed concrete applications of their random walk model to rank nodes in large systems. For instance they have produced a ranked list of scientists based on the hypernetwork representing co-authorship relations in published articles (see Section 9.1 for scientific collaborations as HOrSs). The same model has also been used for classification task. Fig. 16C shows the three-dimensional embedding (defined by the eigenvectors associated to the first three eigenvalues) obtained for the zoo data set.

Chitra and Raphael [346] go beyond the previous approaches, and propose a model of random walks on hypergraphs with edge-dependent vertex weights. Namely, they consider a transition probability assigning different weights even to nodes belonging to the same hyperedge. In their random walk, a walker at node v_j at time t moves to a node v_i chosen in the following way. First, a hyperedge σ is selected among all the hyperedges of v_j with probability $\omega(\sigma)/d(v_j)$, where $\omega(\sigma)$ is the weight of the hyperedge and $d(v_j)$ is the degree of v_j . Then a node v_i is selected from hyperedge σ with a probability $\gamma_\sigma(v_i)/\delta(\sigma)$, where $\gamma_\sigma(v_i)$ is the weight of vertex v_i and $\delta(\sigma) = \sum_{v_i \in \sigma} \gamma_\sigma(v_i)$ is the degree of the hyperedge σ . The novelty of this random walk with respect to previous models on hypergraphs with edge-independent vertex weights consists in the second step, where the probability is not uniform over all the vertices of σ . Chitra and Raphael claim that for a random walk on hypergraphs with edge-independent weights is always possible to find a choice of edge weights such that the process on the hypergraph is equivalent to a traditional random walk on the corresponding projected network with such chosen weights. The proof of equivalence is based on the time-reversibility of the process, which is a typical property of the associated Markov chain. Such property cannot be extended to hypergraphs with edge-dependent weights,

which happen to be not time-reversible. Therefore, random walks on hypergraphs with edge-dependent vertex weights cannot be reduced to traditional random walks on weighted networks. This generalizes a result already found in [347] for k -uniform hypergraphs.

Notice that, without using edge-dependent weights, another way to another way to obtain a higher-order random walk which is not reducible to the traditional model is, similarly to what happens for diffusion, to insert a non-linearity in the equations, as it has been done by Chan et al. [95], and by Li and Milenkovic in [348], and [158].

In the model by Chitra and Raphael the stationary state $\mathbf{p}^{(\infty)}$, can be analytically computed. If for the traditional processes this can be written as by $p_i^{(\infty)} = \rho \sum_{\sigma \in E(v_i)} \omega(\sigma)$, with $E(v_i)$ the set of hyperedges containing v_i , the process proposed by Chitra and Raphael brings to $p_i^{(\infty)} = \sum_{\sigma \in E(v_i)} \rho_{\sigma} \omega(\sigma) \gamma_{\sigma}(v_i)$, i.e. the proportionality constant ρ depends on the hyperedge and each term in the sum is multiplied by the vertex weight.

By making use of this definition the authors also provide an application example, again based on scientific collaborations. They obtain the ranking of different scientists according to a hypergraph where hyperedges represent articles and the authors have weights which reflect their appearance order (first/last or middle authors), and they compare such ranking to that obtained by a random walk on the corresponding edge-independent hypergraph. Other applications of edge-dependent hypergraphs include e-commerce [349], text ranking [106], image visualization and processing [350–354].

Random walks on hypergraphs have also been used to study graph expansion. Louis in [94] introduces a non-linear Laplacian operator on hypergraphs as a generalization of the random walk Laplacian operator on graphs and studies its spectrum. He in particular proves that the second smallest eigenvalue is related to the expansion of the hypergraph, generalizing the Cheeger's inequality. A similar process is analyzed by Chan et al. [355] considering a diffusive flow from the node with maximum density to the one with minimum density within a hyperedge. The two works are merged together in [95]. A generalization of this process is provided in [96], while in [356] the framework is extended to directed hypergraphs. Li and Milenkovic [158] answer the same questions on a different kind of higher-order network, named submodular hypergraph, for which they define a different Laplacian and analyze its spectrum.

Higher-order random walks have also been used for applications such as node ranking [106], community structure detection [357], topological data analysis [358], machine learning [359,360], and even quantum walks have been extended beyond pairwise connections [361]. The traditional definition of cover time in random walk, i.e. the maximum expected time to visit all the vertices of a graph, has been extended to hypergraphs in [362]. While Avin et al. [107] define a higher-order random walk suitably designed to describe communication over a wireless shared channel, which is not well captured by a traditional network.

Another interesting extension is to investigate the interplay between higher-order topology and dynamics in settings with coupled species [363], where flow patterns stem as a cumulative response of nodes. Indeed, the basic mechanism for pattern formation is historically associated to reaction–diffusion systems [364–370]. This framework has been recently extended to hypergraphs by Carletti et al. who in Ref. [371] analyze a dynamical process involving two interacting species whose dynamics is governed by the Laplacian proposed in Ref. [345], combined with a local reaction function. This study reveals spatio-temporal patterns emerging when higher-order interactions among nodes are considered, and which cannot be observed in the projected version of the network where all interactions are reduced to pairwise edges.

6. Synchronization

Synchronization is the emergence of order in populations of two or more coupled dynamical systems. It shows up in many physical, biological and social systems, and at different scales, with typical examples including the synchronized motion of weakly coupled pendulum clocks [372], the clapping of an audience [373] or the flashing of fireflies [374]. Synchronization has been an active research topic in the last decades with successful applications ranging from neuroscience to climatology and engineering [375–378]. Interactions play a key role in the emergence of synchronization, which is why network science provides natural and powerful tools to inquire about the nature and the underlying mechanisms of synchronization. In synchronization on networks, each node of a graph is a dynamical system, and its dynamics is influenced by its neighbors through pairwise interactions. Synchronization occurs when the interactions are such that all, or a macroscopic fraction of, the oscillators reach a coherent state. Historically, this was made clear by Kuramoto and his mathematically tractable model of all-to-all coupled phase oscillators [379]. The Kuramoto model paved the way for others to study the effects of complex topologies [380–382]. Key results have shed light on the relationship between network synchronizability and topology, e.g. the improved synchronizability of small-world networks [383], and have revealed different routes to synchronization, such as abrupt synchronization in scale-free networks [384,385]. In addition, different types of synchronized behaviors have been identified and linked to specific properties of the network structure, including remote synchronization [386], cluster states [387], chimera [388] and Bellerophon [389] states. The existence and properties of these phenomena depend on the type of interactions, but also on the topology of the network. Another line of research concerns the study of coupled cell networks [390,391] from the viewpoint of symmetry and groupoid formalism [392], and how this yields insight into patterns of synchrony [393,394]. See Refs. [378,381,382] for comprehensive reviews on synchronization.

In this Section, we discuss how coupled dynamical systems can be extended to HORs, and how the presence of higher-order interactions can affect synchronization in both phase oscillators and nonlinear dynamical systems. As we will show below, higher-order interactions can change the nature of the transition to synchronization, can favor the emergence of certain collective phenomena, e.g. cluster states, and can even give rise to new dynamical regimes.

6.1. Phase oscillators

In this section, we report on studies that investigate synchronization in populations of phase oscillators: the most basic oscillatory unit which is fully described by a phase.

6.1.1. Higher-order Kuramoto model

The Kuramoto model captures the essence of the emergence of synchronization in a mathematically tractable setting [379]. In the original model, the state of oscillator i ($i = 1, \dots, N$) at time t is described by its phase $\theta_i(t) \in [0, 2\pi[$. The dynamics of each oscillator is governed by its interactions with all other oscillators (all-to-all interactions) according to:

$$\dot{\theta}_i = \omega_i + \frac{K_1}{N} \sum_{j=1}^N \sin(\theta_j - \theta_i), \quad (40)$$

where ω_i denotes the natural frequency associated to i , drawn from a given distribution $g(\omega)$, and $K_1 > 0$ is the (pairwise) coupling constant. In this model, two opposing driving forces are at play: heterogeneity in the natural frequencies pushes the oscillators away from synchronization, while interactions favor synchronization. As a result of this, we observe a phase transition. Above a critical value, K_1^* , of the coupling strength, the oscillators synchronize their frequency, so that their phase difference does not change in time (this is known as phase locking). This phase transition from incoherence to synchronization can be captured by the usual complex order parameter $Z_1(t) = R_1(t)e^{i\Phi_1(t)} = \frac{1}{N} \sum_{j=1}^N e^{i\theta_j(t)}$, a macroscopic quantity that characterizes the collective dynamics of the entire system. The modulus $0 \leq R_1(t) \leq 1$ measures the phase coherence, while $0 \leq \Phi(t) < 2\pi$ is the average phase of the whole population of oscillators. When $K_1 < K_1^*$, the oscillators behave incoherently and $R_1 \approx 0$. When K_1 is above the critical value, instead, the oscillators synchronize and $R_1 \neq 0$. As K_1 tends to large values, R_1 tends to 1, corresponding to all oscillators having exactly identical phases, a case that can be obtained for identical oscillators, i.e. when $\omega_i = \omega \forall i$ [395,396]. To make the driving of the mean field explicit, the system in Eq. (40) can be rewritten as:

$$\dot{\theta}_i = \omega_i + K_1 R_1 \sin(\Phi_1 - \theta_i). \quad (41)$$

About ten years ago, Ott and Antonsen proved that the dynamics of the system in Eq. (41) reduces to a stable low-dimensional synchronization manifold, by applying self-consistency arguments to the evolution of the distribution of the oscillator phases [397]. Meanfield reduction approaches such as theirs and that of Watanabe and Strogatz [395] are powerful tools (see [398] for a recent review including a discussion of their applicability to higher-order interactions).

The Kuramoto model can be extended from the original all-to-all interactions to the case in which the oscillators are the nodes of a network and their couplings are governed by the adjacency matrix $A = \{a_{ij}\}$ of the network. Formally, this is equivalent to consider the equations:

$$\dot{\theta}_i = \omega_i + \frac{K_1}{N} \sum_{j=1}^N a_{ij} \sin(\theta_j - \theta_i). \quad (42)$$

The Kuramoto model has been studied on different types of complex networks, and particular attention has been devoted to investigate how the structural properties of a network affect synchronization. A review of the main results obtained can be found in Refs. [380,381]. In what follows, we will review more recent works that extend the Kuramoto model to higher-order networks, starting with a short detour on synchronization on motifs.

Motifs are small graphs that appear in a statistically significant way in real networks [72]. This is why studying synchronization in motifs can help understanding the dynamics of large networks and is also the first step towards an explicit treatment of synchronization in a HORs.

A first study by Moreno et al. [399] investigated if some motifs of Kuramoto oscillators are more synchronizable than others. For each undirected small graph of $N = 3$ and 4 nodes, the authors evaluated its probability to synchronize by considering many random realizations of the set of natural frequencies $\{\omega_i\}_{i=1}^N$ drawn from a given distribution $g(w)$, and computing the fraction of realizations for which the graph synchronizes. As expected, the probability of synchronization increases with the coupling strength K_1 . Additionally, they have evaluated a threshold coupling strength \bar{K}_1 , as the value of K_1 above which the probability of synchronization is greater than 0.5. The main result of the study is that, at fixed number of nodes, the larger the number of links is, the lower the value of \bar{K}_1 , i.e. the easier it is for the graph to synchronize. This is shown in Fig. 18 for graphs with four nodes. The authors suggest this could help understand why some motifs, which appear in biological networks and are more conserved across evolution, have a higher link density than others.

In a following study, D'Huys et al. have investigated the influence of time delays in the synchronization of motifs [400]. The authors studied the existence and stability of several types of synchronized behaviors, in unidirectionally and bidirectionally coupled small rings, pairs of oscillators, and open chains. The work showed that delays tend to induce multistability in unidirectional rings, in contrast to what happens in bidirectional rings.

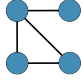
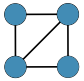
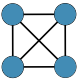
| Motif |  |  |  |
|---------------|---|---|---|
| # links | 4 | 5 | 6 |
| \tilde{K}_1 | 0.22 | 0.18 | 0.14 |

Fig. 18. Critical coupling and motifs. In motifs, i.e. small graphs recurrent in various biological, social and technological networks, the critical coupling strength \tilde{K}_1 for synchronization decreases as the number of links increases.
Source: Figure adapted from Ref. [399].

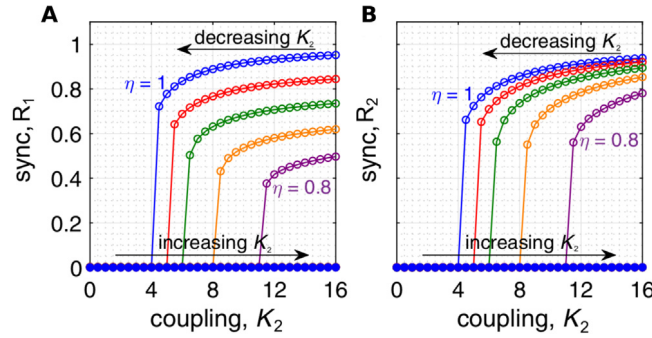


Fig. 19. Abrupt desynchronization induced by higher-order interactions in the model in Eq. (43). The two order parameters R_1 and R_2 are shown as a function of the three-body coupling strength K_2 , in (A) and (B) respectively. The system exhibits multistability, and each stable branch represents a two-cluster state with a proportion of η oscillators in the first cluster.
Source: Figures adapted from Ref. [401].

More recent works have studied variations of the Kuramoto model that explicitly include higher-order interactions. Skardal and Arenas [401] have investigated what happens when all-to-all pairwise interactions are replaced by pure three-body interactions, considering the system:

$$\dot{\theta}_i = \omega_i + \frac{K_2}{N^2} \sum_{j=1}^N \sum_{k=1}^N \sin(\theta_j + \theta_k - 2\theta_i), \quad (43)$$

which is a direct generalization of the original Kuramoto model in Eq. (40). Now, the dynamics is ruled by interactions of all possible triplets of oscillators (i, j, k) in the system (corresponding to a hypergraph with all 3-node hyperedges). The value of the coupling strength K_2 tunes the strength of such interactions. Notice that the number of three-body interactions node i is involved in, scales as N^2 , which explains the presence of the normalization factor $1/N^2$ to ensure a smooth thermodynamic limit. The system in Eq. (43) can be cast into the following form:

$$\dot{\theta}_i = \omega_i + K_2 R_1^2 \sin[2(\Phi_1 - \theta_i)], \quad (44)$$

where $R_1(t)$ and $\Phi_1(t)$ are, as in Eq. (41), the modulus and the phase of the complex order parameter $Z_1(t)$. By arguments of continuity and self-consistency of the oscillator density, the authors then derived analytical formulas for the dynamics of $Z(t)$ and of a second order parameter $Z_2(t) = R_2(t)e^{i\Phi_2(t)} = \frac{1}{N} \sum_{j=1}^N e^{i2\theta_j(t)}$, which is a typical indicator of 2-cluster states. Indeed, $R_2 \approx 0$ for incoherent states, while $R_2 \approx 1$ for 2-cluster states when the two clusters have a phase difference equal to π . Two main novel dynamical phenomena were identified. Firstly, the three-body interactions give rise to an abrupt desynchronization transition, which is not present in the classical Kuramoto model of Eq. (40). In other words, as shown in Fig. 19, as the coupling strength K_2 is decreased from large values, the order parameter R_1 drops from positive values to zero. On the other hand, increasing K_2 back does not yield a transition to coherence since the incoherent state is stable for any coupling strength. Second, the three-body interactions yield multistability: for large enough values of the coupling strength K_2 , there exist infinitely many stable coherent branches that correspond to 2-cluster solutions. Each of these stable 2-cluster solutions can be distinguished by the relative size η of the two clusters, i.e. the relative number of oscillators in the two clusters. Interestingly, each of the stable branches undergoes an abrupt desynchronization transition at a different value of K_2 , so that there is actually a continuum of transitions. Very recently, Xu and coworkers have studied the same system using bifurcation theory and the symmetries of the SO_2 group to reveal scaling properties of the transitions [402]. The authors show that their analysis generalizes to a coupling scheme where natural frequencies are correlated to the coupling strength.

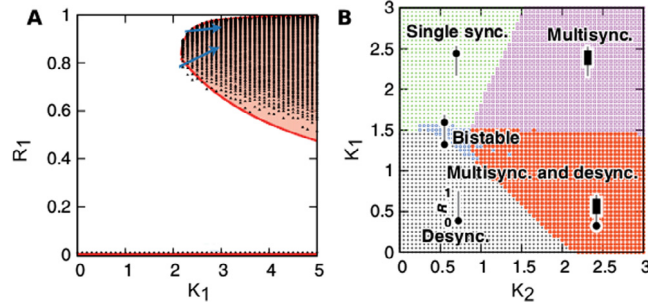


Fig. 20. Phase diagrams of the model with higher-order interactions in Eq. (45). (A) Case $K_2 = 0$ when only three-body interactions are present. (B) General case with both two- and three-body interactions. Vertical black lines represent the interval $[0, 1]$ of values the order parameter R_1 can take. On these lines, black circles and boxes represent the value of R_1 for all coexisting stable states. Source: Figures adapted from Ref. [403].

That higher-order interactions favor multistability is a general trend, and this is also in agreement with the results of some earlier studies [403–405]. Already in 2015, Komarov and Pikovsky [405] studied Eq. (43) in great detail for identical and distributed frequencies, with or without common noise. The main focus of their study is different to Ref. [401]: here, the authors show that while the incoherent state $R_1 = 0$ is always stable in the thermodynamic limit, finite-size fluctuations can induce a transition to synchrony $0 < R_1 \leq 1$. The authors explained this transition by showing that, remarkably, the order parameter scales as $R_1 \sim 1/\sqrt{N}$ with the size of the system, which vanishes in the thermodynamic limit. Even earlier, in 2011, motivated by the importance of many-body interactions in signal transmission between neurons, Tanaka and Ayogi [403] studied a system similar to the one in Eq. (43). They have considered a coupling function of the form $\sin(\theta_j - \theta_i) \cos(\theta_k - \theta_i)$, which indeed corresponds to the first of the two terms to which the original coupling function in Eq. (43) reduces when using the trigonometric identity for the sine of a sum [403]. As shown in Fig. 20A, the model exhibits multistability similar to that in Fig. 19. Additionally, Tanaka and Ayogi have studied the effect of having, at the same time, both all 2- and all 3-body interactions, with respective coupling strength K_1 and K_2 :

$$\dot{\theta}_i = \omega_i + \frac{K_1}{N} \sum_{j=1}^N \sin(\theta_j - \theta_i) + \frac{2K_2}{N^2} \sum_{j=1}^N \sum_{k=1}^N \sin(\theta_j - \theta_i) \cos(\theta_k - \theta_i). \quad (45)$$

In our language this means considering all possible 2-simplices. The phase diagram of this more general model is reported in Fig. 20B and shows the existence of different regimes, many of them exhibiting multiple coexisting stable states. For example, in the region indicated as “Bistable”, both the incoherent state with $R \approx 0$ and the synchronized state with $R \approx 1$ are stable.

In a second study, Skardal and Arenas added two layers of complexity to the previous models: (i) a combination of interactions of different orders up to four-body interactions, (ii) a microscopic description of such interactions in the form of a simplicial complex [406]. They showed numerically that higher-order interactions were sufficient to induce an explosive transition from incoherence to synchronization in a real-world higher-order system. In practice, they have used a Macaque brain data set with 248 nodes and pairwise connections in which any 3-node clique was promoted into a 2-simplex, and any 4-node clique into a 3-simplex. We refer to simplicial complexes constructed this way as “maximal”, because from a_{ij} all possible q -simplices are constructed. A maximal simplicial complex cannot thus have, e.g. any empty triangle (three 1-simplices), but only filled triangles (three 1-simplices and one 2-simplex). The resulting network has 1-, 2-, and 3-simplex interactions, with the 2-simplex interactions term for oscillator θ_i written as

$$\frac{K_2}{2! \langle k^{(2)} \rangle} \sum_{j=1}^N \sum_{k=1}^N a_{ijk} \sin(2\theta_j - \theta_k - \theta_i), \quad (46)$$

and where the 1- and 3-simplex interaction terms have similar structure. Note the choice of an asymmetrical coupling function in Eq. (46) which is different from the symmetrical choice in Eq. (43). This will be discussed in more detail in the next paragraph. Here, $\mathbf{A} = \{a_{ijk}\}$ denotes the 2-simplex interaction tensor with a_{ijk} equal to 1 if there is a three-body interaction among oscillators i, j and k , and 0 otherwise. The $\langle k^{(2)} \rangle$ represents the average degree of 2-simplex degree, i.e. the average number of distinct 2-simplices nodes are part of. In general, the average q -simplex degree is written $\langle k^{(q)} \rangle$, and the coupling coefficient K_q is rescaled by $q! \langle k^{(q)} \rangle$. The complexity of the model makes it hardly tractable analytically. However, by means of self-consistency arguments similar to those used in Ref. [401], the authors were able to obtain a closed equation for the order parameter R_1 in a simplified all-to-all version of the model. They obtained the bifurcation diagram reported in Fig. 21, which shows the following two main findings. Firstly, higher-order interaction are able to induce an abrupt transition from incoherence to synchronization. Indeed, above a critical value of $K_{2+3} = K_2 + K_3 = 2$, the system becomes bistable and exhibits a hysteresis cycle, yielding abrupt transitions.

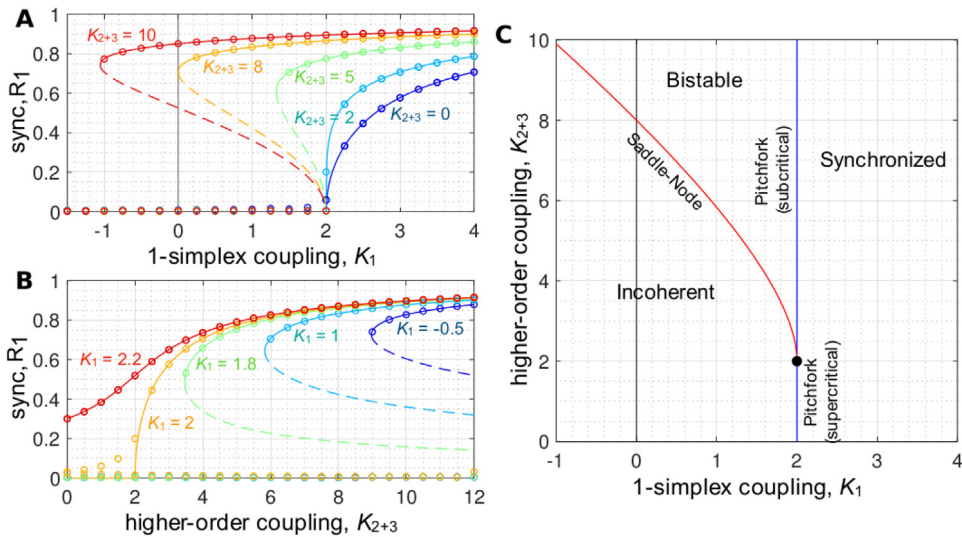


Fig. 21. Phase diagrams of the simplicial complex oscillator model of Ref. [406]. (A) Higher-order interactions induce abrupt transitions between incoherence and synchronization. (B) Moreover, higher-order interactions can stabilize the synchronized state, even when pairwise (1-simplex) interactions are repulsive ($K_1 < 0$). (C) Two-parameter bifurcation diagram identifying the region of bistability. Analytical predictions (solid curves) are in agreement with the numerical simulations (open circles).
Source: Figures adapted from Ref. [406].

Since the incoherent and synchronized states have been linked to resting and active states, respectively, such abrupt transitions provide a potential mechanism for fast switching between brain states. Second, strong enough higher-order interactions (large enough values of K_{2+3}) can stabilize the synchronized state even when the 1-simplex interactions are repulsive, i.e. when $K_1 < 0$. Notice that explosive synchronization was first observed in global coupling with evenly spaced frequencies [407] and then in scale-free networks with frequency-degree correlations [384]. Several other structural or dynamical ingredients have then been identified that can also lead to explosive synchronization, such as multilayer couplings [408] or time delays [409]. Here, Skardal and Arenas have been able to show that higher-order interactions are sufficient to induce explosive synchronization. Explosive synchronization and chimera states have also been studied in simplicial complexes by Berce in Refs. [410,411]. More recently, Khuen and Bick [412] gave a mathematical argument as to why abrupt transitions can be induced by higher-order interactions, and illustrated their framework on epidemic dynamics, synchronization, and a percolation transition.

The choice of coupling function is known to affect the dynamics of coupled dynamical systems [413]. In coupled oscillators, a typical choice at order 1 is the sinusoidal function $\sin(\theta_j - \theta_i)$ that vanishes when oscillators are synchronized and that is 2π -periodic in its phases, as in the Kuramoto model of Eq. (40). For interactions of more than two oscillators, however, there are more choices of functions that satisfy those requirements. Indeed, even if we restrict ourselves to the simplest case, i.e. 2π -periodic sinusoids with no harmonics and no phase-shift, we are faced with two possibilities for the functional form accounting for three-body interactions in the equation for oscillator i , namely $\sin(\theta_j + \theta_k - 2\theta_i)$, or $\sin(2\theta_j - \theta_k - \theta_i)$. The first choice was used for example in Eq. (43). This function is the natural generalization of the pairwise function above, in that it is symmetric in i , meaning that it is invariant under any permutation of the other indices. This choice was also made in Ref. [159] where it was generalized to all possible orders. The second choice, which was used for example in Eq. (46), is asymmetric, in the sense described above. It can, however, arise naturally from the phase reduction of nonlinear oscillators, see for example Eq. (52) and Refs. [414]. For coupling functions of larger numbers of oscillators, there is always one symmetric choice, but the number of asymmetric choices increases. However, to the best of our knowledge, the implications of the precise choice of higher-order coupling functions on the dynamics have not been investigated systematically as deserved so far. We hope this review will encourage works in this direction.

A radically different approach from those discussed above has been proposed by Millán et al. who have formulated a higher-order extension of the Kuramoto model in which the oscillators are placed not only on the nodes but also on the higher-order simplices, such as the links or the triangles, of a simplicial complex [415]. The authors showed that the dynamics defined on q -simplices can be projected, through Hodge decomposition (also see Section 3.5.2), on the dynamics defined on $(q-1)$ and $(q+1)$ dimensional simplices. This means, for instance, that the dynamics on edges can be projected on nodes and triangles. Interestingly, when the two projected dynamics on $(q-1)$ - and $(q+1)$ -simplices are adaptively coupled the transition to synchronization is explosive, while it is continuous in the uncoupled case. This implies for instance that a dynamics defined on links can induce a simultaneous explosive synchronization on the dynamics projected on nodes and triangles. The phenomenon is illustrated in Fig. 22, which reports the results of numerical simulations on a simplicial complex generated by a configuration model (see Section 4).

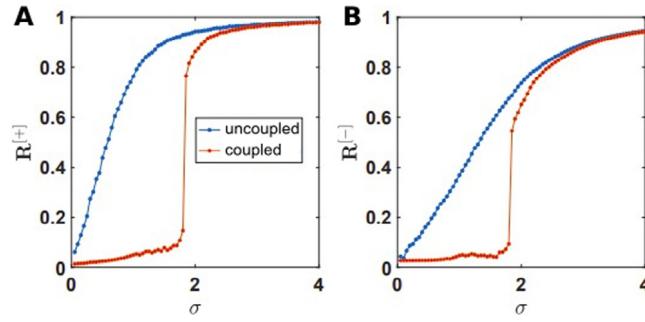


Fig. 22. Explosive synchronization in the higher-order Kuramoto model. In Ref. [415], the oscillators are associated not to the nodes, but to the q -simplices (with $q \geq 1$) of a simplicial complex. $R^{(+)}$ and $R^{(-)}$ denote the order parameter of the dynamics projected on $(q-1)$ - and $(q+1)$ -simplices, respectively shown in (A) and (B). The model has been implemented on simplicial complexes constructed by a configuration model (see Section 4). When the projections are uncoupled the transition is continuous, while when the projections are adaptively coupled, the transition is explosive. Source: Figures adapted from Ref. [415].

The three authors of Ref. [415] have also studied synchronization in so-called Complex Network Manifolds (CNMs), which are growing simplicial complexes of dimension d , i.e. built with d -simplices [341,416] (see Section 4.2.4). Note that simplicial complexes were only used here to construct the adjacency matrix $\{a_{ij}\}$ of networks with an easily tunable spectral dimension, in addition to being small-world and having a highly modular structure. Indeed the goal of these studies was to study the effect of the spectral dimension of the underlying graph on network synchronization. The spectral dimension of a graph describes the power-law scaling of the eigenvalue density of the standard Laplacian L . Most complex networks have a spectral gap, i.e. the second eigenvalue λ_2 of the standard Laplacian L does not tend to zero as the size of the network is increased. In CNMs, however, λ_2 does tend to zero, so that a spectral dimension d_s of the network can be defined. Remarkably, in CNMs, the eigenvalue density scales roughly with the dimension d of the simplicial complex, $d_s \simeq d$. Hence, one can investigate the effect of d_s just by changing the dimension of the simplicial complex used to construct the network. In [416], the authors have reported the observation of frustrated synchronization, a dynamical regime in which the order parameter is non-stationary and exhibits large fluctuations even at large times. In [341], they have further shown via a linear approximation that the synchronized state is thermodynamically stable only in networks with $d_s > 4$. In other words, for smaller spectral dimensions, the average fluctuations of the phases diverge as the network size $N \rightarrow \infty$. Hence, frustrated synchronization is only possible for $d_s < 4$. Additionally, $d_s > 4$ is a necessary condition for a stable synchronized state in the thermodynamic limit, as also confirmed numerically.

Higher-order interactions can yield interesting dynamics even when the oscillators have identical frequencies, as shown by two very recent studies [159,417].

In the first of these works [417], Gong and Pikovsky have considered the following system of all-to-all coupled oscillators with identical frequencies and higher-order harmonics:

$$\dot{\theta}_i = \omega(t) + \Im[H(t)e^{-iq\theta_i}], \quad (47)$$

with pure harmonics of order $q \geq 2$. The quantity $H(t)$ in the equations represents the coupling and depends on the generalized complex order parameters $Z_q(t) = R_q(t)e^{i\Phi_q(t)} = \frac{1}{N} \sum_{j=1}^N e^{iq\theta_j(t)}$. The model reduces to the original Kuramoto model in Eq. (40) when $H = Z_1$ and only the first harmonic $q = 1$ is considered. With $H = Z_2$ and only the second order harmonic $q = 2$, one obtains a coupling function of the type $\sin(2(\theta_j - \theta_i))$. This does not imply higher-order interactions, which can instead be obtained by considering nonlinear meanfield couplings, i.e. powers of Z_q . For example, by taking $H = Z_1^2$ and $q = 2$, one recovers the system in Eq. (43) with pure three-body interactions. Higher-order harmonics and higher-order interactions are linked in that they both allow q -cluster states at order q , for example. Eq. (44) can also be seen as driven by the meanfield with a second order harmonic.

In their work, the authors extend the Watanabe-Strogatz theory to account for any pure higher-order harmonics, $q \geq 2$, for a general form of H that can include higher-order interactions. The Watanabe-Strogatz theory provides a lower-dimensional description of all-to-all coupled oscillators with identical frequencies [395,396], similarly to the Ott-Antonsen theory for distributed frequencies [397]. As an example, Gong and Pikovsky have applied their theory to the cases of pure 3-body and pure 5-body interactions, and have been able to study the basin of attractions of the 3- and 5-cluster states, respectively. It is worth mentioning here three other earlier but related studies by Pikovsky and coworkers [418–420]. In Refs. [418,419], had already considered the effect of nonlinear mean field coupling, i.e. where H is a function of powers of Z_1 , as opposed to only the first power as in the Kuramoto model (40). The authors found that this additional nonlinearity yields richer dynamics, including self-organized quasiperiodic behavior. Similarly, in Ref. [420], the authors consider coupling functions that depend nonlinearly on R_1 .

In the second of these works [159], Lucas et al. have focused directly on higher-order interactions rather than harmonics, and proposed a natural generalization of the usual Laplacian formalism to account for complex topologies

(instead of all-to-all) and with a mix of orders. They introduced a multi-order Laplacian and applied it to simplicial complexes (though the formalism is valid for hypergraphs in general) of identical phase oscillators. This Laplacian allows to assess the stability of the fully synchronized state $\theta_i(t) = \theta^S(t) = \omega t$ for all i . Formally, the authors considered the following system:

$$\begin{aligned} \dot{\theta}_i = & \omega + \frac{K_1}{\langle k^{(1)} \rangle} \sum_{j=1}^N a_{ij} \sin(\theta_j - \theta_i) + \frac{K_2}{2! \langle k^{(2)} \rangle} \sum_{j,k=1}^N a_{ijk} \sin(\theta_j + \theta_k - 2\theta_i) \\ & + \frac{K_3}{3! \langle k^{(3)} \rangle} \sum_{j,k,l=1}^N a_{ijkl} \sin(\theta_j + \theta_k + \theta_l - 3\theta_i) + \dots \\ & + \frac{K_{q_{\max}}}{q_{\max}! \langle k^{(q_{\max})} \rangle} \sum_{j_2, \dots, j_{q_{\max}+1}=1}^N a_{ij_2 \dots j_{q_{\max}+1}} \sin \left(\sum_{m=2}^{q_{\max}+1} \theta_{j_m} - q_{\max} \theta_i \right), \end{aligned} \quad (48)$$

which is a natural extension of the Kuramoto model with all oscillators having identical frequencies ω , and K_q denoting the coupling strength of q -simplex interactions. Here, the complex topology, which is as in Ref. [406] remains mathematically tractable because oscillators have identical frequencies. All cliques in the graph defined by the adjacency tensors $\mathbf{A}^{(q)} = \{a_{ij_2 \dots j_{q+1}}\}$ with q indices: for example, at order $q = 2$, $a_{ijk} = 1$ if there is a triplet interaction (i, j, k) and 0 otherwise. Coupling functions at each order are also a natural generalization of the standard pairwise sine function, as they are chosen to be symmetric with respect to oscillator i , meaning that any permutation of the other indices leaves the coupling function invariant. The authors have shown that each term in Eq. (48) can be rewritten in terms of a newly defined Laplacian matrix, and all such matrices can be combined into a multi-order Laplacian controlling the dynamics of the whole system. The authors denote as $k_i^{(q)}$ the connectivity of order q , i.e. the number of distinct q -simplices that node i is part of, and as $\hat{a}_{ij}^{(q)} = \{\hat{a}_{ij}^{(q)}\}$ the adjacency matrix of order q , i.e. the number of distinct q -simplices that the pair (i, j) is part of. These definitions recover the usual definitions for $q = 1$. Note that the adjacency matrices $\hat{A}^{(q)}$ are different objects than the adjacency tensors $\mathbf{A}^{(q)}$: the former have dimension 2 and can take any integer value, whereas the latter have dimension $q+1$ and only takes binary values. Infinitesimal heterogeneous perturbations $\delta\theta_i$ around the synchronized state $\theta^S(t) = \omega t$, defined as $\delta\theta_i = \theta_i - \omega t$, evolve according to the linearized dynamics. In a system with q -simplex interactions, this dynamics is determined by a Laplacian $L^{(q)} = \{l_{ij}^{(q)}\}$ of order q defined as:

$$l_{ij}^{(q)} = q k_i^{(q)} \delta_{ij} - \hat{a}_{ij}^{(q)}, \quad (49)$$

which is a natural generalization of the usual pairwise Laplacian. For instance, in the case of pure 3-simplex interactions, $K_q = 0$ for all $q \neq 3$, the linearized system reads:

$$\delta\dot{\theta}_i = - \frac{K_3}{\langle k^{(3)} \rangle} \sum_{j=1}^N l_{ij}^{(3)} \delta\theta_j. \quad (50)$$

The stability of the synchronized state is then measured by the second Lyapunov exponent $\lambda_2^{(3)}$, which is proportional to the second eigenvalue $\Lambda_2^{(3)}$ of the Laplacian $L^{(3)}$. When interactions of all different orders are present, it is practical to define a *multi-order Laplacian* $L^{(\text{mul})} = \{l_{ij}^{(\text{mul})}\}$ as $l_{ij}^{(\text{mul})} = \frac{K_1}{\langle k_1 \rangle} l_{ij}^{(1)} + \frac{K_2}{\langle k_2 \rangle} l_{ij}^{(2)} + \dots + \frac{K_{q_{\max}}}{\langle k_{q_{\max}} \rangle} l_{ij}^{(q_{\max})}$ so that the linearized equations read:

$$\delta\dot{\theta}_i = - \sum_{j=1}^N l_{ij}^{(\text{mul})} \delta\theta_j, \quad (51)$$

and the stability of the synchronized solution can be assessed by simply computing the second Lyapunov exponent $\lambda_2^{(\text{mul})}$, which is proportional to the second eigenvalue $\Lambda_2^{(\text{mul})}$ of the multi-order Laplacian $L^{(\text{mul})}$. The authors have then applied the multi-order Laplacian framework to simplicial complexes of increasing complexity. In the case of all-to-all higher-order interactions, where all possible interactions take place at each order, a full analytical spectrum can be obtained. When only attractive couplings are present, the spectrum indicates (i) that the higher the order of pure interactions, the more these interactions stabilize synchronization, as shown in Fig. 23A-C, and (ii) that the more orders are taken into account, the more stable synchronization is, as shown in Fig. 23D. When instead the coupling is attractive at some orders, and repulsive at others, the interplay of the different terms can either lead to stability or instability, which confirms and extends a result found in Ref. [406]. Decaying couplings strength have also been considered in analogy with higher-order phase reduction techniques discussed in the next section. The multi-order Laplacian is also applied to other models of simplicial complexes, such as the simplicial star-clique model, and real-world brain system. The multi-order Laplacian is a general tool that can be used to investigate the effects of higher-order interactions in other oscillatory systems.

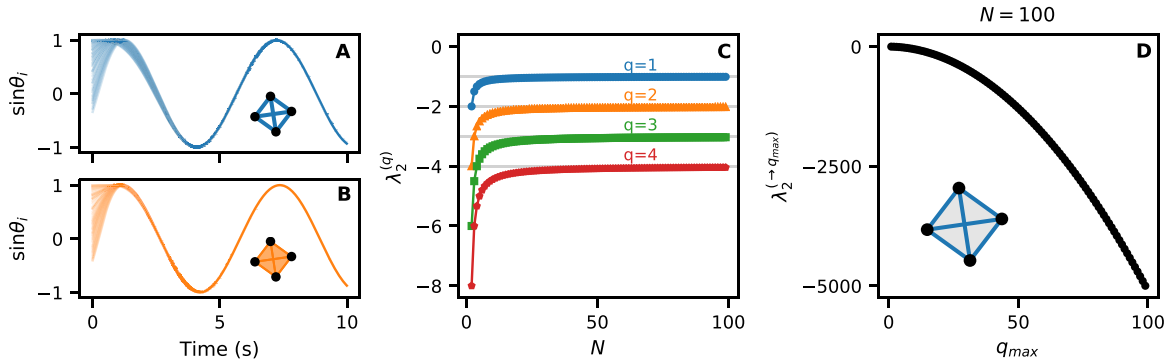


Fig. 23. Higher-order oscillator model of Ref. [159] in the case of all-to-all higher-order interactions. The higher the order of interactions taken into account, the more stable the synchronized state. Convergence of $N = 100$ oscillators with (A) only 1-simplex interactions and (B) only 2-simplex interactions. Convergence is faster in the second case. (C) This is confirmed by the analytical first non-zero Lyapunov exponent at each order q , which is proportional to q . Here, it is plotted against N . (D) Multi-order Lyapunov exponent more negative as q_{\max} is increased. Source: Figures reproduced from Ref. [159].

6.1.2. Higher-order interactions from phase reduction

Real-life oscillators are often nonlinear, and their dynamics is more complex than that of a simple phase oscillator. However, one can obtain phase models that approximate the original dynamics by using phase reduction techniques [421,422]. This makes phase models very powerful since they can capture the dynamics of networks of general nonlinear oscillators, as long as they are weakly coupled. For example, the Kuramoto-Sakaguchi model can be obtained via a phase reduction of the mean-field complex Ginzburg-Landau equations [414]. The Kuramoto-Sakaguchi model is an extension of the original Kuramoto model obtained by the addition of a phase shift α in the coupling function $\sin(\theta_j - \theta_i + \alpha)$ in Eq. (40). However, the Kuramoto-Sakaguchi model is still a first-order phase approximation in the weak coupling parameter limit, and it only displays full incoherence or synchronization (see Refs. [395,396] for the case of identical oscillators). Other nontrivial dynamics such as chaos, cluster states, or weak chimeras, have only been observed by introducing different symmetries or more harmonics in the coupling function [423]. Ashwin et al. have noted ahead of time that, even though adding harmonics does unfold degeneracies, there might be some that will only unfold by considering non-pairwise interactions [423]. More recent results indicate, however, that many-body interactions emerge naturally when considering phase reductions including higher-order terms in the weak coupling parameter [404,414,424]. Moreover, these studies show that the inclusion of higher-order terms unlock nontrivial dynamical regimes as well as transitions between them. In this section, we will only review studies approaching phase reduction of higher-order networks of oscillators from a theoretical point of view. Section 6.3 will then be complementary to this section, as phase reduction will there be approached from the inverse-problem point of view of network inference.

Ashwin, Bick, Rodrigues, and coworkers have produced a series of important contributions for phase reduction of populations of identical oscillators [404,425–428]. The authors of Ref. [423] have suggested that interactions beyond pairwise might be the only way to unfold some degeneracies and unlock nontrivial dynamics [423]. In a paper published in the same year [404], Ashwin and Rodrigues have shown that the application of phase reduction to a systems of generic nonlinear identical systems with global symmetric coupling yields the Kuramoto-Sakaguchi at the lowest order, but at the next order, terms including 2-, 3-, and 4-body interactions naturally emerge:

$$\dot{\theta}_i = \tilde{\Omega}(\theta, \epsilon) + \frac{\epsilon}{N} \sum_{j=1}^N g_2(\theta_j - \theta_i) + \frac{\epsilon}{N^2} \sum_{j,k=1}^N g_3(\theta_j + \theta_k - 2\theta_i) + \frac{\epsilon}{N^2} \sum_{j,k=1}^N g_4(2\theta_j + \theta_k - \theta_i) + \frac{\epsilon}{N^3} \sum_{j,k,l=1}^N g_5(\theta_j + \theta_k - \theta_l - \theta_i). \quad (52)$$

The inclusion of such terms allows for a wider range of dynamical behaviors such as cluster states, and predictions that are valid for longer timescales. Moreover, the authors have been able to demonstrate that non-pairwise interactions yield multistability via the coexistence of many two-cluster states, with varying cluster size, just as in Refs. [401,403]. Here, the many-body interactions terms are traced back to cubic nonlinearities in the original nonlinear system.

Bick et al. have further investigated the dynamics of the phase reduced system of Eq. (52), looking in particular for the possibility of chaos in small networks [425]. Previously, it was thought that for populations of identical oscillators, higher harmonics in the coupling functions, or nontrivial amplitude dynamics, were necessary to observe chaos in small networks ($N = 4$ is smallest theoretical size to exhibit chaos). In fact, for pure pairwise interactions, for $N = 4$, the only known coupling function to yield chaos has a minimum of four nontrivial harmonics (for larger networks, less harmonics are needed) [429]. Remarkably, the authors of Ref. [425] were able to show that two nontrivial harmonics are sufficient to see chaos, even in the case $N = 4$, when many-body interactions are considered. In the last two years, Bick and coworkers have produced three more pieces of work in the same direction, focusing in particular on heteroclinic cycles [426–428]. In the first paper Bick has considered M populations of N oscillators each, with pairwise interaction

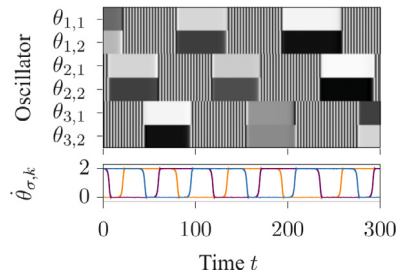


Fig. 24. Switching dynamics in the Bick model of Ref. [426] with three populations of two oscillators each. The oscillators in the three populations intermittently synchronize and desynchronize.
Source: Figure reproduced from Ref. [426].

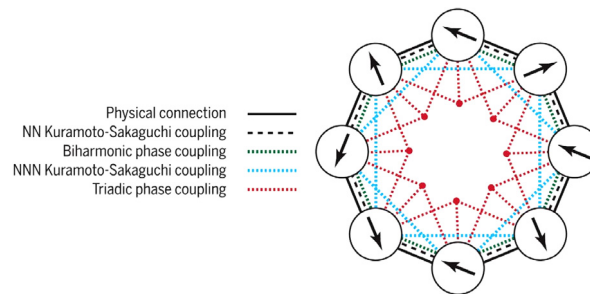


Fig. 25. Ring of eight nano-electromechanical nonlinear oscillators from Ref. [424]. The solid black lines represent physical connections between the oscillators. Dashed and dotted lines represent effective higher-order coupling that appear in the phase reduced model. This systems exotic complex dynamics.
Source: Figure reproduced from Ref. [424].

between oscillators in the same population, and non-pairwise interactions among oscillators of different populations [426]. In Bick's setup, all oscillators have identical frequencies, and it is the presence of nonpairwise interactions that yields the heteroclinic connections joining the weak chimeras. Indeed, as shown in Fig. 24 switching between states of so-called localized frequency synchrony were observed [426]. Bick has further built on that paper to formally prove the existence of those heteroclinic cycles in Ref. [427], and finally to assess their stability together with Lohse in Ref. [428]. Another example of multi-population setups, relating to higher-order interactions, can be found in [430], this time with distinct but resonant frequencies between populations.

More recently, León and Pazó have produced a very thorough study of the higher-order phase reduction of the mean-field complex Ginzburg-Landau equation (MF-CGLE) [414]. To date, the phase reduction of MF-CGLE was only known up to the first order, and produces the standard Kuramoto model of Eq. (40). The Kuramoto model exhibits two dynamical regimes only, synchronization and incoherence, but is unable to reproduce more exotic regimes of the MF-CGLE, such as quasiperiodic partial synchronization and cluster states. To remedy that, the two authors have proposed a isocron-based phase reduction method up to the second and third order. Crucially, the authors demonstrate the accuracy of their technique by showing that the obtained phase model does exhibit the exotic dynamics of the weakly coupled MF-CGLE.

Finally, Matheny et al. have published a very complete study combining experiments, numerics, and analytics [424]. They have performed experiments with a ring of eight nano-electromechanical nonlinear oscillators, and have observed exotic and complex dynamics including weak chimeras, decoupled states, traveling waves, and inhomogeneous synchronized states. Then, they have obtained a phase approximation of their initial nearest-neighbor (i.e. pairwise interactions) network of so-called saturated oscillators, up to the second order in the coupling strength. As in the other studies, terms with three-body interactions naturally emerged in the phase description, with the addition of next-nearest neighbor and biharmonic terms as illustrated in Fig. 25. The strength of their phase model is that it is able to qualitatively reproduce all the complex dynamics regimes observed both in the experiments and in the initial nonlinear model.

In conclusion, phase reduction naturally yields higher-order interactions between the phases. Progress in analytical phase reduction up to higher-order can potentially help us understand the exotic and complex dynamics of network of general nonlinear oscillators, which cannot be captured by first-order phase models. Moreover, it will certainly be helpful in the future to the network inference area presented in Section 6.3. Finally, it is also worth mentioning that some efforts have been made to compute phase reductions numerically, when no analytical derivation is available [431].

6.2. Nonlinear oscillators

6.2.1. Chaotic oscillators

When chaotic oscillators are coupled, they can synchronize in various ways. The study of chaotic synchronization started with two seminal papers published in the 90s [432,433]. In the first of these works, Pecora and Carroll discovered the phenomenon of *complete synchronization*, a regime in which coupled chaotic oscillators converge to an identical state and evolve with the same trajectory [432]. Then, Rosenblum, Pikovsky and Kurths, showed that chaotic oscillators can *phase synchronize*, while their amplitudes vary chaotically and are uncorrelated [433]. The richness of the dynamics of chaotic oscillators allows for more complex behaviors in networked systems than those observed with phase oscillators, and has been the object of interest in the scientific community [376]. However, all the studies on chaotic synchronization, with very few exceptions [434–436], have considered pairwise interactions. We will therefore start our discussion of higher-order effects with a series of studies related to network motifs.

In Ref. [437] Lodato et al. have investigated whether there can be an underlying dynamical reason to explain the existence of network motifs. In particular they have focused on synchronization and have evaluated analytically the stability of the synchronous state in all directed and undirected 3- and 4-node graphs of chaotic oscillators. They have then compared the results with the known abundance of these small graphs as subgraphs (motifs) of real biological systems. Interestingly, the authors were able to show that 3- and 4-node graphs exhibiting more stable synchronous states in general coincide with network motifs preserved across evolution, while the bifan motif, one of the three most relevant biological motifs [72], was not compatible with synchronization for any type of chaotic dynamics. In another study [438], Soriano et al. have investigated the link between generalized synchronization and correlation between the oscillators present in a motif, remarkably showing that it is possible to construct small graphs of oscillators that synchronize but at the same time do not exhibit correlations. This result, important for network inference, stresses how indirect connections might be systematically underestimated. Finally, it is worth mentioning here one more study on motifs [439]. Although the oscillators considered were not chaotic, a fractal topology was used. The authors were able to analytically compute the stability of various dynamical regimes. As an example, they showed that oscillation death was possible in that setting, even with a symmetric coupling function.

We continue with four studies of synchronization in bipartite setups representing two types of populations of oscillators, with inter-population links. The first study considered a complete bipartite network of nonlinear maps (chaotic or periodic) [440]. The existence and stability of synchronization and cluster synchronization was assessed via Lyapunov exponents through the Master Stability Function (MSF) formalism [13,383,441]. Similarly, the second study investigated chaotic synchronization in coupled Bernoulli maps by using the same formalism [442]. The bipartite setting was one of the settings investigated, and the study concluded that synchronization was not possible in that setting. In the third study [443], Sorrentino and Ott used a bipartite setting as a special case of multiple interacting populations of oscillators. The authors found that adding intra-population links could enhance the stability of so-called multisynchronous states. Finally, bipartite networks (together with random and tree-like networks) were one of three settings in which Pecora et al. showed the possibility for cluster synchronization and so-called isolated desynchronization [387]. The latter is a dynamical regime in which one or more clusters desynchronize while the other clusters remain synchronized.

It was as early as 1998 that the synchronization of coupled chaotic circuits was studied by Wu on hypergraphs [434]. The system under consideration consisted of identical chaotic circuits (the nodes of the hypergraph) coupled via multi-terminal resistance-devices, effectively yielding multi-circuit interactions (the hyperlinks). For the sake of mathematical tractability the author restricted his study to a case with only triplet interactions. By looking at the algebraic connectivity of the hypergraph, defined as the smallest nonzero eigenvalue of the hypergraph Laplacian, he was then able to derive sufficient conditions for the complete synchronization of the circuits. Indeed, a large algebraic connectivity and linear but passive coupling were required to yield synchronization. Note that all computations rely on the hypergraph structure, even if the system was represented as a bipartite network in the figures of the original paper. A more recent study by Krawiecki has gone much further in complexity [435]. In particular, the author has considered a system of identical chaotic (Lorenz) oscillators placed on the nodes of scale-free q -hypergraphs (with $q \geq 2$), i.e. hypergraphs that exhibit only $(q - 1)$ -simplex interactions, i.e. in which each hyperedge connects exactly q nodes, and the number of hyperedges attached to a node follows a power-law distribution. He found out that a state of complete synchronization can be achieved and coexists with a state of oscillation death [444]. Remarkably, the traditional Master Stability Function formalism was generalized to hypergraphs so as to investigate the stability of the complete synchronization state. Furthermore, the study has reported the existence of other dynamical regimes such as partial anti-synchronization.

In another study [316], Wu et al. have derived analytical criteria for the synchronization of Chua oscillators in q -hypergraphs. The hypergraphs have a power law distribution of hyperdegrees such that when $q = 2$, the structure reduces to that of a Barabási-Albert network. Recently, Mulas et al. [445] used the Master Stability formalism to derive stability criteria in coupled nonlinear oscillators on hypergraphs with the particularity that they are directed.

Finally, very recently, Gambuzza et al. [436] have generalized the Master Stability Function formalism to the most general case of simplicial complexes. They have considered a system of N dynamical units, which are placed on the nodes of a simplicial complex of any dimension q_{\max} and can be involved in q -simplex interactions, with $q = 1, 2, \dots, q_{\max}$, as described by the structure of the simplicial complex. The equations of motion of the system read:

$$\begin{aligned} \dot{\mathbf{x}}_i = & \mathbf{f}(\mathbf{x}_i) + \sigma_1 \sum_{j_1=1}^N a_{ij_1}^{(1)} \mathbf{g}^{(1)}(\mathbf{x}_i, \mathbf{x}_{j_1}) + \sigma_2 \sum_{j_1=1}^N \sum_{j_2=1}^N a_{ij_1 j_2}^{(2)} \mathbf{g}^{(2)}(\mathbf{x}_i, \mathbf{x}_{j_1}, \mathbf{x}_{j_2}) + \dots \\ & + \sigma_{q_{\max}} \sum_{j_1=1}^N \dots \sum_{j_{q_{\max}}=1}^N a_{ij_1 \dots j_{q_{\max}}}^{(q_{\max})} \mathbf{g}^{(q_{\max})}(\mathbf{x}_i, \mathbf{x}_{j_1}, \dots, \mathbf{x}_{j_{q_{\max}}}), \end{aligned} \quad (53)$$

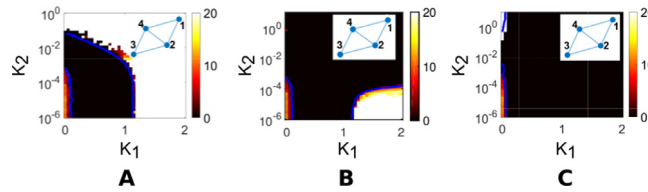


Fig. 26. Coupling functions affect synchronization in simplicial complexes of coupled chaotic oscillators as in the framework of Ref. [436]. Synchronization phase diagram of a system of four Rössler systems are coupled in pairs and triplets according to the simplicial complex sketched. A baseline case (A) is compared to (B) where the pairwise coupling function is changed, and (C) where the triplet coupling function is changed. The predictions of the Master Stability Function formalism (blue lines) are in good agreement with the regions of synchronization obtained by numerical simulations (black).

Source: Figures adapted from Ref. [436].

where $\mathbf{x}_i \equiv \mathbf{x}_i(t)$ is the m -dimensional vector describing the state of node (dynamical unit) i at time t , the real valued parameters $\sigma_1, \dots, \sigma_{q_{\max}}$ tune the strength of the interactions at the different orders $q = 1, \dots, q_{\max}$, and $a_{ij_1 \dots j_q}^{(q)}$ are the entries of the adjacency tensor $\mathbf{A}^{(q)}$ representing the structure of the simplicial complex. Furthermore, $\mathbf{f} : \mathbb{R}^m \rightarrow \mathbb{R}^m$ is the most general function describing the local dynamics, which is assumed to be identical for all units, while $\mathbf{g}^{(q)} : \mathbb{R}^{(q+1) \times m} \rightarrow \mathbb{R}^m$, with $q = 1, \dots, q_{\max}$, are the functions governing the interaction forms at different orders. The authors have been able to study analytically the stability of the complete synchronized state $\mathbf{x}_i(t) = \mathbf{x}^S(t) \forall i$, under the only assumption that the coupling functions are synchronization non-invasive, i.e. that $\mathbf{g}^{(q)}(\mathbf{x}^S, \mathbf{x}^S, \dots, \mathbf{x}^S) \equiv \mathbf{0} \forall q$. Based on a set of Laplacian matrices similar to those in Eq. (49), they have derived a Master Stability Function with the negativity of the maximum Lyapunov exponent as the stability criterion. The method has been illustrated on simplicial complexes of coupled chaotic oscillators, such as Rössler and Lorenz dynamical systems, with both pairwise and triplet interactions. When nonlinear oscillators are coupled, the Lyapunov exponents depend nonlinearly on the eigenvalues of the Laplacian of the system. Hence, it is possible to have bounded regions of the parameter space where synchronization is stable, as defined by a negative maximum Lyapunov exponent. The authors have investigated how the region of stability depends on the structure of the simplicial complex and on the coupling functions. Fig. 26 shows an example of coupling functions for which the region of synchronization is respectively bounded (Fig. 26A) and unbounded (Figs. 26B,C), for a given node dynamics and structure of the simplicial complex. This framework will hopefully be used in further studies along those lines, for various oscillators, topologies, and coupling functions.

Finally, a different approach based on the Laplacian introduced in Ref. [345] was recently used to extend the Master Stability Function formalism to hypergraphs [371].

6.2.2. Neuron models

The brain provides a very rich and important terrain to study synchronization of neurons with higher-order interactions. However, so far, little is known about synchronization of neuron models in higher-order networks from the theoretical side. In the theoretical study of neuronal networks, various oscillators models are used to represent neurons, depending on the context and the goals of the modeler [446,447]. Historically, the most famous model is that of Hodgkin and Huxley, dating back from 1952 and for which they won a Nobel Prize in Physiology or Medicine. Their model describes how the neurons spike, and consists of a set of nonlinear differential equations for the membrane potential. Other models such as neural mass models have been developed since and have been used successfully to understand synchronization phenomena in the brain. Here, we report the different higher-order settings in which synchronization of neuron models has been carried out.

We start with a bipartite setting that was investigated in [448]. Here the authors use that setting as a mean to study the interactions between two populations of neurons, and in fact study two coupled bipartite networks. The authors concluded, by analytical and numerical calculations, that the two networks can be synchronized with the help of adaptive feedback.

Only a few studies have considered synchronization in motifs of neurons [449–453]. Shilnikov and collaborators [449] provide a detailed analysis of synchronization in motifs of both inhibitory and excitatory, and inhibitory-only neurons, see for example Fig. 27. The authors showed that the neurons can self-organize to designate the pacemaker among them by shortening the burst duration of the (secondary) driven neuron. This effect holds in inhibitory-only motifs, but the synchronous patterns can coexist with asynchronous patterns. The authors show that the addition of excitatory links ensure synchronous patterns of bursting. Finally, the inhibitory-only motifs exhibited multistability with as much as eight coexisting attractors. The authors suggest these attractors could be associated with patterns known to control certain animal and human locomotion activities. More recently, more insight was provided about bifurcations in 3-neuron motifs [452,453], and polyrhythmic synchronization [449].

In the second study [450], so-called anticipated synchronization was shown to exist and be stable in biologically plausible 3-neuron motifs including inhibitory and excitatory synapses with time delays. All parameters have a clear biological interpretation, and the authors identified a transition from delayed synchronization to anticipated synchronization when synaptic conductances are increased within physiological ranges.

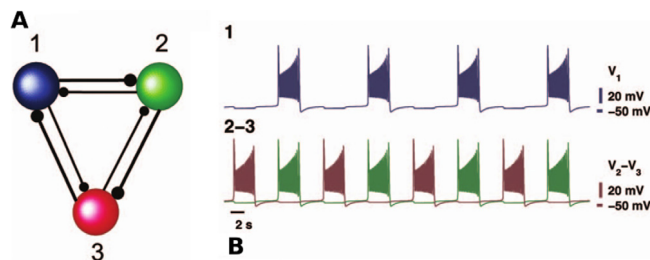


Fig. 27. Synchronization pattern in inhibitory motif from Ref. [449]. The pacemaker neuron (blue) is the one with the longer interburst time. Source: Figure adapted from Ref. [449].

In the third study [451], Gollo et al. identified a mechanism by which zero-lag synchronization is facilitated. Zero-lag synchronization is of widely accepted importance in brain studies. Indeed, experimental evidence shows zero-lag synchronization between distant regions of the brains. A mechanism called “dynamical relaying”, related to a specific motif, was proposed to account for such phenomenon in the presence of conductance delays. However, Gollo and coworkers showed that the motif was not always a reliable condition for zero-lag synchronization. Instead, they narrowed down a “resonance pair” of reciprocally connected neurons, which ensures zero-lag synchronization. They did so by systematically analyzing synchronization in small network motifs of Hodgkin–Huxley, neural mass, and Izhikevich neurons.

Finally the few studies that considered synchronization in larger networks of neurons relied either on numerics or phase reduction techniques, such as [403], and were described in the corresponding sections above. For more applied studies on the higher-order structure of brain networks in neuroscience, see Section 9.2.

6.3. Inference of nonpairwise interactions in coupled oscillators

In networks of coupled dynamical units, the standard approach is to fix the structure of the network and to study how the system evolves. However, when modeling real oscillatory networks, we very often have to face the so-called inverse-problem too: can we reconstruct the underlying network structure by just looking at the dynamical evolution of the system? This is a problem with relevant applications. In neuroscience, for example, one wants to infer the brain neuronal network from EEG data, i.e. times series of the electrical activity of neurons or cortical areas. This task, known as network inference, is highly non trivial, and three main approaches have been proposed in the literature to reconstruct directional pairwise interactions based on information theory [454], state-space approaches [455], and phase dynamics [456]. Here, we report on the few studies that have addressed the inference of higher-order interactions, i.e. of interactions between three or more oscillators, based on the third approach using phase dynamics.

Following [457], let us start by considering the general system of N coupled dynamical equations:

$$\dot{\mathbf{x}}_i = \mathbf{G}_i(\mathbf{x}_i) + \epsilon \mathbf{H}_i(\mathbf{x}_1, \dots, \mathbf{x}_N), \quad (54)$$

with $i = 1, \dots, N$, where function \mathbf{G}_i determines the local (uncoupled) dynamics of oscillator i , ϵ is the coupling strength, and \mathbf{H}_i is the function describing the structural coupling. It is assumed that the \mathbf{G}_i are such that each uncoupled oscillator has a stable limit cycle, which can be parametrized by a phase θ_k . The *structural couplings* are directed physical couplings, e.g. synapses in the case of neurons. If \mathbf{H}_i does not depend on \mathbf{x}_k , we say there is no structural coupling from k to i . In general, \mathbf{H}_i can contain terms of pairwise coupling, $\mathbf{H}_{ij}(\mathbf{x}_i, \mathbf{x}_j)$, triplet couplings, $\mathbf{H}_{ijk}(\mathbf{x}_i, \mathbf{x}_j, \mathbf{x}_k)$, or coupling between any larger numbers of oscillators. For example, one can write $\mathbf{H}_i = \sum_j \mathbf{H}_{ij}(\mathbf{x}_i, \mathbf{x}_j)$, if only pairwise interactions are present in the network. In the case of weak coupling, i.e. in the small ϵ limit, each individual limit-cycle is perturbed weakly enough so that system (54) has an attracting N -torus solution which can be written in terms of N phases $\theta_1, \dots, \theta_N$ [457] as:

$$\theta_i = \omega_i + h_i(\theta_1, \dots, \theta_N). \quad (55)$$

The new coupling functions can then be written as an expansion in the small coupling parameter ϵ

$$h_i(\theta_1, \dots, \theta_N) = \epsilon h_i^{(1)}(\theta_1, \dots, \theta_N) + \epsilon^2 h_i^{(2)}(\theta_1, \dots, \theta_N) + \dots, \quad (56)$$

by performing a perturbative reduction of Eq. (54) (see Section 6.1.2). We refer to the couplings functions h_i in system (55) as *effective phase couplings*. It is important to note that, as in Section 6.1.2, the effective phase couplings h_i differ from the original structural couplings \mathbf{H}_i . More specifically, there can be an effective phase coupling from j to i even if there is no structural coupling, but the opposite is not true. So, there are more effective links than structural links. However, if ϵ is sufficiently small, structural and effective couplings are practically identical. Indeed, the additional effective links appear only in the second-order terms $h_i^{(2)}(\theta_1, \dots, \theta_N)$ which is rescaled by ϵ^2 , and in the higher-order terms which scale in higher powers of ϵ .

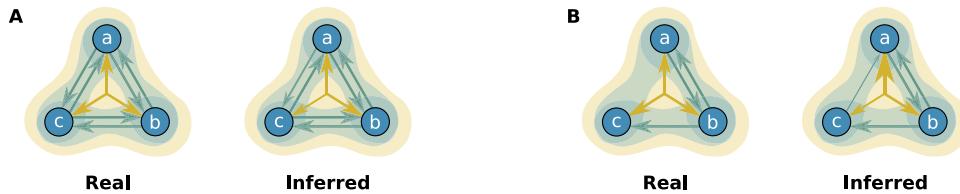


Fig. 28. Inference of directed pair and triplet couplings among three Van der Pol oscillators from the method in Ref. [457]. An arrow from the center to a node i indicates a directed triplet interaction from (j, k) to i . Panels (A) and (B) show two examples of the original structural network and the reconstructed one. While the inference in the first case is good, the method yields a spurious links from node c to a . Source: Figures adapted from Ref. [457].

The goal of the methods proposed in Refs. [457,458] is to reconstruct the effective coupling of the system in Eq. (55), including couplings beyond pairwise, starting from at least one scalar time series for each node of the original system in Eq (54). A situation where only a scalar time series is available for each node is common for example in neuroscience with EEG recordings, and in such cases, the information can be sufficient to reconstruct the phase system (55) but not the original system (54). Such a goal is achieved in two main steps: first, by reconstructing phases from the original time series, and second, by reconstructing the effective phase couplings h_i from the phases. Finally, weighted directed links are extracted from the coupling functions by measuring the so-called partial norms [457] associated to each link. Indeed, since the h_i are 2π -periodic functions of N phases, they can be decomposed into a Fourier expansion for the phases. Then, the pairwise interaction from i to j is determined by the coefficients in the expansion that depend only on i and j , and it can be measured as the sum of the square of those coefficients. More specifically, in Ref. [457] Kraleman et al. have generalized this method of spectral decomposition of the effective coupling functions from Ref. [459] to the case of interactions among more than two oscillators. Hence, each term corresponds to a coupling among two or more oscillators, and its associated partial norm indicates its strength. The numerical method has been successfully tested on networks of size 3, 5, and 9 of van der Pol oscillators. Fig. 28 shows an example of the results obtained in the case of networks with three nodes. In general, the effective links detected by the method reliably reveal the true structural links (pairwise or higher-order). However, the method also detects some additional links, as expected: some are true higher-order links of the phase description, while some others are spurious links, due to a systematic error of the method. Unfortunately, no analytical derivation of the phase reduction exists yet for these systems (see Section 6.1.2 for other systems), so that there is no clear way to distinguish, of those additional links, which are true and which are spurious, to date. The method also successfully avoids detecting functional links. Two oscillators are said to be *functionally coupled* if their dynamics is correlated. Functional coupling is a concept typical of brain activity studies, and it may only be loosely related to structural and effective coupling [460].

It is worth mentioning here that Rosenblum and Pikovsky have developed in parallel a numerical phase reduction beyond the first order to remedy the missing analytical derivations and complement the existing ones [431]. For such a method to work, the available time series data must satisfy two criteria: they must not come from a fully synchronized trajectory, and it must be of sufficient length. Indeed, to infer the coupling functions, the phases must cover the N -torus. Hence, first, when the system is synchronized, however, the dynamics only happens on a limit-cycle, and no information can be extracted. Second, the time series must be long enough to cover the N -torus. Because of this, the method, is practically useless for large networks, as the data needed to cover a N -dimensional space rapidly grows with N . To be able to deal with networks larger than $N > 3$, only partial phase dynamics reconstruction is possible. Typically, one assumes pairwise interactions, and only considers the phases θ_i and θ_j to infer the coupling functions h_{ij} from j to i . The idea is to do so for all pairs of oscillators, and instead of reconstructing the full system in Eq. (55), one only allows for pairwise links to be inferred. However, this method yields spurious effective phase links that do not exist in the full system in Eq. (55) or the original structural connectivity of system in Eq. (54).

To overcome this, Kraleman et al. have extended their previous method discussed above, and have proposed a partial triplet analysis [458]. They have considered all the triplets of phases of the type $\theta_i, \theta_j, \theta_k$ to reconstruct the coupling functions $h_{ijk}, h_{jki}, h_{kij}$. From these functions, pairwise connections have been obtained from the partial norm of the spectral decomposition, as above. The authors have showed that triplet partial analysis performed better than the pairwise partial analysis in networks of 3 and 4 Van der Pol oscillators. Indeed, the true links were detected equivalently well, but the triplet partial analysis successfully avoided detection of spurious links produced instead by the pairwise analysis.

As mentioned above, all these methods need input data that do not come from synchronized trajectories. This can be checked by evaluating the usual pairwise $n:m$ synchronization index $\gamma_{j,k} = |\langle e^{i(n\theta_j - m\theta_k)} \rangle|$, where $\langle \cdot \rangle$ indicates temporal averaging, and where n and m are integers [376]. This index is close to 1 if oscillators j and k are phase locked. Complete network synchronization can be checked by computing the index for all pairs of oscillators. However, triplet synchronization is not revealed by this index. Indeed, it is well possible that three phases $\theta_i, \theta_j, \theta_k$ satisfy the relation $n\theta_i + m\theta_j + l\theta_k = \text{constant}$ for three integers n, m, l , even though the pairwise index of each pair is not close to 1. To reveal triplet synchronization from data, the following triplet synchronization index has been introduced in Ref. [461]:

$$\gamma_{i,j,k} = |\langle e^{i(n\theta_i + m\theta_j + l\theta_k)} \rangle|. \quad (57)$$

Notice that a value of $\gamma_{i,j,k}$ close to 1 is not a sufficient condition for synchronization. Indeed, it only indicates its possibility, since a large value of the index can also be the consequence of other types of interdependence between the phases. Finally, as mentioned by the same authors, the index can be readily extended to higher-order synchronization indices, valid for quadruplets and higher-resonances. Jia et al. have built on that, showing experimentally the existence of states where triplets are synchronized but pairs are not [462].

In Ref. [413], Stankovski et al. have proposed another method to reconstruct the effective phase connectivity of a network. The specificity of their method is that it works for network of oscillators with time-varying coupling and frequencies, and that are subject to noise. The method is based on dynamical Bayesian inference [463], and detects coupled pairs, triplets, and quadruplets of oscillators. The method computes the values of a set of parameters that fully determine the couplings. The values of the parameters are inferred by making use of Bayes' theorem, which takes a prior distribution and evolves it into a posterior distribution, by using time series of the system and building a likelihood function. The authors have demonstrated the accuracy of the method on a simulated 5-oscillator network, as well as on real multi-channel EEG data. The method has been shown to outperform inference based on pairwise interactions only. Unfortunately, similarly to the other methods presented above, this method works for relatively small networks.

For applications of inference methods of higher-order interactions on real brain networks data, see Section 9.2.

7. Spreading and social dynamics

Dynamical processes that emulate human behaviors have been the focus of many studies, where social relationships and interactions are typically considered as an underlying structure [3,15]. Social interactions are a natural testing ground for higher-order approaches. Since individuals can interact in pairs or groups, the dynamics should in turn account for the higher-order effects that the non-pairwise interactions might lead to. In this section, we review a broad variety of models, initially introduced and studied on graphs, that have been extended as dynamical processes on HORs. We start reviewing *spreading processes*, historically embedded within the literature of epidemics on networks [464–467], but often revisited to fit the dynamics of social contagions [468,469]. We then continue with a wider class of models of *social dynamics* mostly devoted to the formation of opinions and consensus [470–474].

7.1. Spreading in higher-order networks

The study of spreading processes on networks is one of the branches of network science that attracted more attention among the community. Building on top of classical epidemiological compartmental models [475–477], the recent success of these models is partially due to the increasing availability of large-scale data that opened up new avenues along the research line initiated by Pastor-Satorras and Vespignani [464]. In this fashion, researchers make use of the newly available data sources to better inform models built to forecast and possibly control the disease spreading [478–484]. In light of these new advancements, network scientists have been slowly, but extensively, introducing more and more details into the modeling framework in order to increase its accuracy and ultimately its predictive power.

The two most studied compartmental models are the Susceptible–Infected–Recovered (SIR) and the Susceptible–Infected–Susceptible (SIS). In both models, susceptible individuals (S) can get infected by mean of an interaction with infectious ones (I). This SI process always leads, by construction, to the absorbing state in which all individuals are infected. The introduction of an additional transition leads to richer phenomena. More specifically, in the case of the SIS, individuals can switch multiple times between the S and I states, eventually reaching a steady state in which the epidemic is sustained by a non-zero number of individuals. Contrarily, in the SIR, individuals gain immunity to reinfections after a certain amount of time, or with a given probability per unit time. These immune individuals are then called recovered (R) and do not participate to the spreading dynamics anymore. This type of models is therefore used when it comes to modeling infectious diseases such as Ebola, or seasonal influenza, in which individuals can acquire immunity against reinfections. As a consequence, the SIR presents also the disease-free state as an absorbing state.

Many theoretical approaches have been developed to analytically describe, with increasing level of complexity also given by the chosen representation, the dynamics of epidemic spreading on complex networks. An accurate analytical description should include the interplay between the structure of the contact patterns and the dynamics of the spreading process on top [38,467,485–489]. Here, instead of going through the assumptions, advantages and drawbacks of all the possible descriptions, from the mean-field (MF) and the heterogeneous mean-field (HMF), to the most accurate microscopic Markov-chain approaches, we refer the interested reader to Refs. [466,490–494] and references therein.

While the aforementioned models have been widely used to study the spread of diseases, there is a variety of other domains where they have been successfully applied. Indeed, there is another long tradition of modelers that used similar frameworks to characterize the spreading of social phenomena, such as the diffusion of rumors and fads or the adoption of novelties and technological innovations [495–499]. However, in all these situations the social nature of the contacts that mediate these processes calls for ad-hoc modeling adjustments that are not present in simple disease epidemics models. These approaches, developed under the name of *complex contagion*, are meant to include additional ingredients, such as mechanisms of social influence and peer pressure, already widely studied within the social sciences [32,65,500]. The requirement of these new features, not needed when dealing with the spreading of a pathogen, gave rise to a plethora of models that have been already extensively reviewed in Ref. [501].

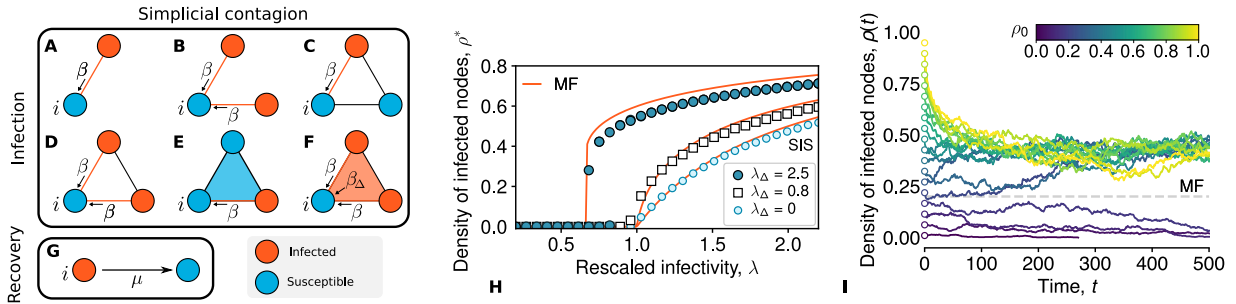


Fig. 29. Simplicial contagion model ($D = 2$) [283]. (A-F) Different channels of infection for a susceptible node i are shown. Notice (F), where node i can get the infection from each of the two 1-simplices with probability β , and also from the 2-simplex with probability β_Δ . Behavior on synthetic random simplicial complexes: In (H) the average fraction of infected obtained by means of numerical simulations is plotted against the rescaled infectivity $\lambda = \beta(k)/\mu$ for different values of λ_Δ ($\lambda_\Delta = 0$ gives results for the standard SIS model without higher-order effects). The red lines correspond to the analytical MF solution described by Eq. (58). When λ_Δ ($\lambda_\Delta = 2.5$) we observe a discontinuous transition with the formation of a bi-stable region where healthy and endemic states co-exist. (I) Temporal evolution of the densities of infectious nodes in the bi-stable region ($\lambda = 0.75$, $\lambda_\Delta = 2.5$). Different curves—and different colors—correspond to different values of ρ_0 , the initial density of infectious nodes. The dashed horizontal line corresponds to the unstable branch of the MF solution, separating the two basins of attraction. Source: Figures adapted from Ref. [283].

Here, keeping the focus on the dynamics of social contagion, we shift the attention towards the structural aspect of the social contacts on top of which the dynamics evolves. Moving from pairwise to higher-order structures, we investigate the dynamical effects brought by the novel representations. There is a matter of discussion whether social relationships could be better modeled by using simplicial complexes rather than hypergraphs. In the end, depending on the situation, it might be reasonable or not to assume that in a group interaction all the sub-interactions among the group members should be considered as well [502]. In what follows, we distinguish between the two approaches and discuss recent developments towards the inclusion of HORs in the modeling approach. Our limited goal is to introduce some of the recent efforts in this direction without imposing selective constraints on how a “pure” higher-order dynamics should be defined on these new structures. This leads to a mixture of models based on higher-order and not-so-higher-order dynamics on HORs. We explicitly distinguish between the HORs, starting from spreading processes that take place on simplicial complexes and then moving to hypergraphs.

7.1.1. Spreading on simplicial complexes

In the simplicial contagion model proposed by Iacopini et al. [283], a simplicial complex is used to represent the social structure on top of which the contagion dynamics takes place. By definition, all the sub-interactions contained in each group interaction are considered. Therefore, the dynamics of the model specifically relies on the different channels of infections (1-simplex, 2-simplex, etc.) through which, with different transmission rates, a contagion can happen. The SIS-like model of order D is controlled via a set of control parameters $\beta_1, \beta_2, \dots, \beta_D$, whose elements represent the probability per unit time for a susceptible node i that participates to a simplex σ of dimension D to get the infection from each one of the infectious faces composing σ (faces in which all nodes but one are infected). At order $D = 2$, one has β_1 and $\beta_2 = \beta_\Delta$ corresponding respectively to the probability that a susceptible node i receives the infection from an infected node j through the link (i, j) and to the probability of receiving it from an infectious 2-simplex (i, j, k) incident on i . The recovery dynamics is controlled by the standard recovery probability μ , which, being node-dependent, does not “feel” the higher-order structure (Figs. 29A-G).

Even the inclusion of only the lowest higher-order interactions (2-simplices) dramatically changes the nature of the spreading process, going from a continuous to a discontinuous phase transition in the prevalence as a function of the 1-simplex infectivity λ (Fig. 29H). Notice that the nature of the transition depends on the 2-simplex infectivity λ_Δ . This behavior is confirmed by numerical simulations on empirical data obtained from the Sociopatterns collaboration [503] and on synthetic random simplicial complexes (see Section 4.1.5), where a bi-stable region in which healthy and an endemic states co-exist appears. This is illustrated in Fig. 29I, in which different curves represent different realizations of the model starting from seeds of infectious nodes of different sizes (colors). Further analytical insights on this bi-stability can be found in Ref. [504].

The authors further explained the observed phenomenology through an analytical investigation based on an extension of the standard mean-field (MF) approach for networks, specifically adapted to the case of HORs. In this case, the general equation for the evolution of the stationary density of infected nodes, $\rho(t)$, reads

$$d_t \rho(t) = -\mu \rho(t) + \sum_{d=1}^D \beta_d \langle k_d \rangle \rho^d(t) [1 - \rho(t)] \quad (58)$$

with $\langle k_d \rangle$ denoting the average generalized degree, i.e., the number of d -dimensional simplices incident on average on each 1-dimensional simplex α : $\langle k_d \rangle = \langle k_{d,1}(\alpha) \rangle_\alpha$ (see Section 3.2.1). This approach confirmed the results obtained on synthetic

random simplicial complexes, showing that the steady-state dynamics, the position, and the nature of the transition can be predicted analytically on social structures characterized by homogeneous degree distributions. This is shown in Fig. 29H, where the MF curves (red) are compared to the simulated results (points), and in Fig. 29I, where the dashed gray line—corresponding to the unstable solution of the MF approach—correctly detects the two basins of attraction that split the simulated curves.

Further developments of the simplicial contagion model based on probabilistic descriptions showed that more complex analytical formulations, namely the microscopic Markov-chain approach [505] and the link equation [506], can improve the accuracy of predictions [507]. Differently from the MF approach, these techniques can be used to analytically describe the contagion dynamics on HORs having heterogeneous structures.

7.1.2. Spreading on hypergraphs

In contrast with simplicial complexes, hypergraphs can be used to describe interactions that only take place in groups, lifting the constraint of having to include all the sub-interactions within the groups themselves. Therefore, hyperedges can efficiently be used to represent clusters or communities, when such sub-interactions are unlikely to be relevant ingredients in the description of social HORs [266,508]. Previous results on spreading dynamics on networks have already showed the impact that the presence of clusters, communities and sub-graphs might have on the epidemic threshold and on the final epidemic size [227,229,240,509–514]. Hypergraphs have been also used to model knowledge diffusion in collaboration networks [515–517].

The idea of modeling communities as hyperedges was first proposed by Bodó et al. [518], who used the nodes of a hypergraph to represent individuals and hyperedges to represent the different communities a node belongs to, such as a household or a workplace [519–521]. The authors studied the behavior of an SIS model on hypergraphs under a continuous time Markov chain formalism in which both infection and recovery are governed by Poisson processes. However, while the recovery is a spontaneous process controlled by a fixed recovery rate γ , the rate of infection r takes into account the higher-order connectivity patterns. In particular, they defined the probability for a susceptible individual to become infected as $1 - \exp(-r\Delta t)$, with r being $r = \tau \sum_e f(i_e)$. The summation runs over all the hyperedges—the communities—containing the susceptible individuals, while $f(i_e)$ denotes a generic function of i_e , the number of infected nodes in the hyperedge e . Bodó et al. chose f to be a piece-wise linear function, with the idea of not increasing the infection pressure for a susceptible node when the number of infected neighbors is higher than a given threshold. This is conceptually different from the conventional threshold mechanism—largely exploited by the complex contagion literature—in which thresholds are used in the opposite way, e.g., to set the critical amount of exposures from the peers that an individual needs in order to adopt a new technology [522,523]. Simulations on hypergraphs having hyperedges of different sizes showed that heterogeneous structures might significantly hasten the initial phase of the spreading when compared to regular hypergraphs, while leading to slightly smaller values of prevalence in the stationary state.

Later, Suo et al. [524] investigated a similar SIS model on hypergraphs particularly designed to study the differences between two different spreading strategies. In the global one, at each time step an infected node i can infect with a probability β all the susceptible neighboring nodes that are connected to i via a hyperedge (global). In the local one, an infected node i randomly chooses e , one of its hyperedges, and then tries to infect all the susceptible nodes in e (local) with probability of success β . This is inspired by the different ways in which an individual might decide to share a content on a social media platform, either to all the contacts or exclusively targeting a particular group. Notice that, differently from the higher-order models previously introduced, here the HOR is used as a structure, but the global contagion dynamics does not specifically “feel” it. Hence, the global spreading strategy would in principle be equivalent to the one defined on the 1-skeleton of the hypergraph, in which each hyperedge is a clique instead. The two different strategies lead to different long term behaviors, with a vanishing epidemic threshold in the global strategy. Contrarily, the particular positioning of the initial seed of infectious nodes—either on high or low hyperdegree nodes—seems to affect only the early evolution of the process: as expected, choosing nodes with a high hyperdegree as seeders can significantly speed up the contagion in the early times. No differences in the stationary states were found.

The two models just presented made use of the HOR to define the neighborhood of a node that might be responsible for a contagion event, but no explicit mechanism of peer pressure was included in the modeling framework. Here, we briefly discuss two following works in which, differently from before, the higher-order representation explicitly enters into the contagion dynamics to account for reinforcement effects that might occur at the group level.

Jhun et al. [525] extended the simplicial contagion model discussed in Section 7.1.1 to the more general case of hypergraphs. The SIS-like model works exactly as the one proposed by Iacopini et al. [283], but this time the spreading process takes place on top of d -uniform hypergraphs in which all the hyperedges have the same size d . As for the simplicial model, a susceptible node that is part of a hyperedge α of size d can get an infection from α , with rate β_d , only if the remaining $d - 1$ nodes composing α are infectious. As for the recovery, the standard recovery probability μ is used. The authors considered the case of scale-free (SF) uniform hypergraphs. Notice that even if all the hyperedges have the same size, different nodes can belong to a different number of these hyperedges. In this sense, the heterogeneity is given by the number of hyperedges a node belongs to, which is distributed as $\sim P(k)^\gamma$. The heterogeneous mean-field formalism (HMF)—in which nodes of the same hyperdegree class are considered equivalent [464]—leads to the following equation for the evolution of the stationary density of infected nodes of hyperdegree k :

$$d_t \rho_k = -\mu \rho_k + \beta_k (1 - \rho_k) k \Theta^{d-1} \quad (59)$$

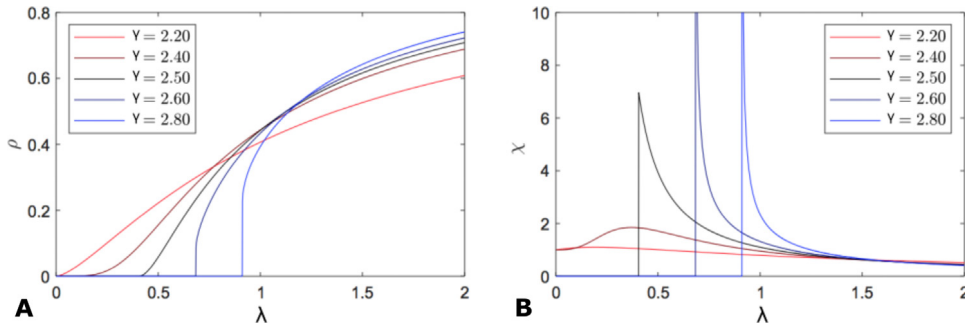


Fig. 30. Behavior of the higher-order contagion model on scale-free uniform hypergraphs ($D = 3$) [525]. (A) Stationary density of infected nodes against control parameter $\lambda \equiv \beta/\mu$ for different values of the SF exponent γ . For $\gamma = 2.2$ and 2.4, the epidemic threshold vanishes ($\lambda_c = 0$), while λ_c is finite for higher values of γ . For $\gamma = 2.2, 2.4$ and 2.6, the transition is second-order, and for $\gamma = 2.6$ and 2.8 the transition is hybrid. (B) Susceptibility χ versus λ . For $\gamma \leq \gamma_c$, χ converges to a finite value $1 + d(d-2)$. In contrast, for $\gamma > \gamma_c$, the susceptibility diverges as $\lambda \rightarrow \lambda^+$. Source: Figures adapted from Ref. [525].

The contagion term on the r.h.s. considers the probability that a susceptible node of hyperdegree k gets the infection from one of the hyperedges. This is, as usual, proportional to the infection rate β_k , the number of hyperedges k , and the probability Θ^{d-1} to be connected to a hyperedge having all the other nodes infected. A comparison of Eq. (59) with Eq. (58) highlights the difference in the representation used. Indeed, differently from the simplicial case, here the contagion term does not depend on the lower order faces.

The resulting phase diagram of the model for a 3-uniform hypergraph is reported in Fig. 30A, where the stationary density of infected nodes ρ is plotted against the re-scaled control parameter $\lambda \equiv \beta/\mu$ for different values of the SF exponent γ . The system presents a characteristic exponent $\gamma_c = 2 + 1/(d-2)$ of the degree distribution that determines the nature of the transition. In particular, for $\gamma < \gamma_c$ the epidemic threshold vanishes ($\lambda_c = 0$), as it is confirmed by the finite value of the susceptibility χ reported in Fig. 30B. By contrast, if $\gamma = \gamma_c$ a second order transition appears, that becomes hybrid when higher values of γ are considered (see curves for $\gamma = 2.6$ and 2.8). The associated values of the susceptibility diverge at the transition point, as expected [526,527]. These results are consistent with simulations on SF uniform hypergraphs, confirming the validity of the HMF approach on such topologies.

Another version of the higher-order social contagion model on hypergraph was recently proposed by de Arruda et al. [258]. Based on a similar SIS framework, the fundamental difference with respect to the other models relies on the explicit inclusion of a critical-mass dynamics into the contagion process that generalizes the one in Ref. [283]. In the simplicial contagion model previously discussed, a susceptible node i belonging to hyperedge α (or a simplex) of size d could get the infection from α only if all the remaining $d-1$ nodes composing it are infected. Here, the authors relax the constraints by (i) moving from simplicial complexes to hypergraphs and (ii) allowing a hyperedge α to be potentially infectious for $i \in \alpha$ if the number of infected nodes composing α is greater or equal to a given threshold Θ_α . The standard SIS model is then recovered by restricting this threshold mechanism to hyperedges of size greater than two, so that a contagion through active links can always happen (no threshold). This model reveals a similar phenomenology to the one on simplices, characterized by the appearance of first and second-order transitions and hysteresis. Further insights on the conditions for the continuity of the phase transition and the stability of general dynamical process on hypergraphs have been subsequently given in Ref. [528]. In addition, the authors provide further analytical results on two particular regular hypergraphs, namely a hyperblob (a random regular network with one hyperedge containing all the nodes) and a hyperstar (a star network with one hyperedge containing all the nodes). The critical values analysis is then extended with the introduction of the concept of a “social latent” heat, interpreted as the fraction of individuals to be added or removed to move the dynamics from one solution to the other.

These findings provide a possible phenomenological explanation for some apparently contradictory results previously obtained. In fact, experimental work has shown different values of critical mass levels needed to initiate a social change, i.e., to revert an existing equilibrium to a new one by mean of a committed minority [529–531]. These threshold values, spanning from 10% to 40%, could be consistently seen as the effect of the interplay between a global critical mass and the local thresholds as given by Θ_α , which also depend on the size of the interacting group.

Finally, Ma and Guo [532] introduced different extensions of the SIR model to hypergraphs. In their model, placed within the framework of rumor spreading [498,533], individuals are divided into the three standard classes corresponding to ignorant (S), spreader (I), and stifler nodes (R). In this particular context, the spreading process models the transmission of information between different members of an enterprise, whose internal structure is characterized by informal organizations (spontaneous groups). In particular, Ma and Guo consider different variations of the mechanism of information transmission. Fig. 31 reports an illustrative example of the probabilistic transmission, as defined by the authors. At $t = 0$ (Fig. 31A), all the nodes are ignorant (blue). At $t = 1$ (Fig. 31B), the information starts to spread, with a given probability, from a randomly selected spreader node (red) to the other nodes within the same hyperedge. Subsequently, the rumor

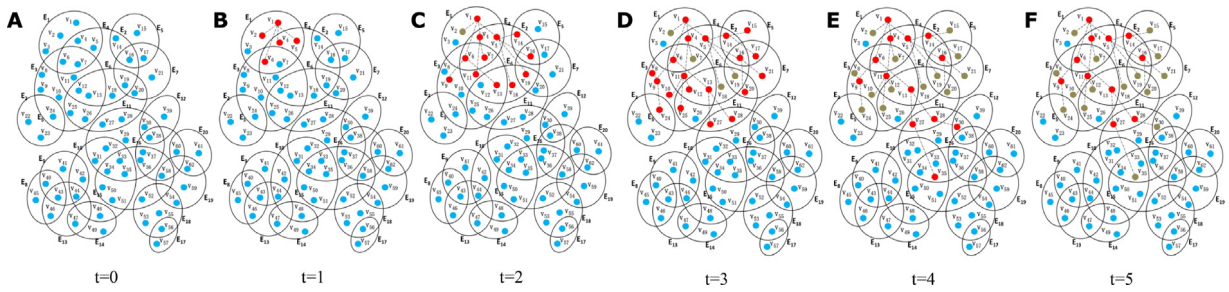


Fig. 31. SIR model on hypergraphs[532]. Ignorant (S), spreader (I), and stifler (R) nodes are respectively depicted in blue, red, and green. At each time step a spreader can transmit the information to ignorant nodes within the same hyperedge with a given probability.

Source: Figures adapted from Ref. [532].

reaches more and more nodes while some nodes become stifler (green) and can no longer spread the information. Other variations where the information passes to the entire hyperedge at once or to a constant number nodes within the same hyperedge are also considered.

7.2. Opinion and cultural dynamics beyond pairwise interactions

In this subsection, we will review some of the best known models of opinion and cultural dynamics. These agent-based models describe social dynamics by relying on simple rules inspired from the physics and mathematics literature, such as spin models and interacting particle systems. Many different variations and extensions have been proposed and extensively studied, therefore we will limit our focus to those for which, in the spirit of this review, an higher-order extension exists. We refer the reader interested in the more general world of sociophysics, statistical physics, and computational social science, to the dedicated reviews [470–474,534–537].

7.2.1. Voter model

With its origins deeply rooted in the statistical physics literature, the voter model is one of the simplest models of opinion dynamics [538]. In the most basic version, it consists in a population of N interacting individuals located on the sites of a lattice, each endowed with a binary variable (spin) $\sigma_i = \{-1, 1\}$, $i = 1, \dots, N$, representing an opinion, or a vote. The fundamental mechanism of the model relies in the node-update rule, according to which, at each time step, a randomly selected node copies the opinion of a randomly selected neighbor (Fig. 32A). This dynamics is iterated until one of the absorbing states of full consensus is reached. Despite its simplicity, this model presents a non-equilibrium dynamics leading to non-trivial behaviors [539]. Extending the voter dynamics from a lattice to a network requires a change of perspective. Indeed, in order to maintain the average magnetization of the system, one has to move from the aforementioned node-update rule to a link-update rule [540] (Figs. 32B,C). This is because the degree heterogeneity potentially present in a network biases the random selection of the neighboring nodes in favor of the most connected ones, ultimately making the “order of play” matter. As for many other dynamical processes on structured populations, the interplay between structure and dynamics has been the focus of many studies [541]. Introducing the many different—and sometimes multilayered [542]—variations of the voter model and their applications [543] goes beyond the scope of this review, therefore we now focus on the particular version that has been generalized in order to account for higher-order interactions.

If we let the node variables take more than two values—going beyond binary opinions—we can call colors these different opinions, and as a consequence the voter dynamics becomes a coloring *coordination game* (see Section 8). Motivated by coloring game experiments [544,545] in which agents make informed decisions based on some local information available, i.e., a subset of nodes, Chung and Tsistas used hyperedges as a natural way to encode these group interactions [546]. In their model, voters have non-pairwise relationships which are represented as hyperedges of a hypergraph, and the dynamics obeys to the following hyperedge-update rule (Fig. 32D). At each time step a hyperedge is selected, and the nodes composing it simultaneously change their vote according to a given probability. In the simplest case this probability does not depend on the status of the voters at the time of the interactions. Further insight on the process can be gained by using the duality of the process with a random walk on an associated weighted graph whose weights encode the transition probabilities among different voting configurations. By performing this mapping, Chung and Tsistas were able to study the dynamics of the memoryless game in terms of the spectral properties of the random walk.

Another prominent research topic in network science deals with the investigation of dynamical processes that directly affects the structure of the network. This co-evolution of network structure with the dynamics that takes place on it is particularly relevant when it comes to modeling social systems, in which the states of the nodes or a behavioral change might force the network to react by changing its connectivity patterns. Voter models with binary opinions have been

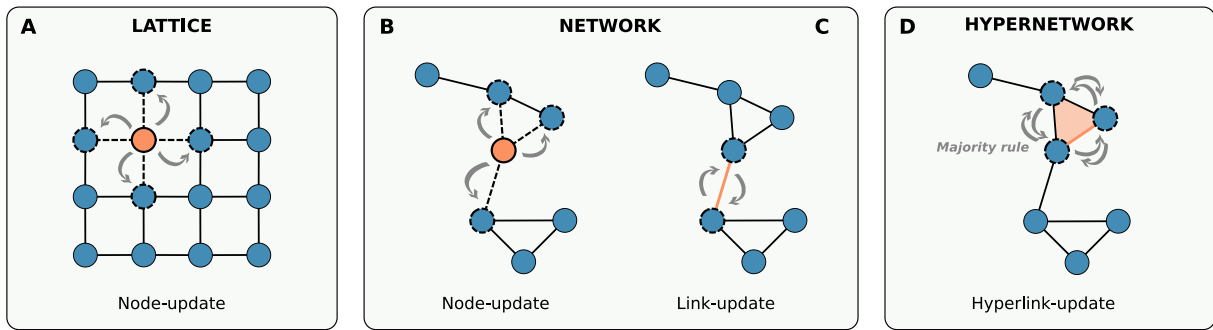


Fig. 32. Voter dynamics on different structured populations. (A) Node-update rule on a lattice and (B) on a network: a randomly selected node copies the opinion of a randomly selected neighbor. (C) Link-update rule on a network: one of the two nodes of a randomly selected edge adapts its opinion to the one of the other, ultimately making e inactive. Recently, Horstmeyer and Kuehn have extended this model in order to account for higher-order structures, such as simplicial complexes [549]. In their model, studied for simplicity up to the level of the 2-simplices, an edge e (1-simplex) is randomly selected. If e is not part of a 2-simplex the standard rules just defined on networks apply. Alternatively, if e is active and part of at least one 2-simplex then a new mechanism of peer pressure might appear. This is controlled via a second parameter $q \in [0, 1]$ representing the probability of the higher-order structure affecting the dynamics through a majority rule. When this happens, with probability q , one of the 2-simplices containing e is selected at random, and all its nodes adopt the opinion of the majority with probability p . Similarly to the standard case, with probability $1 - p$ a rewiring happens, but this time on the 2-simplices. In particular, all the 2-simplices containing e are “downgraded” to three standard 1-simplices and an equal number of new 2-simplices is created by randomly “promoting” triangles of the network formed solely by 1-simplices. However, this mechanism combined with the rewiring leads to a natural depletion of 2-simplices that determines the stopping criterion for the simulations (when there are no triangles left to “promote”). This model reduces to the standard one when $q = 0$, while for $q > 0$ the simplicial structure plays a relevant role on the dynamics. In this last regime, the characteristic behavior of the adaptive voter model does not change and one can still observe a transition at a critical value p_c between an active phase with a nonzero stationary density of active links and a frozen phase in which the system breaks up into two disconnected components having opposite opinions. However, the higher-order structure has several effects on the model dynamics. When $q > 0$ the speed at which the dynamics reaches the two phases is increased, the critical p_c separating the phases is shifted towards lower values of rewiring, and the stationary density of active edges in the first phase is lowered due to the peer pressure mechanism introduced.

widely extended in this direction, and many versions of adaptive voter models have been proposed [547]. The minimal adaptive voter model on networks works as follows [548]. At each time step an edge e is randomly selected. If e is inactive, i.e., it connects nodes with the same opinion, nothing happens. Contrarily, if e is active, there are two possible mechanisms, both leading to the death of this active link in favor of an inactive one. More precisely, with probability $p \in [0, 1]$ a rewiring happens. In this case a randomly selected node between the two composing e rewires to a random node in the network that shares its own opinion. Otherwise, with probability $1 - p$ one of the two nodes of e , selected at random, adapts its opinion to the one of the other, ultimately making e inactive. Recently, Horstmeyer and Kuehn have extended this model in order to account for higher-order structures, such as simplicial complexes [549]. In their model, studied for simplicity up to the level of the 2-simplices, an edge e (1-simplex) is randomly selected. If e is not part of a 2-simplex the standard rules just defined on networks apply. Alternatively, if e is active and part of at least one 2-simplex then a new mechanism of peer pressure might appear. This is controlled via a second parameter $q \in [0, 1]$ representing the probability of the higher-order structure affecting the dynamics through a majority rule. When this happens, with probability q , one of the 2-simplices containing e is selected at random, and all its nodes adopt the opinion of the majority with probability p . Similarly to the standard case, with probability $1 - p$ a rewiring happens, but this time on the 2-simplices. In particular, all the 2-simplices containing e are “downgraded” to three standard 1-simplices and an equal number of new 2-simplices is created by randomly “promoting” triangles of the network formed solely by 1-simplices. However, this mechanism combined with the rewiring leads to a natural depletion of 2-simplices that determines the stopping criterion for the simulations (when there are no triangles left to “promote”). This model reduces to the standard one when $q = 0$, while for $q > 0$ the simplicial structure plays a relevant role on the dynamics. In this last regime, the characteristic behavior of the adaptive voter model does not change and one can still observe a transition at a critical value p_c between an active phase with a nonzero stationary density of active links and a frozen phase in which the system breaks up into two disconnected components having opposite opinions. However, the higher-order structure has several effects on the model dynamics. When $q > 0$ the speed at which the dynamics reaches the two phases is increased, the critical p_c separating the phases is shifted towards lower values of rewiring, and the stationary density of active edges in the first phase is lowered due to the peer pressure mechanism introduced.

7.2.2. Majority models

A similar class of models is the one of the *majority models*, originally proposed by Galam [550]. In the most basic formulation, individuals are endowed with binary state variables denoting opinions, and interact without specific topological constraints. These models behave similarly to the voter-like models discussed above, but with one fundamental difference in the updating rule. In fact, as the name suggests, here the copying mechanism is replaced by a deterministic majority rule according to which, at each time step, a subset of n individuals is chosen and their opinion is set to the one of the majority within the subset. An additional bias—justified as social inertia—that favors a particular opinion is usually introduced to resolve ties when n is even. Typical quantities of interests are the probability of reaching a particular type of consensus as a function of the initial configuration and the time required to reach it. Many studies have been conducted in this regard by using models on lattices and graphs, highlighting the key role played by the dimensionality of the system, together with changes in the dynamics when finite or infinite systems are considered. In all these cases, i.e., when a structured population is used, the node-update consists in adopting the opinion of the majority of the neighboring nodes. In this sense, the majority rule model can be seen as a special case of a threshold model in which the threshold parameter of each node is set to half of the number of neighbors [551].

The spatial version of the majority rule model proposed by Lanchier and Neuffer [552] is based on the idea that social groups are better defined in terms of hyperedges rather than dyadic interactions. Thus, they extended the majority rule model on HORs defined as hypergraphs, so that nodes within each hyperedge simultaneously change their opinion to

the majority opinion of the hyperedge they are part of. By focusing on a particular regular social structure, in which a hyperedge consists of a $n \times \dots \times n$ block on a lattice, they were able to show through analytical results and simulations that, for each dimension, the model dynamics behaves similarly to the voter model when a fixed odd number n of interacting nodes is selected. This means that for hyperedges of even size n the system always reaches a consensus where all the nodes have the opinion favored by the bias, while if n is odd, the system presents growing clusters that eventually reach consensus. This is radically different from the voter model in high dimensions ($d \geq 3$), in which the system reaches a stationary state in which the two opinions co-exists (see Section 9.3).

A popular variation of the majority rule is the *majority model* [538], in which a parameter $q \in [0, 1]$ is introduced so that a node changes its state to the one of the majority of its interacting nodes with probability $(1 - q)$. Since q controls the randomness, sometimes the model goes under the name of majority vote model with noise, and it obeys the following update rule. At each time step, an individual i is selected, and its opinion σ_i is flipped with probability

$$w(\sigma_i) = \frac{1}{2} \left(1 - (1 - 2q) \sigma_i \operatorname{sgn} \left(\sum_j \sigma_j \right) \right) \quad (60)$$

where the sum $\sum_j \sigma_j$ runs over all the nodes j that are interacting with i so that $\operatorname{sgn}(\cdot)$ takes either the sign of the argument or is equal to 0 in case of a lack of majority (zero sum).

Results on regular lattices show that the model undergoes an order-disorder phase transition at a critical value q_c [553], with critical exponents falling within the universality class of the corresponding equilibrium Ising model, with q acting as a temperature. A similar behavior was found on Erdős-Rényi random graphs [554]. By contrast, in small world networks [5,555] the position of the transition point was found to be a function of the rewiring probability [556,557], with critical exponents not belonging to the same universality class of the corresponding Ising model. The same holds for directed and undirected networks with heterogeneous degree distributions $P(k) \propto k^{-\alpha}$ [558,559].

Gradowski and Krawiecki extended the majority vote model to the case of hypergraphs [560]. They introduced two different higher-order versions, a first one based on a node-update rule and a second one based on a hyperedge-update rule. According to the hyperedge-update dynamics, a hyperedge, representing a group, is randomly selected. The majority is then checked within the group. With the node-update dynamics, a random node is selected at random and then the majority rule acts on one of its hyperedges, selected at random as well. In both cases, when a hyperedge α is selected the opinions of all the nodes in α are updated according to the standard rule, as in Eq. (60), but with the sum $\sum_j \sigma_j$ running over all the nodes $j \in \alpha$ instead (including the node of the node-update rule). The main difference between the two rules is in the interaction dynamics. While in the first case each node at each time step interacts with all the other nodes in a shared group, in the second case just the nodes of a single group are considered. Obviously, this difference becomes significant when heterogeneous structures are considered. Thus, Gradowski and Krawiecki studied the model on SF hypergraphs having a hyperdegree distribution that follows a power law $P(k) \propto k^{-\gamma}$ with $\gamma = 1 + \frac{N}{N-m}$, constructed by using a growth model with preferential attachment [312] (see Section 4.2.3). Both dynamics present a similar behavior, with a second-order phase transition appearing at a finite critical value q_c . Notice that here the transition appears even for a SF exponent $2 < \gamma < 3$, while the Ising model on SF networks presents a phase transition at finite temperature only for $\gamma > 3$ [561]. As expected, the heterogeneous structure affects the two dynamics in different ways. In the case of the hyperedge-update, the topology does not have a strong influence on the critical exponents, and the hyperedge dynamics locally behaves as a mean-field for the Ising model. In contrast, when the node-update rule is considered the hypergraph topology matters, and the values of the critical exponents strongly differ from the corresponding equilibrium Ising model on SF networks having the same γ .

7.2.3. Continuous models of opinion dynamics

The different models discussed so far describe the dynamics of interacting agents having discrete opinions. These approaches are suitable in those cases in which an individual can only have a clear and well-defined opinion on a subject, such as in politics, where one could be for or against the introduction of a given policy or the adoption of a given strategy. However, to model the more general dynamics of political orientation, discrete opinion variables might be too restrictive, leaving only “black or white” polarized options. In these cases, the opinion of an individual might be better represented by a continuous variable $x_i \in [0, 1]$ spanning between two extremes [562,563]. Neuhäuser et al. [338] have investigated the effects of non-linear interactions in a model of continuous opinions dynamics on HOrSs. Starting from the formalism of dynamical systems on networks (see Section 5), they have proposed a generalization with (3-body) higher-order interactions that captures the two important social mechanisms of peer pressure and homophily [50,564]. In their model, nodes interact through the hyperedges of size 3 of a hypergraph. The evolution of the N dynamical variables x_i is given by:

$$\dot{x}_i = \sum_{j,k=1}^N A_{ijk} \underbrace{s(|x_j - x_k|)}_{\text{Influence function}} \underbrace{[(x_j - x_i) + (x_k - x_i)]}_{\text{Linear term}} \quad (61)$$

where the adjacency tensor A_{ijk} restricts the interactions between nodes that share a hyperedge (see Section 3.1.2). Notice that the standard linear term, denoting the influence of the two nodes j and k on i , is modulated by an additional influence

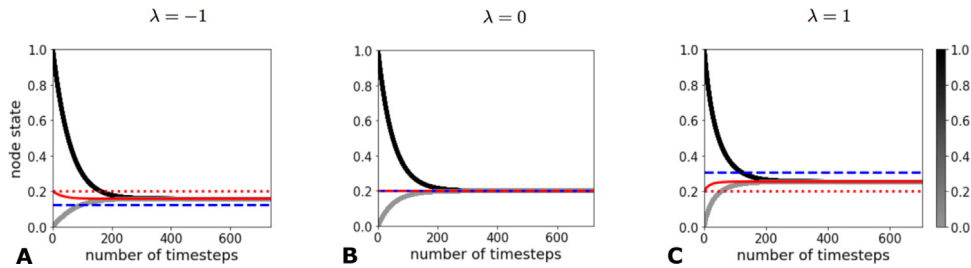


Fig. 33. Average node state for the 3-body non-linear consensus dynamics with continuous-valued opinions on a fully-connected hypergraph. At $t = 0$ an asymmetric opinion initialization is considered, such that $\bar{x}(0) = 0.2$. The interaction function is $\text{iss}(x) = \exp(\lambda x)$. Dotted red lines indicate the initial value of the average node state. Black and gray solid lines represent the evolution of the state of nodes in the two initial configurations, one and zero respectively. Dashed blue lines denote the approximated final state. (A) If $\lambda < 0$ (similar node states reinforcing each other) the asymptotic average opinion state drifts towards the majority opinion. (C) The opposite effect is observed for $\lambda > 0$, where the dynamics shows a drift towards balance. (B) When $\lambda = 0$ the linear dynamics with a conserved average state is recovered.

Source: Figures adapted from Ref. [338].

function $s(x)$ which depends on the difference between the states of the other nodes composing the hyperedge. According to the choice of $s(x)$, this model can reproduce the reinforcing or inhibitory effects that two nodes of a 2-simplex can have on the third one. For example, with a form $s(|x_j - x_k|) = \exp(\lambda |x_j - x_k|)$ and $\lambda < 0$, similar states of j and k can accelerate the dynamics of i (or decelerate if $\lambda > 0$). As expected, if the influence function is constant, i.e. $\lambda = 0$, the standard linear case is recovered and the dynamics conserves the average state at time t , typically defined as $\bar{x} = \frac{1}{N} \sum_i x_i(t)$. Interestingly, this is not true when non-linear interactions are considered. Neuhäuser et al. have showed that in the mean-field approach the higher-order interactions may produce a shift on the average state of the system depending on the initial state of the nodes. In particular, for an unbalanced binary initialization ($\bar{x}(0) \neq 0.5$) the asymptotic average state is shifted towards the majority if $\lambda < 0$ (Fig. 33A) or towards balance if $\lambda > 0$ (Fig. 33C). These results are confirmed by numerical simulations on fully connected hypergraphs. Further analyses on modular hypergraphs have highlighted the additional role played but local sub-graphs in driving the system towards an asymmetric dynamics when non-trivial topologies are considered [338].

7.2.4. Cultural dynamics

In the previous Section, we reviewed models that made use of scalar variables to represent evolving opinions. There is a general agreement in calling models with such characteristics *opinion models*. A separate class of *cultural models*, originally proposed by Robert Axelrod [565], define the cultural profile of an individual as a vector rather than a scalar. This approach, useful to model the emergence of multiculturalism, incorporates two basic mechanisms of homophily and social influence into what is called now, unsurprisingly, the Axelrod model. In this model, individuals interact through the links of a social network by imitating each other, that is by copying an element of the feature vector of a neighbor. The imitation probability is proportional to the so-called *cultural overlap* among the two nodes, which in the original model corresponds to the fraction of common cultural features. The model has been widely investigated by physicists [566–568], and has been recently extended to multiplex networks, where interactions among individuals on different topics, such as religion, sport or politics, happen on different layers [569]. This approach allows for interaction patterns that are topic specific, therefore limiting the social influence among two individuals to the subset of features on which there is an actual social interaction (a link in the topic layer).

Even if a “proper” extension of these model to HORs is still missing, HORs have still found their way into these modeling approaches. For example, Maletić and Rajković [570] proposed to move away from the vectorial representation of cultural features and adopt a higher-order representation instead. In this case, an opinion can be represented as a set of interconnected judgments, so that different judgments forming an opinion represent the vertices of a simplex. In this formulation, overlapping opinions sharing arguments or judgments correspond to simplices sharing faces and ultimately forming a simplicial complex of opinions. This framework opens up new research directions in which overlapping opinions can then be used to shape social interactions [571].

8. Evolutionary games

Imitation is an important mechanism to model social dynamics, at the heart of many processes described in Section 7. Yet, in several cases individuals do not make decisions simply based on peer pressure and social influence [572]. In many contexts, they can set and update their behavior based on strategic choices. In biology, for instance, the selection of a specific physical trait among the many alternatives typically occurs because of the beneficial effects which it brings to the survival of the species. Similarly, human decisions, or *dilemmas*, are frequently based on computing and evaluating a trade-off between the positive and negative consequences of different scenarios.

Games are often studied in a simple dyadic setting, where pairs of individuals are given the chance to pursue either a selfish strategy and defect (D), or a cooperative choice (C), with the selfish strategy being the more rewarding unless both of them undertake it. In the most general set-up, pairwise games can be defined according to a payoff matrix:

$$\begin{array}{c|c} & \begin{array}{c} C \quad D \end{array} \\ \begin{array}{c} C \\ D \end{array} & \begin{pmatrix} R & S \\ T & P \end{pmatrix} \end{array} \quad (62)$$

where R is the *reward* obtained by a cooperator playing against another cooperator, S is the *sucker* payoff received by a cooperator when its opponent is a defector, T is the *temptation* a defector has to resist when it plays against a cooperator, and P is the *punishment* that a defector receives when it plays against another defector. Games where more than two strategies are possible, such as the rock–paper–scissors [573,574], are not discussed in this section. Games can be categorized into different classes, based on the relative order of the four payoffs previously introduced.

The most famous game is the prisoner's dilemma [575,576], where two members of a criminal gang are arrested and isolated from each other. As each prisoner could be convicted of a small charge, but there is not sufficient evidence to convict them for the main greater charge, both prisoners are given the opportunity to bargain, i.e. defecting by stating that the other committed the crime, and being in exchange set free. Cooperation is harmed by a high temptation T , as in this setting the payoff associated to defect against a cooperator yields a higher payoff than the reward R associated to both players cooperating and staying silent. Besides, cooperating against a defector gives the lowest earning, typically known as sucker S payoff, and the payoff ordering of the game is $T > R > P > S$. As no defecting player can benefit by changing strategy if the others keep theirs unchanged, this makes the decision of both players to defect, i.e. punishment P , the Nash equilibrium of the system, despite being a less rewarding situation than full cooperation.

Many alternative real-life situation have been described as social dilemmas. The stag-hunt game describes the dilemma of two hunters, which must cooperate to kill a stag and avoid going hungry [577,578]. It is described by the ordering $R > T > P > S$, and suitable to formalize conflicts between cooperation and safety. Differently from the prisoner's dilemma, this game has two distinct pure Nash equilibria, full cooperation, leading to the highest payoff, and full defection, which is risk-dominant as it prevents from the risk to be the only hunter involved in the attempt to kill the animal. The stag-hunt is a coordination game, as it requires the two individuals to coordinate in order to converge towards the payoff-dominant equilibrium.

Other games are described by the payoff ordering $T > R > S > P$. This ordering is associated to the chicken game, where two individuals drive towards each other looking for a free way at the risk that both may die in the crash, but hoping that the other swerves away (acting cowardly like a poultry). Outside the political sciences, the same ordering of payoff is typically referred to as the snowdrift game. In this game, a snowdrift is blocking the way, and at least one of two individuals has to shovel away snow to free the road. This setting describes well situations where defectors benefit from cooperators without paying a cost for accomplishing a given task, but at least a cooperator is needed for the task to be performed. Here the player's optimal choice depends on what their opponent is doing, as one should yield only if the opponent fails to. For this reason, the chicken game is an anti-coordination game [579]. It is worth to notice that the same ordering is also associated to the hawk-dove game, where two players compete for a resource to be shared, an outcome which is possible without damage only when two doves meet [580–582]. All these games have two pure Nash equilibria, in which each player plays one of the pair of strategies, and the other player chooses the opposite one.

These dilemmas were introduced as static games. Almost fifty years ago the pioneering work of John Maynard Smith [583] first considered the dynamics of a population with repeated strategic interactions, a discipline now known as *evolutionary game theory*. In the well-mixed scenario, where all agents have equal probability to interact with each other, the evolution of the fraction of cooperators x_c can be tracked by the differential equation describing the so-called replicator dynamics [584–587]

$$\dot{x}_c = x_c(1 - x_c)(\bar{\pi}_C - \bar{\pi}_D) \quad (63)$$

where $\bar{\pi}_C$ is the average payoff of a cooperator, and $\bar{\pi}_D$ the average payoff of a defector. The replicator equations are also widely used to model species interactions, as we will discuss in Section 9.3.

Numerically, the dynamics of games are often studied as agent-based models [588]. The importance of numerical simulations, in particular in the case of agents placed on a network, is also linked to the limitations achieved by analytical methods. A first approach is the so-called best response, where individuals choose the strategy which produces the best outcome for them taking the strategies of the other players as given. However, more complex update processes are often considered, where players can update their strategy by imitating the behavior of the most successful individuals, where the higher copying probability the larger the difference in earnings. This allows to consider more realistic scenarios, where agents can also make mistakes.

For the prisoner's dilemma, in well-mixed population (where at each round individuals have the same probability to play with any other agent in the population) the evolutionary dynamics brings the system into a state of full defection [585]. This is in spite of the low payoff associated to the outcome, a situation sometimes referred to as the tragedy of the commons [589]. When populations are structured, meaning that interactions between agents—often limited by spatial constraints—can be described by a network of relationships, cooperators are able to emerge even in adverse settings. This was first proposed by Nowak and May, who carried out computer simulations by placing agents at the

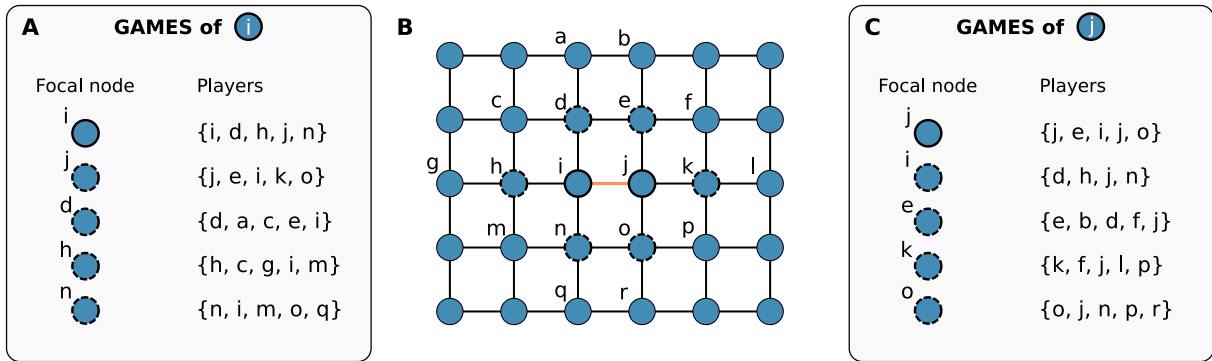


Fig. 34. Traditional graph implementation of a multiplayer game. At each elementary step a player i and one of its neighbors j are chosen at random. Each individual accumulates earnings by playing all games in which it is involved, namely the game in which it is the focal individual of the group, and the k games where it participates in a group centered on one of its neighbors. All groups in which i and j participate are listed in panels (A) and (C), for a simple two-dimensional lattice (B). Finally, i compares its payoff to that of j , updating its strategy by imitating the strategy of the neighbor with a probability which depends on the relative difference of the payoff. The presence of links among neighbors of i and j (clustering) does not affect the definition of the groups.

nodes of a simple square lattice, observing that repeated games between the same pairs of individuals allow for *network reciprocity*, i.e. the creation of robust mutual interactions based on trust, even if the temptation to defect would prove to be more rewarding in a single individual round [590]. Further theoretical and computational studies showed that graphs which are heavy-tailed [591,592] or clustered [593] provide the best conditions for the emergence of cooperation, exploiting the beneficial effect of prosocial hubs and the presence of tightly connected communities to sustain the formation of trust among players. It is worth to note that these expectations have been challenged by experiments, where human subjects play in lattices or scale-free networks. Indeed, in most experiments performed in the lab cooperation does not survive [594–599], with the exception of the one described in Ref. [600]. For a detailed discussion of the comparison between theoretical predictions and experimental results, we refer the reader to Ref. [601].

In the snowdrift game the relative values of the sucker payoff and punishment are inverted compared to the prisoner's dilemma, as a lone cooperative shoveler still has a better cost-to-benefit ratio than an individual in a pair where both agents defect. This apparently small difference generates the emergence of a stable state with coexisting cooperators and defectors in structuredless population, differently from the prisoner's dilemma [585]. Surprisingly, spatial structures were shown to be detrimental for the emergence of cooperation in the first computational studies on the snowdrift game [602].

In the last 15 years the fields of evolutionary game theory and network science have become significantly closer, and we are now witnessing an explosion of contributions at the boundary of these topics [603–605]. In the following of this Section, going beyond the traditional pairwise scheme, we provide an overview of the main results on evolutionary games in networks with group and higher-order interactions.

8.1. Multiplayer games on networks

8.1.1. Public goods game

Many dilemmas do not involve pairs of individuals, but occur at the level of groups. This is the case of taxes for welfare state, which are beneficial from an individual perspective only if most individuals are willing to contribute. The public goods game is the paradigmatic game to describe social dilemmas in the case of group interactions [606–609], and it is considered the generalization of the prisoner's dilemma to $N > 2$ players. In the most simple implementation, players, belonging to a group of size G , are asked to contribute to a common pool. Cooperators contribute with a token t whereas defectors do not contribute at all. The tokens are then multiplied by a synergy factors R , with $R < G$, and shared evenly across the population no matter the strategy of the agents. For this reason, if we indicate with N_c the number of cooperators in the group, cooperators earn a payoff $\pi_c = t(N_c R/G - 1)$, whereas defectors obtain $\pi_D = t(N_c R/G)$. To simplify the payoffs and without loss of generality, t can be set equal to 1. The game is fully controlled by the effective parameter $r = R/G$, which is known as the reduced synergy factor. The traditional implementation of a multiplayer game on a graph is illustrated in Fig. 34. As explained later on, different implementations are necessary if one wants to explicitly take into account the real pattern of higher-order interactions among individuals.

Similarly to the prisoner's dilemma, the network structure affects the emergence of cooperation also in the public goods game [591,610]. Simulations on lattices first showed that structured interactions sustain cooperation for values of the synergy factor well below the critical condition $R = G$ [611,612]. Yet, interest in the public goods game sparked when more realistic network structures with heterogeneous degree distributions were considered [613]. In heterogeneous networks, at every round each agent is involved in $k + 1$ games (where k is the degree of each node), meaning that hubs play significantly more games than agents placed on poorly connected vertices. In the implementation known as *fixed*

cost per game, in particular, $(k + 1)$ is also the total contribution of each agent after a full round. Because of this inequality, another set-up has also been widely investigated, where each agent has a *fixed cost per individual* t , and hence each game contributes to its total payoff as $1/(k + 1)$. Fixed costs per individual are considered a suitable setting to model cumulative costs, such as in the case of taxes, while fixed costs per individual are best suited to model a scenario in which the resource associated to the cost is finite, and it is equally distributed among players. In scale-free networks cooperation was found to be significantly enhanced through network reciprocity if cooperators pay a fixed cost per individual, whereas the same effect is reduced when prosocial individuals pay a fixed cost per game [591]. The enhanced cooperation of the first scenario is due to the disproportionately higher payoff obtained by those agents participating in a very large amount of groups.

The beneficial effect from interacting according to a scale-free networks can be lost if the underlying structure is characterized by positive degree-degree correlation, reducing the evolutionary advantages of individuals with high-degree who decide to cooperate [614]. Similarly to pairwise games, tight community structure and clustering can sustain positive feedback and the survival of cooperators for low values of the synergy factor also in the public goods game [615]. Prosocial behavior may be further promoted by allowing heterogeneous contributions, for instance by making them proportional to the cooperation of each group [616,617]. However, interestingly, increasing group size does not always lead to the dynamics of well-mixed populations in such a multiplayer game [618].

Multiplayer games are considered to be inherently different from the corresponding pairwise games, as the emergent collective behavior in the case of group interactions might be different [619]. This is rooted in the formation of indirect links between players who belong to the same group but are actually disconnected. As an important consequence of this, the details of the local topology of the network of interactions for multiplayer games are often irrelevant for the final outcome, as discussed in Ref. [620]. Besides, multiplayer games also show qualitatively different evolutionary dynamics, giving rise to new forms of self-criticality which have not been observed in pairwise games [621]. Among those, we report the emergence of new temporal and spatial patterns of dominance, such as the so-called indirect territorial competition, first reported in a modified public goods game in Ref. [622].

More recently, the role of multiplexity has also been taken into account. In this setting, different layers are associated to different games (different values of the synergy factor) and individuals may have different neighbors depending on the layer. While not making possible direct strategy exchanges between the networks, interconnectedness can affect the utility function of players, who do not have access to the earnings of their neighbors on each of the layers but only to a (possibly non-linear) combination of them [623]. Interestingly, this simple payoff coupling was shown to further enhance cooperation in the whole system, through a mechanism dubbed *interdependent network reciprocity* [624]. Despite the presence of the same synergy factors at different layers, the system naturally self-organizes into a configuration where one layer is more cooperative than the others through spontaneous symmetry breaking [624]. However, interdependent network reciprocity is not a universal property of all interconnected systems, but strongly depends on the structure of the layers. In particular, interdependent network reciprocity is proportional to the fraction of edges shared by the different layers (i.e. edge overlap [625]), and the beneficial effects of multiplexity completely disappear when the overlap between the network structures goes to zero, no matter the number of layers [626]. In this detrimental configuration, cooperators can appear in the system only if the synergy factors of all layers are at least as high as the critical conditions associated to each network in isolation [626]. Further coverage on the effects of multiplexity and network interdependence on evolutionary games is provided in Ref. [605].

Much attention has also been devoted to the case of coevolutionary games, where the structure of the networks of social interactions may change over time as a result of the outcome of the strategic interactions among players [588]. When individuals can alter the connections in their social network in response to unsatisfactory interactions, coevolution between cooperation and spatial organization in the public goods game naturally leads to increased social cohesion [627] and prosocial behavior [628]. A different setting is considered in Ref. [629], where a survival cost parameter is introduced, and agents with low payoff are replaced in the games by new random players. With this mechanism, cooperation emerges if the synergy factor is higher than the average degree, and the population self-organizes into a scale-free network of interactions, naturally more beneficial to sustain prosocial behavior. Finally, coevolutionary rules have been implemented in the case of interdependent network of players, leading to complex social structures where strong inter-layer links were promoted around agents performing the best [630].

As most of these results rely on numerical simulations, it is important to highlight the importance of proper simulations practices. An important contribution to the topic is found in Ref. [631], which investigates the stability of observations from agent-based model simulations going beyond traditional finite-size scaling, or on the role of noise [632]. In particular, only a complete stability analysis of all subsystems solutions (solutions that are formed by a subset of all possible individual strategies) can be explicitly linked to the existence of a phase transition in the thermodynamic limit in multiplayer games where competing strategies are more than two. For a complete review on the public goods game on networks, we refer the interested reader to the work by Perc et al. “Evolutionary dynamics of group interactions on structured populations: A review” [608].

8.1.2. Other multiplayer games

The public goods game is not the only multiplayer game whose evolutionary dynamics has been studied on graphs. An interesting alternative is the generalized multiplayer snowdrift game, where individuals receive a benefit b if the task is performed by one or more agents belonging to their same group, no matter their strategy [633]. In this game cooperators

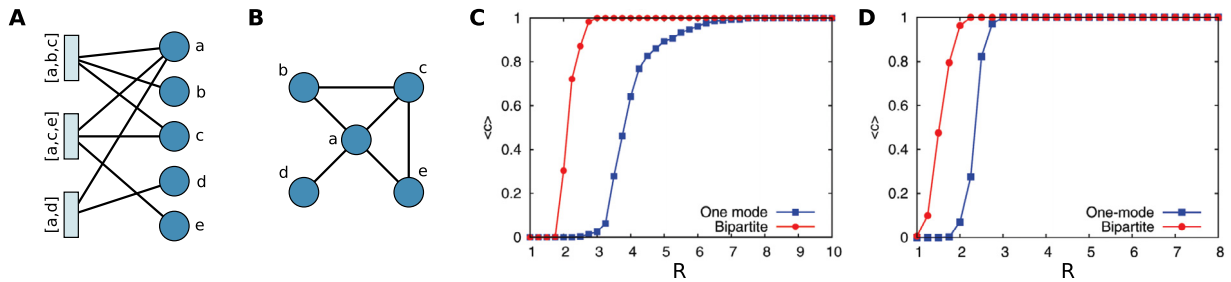


Fig. 35. Public goods game on bipartite graphs. Information on the exact group structure encoded in a bipartite network (A) is lost when its one-mode projection is considered, where two individuals are directly linked if they both participate in at least one group (B). Cooperation is enhanced when the game is played by considering the real group structure instead of the projected graph, both for the fixed cost per game (C) and fixed cost per individual (D) implementation. Prosocial behavior is greater when fixed costs per individual are considered.

Source: Figures C and (D) reproduced from Ref. [643]

share the workload and have a payoff $\pi_C = b - c/N_c$, while defectors have a payoff $\pi_D = b$ as long as there is at least a cooperator in the group, otherwise $\pi_D = 0$. In well-mixed populations cooperation decreases with high cost-to-benefit ratio, as well as a function of the number of agents in a group [633]. When network structures are considered, the introduction of an underlying homogeneous graph steadily promotes prosocial behaviors, similarly to the corresponding game played on well-mixed populations. By contrast, heterogeneous networks typically generate multiple new internal equilibria [634]. The introduction in the game of dynamical grouping, where agents are placed in groups of different sizes at different times, and players of different strategies are dynamically mixed was found to greatly enhance prosocial behavior [635]. A common modification of the traditional multiplayer snowdrift games links the benefit of accomplishing a task to the existence of a minimum threshold of cooperative individuals [636–638]. Despite its peculiarity, the game is sometimes considered as a particular type of public goods game.

More recently, a generalization of the hawk-dove game to multiple interacting players was proposed [639]. In particular, whereas in the corresponding pairwise settings the game is considered equivalent to the snowdrift game, this is not true when interactions occur between groups of players. In particular, while in the snowdrift game the accomplishment of the task benefits all individuals, in the hawk-dove problem only strategists of a particular kind (hawks) benefit from the shared resource, excluding the opponent type (dove) from the distribution, unless a sufficiently high number of cooperative doves is present in the group. The emerging evolutionary dynamics is very rich: different scenarios associated to dominating hawks, coexistence, bi-stability, multiple interior equilibria and dominating doves can be obtained as a function of the dynamical parameters describing the resource to be shared, cost and minimum number of doves in a group for prosocial individuals to benefit.

The games discussed so far are multiplayer generalizations of pairwise dilemmas described by the payoff matrix in Eq. (62). It is worth to mention that also different families of pairwise games have been investigated in the setting of wider group interactions. An example is that of the ultimatum game, where two players, one acting as a proposer and one as a receiver of an offer, bargain to split a sum of money [640,641]. In the multiplayer case, offers can have an arbitrary number of receivers, who can reject or accept the proposal individually. Similarly to a threshold model [522], the offer is accepted and shared equally among responders only if the number of individual acceptances is above a given threshold. The game is significantly affected by the value of this parameter, with higher values associated to more generous and fair outcomes [642].

8.2. Games with higher-order interactions

8.2.1. Public goods game on bipartite networks

Networked implementations of multiplayer games discussed so far lack control on the real higher-order structure of interactions. For instance, a scale-free degree distribution $P(k) \sim k^{-\gamma}$ generates a similarly heavy-tailed distribution of group sizes $P(G)$. This is not a realistic feature of many real social networks, such as collaboration networks, where individuals tend to collaborate together in fairly small groups of homogeneous size [295].

Motivated by this finding, in Ref. [643] Gómez-Gardeñes et al. studied the public goods game on an empirical bipartite network of scientific collaborations, where the two sets of nodes describe respectively scientists and papers. The authors compare the results with what is obtained by implementing the game on the corresponding one-mode projection, acting as a null-model, where scientists who co-authored at least a paper are linked together, as shown in Figs. 35A,B. The main finding is that—no matter the details of the updating rule for the evolutionary dynamics—cooperation is systematically enhanced by considering the real higher-order structure described by the bipartite network. This is due to the interplay between the heterogeneous distributions of the number of games in which each player is involved, and the homogeneous distribution of the groups. Taken together, these two features allow for the existence of a fairly high number of agents with high payoff involved in small groups, making this scenario responsible for further promoting prosocial behavior.

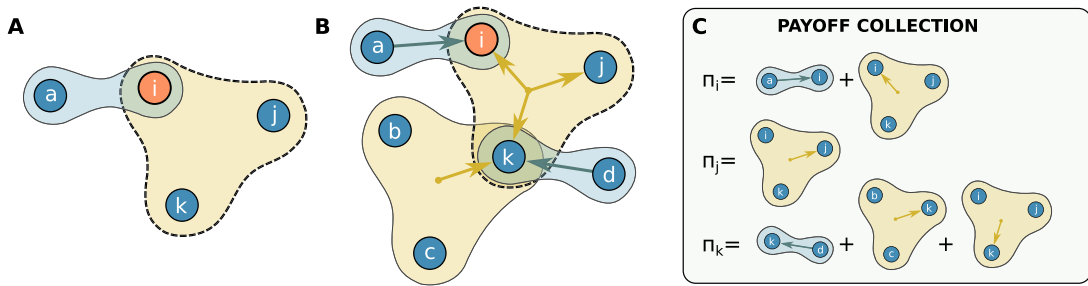


Fig. 36. Hypergraph implementation of strategic group interactions. (A) At each time step, a node i is chosen randomly, and one of the hyperlinks to which it participates is selected. (B) All the members of the hyperlink play a game for each of the hyperlinks they are part of, and (C) accumulate payoffs accordingly.

Enhanced cooperation with respect to the one-mode projection is observed consistently in both settings of fixed cost per game (Fig. 35C) and fixed cost per individual (Fig. 35D): the degree of cooperation is always greater when fixed costs per individual are considered rather than fixed costs per game, consistently with what is found for classical monopartite networks, though the differences are now smaller. The boost in cooperation for fixed cost per individual is linked to the long tail in the distribution of degrees and number of games. However, this effect is mitigated when the real structure is considered. This can be understood by considering the agents who participate in a single collaboration, whose contribution is the same in the bipartite network both for fixed cost per individual and fixed cost per game scenarios, while this is not the same in the projected one-mode network where a node in general participates in $k + 1$ groups. Interestingly, the authors remark that the final cost per individual is a better setting to model collaborations, where researchers have a limited amount of time to be shared among parallel projects, and where those involved in only a few collaborations tend to take most of the workload. Finally, increasing the number of members of a group leads to a decrease of the level of cooperation in a population.

In a following work, Gómez-Gardeñes et al. deepen their investigations of higher-order structure by studying the effect of bipartite networks which have groups of the same sizes, but where the number of groups in which a player can participate is a tunable parameter [644]. Surprisingly, the average level of cooperation achieved with homogeneous connectivity is remarkably larger than that for scale-free substrates. This finding indicates that the ability of scale-free networks to outperform the promotion of cooperators in homogeneous structures, first discussed in Ref. [591], is not directly linked to the fat-tail in the distributions of number of games per player. At difference, instead, it rather depends on the entanglement of social and group heterogeneities which is unavoidable in the one-mode projection. Further analyses on the impact of different distributions for group sizes and the number of individual contacts reveal the importance of overlap between groups for cooperation, similarly to the role of clustering on one-mode projected networks [645].

An interesting modification of the game considers the possibility that information on the earnings is shared between groups. This can be done by introducing an effective payoff, where the normal payoff associated to a member playing in a group is combined with the earnings of the same agents from the other groups in which it participates. The strength of this second term can be tuned with a parameter α , which describes the degree of cross-information among groups. Interestingly, information exchange is positively correlated with an enhancement of the cooperation in the system [646]. The positive effect induced by cross-information is analogous to that of interdependent network reciprocity for multiplex networks, where individual payoffs are aggregated across the layers of the system.

8.2.2. Public goods game on hypergraphs

Recently, Alvarez-Rodriguez et al. introduced a new formalism to describe the evolutionary dynamics of higher-order interactions [647]. In this set up, groups of individuals are described by the hyperlinks of a hypergraph, making explicit the lift of interaction networks to the case of non-dyadic interactions. The Monte Carlo implementation of the dynamic is illustrated in Figs. 36A-C. In the manuscript, the authors finally normalize the payoffs by the number of played games, in an implementation reminiscent of the fixed cost per game scenario. The update process is also modified, and i imitates the strategy of its best performing neighbor k with a probability which depends on the difference $\pi_i - \pi_k$.

The stable state achieved from the evolutionary dynamics is first studied on uniform random hypergraphs, where all players are involved in the same number of hyperlinks of equal size, $G = 2, \dots, 5$. Fig. 37A shows the fraction of cooperators x_c as a function of the reduced synergy factor r , where the hyperdegree of each node is the minimum one to guarantee a connected hypergraph. As shown, the presence of larger groups promotes the onset of cooperation in more adverse conditions described by a low value of r . When density increases—no matter the group size—the hypergraph implementation of the public goods game converges to the limit of well-mixed population, as shown in Fig. 37B. Besides, the relaxation time T of the dynamics can be computed with good analytical accuracy with a mean-field approach.

The introduced formalism also allows for an analytical treatment of heterogeneous random hypergraphs, where nodes participate in groups of different order with a weight described by a probability distribution. For simplicity, the authors

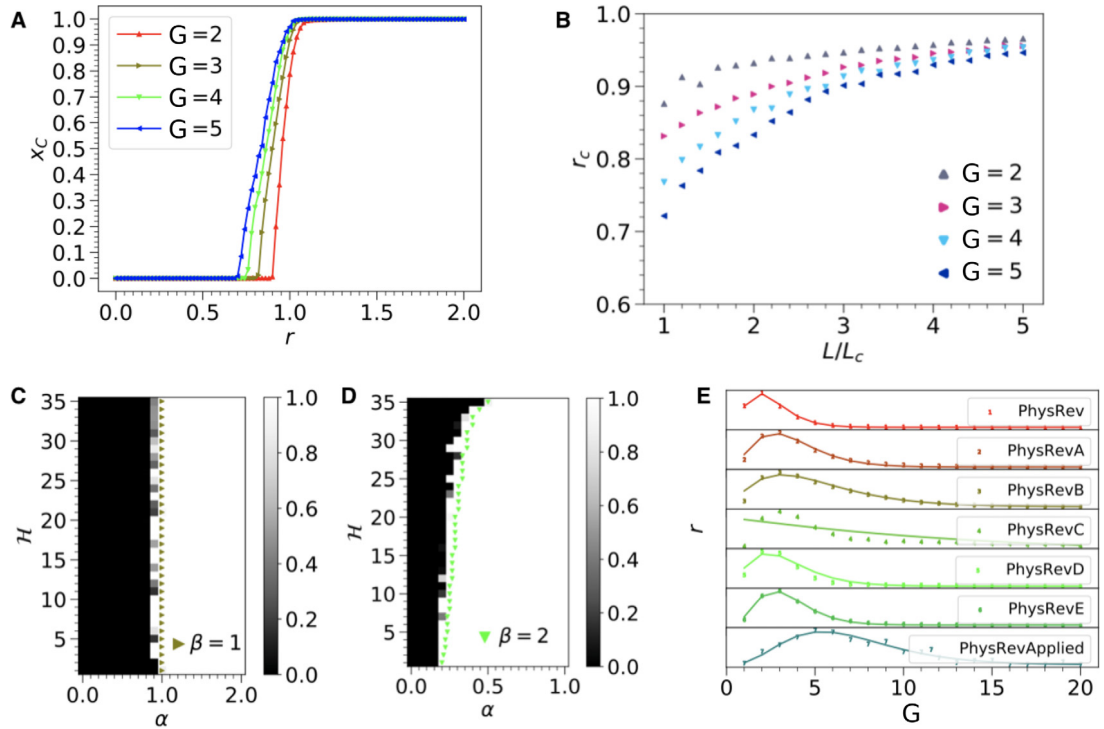


Fig. 37. Cooperation in the public goods game on hypergraphs. (A) Average fraction of cooperators as a function of the reduced synergy factor r for homogeneous hypergraphs with interactions of different order G . (B) Critical value r_c for the emergence of cooperation as a function of the density of the hypergraphs L/L_c , where L_c is the critical number of hyperlinks for a connected hypergraphs, for different values of g . Classes of 35 different heterogeneous hypergraphs \mathcal{H} with hyperlinks of orders $g = \{2, 3, 4, 5\}$ are considered. The synergy factor $R(\alpha, \beta)$ scales according to Eq. (64). Results for two values of the exponent, $\beta = 1$ (C) and $\beta = 2$ (D), are shown. (E) Dependency of synergy factors from hypergraphs describing co-authored publications in journals of the American Physical Society assuming the collaboration process is optimal.

Source: Figures reproduced from Ref. [647].

focus on heterogeneous hypergraphs with a different frequency of groups f_G of order from 2 to 5 and $\sum_G f_G = 1$, giving rise to 35 different hypergraphs classes. In this set-up, it is interesting to investigate the collective outcome of the game in scenarios where larger or smaller collaborations can be more or less effective. These different conditions are easily described by setting the synergy factor R to be a function of the group size G , i.e.

$$R(G) = \alpha G^\beta, \quad (64)$$

where $\alpha > 0$ and $\beta \geq 0$ and different from 1. The emergence of cooperation is in general affected by both parameters α and β . In the particular case $\beta = 1$, all classes of hypergraphs show the same behavior as a function of α (Fig. 37C). This is not true for different values of the exponent, such as $\beta = 2$ (Fig. 37D). Besides, the average relaxation time T of the dynamics as a function of the critical point α_c for the emergence of cooperation scales linearly with α if $\beta \neq 1$. Interestingly, while a degeneracy is observed for $\beta \leq 1$, this is broken for the superlinear case. This means that it is possible to exploit this additional degree of freedom by choosing an adequate hypergraph to set independently a chosen critical point and relaxation time.

Finally, the authors considered several datasets describing synergies and group tasks in the real-world. By imagining that these collaborations—ideally described by a public goods game—evolved over time to produce an optimal hypergraph structure and that a coordination cost is added to sustain too large collaborations, they inferred the ideal synergy factor associated to prosocial behavior. As an example, results for collaborations among physicists publishing in different journals of the American Physical Society are shown in Fig. 37E). Journals in experimental and applied physics typically have an optimal synergy factor for larger values of the group size G .

To conclude, even more than for the dynamical processes considered in Sections 5–7, the landscape of HORs in the field of social dilemmas is still widely unexplored. In the future, we foresee that an explicit treatment of higher-order interactions could be applied to the many games discussed in Section 8.1.2, as well as others such as the naming game [648,649], the sender-receiver game [650–652], or problems of collective risk [653].

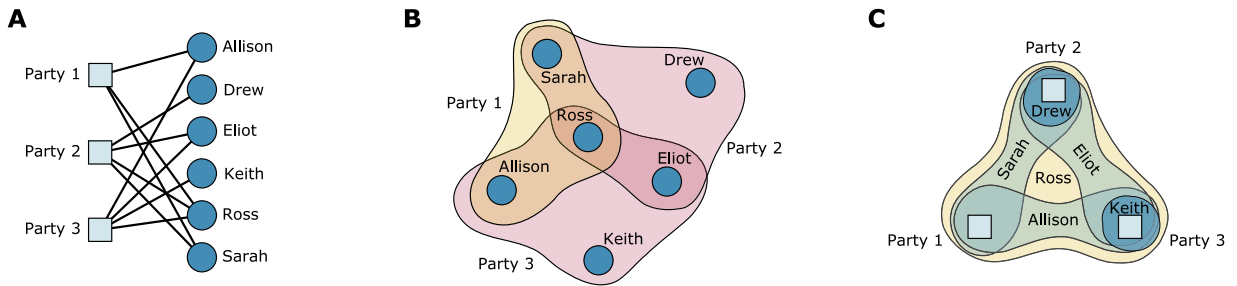


Fig. 38. Affiliation network of six children and three parties. The interactions are shown respectively as (A) a bipartite network actor-events, (B) as the hypergraph with the six children as the nodes, and (C) as the dual hypergraph with the three parties as the nodes.
Source: Figures adapted from Ref. [65].

9. Applications

Non-pairwise interactions are common in various types of systems in the real world. Important examples include group interactions in both offline and online social networks [65,654–656], multi-authors scientific collaborations [115], network motifs in transcription networks [657] and trigenic interactions in gene regulatory networks [658], beyond pairwise mechanisms of species coexistence in ecological communities [30], and higher-order correlations in neuronal [659] and whole-brain functional patterns [25,660]. In this section, we present a selection of some of the possible applications of HorSs in fields spanning from social sciences to neuroscience and biology.

9.1. Social systems

Social scientists have realized since long time the importance of hypergraphs and simplicial complexes to describe and study affiliation data [65]. *Affiliation networks*, also known as *membership networks*, are a special kind of two-mode social networks representing the affiliation of a set of n actors to a set of m events, or social occasions. As an example, Fig. 38A shows the bipartite network of the attendance of $n = 6$ children to $m = 3$ birthday parties. This system can be naturally described as a hypergraph whose nodes are the children and the hyperedges are the set of events (Fig. 38B). Notice that the data can be represented equally well by the dual hypergraph, obtained by reversing the roles of nodes and edges (Fig. 38C). In this latter case the three nodes are the three parties, while each child is a hyperdegree.

The literature on applications of hypergraphs and simplicial complexes in the social sciences is vast. We will then limit our survey to the pioneering works and to some recent results. Ref. [661] presents one of the earliest use of hypergraphs to investigate affiliation to voluntary organizations. The work focuses on the issue of sampling and proposes estimators for the number and size distribution of organizations in cities, the density of relations among individuals generated by organizations, and the amount of membership overlap among organizations. Such estimators are then applied to data from a sample of individuals in different towns in the state of Nebraska. Results show that, while the mean affiliation rate does not systematically vary from city to city, the number of inter-organizational links per organization increases with the size of the city. Hypergraphs have also been used to capture the characteristic fluidity of urban social structures arising from collections of overlapping subsets such as voluntary associations, ethnic groups, action sets, and quasi-groups [662], and to study participation of Thai households to ritual celebrations [663].

Ref. [664] discusses the conceptualization, measurement, and interpretation of centrality in affiliation networks. The main underlying assumption is that, in an affiliation network, also the events can acquire and transmit centrality. Ref. [127] shows how centrality can be adapted to HORs and can turn very useful to capture important properties of real-world systems. The measures proposed in this work are extensions of the Bonacich eigenvector centrality [122,126,665] to the case of hypergraphs (see also Section 3.2). The basic idea is simple. Let I be the incidence matrix of a hypergraph. If we indicate as vectors x and y the centrality scores for the rows and columns, representing the hyperedges and the nodes of the hypergraph respectively, we can write that: $I^T x = \lambda y$ and $I y = \lambda x$, which means assuming that individuals acquire their centrality by attending important events, and important events are attended by central individuals. The vectors x and y are then eigenvectors of two different matrices, although both are associated with the same eigenvalue λ^2 :

$$I I^T x = \lambda^2 x \quad I^T I y = \lambda^2 y \quad (65)$$

The final outcome is a measure of centrality for events, as well as an improved measure of centrality for actors. The authors of the paper show an application to study data describing 56 attacks on European settlements occurred between the years 1509 and 1700 and involving Carabe from 22 different islands. Such data require a description considering more-than-dyadic interaction, as attacks could involve more than two islands at the same time.

Simplices and simplicial complexes provide an alternative way to describe and study membership networks using methods from algebraic topology. This approach draws heavily on the pioneering ideas of Ron Atkin [36,666] and on

his *q-analysis*, which makes use of a geometric interpretation of the relationships between actors and events. Atkin's framework to study social systems is based on a fundamental distinction between what he calls the "backcloth" of social action, namely the structure of ties among the events, and the "traffic" of social activities that can take place over the backcloth, such as the formation of pairwise acquaintanceship between actors. The backcloth is a simplicial complex and the *q-analysis* is designed to describe the patterns of relations among its constituents.

To give a concrete example, we will discuss here an application of Atkin's framework to study the formation of friendship in a scientific community against the backcloth of shared contacts [654]. In his analysis of friendship among a set of 29 social science researchers, Linton Freeman looked at 19 linking events corresponding to scientists been located in the same university department at the same time, or having attended conferences together. Each person is then represented as a simplex of the linking events in which has been involved. 25 of the 29 persons participated at least to one of the 19 events, with 13 of them involved in only one event. These persons are 0-simplices, but there are also six 1-simplices (pairs of events), and four 2-simplices (persons involved in three linking events). The highest order simplices found are two 3-dimensional tetrahedrons. These simplices form the building blocks for the construction of a backcloth for social action. The basic idea is that conferences and universities provide the perfect setting in which friendships between academics can be developed. Therefore to understand the formation of social ties it is important to analyze how the simplices are intertwined into a larger structure, i.e. into a simplicial complex. The simplicial complex corresponding to the system under study is shown in Fig. 39A. The linking events are the nodes of the simplicial complex and are labeled with a number from 1 to 19. The persons are instead indicated with the symbols $P_1 - P_{29}$ and can either be represented as nodes, links, or higher order objects. Notice the two tetrahedrons respectively corresponding to persons $P_{13} = \{11, 13, 15, 16\}$ and $P_3 = \{2, 8, 9, 19\}$. These are the highest-order simplices present in the simplicial complex, which can then be well represented in three dimensions. Two persons can share one or more common linking events. For instance, person P_{20} is linked at dimension 0 to person P_4 since they have only a node (event 3) in common. Person P_{13} and P_{21} are instead linked by two events (nodes 8 and 9). Hence they are 1-connected, as they are glued together by a 1-dimensional line (the edge 8–9). What matter are not only direct connections between simplices, but also chains of connections. For instance, the three simplices P_4 , P_9 and P_{20} are linked in a chain of connection of order 0, as P_4 is 0-connected to P_{20} , and P_{20} is 0-connected to P_9 . Instead P_{13} , P_9 and P_{20} are in the same 1-connected component. Atkin's *q-analysis* describes the sets of chains of connection and their dimensions. The table in Fig. 39B tells us that there are three components at dimension 0, with the largest one containing 21 of the 25 persons. Moreover, there are nine components at dimension 1: the largest one made by P_{13} , P_9 and P_{20} , the second one by P_2 and P_{28} , and seven isolated 1-dimensional simplices (edges). No connections (of any type) are instead observed among simplices of dimension larger than 1. Another interesting feature of the simplicial complex is the existence of a 0-dimensional *q-hole* (akin to a H_1 cycle, see Section 3.4) involving the four persons P_9 , P_{11} , P_{13} and P_{20} and shown as a shaded area in Fig. 39A. This corresponds to a cycle of four nodes only pairwise connected and is an indication of an obstruction to the free flow of social traffic on the backcloth. The main purpose of Freeman was to correlate the formation of personal friendships to the structure of the backcloth. He had data of 12 close mutual friendships reported by the 29 researchers. And he was indeed able to show that the structure of the backcloth constrains the choice of personal friends. In fact, none of the 12 existing social links was among the pairs prohibited by the obstructions in the backcloth. Moreover, 11 of these 12 pairs were among the 31 adjacent pairs which are 0-adjacent in the backcloth.

A similar application of *q-analysis* to study the evolution of social groups was published by Patrick Doreian in the same years [667]. Doreian had data on the participation of 18 women in 14 events through time, and used *q-connectivity* to trace the group structure over time. His primary objective was to investigate conflict within the group and eventually predict the observed split of the group of women into two subgroups. Differently from Ref. [654], the approach here is dynamic: the *q-connectivity* analysis is applied to an enlarging set of successive events in time. Although, on the one hand, the work confirmed that algebraic topological approaches are flexible enough to provide a description of structural changes, on the other hand the results showed that the data used were not rich enough to explain the observed changes. This also pointed to the importance of collecting high-resolution temporal data [22,656,668,669].

Certainly one of the most original applications of simplicial complexes to social networks is the structural analysis of a team sport presented in Ref. [670]. In their work, Gould and Gatrell used Atkin's *q-analysis* to define and characterize intuitive notions of structure in a soccer match. They focused on the England FA Cup Final between Liverpool and Manchester United played on 21 May 1977 at Wembley Stadium, London. Although commentators generally rated the play of Liverpool as superior, Manchester United won the match by 2 goals to 1. The authors considered the 22 players and defined a relation in this set using a variable threshold on the number of times the ball passed from one player to another. Then they examined the internal structure of the two teams separately, and also the relations between the two sets of players, defined by the loss of the ball by one team to the other. The analysis is able to show the relevance and role of different players and groups of players. The results also indicate that the injection of *q-holes* by the defense of the Manchester United, created an obstruction to the free flow, contributing to the fragmentation and loss of the Liverpool. It could be very instructive to apply and validate this type of analysis on a larger scale, now that soccer analytics is attracting increasing interest and detailed data on all the spatio-temporal events (passes, shots, fouls, etc.) occurring during a match are available for entire seasons and different soccer competitions [671].

More recently, simplicial complexes have also been used to investigate online social networks [655,672], information sharing [673] and social resource sharing systems [674]. For instance, the authors of Ref. [655] have assessed the role

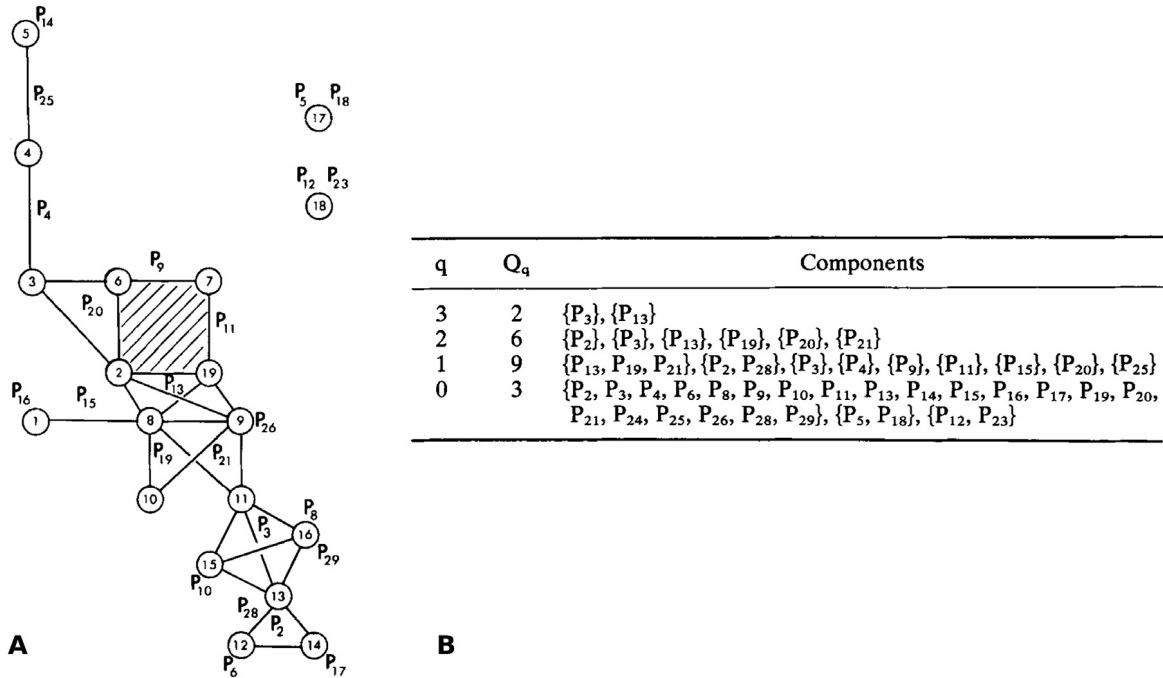


Fig. 39. Early simplicial representation of interactions among social science researchers. (A) Simplicial complex showing the pattern of links between social science researchers, P_1 – P_{29} , through shared linking events, nodes 1–19, indicating participation to events or affiliation to university departments. (B) Table showing the q -analysis of the simplicial complex. The first column is the dimension of components made up of chains of simplices. The second column is the number of chains at each level, while the third column reports the names of the simplices making up each chain.

Source: Figure and table reproduced from Ref. [654].

of an individual in MySpace computing what they name the node structure vector, which allows to characterize the topological space around a node. This is defined, for a node i , as the vector $\mathbf{Q}^i = \{Q_0^i, Q_1^i, \dots, Q_{d_{\max}}^i\}$ whose $d_{\max} + 1$ components denote respectively the generalized node degree $k_{d,0}(i)$ of order d introduced in Section 3.2, i.e. the number of d -dimensional simplices, with $d = 0, 1, \dots, q_{\max}$, to which node i participates, and d_{\max} is the dimension of the largest simplex in the complex. The study of the simplicial node degree $k(i) = \sum_{d=0}^{d_{\max}} Q_d^i = \sum_{d=0}^{d_{\max}} k_{d,0}(i)$, also known as the node topological dimension, provides a good measure of the social capital of the corresponding individual. In fact, it has been found that the so called Simmelian brokerage [675], which quantifies a node's ability to act as a broker in a community, scales as a power of the node topological dimension. Moreover, the analysis of the components of the node vector over the different social layers and communities of MySpace reveals that influential individuals connect higher-order simplices and build their social capital by combining their connections in different layers.

Authorship of scientific articles is a particularly interesting type of affiliation networks, as it provides important insights on patterns of collaboration within the academic community. In this case, the two sets of nodes represent scientists and their publications, respectively. The basic units of scientific collaborations and of the social network of acquaintances among scientists are co-authored publications, which often involve groups of authors rather than just two [676,677]. Hence, in their study on the “shape of scientific collaborations”, the authors of Ref. [115] have proposed to complement the results that have been obtained by methods of network analysis [678–680] with an approach based on a simplicial description of scientific publications and on the use of tools from algebraic topology. They have considered all the papers posted on the arXiv, a repository of electronic preprints spanning from physics to quantitative biology and mathematical finance, in the period 2007–2016, and have constructed 18 different simplicial complexes, one for each of the different categories of arXiv. Each paper with k authors corresponds to a $(k - 1)$ -simplex, and only papers with author sets not fully contained in the author sets of other papers have been retained in the construction of the simplicial complexes in order to preserve their basic structural properties. Both the size distribution of facets (maximal simplices, see Section 2) $P(s)$ and the simplicial node degree distributions $P(d)$ of the complexes display broad tails, indicating the presence of large collaborations and of authors with a large number of different collaborations, respectively. The 18 different categories can then be grouped in only two large classes based on their $P(d)$, showing that the number of collaborations to which an author is able to participate is quite well conserved across fields. Also, all the 1-dimensional homological cycles, i.e. the two-dimensional holes bounded by edges, of the various co-authorship simplicial complexes have been studied. In particular, focusing on the shortest possible cycles, triangles, and counting how many of the set of three edges arranged in a triangle are covered by a full triangle (2-simplex), allows to investigate the concept of simplicial closure (the extension of

triadic closure to simplicial complexes [681]) in the data. Results indicate the presence of very strong simplicial closure for all categories of arXiv, meaning that in the great majority of cases whenever three authors have collaborated in pairs, they also have collaborated on a paper together. An application to collaboration networks of a similar extension to hypergraphs of the concept of clustering coefficient, and of that of subgraph centrality can be found in Ref. [120].

9.2. Neuroscience and brain networks

Lively debated over the last decade, the question of whether high-order correlations – in addition to the basic pairwise interactions – were needed to properly account for brain function was met with strong evidence of a positive answer. Using higher-order connected correlation functions [659], Schneidman et al. [682] revealed that high-order correlations exist in neural populations. Similarly, Ganmor et al. [29] and Yu et al. [683] provided evidence that introducing higher-order interactions between neurons allowed to improve predictions at mesoscopic scales, e.g. for cortical dynamics such as neuronal avalanches in awake monkeys or visual responses in anesthetized cats. More recently, further research in neural spike trains provided methods to measure the strengths of multi-spike interactions [684], and showed their importance in shaping the dynamics of cortical columns [685] and in population coding [686,687].

The models used to estimate higher-order interactions in the cases mentioned above are usually tailored after the generalized Ising model [682], which can themselves be linked back to earlier higher-order proposals [688,689]. In these models, the probability of observing a pattern of firing neurons $(\sigma_0, \sigma_1, \dots, \sigma_n)$ is given by

$$P(\sigma_0, \sigma_1, \dots, \sigma_n) = \frac{1}{Z} \exp\left(\sum_i \alpha_i \sigma_i + \sum_{i < j} \beta_{ij} \sigma_i \sigma_j + \sum_{i < j < k} \gamma_{ijk} \sigma_i \sigma_j \sigma_k + \dots\right) \quad (66)$$

where $\alpha, \beta, \gamma, \dots$ control the self-, pairwise- and third-order interactions among firing units. These models, while very powerful, have several limitations. First, they are designed for systems with discrete states. Neurons are usually considered to be firing or quiescent so are well described by Ising spins, which take values ± 1 . Conversely, continuous data (e.g. local field potentials, EEG or BOLD signals) need to be binarized to be amenable to this type of analysis, and this can represent an important problem when we want to deal with macroscopic brain networks [690,691]. Second, and more importantly, these models neglect the information encoded in the spatial and temporal structure of the interactions. Third, their scalability to large networks is made more complicated by the requirement of large amounts of data (e.g. long time series) to estimate model parameters.

Against this context, Giusti et al. [692] studied how the correlations of spike trains can be used to detect intrinsic structures in neural activity, without recurring to external stimuli or receptive fields, and how they relate to the topology and geometry of the animal's space. In particular, they computed pairwise correlations from the cross-correlograms of pyramidal neurons in freely roaming mice. Each correlation matrix was then transformed into an order complex. This is a filtration of simplicial complexes, obtained in their stead from a sequence of progressively denser graphs. At each density, only the strongest edges until the fixed density were retained. In such a way, for each density a binary graph was built and the corresponding clique complex computed, that is, in each graph all the cliques were considered as simplices (Fig. 40A). Giusti et al. [692] then compared the Betti curves of the real order complex with those obtained from randomized versions, which were built by reshuffling the original correlation matrices. They found that the Betti curves, which encode the topological complexity of the cell activation patterns, displayed consistently lower values than those from the randomized models. These observations suggested that the correlation structure of hippocampal neurons intrinsically represented the low dimensional input space (a two-dimensional roaming space in this case).

These results confirmed previous evidence on the role of hippocampal place cells in encoding primarily a space's topological qualities rather than its geometry [693,694], but also showed that some coarse geometrical information can be encoded in the fabric of correlations. Even more interestingly, Babichev et al. [695] extended previous hypotheses on the topological nature of the hippocampal map [693,694] to account for the temporal nature of interactions among place cells. Indeed, the mammalian hippocampus is thought to be able to learn an internalized cognitive map representing the ambient space. It is however unclear how such a map is conserved in time and updated due to the transient nature of synaptic connections and of the downstream neuronal networks. To investigate this mechanism, Babichev et al. [695] represented the instantaneous state of the internalized map as a coactivity complex, in which simplices represent groups of coactive place cells. At the beginning only few groups of place cells, hence simplices, are present. In time however by accumulation of activity, the coactivity complex should approximate the topology of the underlying space in which the animal moves. An open question however is how it is possible to preserve a consistent representation of a space while the animal is moving, place cells are constantly remapping and in general the population coding fluctuates. Studying the robustness of the topological features of coactivity complexes, Babichev et al. [695] strongly suggested that the temporal stability of the hippocampal map is a generic phenomenon stemming from a compensatory mechanism in which neuronal activity compensates deterioration in the network structure to preserve hippocampal function (see Fig. 41).

Reimann et al. [696] investigated the topology of excitation networks built from simulated activity on reconstructed cortical micro-circuitry. They found that different stimuli elicited a surprisingly large number of high-dimensional directed cliques and created a wide variety of high-dimensional homological holes. In particular, simulations on a variety of synthetic and null models did not display such an array of topological responses, suggesting these topological metrics do not emerge from traditional constraints on graph structure (e.g. degree sequences, clustering, etc.), but rather from

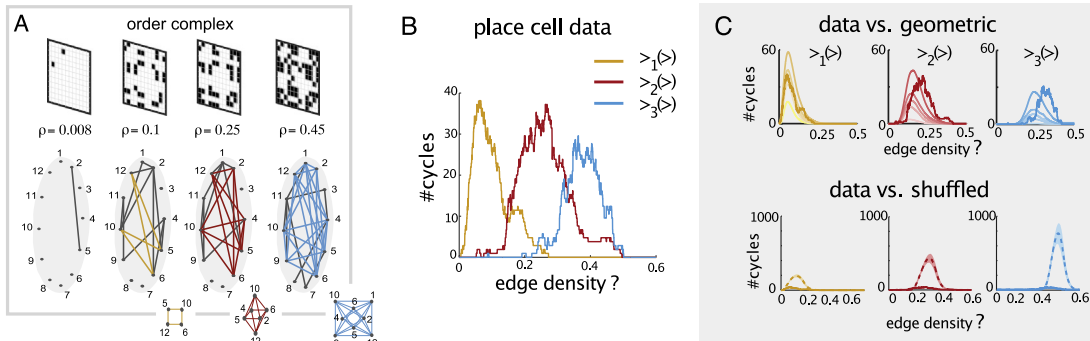


Fig. 40. Topology of hippocampal cells' activations encodes geometrical information about the environment. (A) an example of construction of order complex from a full correlation matrix. At each step the order complex (top row) encodes the topology of the density-filtered correlation graph (bottom row). (B) Betti curves of the pairwise correlation matrix for the activity of $N = 88$ place cells in hippocampus during open-field spatial exploration. (C) The same Betti curves from B (bold lines) shown overlaid on the mean Betti curves from random geometric complexes (top) and from complexes built from shuffled correlation matrices (bottom). Note the differences in when Betti numbers emerge in the case of random geometric complexes and in the magnitude itself for shuffled weight complexes.

Source: Figures adapted from Ref. [692].

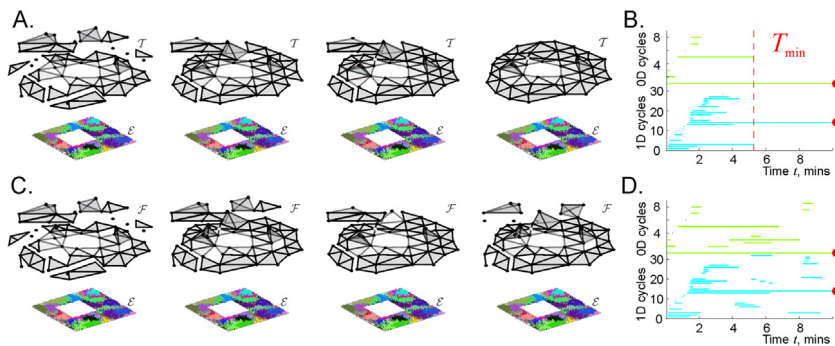


Fig. 41. The structure of coactivation complexes. (A) Simulated place field map $M(\epsilon)$ of a small planar environment ϵ with a hole in the center. The series of snapshots illustrates the temporal dynamics of the coactivity complex: the complex goes from being small and fragmented, in the early part of the exploration, to becoming a stable representation of the shape of the underlying environment. (B) The timelines, encoded as barcodes, of topological persistent H_0 and H_1 cycles in the coactivity simplicial complex: 0-dimensional persistent generators are shown in light-blue lines, 1-dimensional ones in light-green. Most loops correspond to accidental, short-lasting structures, effectively representing noise in the complex. The persistent topological loops (marked by red dots) represent physical features of the environment. The time to eliminate the spurious cycles can be used as a theoretical estimate of the minimal time needed to learn the path connectivity of ϵ . (C) Simplices can also disappear, and hence the coactivity complex may be flickering, instead of stable. (D) The timelines of the topological cycles in such complex may remain interrupted by opening and closing topological gaps produced by decays and reinstatements of its simplices.

Source: Figures reproduced from Ref. [695].

particular species-specific coordination among links. Moreover, they observed also that, in response to sensory stimuli, pairwise correlations grew with the number and order of the simplices to which the neurons belonged, suggesting that the hierarchy in physical structure results in hierarchically correlated activities.

At the macroscopic brain network level [697], the question of the importance (or lack thereof) of higher-order interactions appears less settled. On the one hand, for example, Huang et al. [698] suggested that weak higher order interactions might indeed be present in macroscopic functional networks, but also that, due their weakness, pairwise interactions are dominant in shaping brain activities, hence justifying functional connectivity descriptions based on pairwise interactions alone. On the other hand instead, higher order features were shown to be reliable under test-retest analysis [699], and important as indicators of aberrant connectivity in mental disorders [700] and mild cognitive impairment [701]. Also, higher order interactions were useful in the inference of the parameters of coupled oscillator models of EEG signals (for example [458]), which we discussed in more detail in 6.3.

Recent seminal research has shown the potential and impact of topological approaches, in particular those inspired by topological data analysis. Structurally, persistent homology techniques were adopted to describe and discriminate healthy and pathological states in developmental [702] and neurodegenerative diseases [703]. Sizemore et al. [26] described the white matter network of fibers between brain regions as a weighted network and then studied both its dense portions, in terms of cliques, and its cavities, in terms of homology. They found that large cliques are much more frequent than expected in an appropriate randomized model built using biologically-inspired principles of parsimonious wiring

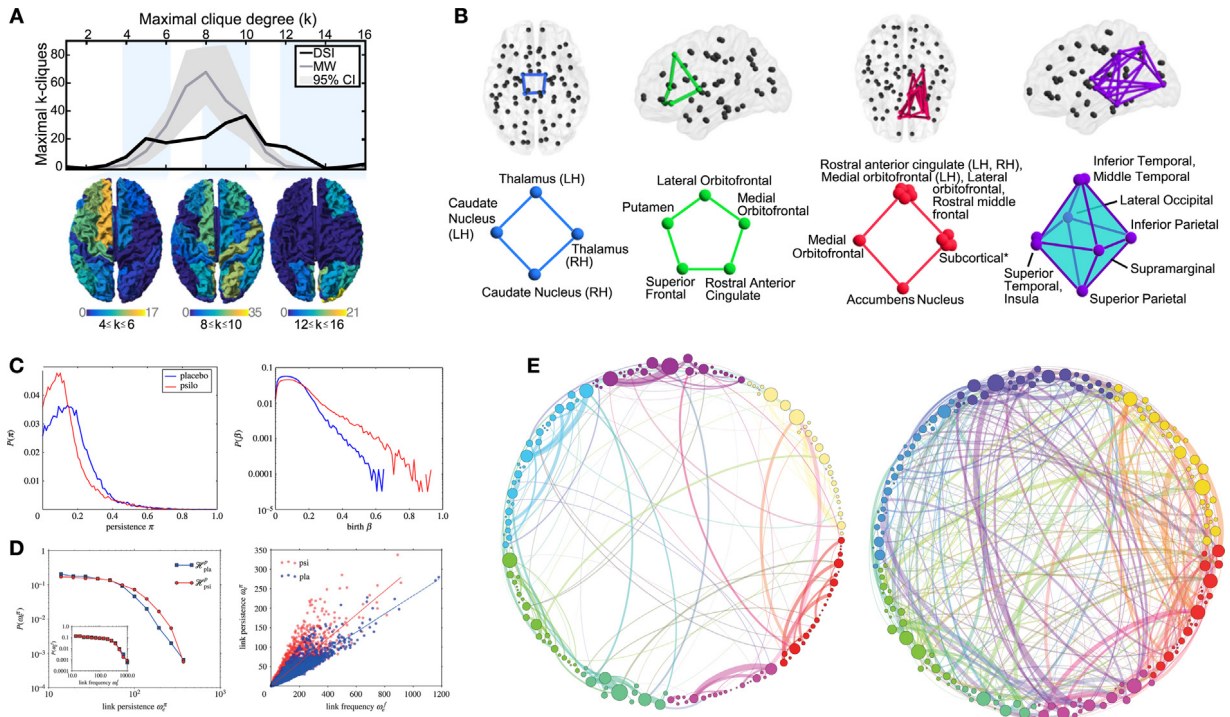


Fig. 42. Persistent homology of structural and functional brain connectivity. (A) Distribution of maximal cliques in the average DSI (black) and individual minimally wired (gray) networks, thresholded at an edge density of $\rho = 0.25$. Heat maps of node participation shown on the brain surfaces for a range of clique degrees equal to 4–6 (left), 8–10 (middle), and 12–16 (right). (B) Minimal cycles representing each persistent cavity at the density at birth represented in the brain (top) and as a schematic (bottom) (adapted from [26]). (C) Comparison of persistence p and birth b distributions. Left, H1 generators' persistence distributions for the placebo group and psilocybin group. Right, distributions of homology cycles' births. (D) Statistical features of group homological scaffolds. Left, probability distributions for the edge weights in the persistence homological scaffolds (main plot) and the frequency homological scaffolds (inset). Right, scatter plot of the scaffold edge frequency versus total persistence for both placebo and psilocybin scaffolds. (E) Simplified visualization of the persistence homological scaffolds for subjects injected with placebo (left) and with psilocybin (right). Colors represent communities obtained by modularity optimization on the placebo scaffold and display the departure of the psilocybin connectivity structure from the placebo baseline.

Source: Figures adapted from Ref. [25].

(Fig. 42A). These cliques were interpreted as local dense units able to perform rapid processing, and were found to be positioned around topological cavities, which in turn acted as obstructions and guides for the information flows. These cavities were also reproducible across subjects and appeared to connect regions belonging to different phases of brain evolutionary history (Fig. 42B). Similarly, Bendich et al. [704] described the morphology of brain arteries using topological observables. In particular, using persistent homology of trees, they characterized arterial morphology using the structure of branching and looping of vessels at multiple scales, and found distinctly different patterns at different ages.

Topological differences have been also found at both population and individual levels in functional connectivity in healthy and pathological subjects [705–707]. Higher dimensional topological features have been employed to detect differences in brain functional configurations in neuropsychiatric disorders and altered states of consciousness relative to controls [25,708], and to characterize intrinsic geometric structures in neural correlations [692,709].

As an example, Petri et al. [25] compared the topology of the functional connectivity of subjects that had been subministrated with psilocybin, a psychedelic drug, with their own under placebo. They found that the topological structure of the two conditions was very different and such difference could be quantified already at the level of persistence diagrams (Fig. 42C). While the difference between topological summaries obtained from persistent homology, was already discernible, it provided little information on how topological information mapped back to the underlying brain regions. The authors solved this problem by defining a topological backbone, called *scaffold*, built on approximated minimal homological generators (Fig. 42D), which allowed them to show that altered states of consciousness induced by psilocybin (and likely, other psychedelics) stem from very different patterns of information integration and importance of the brain regions [710] with respect to the normal state (Fig. 42E). Other examples can be found in the following series of works. Lee et al. [706] have proposed methods to discriminate between cohorts of children with attention deficit hyperactivity disorder, autism spectrum disorder and pediatric control subjects on the basis of their functional topology. Lee et al. [711] instead represented the topological substructure of brain networks through the eigenvectors of the corresponding Hodge Laplacians and used it to discriminate between mild and progressive cognitive impairments,

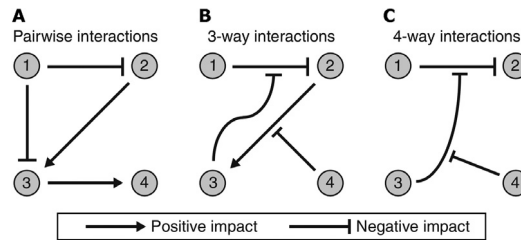


Fig. 43. Pairwise and higher-order interactions in ecological systems. (A) Direct pairwise positive and negative interactions among species. (B) Three-ways interactions: for example species 3 attenuates the direct inhibitory effect of species 1 on species 2. (C) Four-way interactions: species 4 inhibits the inhibition produced by species 3 on the interaction between 1 and 2.

Source: Figures adapted from Ref. [723].

and Alzheimer's disease. Chung et al. [712] described the heritability of differences in whole-brain functional topology in a cohort of twins. Ibáñez-Marcelo et al. [660] related the topological functional structure of EEG data during imagery to functional equivalence in a population of skilled versus unskilled imagers [713].

Going beyond functional connectivity, Saggat et al. [714] constructed a simplified topological backbone representation of the full fMRI activation space and showed that the properties of these backbones associated with behavioral performance in a series of cognitive tasks. In the context of event-related fMRI, Ellis et al. [715] investigated the feasibility of topological techniques for recovering signal representations from BOLD signals. In particular, they embedded specific signal configurations by a convolution of the signal with the hemodynamic response, showing that the persistent homology was able to recover the signal topology with high accuracy.

Finally, moving from neuroimaging to applications in cognitive neuroscience, Sizemore et al. [325] mapped the evolution of early semantic networks in toddlers by identifying words with nodes and considering higher-order interactions among them. They found that sparse regions of the resulting HORs displayed remarkable similarities at the topological level across subjects, and the timing of their disappearance was more closely related to the patterns of connections among words than to their actual semantic content, thus suggesting that knowledge acquisition might generally happen via filling knowledge gaps. For an extended review of the current research on the effects of non-pairwise interactions in neuroscience, we refer the reader to the following references [92,716,717].

9.3. Ecology

Higher-order interactions have been studied for decades in the context of ecological models [718–720]. However, only very recently it has been highlighted their crucial role for the stability of large ecological communities and for the remarkable biodiversity observed in nature. While pairwise interactions in ecology consider the direct effect, either positive or negative, of a species on another, as shown in Fig. 43A, higher-order interactions include all the cases where the relation between two species can be modified by the presence of other species, which may also be not directly affecting the former [721,722]. For instance, this happens when there is a microbial species that produces an antibiotic to interfere with a competing species, and a third species produces an enzyme which degrades the antibiotic thus reducing the strength of the interaction among the other two [723]. This is illustrated in Fig. 43B, where species 1 inhibits species 2, and species 3 produces the enzyme that reduces the direct inhibitory effect of species 1 on species 2. Such a mechanism gives rise to a so-called “trait-mediated indirect interactions” (TMIIs) between species 3 and 2, which is different from a possible direct pairwise interaction between 3 and 2 (also reported in the figure), being intrinsically a three-species interactions. As finally shown in Fig. 43C, the enzyme produced by species 3 can in turn be inhibited by a compound introduced by a species 4, creating a four-species inseparable/entwined interaction, and so on [724–726]. Similar effects can also arise from an adaptive behavior, for instance a predator which changes its target prey because another prey becomes available [727]. In this case there is no direct interaction between the two preys but they are part of a higher-order interaction, and considering only pairwise interactions would not allow to correctly take into account this effect.

Analyses of ecological networks almost often omit non-pairwise interactions, many classes of which are instead fundamental to the structure, the function and the resilience of ecosystems. It has been shown that the class of three-species interactions in which one of the three species has the effect of mitigating the negative interaction between the other two can have a stabilizing effect [724], while it has been found that increasing the order of the interactions reduces the fraction of extinct species [728] and increases the variance of species abundances at equilibrium [729]. The literature is growing and many scientists have shown that higher-order interactions can have a stabilizing effect under many particular condition settings.

It has been shown that hypergraphs can be a very useful mathematical framework to represent and take into account non-pairwise ecological interactions, such as TMIIs [120,730,731]. As an illustrative example of the value of hypergraphs in describing ecological communities, the authors of Ref. [731] have studied a real-world coffee agroecosystem in southern Mexico, in which resistance to agricultural pests depends upon a large number of TMIIs. Based on field studies, they

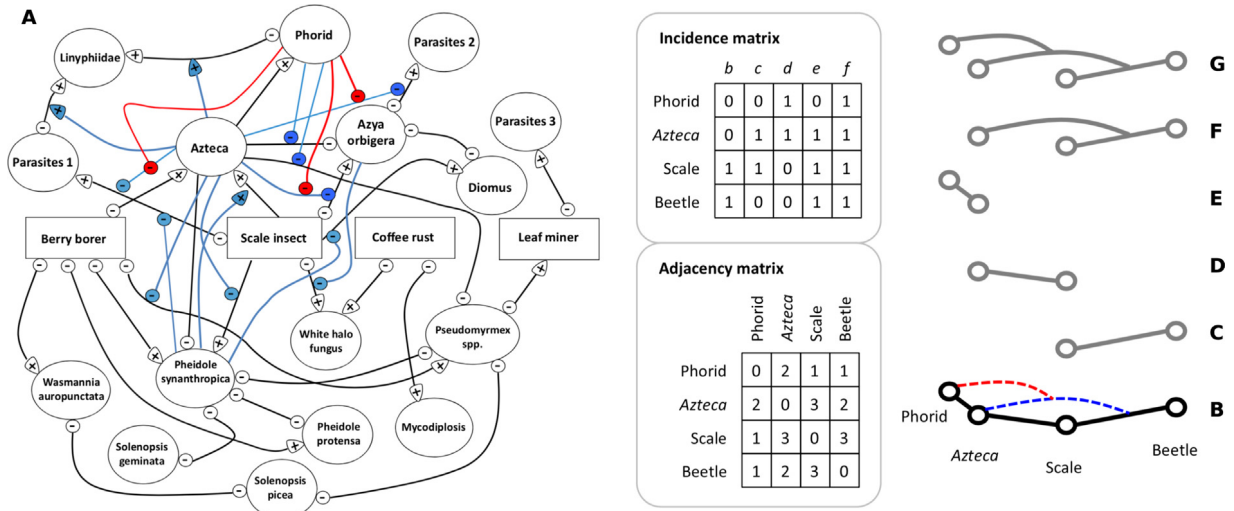


Fig. 44. Hypergraph description of the coffee agroecosystem in southern Mexico [731]. Nodes in (A) represent the different agricultural pests, while lines indicate direct effects (black), modifications of direct effects (blue), and modifications of those modifications (red). Key interactions (B) among four nodes of the system, namely Phorid, Azteca, Scale and Beetle (*Azya orbiger*), are represented in the form of a hypergraph whose hyperedges (C-G) and incidence and adjacency matrices are reported beside them.
Source: Figures adapted from Ref. [731].

have assembled the intricate web of interactions among agricultural pests that is reported in Fig. 44A. Black arrows indicate direct effects, while blue and red arrows represent modifications of those direct effects, and modifications of those modifications, respectively. In particular, some protective effects attributable to TMIs imposed by ants of the genus *Azteca* (blue lines from node *Azteca*), some of which are further modified by ant-parasitizing phorid flies (three red lines from node *Phorid*), have been shown to be crucial for controlling agricultural pests. Interactions within this system can be well represented by a hypergraph. The hypergraph corresponding to key interactions involving the four nodes *Phorid*, *Azteca*, *Scale* and *Beetle* (*Azya orbiger*) is reported in Figs. 44B-G, together with its adjacency and incidence matrices. Notice that positive and negative direct effects, or strengthening and weakening TMIs are respectively indicated by triangular and circular arrow-heads in the interaction web in Fig. 44A. However, this information has been omitted to produce the simpler case of an undirected system shown in (B). Direct effects represented as black lines in (B), and corresponding to the three edge of the hypergraph, include beetles preying on scale insects (C), *Azteca* ants consuming energy from Scales (D), and *Phorid* flies parasitizing *Azteca* ants (E). Indirect effects, consisting of *Azteca* ants reducing the magnitude of the interaction between *Scale* and *Beetle* [dashed blue line in (B)], and *Phorid* flies reducing the magnitude of the effect of *Azteca* ants on the *Scale*-*Beetle* interaction [dashed red line in (B)], are instead represented as the two hyperedges reported in (F) and (G), respectively. This example immediately illustrates the straightforward way in which hyperedges can represent TMIs. The authors of Ref. [731] further elaborate on how the analysis of hypergraph topology, and concepts such as shortest hyperpaths and hypergraph centrality measures, can turn very useful for studying important aspects of ecological systems (such as how a species is affected by the removal of other species from the system) that a network description only based on pairwise interactions alone can fail to faithfully represent.

Bailey et al. have investigated the stabilizing role of higher-order interactions in replicator equations [723]. They have proposed a mathematical model based on random replicator dynamics to study ecosystems when both pairwise and higher-order interactions are present. An ecosystem is described at each time by its state $\mathbf{x} = (x_1, x_2, \dots, x_N)$, where $x_i \equiv x_i(t)$ denotes the abundance of species i at time t , with the physical constraint $\sum_i x_i(t) = 1 \forall t$. The temporal evolution of the abundances are governed by the following set of differential equations:

$$\dot{x}_i = x_i [f_i(\mathbf{x}) - \sum_{j=1}^N x_j f_j(\mathbf{x})] \quad i = 1, \dots, N \quad (67)$$

in the usual form of replicator dynamics [584–587], already introduced in Eq. (63), Section 8, to model the evolutionary dynamics of strategic interactions in a population with cooperators and defectors. The first term in bracket, f_i represents the fitness of species i , which depends on the effect of the other species through the system state \mathbf{x} , while the second term is the average population fitness. The key point is that the fitness function here adopted:

$$f_i(\mathbf{x}) = -x_i + \sum_{j=1}^N a_{ij} x_j + \sum_{j=1}^N \sum_{k=1}^N b_{ijk} x_j x_k + \sum_{j=1}^N \sum_{k=1}^N \sum_{l=1}^N c_{ijkl} x_j x_k x_l + \dots \quad (68)$$

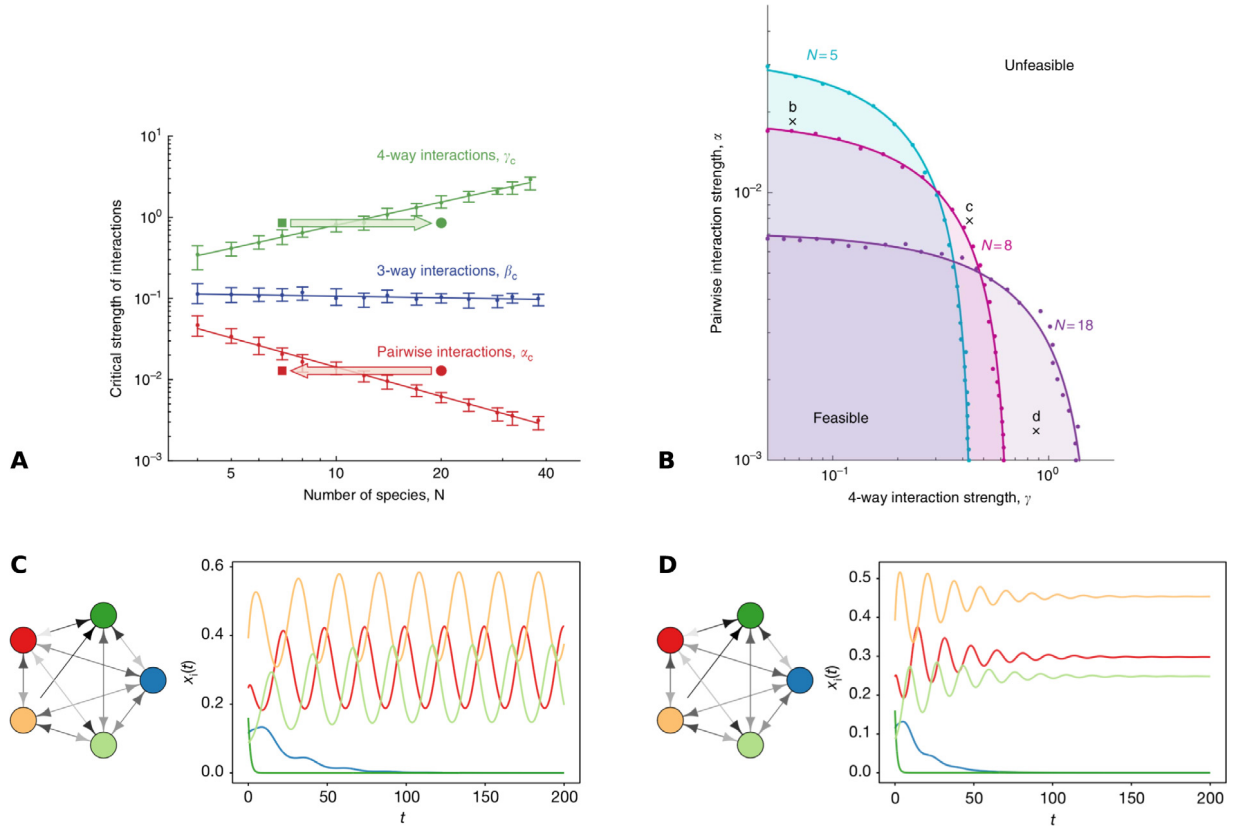


Fig. 45. Dynamical effects of higher-order interactions in ecological systems. (A) Critical strength of interactions in the Bairey et al. [723] model in Eq. (67) and (68) beyond which the coexistence of species is lost as a function of the number of species N . The three curves represent the case of only pairwise, three-species and four-species interactions, respectively. (B) Regions of stability for ecosystems with $N = 5, 8$ and 18 species in the (γ, α) space (assuming $\beta = 0$). (C) Temporal evolution of the abundances of five different species as given by the Grilli et al. [27] model for the competition matrix H reported in the five node graph, and when only pairwise interactions are considered. (D) Same as in the previous panel, but with sampling three seedlings at a time instead of two.
Source: Figures adapted from Ref. [27] and Ref. [723].

includes pairwise but also higher-order interactions. Entry a_{ij} of matrix A determines the effect of species j on species i . Three-dimensional (or third-order) tensor B rules three-species interactions, with the value of the entry b_{ijk} determining the joint effect of species j and k on species i , and so on with the four-dimensional tensor C , etc. Notice that the negative sign of the first term, $-x_i$, implies the stability of the system when interactions are turned off (species are self-limiting in high concentrations). Limiting the analysis to higher-order interactions not involving more than four species, random perturbations of different order to a stable ecosystem are then modeled by setting $A = \sqrt{\alpha}\tilde{A}$, $B = \sqrt{\beta}\tilde{B}$ and $C = \sqrt{\gamma}\tilde{C}$. Here \tilde{A} , \tilde{B} and \tilde{C} are a random matrix (a two-dimensional tensor), and a random three-dimensional and four-dimensional tensors respectively. The elements of \tilde{A} , \tilde{B} and \tilde{C} can either be positive or negative and are drawn from a Gaussian distribution with mean 0 and variance 1. The important parameters of the model are then the values of α , β and γ , which represent the strength of the pairwise, three-species and four-species interactions, respectively. As expected, in a system with only pairwise interactions ($\beta = 0$, $\gamma = 0$), species exhibit extinctions when the strength α is larger than a critical value, and such value decreases with the system diversity, i.e. with the number of species N . Reported in Fig. 45A is the threshold α_c at which coexistence is lost in 5% of the simulations. When the number of species N is increased, the critical threshold α_c decreases as $1/N$, in agreement with the result by May [732]. The situation changes when higher order interactions are considered. In particular, if only three-species interactions are present ($\alpha = 0$, $\gamma = 0$), then the value of the critical strength β_c is not affected by the number of species. Conversely, if only four-species interactions are considered, the threshold γ_c increases with the system diversity. This is a striking result: for a fixed strength of four-species interactions, an ecosystem is stabilized, rather than destabilized, as the number species increases. Thus, while pairwise interactions introduce a higher bound on diversity, a lower bound is instead created by high-order interactions. Or in other words while ecological communities with a large number of species become sensitive to pairwise interactions, communities with a small number of species are sensitive to high-order interactions.

Bairey et al. have also considered the more interesting “mixed case” in which a combination of the three types of interactions can be present at the same time. The resulting stability region for three different sizes N of the system is

graphically represented in Fig. 45B. in the space (γ, α) of pairwise and four-species interaction strengths, in the case of no three-species interactions, i.e. assuming $\beta = 0$. Notice that there is a small area where an ecosystem with $N = 8$ species is feasible, while systems of both sizes $N = 5$ and $N = 15$ are unstable. Since it is plausible that, in the most general case, an ecosystem is characterized by interactions of different orders and by a set of values $(\alpha, \beta, \gamma, \dots)$ for the corresponding strengths, this will imply the existence of both a lower and upper bound for the number of species, for which Bairey et al. provide an analytical estimation. They also found that, if the total strength $\alpha + \beta + \gamma$ is increased, then upper and lower bounds get closer, restricting the range of allowed diversity of the ecosystem.

Grilli et al. [27] have instead studied the role of higher-order interactions in a model of interacting competitors [733–736]. Although the proposed framework is quite general, the model describes the dynamics of a forest with a large but fixed number of trees, in which N different species of trees compete for space. As in the case of the model by Bairey et al. the state of the system is described by the vector $\mathbf{x}(t)$, i.e. by the proportion $x_i(t)$ of trees of each species i at time t , with $\sum_i x_i(t) = 1 \forall t$. The dynamics stems from the fact that at each time step a tree, selected at random (with all the species having the same death rate), dies leaving an empty space in the canopy, which can be filled by a new tree. That is when the competition among seedlings begins. The simplest way to model this mechanism is through a pairwise competition: two species are randomly selected and the winner of the competition will fill the gap. Pairwise competitions are characterized by matrix H whose entry h_{ij} represents the winning probability of species i on species j . In particular, Grilli et al. consider the most general case of a matrix of randomly generated positive numbers between 0 and 1, with $h_{ij} + h_{ji} = 1$, which represents an extension of previous works [737,738]. The dynamics of the N species is ruled by the following set of differential equation:

$$\dot{x}_i = -x_i + 2x_i \sum_{j=1}^N h_{ij}x_j = x_i \sum_{j=1}^N p_{ij}x_j \quad (69)$$

where the negative terms $-x_i$ describe the death process, while the positive term $2x_i \sum_j h_{ij}x_j$ gives the probability of selecting two seedlings of species i and j , with i winning the competition. Notice that the competition process can be seen as a game [739,740], and the right hand side of the equation can be rewritten in the form of a replicator equation for a zero-sum, symmetric matrix game with two players, where the payoffs p_{ij} are the entries of the skew-symmetric payoff matrix $P = H - H^T$ [741,742], similar to the payoff matrix introduced in Eq. in Section 8. Independently from the initial conditions $\mathbf{x}^*(0)$, after an initial transient, Eq. (69) drives the system to a state where some of the N species go extinct, while the remaining ones cycle around a unique equilibrium point \mathbf{x}^* . This is shown for a case with $N = 5$ and a particular random choice of matrix H in Fig. 45C. By changing H the model can lead to arbitrarily many species coexisting, and can generate any possible species-abundance distribution empirically observed. However, the neutral cycling around the equilibrium is problematic, as such cycles are not observed in nature. In addition to this, the main issue with the model is that the equilibrium is highly unrobust: any deviation from perfectly identical death rates destabilizes the dynamics and leads to just one species surviving. Grilli et al. have shown that the problem can be solved by going beyond the pairwise interactions and considering the simultaneous competition among more than two species when a new empty space appears in the canopy. They propose an extension of the model in Eq. (69) where three seedlings are picked at random, the first competes with the second and the winner with the third. The equations now read:

$$\dot{x}_i = -x_i + x_i \sum_{j=1}^N \sum_{k=1}^N (2h_{ij}h_{ik} + h_{ij}h_{jk} + h_{ik}h_{kj}) x_j x_k = x_i \sum_{j=1}^N \sum_{k=1}^N p_{ijk} x_j x_k \quad (70)$$

where $h_{ij}h_{ik}$ is the probability that i beats both j and k , $h_{ij}h_{jk}$ is the probability that first j beats k , and then i beats j , and $h_{ik}h_{kj}$ is the probability that k beats j , and then i beats k . Also in this case the equations can be rewritten in the form of a replicator dynamics for a three-player game with a three-dimensional payoff tensor P whose entry $p_{ijk} = 2h_{ij}h_{ik} - h_{ij}h_{jk} - h_{ki}h_{kj}$ gives the payoff of the first player 1 playing strategy i when player 2 plays j and player 3 plays k . Surprisingly, the evolution of this new model leads to globally stable fixed points instead of cycles. As shown in Fig. 45D for the same matrix H as in Fig. 45C, the system converges to a fixed point characterized by the same vector \mathbf{x}^* that was the center of the oscillation in the model with only pairwise interactions. In addition to this, the fixed point is now globally stable. Hence, sampling three seedlings at a time instead of two produces stability in a system of competitors. The same authors have also proven that the inclusion of fourth- or higher-order terms does not change the equilibrium but simply accelerates the convergence to it. Moreover, when transforming this deterministic model into a stochastic one, the presence of higher-order interactions delays the extinction time, allowing a prolonged coexistence of species. Summing up, the model in Eq. (70) clearly indicates that the inclusion of higher-order interactions in competitive networks stabilizes dynamics, making species coexistence robust to perturbations.

Mayfield et al. [743] have pointed out the role of higher-order interactions in another important aspect, that of estimating the values of fitness in ecological models. They have shown that it is quite difficult to explain the empirically observed fitness outcomes by considering only pairwise interactions. The inclusion of higher-order interactions, defined as changes to the interactions between two species mediated through a third species, can instead improve the ability to perform such an estimation.

Very recently, Valverde et al. [744] have applied a HOoS framework to the analysis of environmentally mediated host-pathogen infections. The hyperlinks of a hypergraph are used to depict three-way associations between plants (hosts),

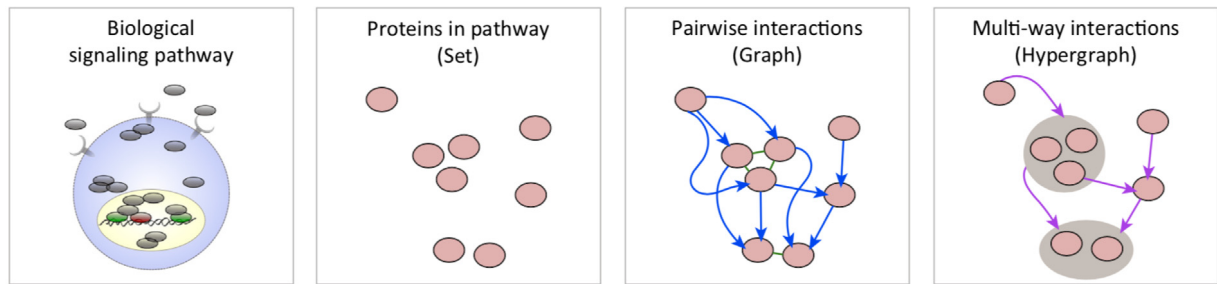


Fig. 46. Different representations of biological signaling pathways. In the simplest representation, a signaling pathway is simply a set of proteins, with no additional information. Networks can only capture pairwise interactions between proteins. Hypergraphs naturally encode multilateral interactions and reactions.

Source: Figure reproduced from Ref. [752].

viruses (pathogens), and different habitats. Projecting this information, it is possible to study the interactions between viruses and different host ecotypes, explicitly including the spatial context in which host-pathogen interactions take place. By building a neutral model for the evolution of host-pathogen networks across multiple habitats, the study showed that real ecosystems live in a continuum between nested and modular networks, going beyond the traditional dichotomy between modularity and nestedness in ecological networks [745]. The model has been empirically validated by the analysis of different ecosystems in an agricultural landscape in Spain.

For a more complete review of the current research on the effects of non pairwise interactions on the mechanisms to maintain biodiversity in ecological systems we refer the reader to the review “Beyond pairwise mechanisms of species coexistence in complex communities” by Levine et al. [30].

9.4. Other biological systems

Over the last decades network science has become an established framework to describe and understand interactions between biological agents, including proteins, metabolites and genes [746–748]. Yet, the complexity of biological processes can only rarely be decomposed as a sum of pairwise interactions. For instance, metabolic reactions often involve multiple partners, and proteins typically interact with each other in small groups known as complexes. As a consequence, traditional pairwise approaches, which neglect the presence of higher-order structures, are at risk of oversimplify the complexity of biological systems.

Among the first higher-order analyses in biology were studies showing that the hypergraphs corresponding to mammalian protein complexes [749] had a scale-free distributions of both node degrees and hyperedge sizes [750]. The full potential of using HORS frameworks, in particular hypergraphs, to characterize complex biological processes taking place in biomolecular systems, was already clear more than ten years ago [751]. An important range of applications is that of signaling pathways in cell biology, where groups of molecules have to work together to efficiently control cell functions, such as death or division [752]. Different representations of signaling pathways are summarized in Fig. 46. Gaudelet et al. [753] have investigated protein interaction hypergraphs by extending the concept of graphlets [754], to the case of higher-order networks. Hypergraphlets were defined as small induced sub-hypergraphs of a given large hypergraph, and an orbit identifies each different set of automorphic nodes. An example of all the hypergraphlets of 1, 2 and 3 nodes is illustrated in Fig. 47. Similarly to motifs [72], hypergraphlets allow to characterize wiring patterns of higher-order networks at the local scale. By focusing on the case of yeast and human pathways, the authors showed that modeling protein interactions as hypergraphs allows for better functional predictions than a description in terms of graphs with pairwise interaction only.

Franzese et al. [755] have challenged the current approaches to molecular connectivity, which they found either too permissive or too restrictive. As an alternative, they have proposed an intermediate optimal solution that interpolates between graph and hypergraph approaches and allows to better capture the importance of small molecules involved in many distinct reactions. More recently, Klimm et al. [756] have used hypergraphs to investigate multiprotein complex data, showing how a pairwise (network) projection produces a hierarchical structure, that is instead not observed when polyadic interactions are considered. After comparing the protein complexes with appropriate null models, the authors found that larger complexes tend to be more essential, with a hyperdegree that better correlates with gene-essentiality information than the standard graph degree. All these results suggest the importance of considering the inherent higher-order structure of protein complexes to reveal complementary information.

Redundancy is an important property of biological systems that guarantees their functionality in the case of malfunctioning of some local components. Percy et al. [757] have used hypergraph percolation to assess the robustness of empirical bacterial metabolic higher-order system to random failures. In particular, they have used site percolation, in which a hyperedge (describing a reaction) is activated only when all metabolites involved in the hyperedge are

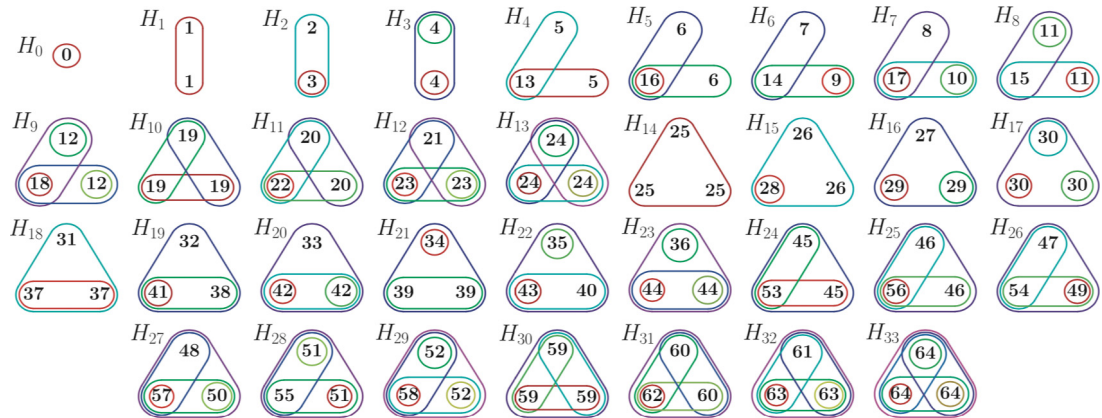


Fig. 47. Hypergraphlet representation of local connectivity patterns in hypergraphs. Complete illustration of the 65 orbits associated to hypergraphlets of order 1, 2 and 3. More than 6000 orbits are associated to hypergraphlets of order 4, and more than a hundred thousands to hypergraphlets of order 5.

Source: Figure reproduced from Ref. [753].

active. Results showed that interacting systems that have evolved in environments with a higher degree of variability are more robust, and that, similarly to their simple network counterparts, metabolic hypergraphs are characterized by the presence of a core-periphery structure. In another study, metabolic networks have been characterized by the spectrum of a symmetric tensor associated with their hypergraph connectivity, successfully capturing the chemical information of enzymes and structural changes of compounds to define novel classes of functional reactions [758]. Other higher-order topological operators such as combinatorial Laplacians (see Section 3.5.2) were shown to provide a more complete characterization of chemical reaction networks [759].

The complexity of biological systems entails that the data we obtain from experiments are often incomplete or characterized by a limited accuracy. For this reason, various works have concentrated on the problem of reconstructing the hypergraphs associated with different kinds of cellular processes where higher-order interactions are at play [760–764]. Recently, higher-order inference frameworks have also been extended to deal with dynamic correlations of abundance levels of genes, transcripts and metabolites changing over time. The results provide a better picture of the global dynamic correlation patterns of the investigated biological systems [765].

Higher-order interactions have also revealed key insights when designing effective drug combinations to prevent or contrast diseases. Indeed, in multiple cases, from cancer to tuberculosis, the combined action of the ingredients of a so-called drug cocktail, even when administered at a low dose, has been shown to be more beneficial than that of single drugs in isolation. Recently, the dose model has been developed as an efficient tool to discover effective drug combinations based on pairwise interactions [766]. While the dose model was originally tested only on triplets and quadruplets of antibiotics, as well as triplets of cancer drugs, very recently the model was shown to successfully predict effective combinations of up to ten drugs used for *E. coli* and the *M. tuberculosis* pathogen [767]. However, when noise in the dataset is more important, prediction of higher-order interactions based on pairs of drugs is less efficient [768]. Notice that alternative approaches to detect effective drug cocktails are available, such as the so-called pairs model, which was shown to be more noise-resistant but less precise [769].

Related to both robustness and drug resistance, the feedbacks between the different levels of genetic information shape to a large degree the link between genotype and phenotype [770,771]. A relevant example is that of epistasis, which Weinreich et al. [772] have defined as “the surprise at the phenotype when mutations are combined, given the constituent mutations’ individual effects”. In other words, epistasis describes the somewhat surprising observation that the effects of multiple individual mutations appear to interact with each other in ways that cannot be quantitatively reduced to sums of pairwise interactions [28]. While the concept of higher order epistasis is not new [773], only recently it has become possible to start a quantitative analysis of its effects in different contexts [774]. For example, Guerrero et al. [775] have investigated how protein quality control machinery influenced the epistasis in traits related to bacterial antibiotic resistance, separating the mutations affecting an essential bacterial enzyme from species-specific effects. Yitbarek et al. [776] have explored higher-order interactions among gut taxa and their effects on host infection risk, using a theoretical model tailored to the type of data that might be empirically collected in the near future. Mickalide and Kuehn [777] have studied a controlled microbial trophic chain and detected an increased invasion resistance of the community, stemming not from resource allocation but from high-order interactions between its species.

Finally, dynamical processes have been recently used to extract information on the structure of higher-order biological networks. For instance, Niu et al. [778] have considered a microbe-disease hypergraph, where nodes are microbes and diseases are hyperedges. A higher-order random walk (see Section 5.2) was shown to have a greater accuracy in the prediction of disease-microbe associations compared to that of traditional random walks.

10. Outlook and conclusions

In this review, we have discussed ways and methods to detect, represent, measure and model systems with higher-order interactions, and we have illustrated that models of higher-order systems substantially differ both structurally and dynamically from traditional pairwise models.

We have seen time and time again that there are crucial conceptual differences between modeling pairwise and higher-order interactions. For example, we have seen that higher-order interactions typically lead to new sources of non-linearity in the systems under study, which are not present in standard network approaches. Further, considering objects richer than links opens up new possibilities and questions: for example, state variables can now be defined not only on nodes, as in standard practices, but also on edges, triangles, tetrahedra and so on, paving the way to concepts like group states, but also necessitating a consideration about their meaning and interpretation [415]. Much of this new landscape is yet unexplored, but we can already make a few important observations.

At the dynamical level, it is evident that the presence or absence of higher-order interactions is especially important. We reviewed explicit examples in which higher-order interactions profoundly change the critical behavior of dynamical processes in both simplicial complexes [86,152,283,339,406,425] and hypergraphs [103,258,345,424,647]. However, even when a dynamical process does not explicitly contain higher-order *dynamical* terms, it is possible to find new effects due to higher-order terms in the *structural* patterns underlying the dynamics. For example, simple contagion processes are usually considered to be largely oblivious to higher-order structures (e.g. large groups, heterogeneous and/or hierarchical clique structure) beyond clustering in the underlying contact patterns. However, membership of nodes to cliques of heterogeneous sizes can result in unexpected mesoscopic localization phenomena, in turn yielding possible outbreak persistence for cases in which standard diffusion models would predict outbreak extinction [779]. Along similar lines, it has been shown that including group activations in a simple contagion model on a temporally evolving contact substrate can shift the critical infectivity, and that the shift depends on a trade-off between the distributions of group sizes and of activity of the nodes [293].

The importance of higher-order interactions is naturally not limited to their effects on dynamics. Recent examples include applications in which higher-order terms allowed better descriptions of group formation in scientific collaborations [115,358,676] and finer classification of the local environment of node [133]. In other cases, they improved the predictions of new interactions beyond the capacity of link-based prediction models, and also significantly denoised signals in complex environments [70,780]. Topological descriptions have even been proposed as a convenient tool to model epistemic models with distributed computing tasks [781–783].

The study of higher-order systems, of their characteristic properties and their effects on dynamics is a recent field, and there are still many open and unexplored directions. Below, we list some of them:

Measures for higher-order structures. We have described the most common measures used in the description of HORs. With the exception of the intrinsically algebraic ones, most of these measures however are straightforward generalizations of those used for networks. Temporal, multiplex and multilayer measures are still lacking, and generally there is a large space to be filled. An example are measures that simply cannot be defined in pairwise networks, the simplicial closure being one of these [31,115,133]. Other examples touch on state variables defined on simplices or hyperedges of arbitrary dimensions: while we have a clear understanding of what synchronization among nodes looks like in models of oscillators, it is much harder to have an intuitive grasp of what the state of an edge, or of a triangle, might mean [784]. Defining measures able to capture these quantities would also be a step toward an understanding of their role and quantitative insights about their effects. A further example is homological information obtained from topological data analysis techniques: it is defined as an equivalence class and therein lies its power and curse, because its resulting non-local nature makes it a powerful descriptive tool, but also very hard to localize on specific elements of the HORs. Efforts to find a solution to this issue already exist [25,785,786], but in many cases the problem is ill-defined and the solution specific to the problem at hand. So, are there standard or, at least, acceptable ways to localize homological features as to use them in further analysis? Or should we give up on localizing shapes, and think only about manifolds? Finally, while hypergraph partitioning [158,787] has a long history, little work has focused on characterizing the mesoscopic structure of simplicial complexes, both in terms of the definition and detection of communities (e.g. [357,788]) and of other types of (quasi-)local (e.g. rich club, assortative behavior, etc.) and spanning structures (e.g. cores [789], minimal spanning trees [790], expander properties [791,792]).

Generative models for higher-order structures. Models able to constrain various features of higher-order structures are crucial because they provide a principled answer to the question of what constitutes a non-trivial and topologically rich HORs. As we have discussed in this review, there are currently few random models of simplicial complexes. Some of the existing models of simplicial complexes reproduce the local connectivity patterns [108,114], but none exist that are able to reproduce or approximate more refined topological structures, like a specific target homology or mesoscopic structures. Finally, exactly like conventional networks, HORs can change in time or be composed by different qualitatively different types of interactions. With few notable exceptions [293,695], to date there are practically no models taking into account the temporal or multiplex structure of higher-order interactions—the vast majority model growth instead [302].

Understanding the driving mechanisms of higher-order dynamics. Developing new measures and generative models is also important to identify the fundamental mechanisms that lie behind the patterns we observe. There is in fact clear evidence that non-trivial higher-order topologies emerge in social [793,794] as well as in biological systems [25,692,693], but very

little understanding of how or why they do emerge. Currently, only few models focus on describing coordination, group interactions and in general growth of HORs at the group level, and none reproduce higher-order topological invariants. This is in part due to the predominance of network descriptions up until now, and in part to the actual difficulties to provide an analytical description that one encounters as soon as higher-order terms are introduced. In addition to the work on contagion mentioned above, early efforts in this direction are already under way, including generalization of Kuramoto models to higher-order interactions [159,339,401,406] and games [647]. A particularly important and recent line of research focuses on extending concepts from percolation to simplicial complexes, dubbed *topological percolation*, both in simplicial [290,291] and homological terms [795]. Overall, despite encouraging recent results [412], we still lack a general understanding of how higher-order terms affect dynamical systems.

Inference from data. What is a truly genuine higher-order interaction? And how do we tease it apart from low-order ones in data? And if it is possible, what type of data do we need to tell the difference between low and higher-order interactions? These are hard questions in general, but for some systems it is easier to approach them with some confidence. Indeed, for systems where the data already comes in the form of sets, it is straightforward to extract higher-order interactions and measure their strengths. This is the case, for instance, of affiliation networks such as coauthorship data, where each paper constitutes an interaction among all authors, or of data about joint presence in locations, or different ingredients in recipes. In many systems, however, interactions are not already identified, but instead need to be inferred from the data [796–798]. The most obvious example is that of time series: brain functional networks are usually estimated by computing correlations, or other measures based on information theory, between fMRI or EEG time series [799]; similarly, financial networks are built starting from stock option prices or timecourse of revenues, and so on [800]. In all these cases, higher-order interactions are seldom considered relevant, or even computed, due to various reasons. First, many-body correlations are often computed as second order approximations of standard correlations, and hence considered as perturbations. Second, measures that can find higher-order effects [801–803] often require long time series, which in many cases are not available. Third, the scarce availability of rich data on dynamical models with and without higher-order interactions makes it impossible to define a proper inference scheme for the presence, nature and strength of higher-order interactions. This last point is crucial and links back to the importance of models to understand the underlying mechanisms. Just like it is hardly possible to distinguish complex from simple contagion from prevalence and incidence data [804], it might well be the case that it is not possible to tease apart the effects of complex contagion from those of simplicial contagion [283] in absence of microscopic mechanistic information. However, currently there are no inference schemes able to test hypothesis about higher-order interactions and provide guidance in these situations [797]. Developing such schemes is therefore paramount to the advancement of the field.

The open directions discussed above focus on theoretical, modeling and methodological issues. HORs have already been fruitful in a smattering of applications, but they still need to find concrete applications to a wider range of topics. Indeed, the real test of their relevance will be in the breadth and depth of their impact on specific problems. While the paradigm of higher-order interactions is general, we envision that problems in biology, ecology, population dynamics, neuroscience and computational social sciences will be the first and the foremost to benefit from these new tools and ideas. We hope that this review will provide a guiding path for researchers interested in HORs, and we look forward to seeing how HORs themselves will reshape the landscape of complex systems research.

Declaration of competing interest

The authors declare that they have no known competing financial interests or personal relationships that could have appeared to influence the work reported in this paper.

Acknowledgments

F.B. acknowledges partial support from the ERC Synergy Grant 810115 (DYNASNET). G.C. and M. L. acknowledge partial support from the “European Cooperation in Science & Technology” (COST): Action CA15109. I.I. acknowledges partial support from the Urban Dynamics Lab under the EPSRC Grant No. EP/M023583/1. V.L. acknowledges support from the Leverhulme Trust Research Fellowship “CREATE: the network components of creativity and success”, RF-2019-059. J.-G.Y. acknowledges support from the James S. McDonnell Foundation. G.P. acknowledges partial support from Intesa Sanpaolo Innovation Center and from Compagnia San Paolo (ADnD project).

The authors acknowledge valuable and stimulating discussions with many members of the network science community on the topic covered in our report, including Antoine Allard, Unai Alvarez-Rodriguez, Alex Arenas, Tomaso Aste, Paolo Bajardi, Albert-László Barabási, Andrea Baronchelli, Alain Barrat, Danielle Bassett, Demian Battaglia, Jaume Bertranpetit, Ginestra Bianconi, Christian Bick, Jacob C.W. Billings, Stefano Boccaletti, Francesco Bonchi, Guido Caldarelli, Timoteo Carletti, Ciro Cattuto, Mario Chavez, Guilherme Ferraz de Arruda, Fabrizio De Vico Fallani, Tiziana Di Matteo, Tina Eliassi-Rad, Paul Expert, Duccio Fanelli, Michael Farber, Mattia Frasca, Luca Gallo, Lucia Gambuzza, Laetitia Gauvin, Fosca Giannotti, Tommaso Gili, Corrado Gioannini, Jesus Gómez-Gardeñes, Heather A. Harrington, Laurent Hébert-Dufresne, Esther Ibáñez-Marcelo, Gerardo Iñiguez, Cliff Joslyn, Márton Karsai, Sonia Kéfi, János Kertész, Julia Koltai, Dima Krioukov, Lucas Lacasa, Renaud Lambiotte, Bruno Lepri, Michael Lesnick, Daniele Marinazzo, Andrea Migliano, Marija Mitrovic Dankulov, Yamir Moreno, Mark Newman, André Panisson, Daniela Paolotti, Luca Pappalardo, Dino Pedreschi, Tiago P.

Peixoto, Matjaž Perc, Nicola Perra, Angkoon Phinyomark, Mason Porter, Márton Pósfai, Mario Rasetti, Martin Rosvall, Manish Saggarr, Anxo Sanchez, Enrica L. Santarcangelo, Samuel S. Scarpino, Michael Schaub, Martina Scolamiero, Ingo Scholtes, Olaf Sporns, Bosiljka Tadić, Stefan Thurner, Michele Tizzoni, Francesco Vaccarino, Alessandro Vespignani, Lucio Vinicius.

References

- [1] P.W. Anderson, More is different, *Science* 177 (4047) (1972) 393–396.
- [2] A.-L. Barabási, The network takeover, *Nat. Phys.* 8 (1) (2011) 14.
- [3] A. Vespignani, Modelling dynamical processes in complex socio-technical systems, *Nat. Phys.* 8 (1) (2012) 32–39.
- [4] M. Boguna, I. Bonamassa, M. De Domenico, S. Havlin, D. Krioukov, M. Serrano, *Network geometry*, 2020, arXiv:2001.03241.
- [5] D.J. Watts, S.H. Strogatz, Collective dynamics of ‘small-world’ networks, *Nature* 393 (6684) (1998) 440.
- [6] A.-L. Barabási, R. Albert, Emergence of scaling in random networks, *Science* 286 (5439) (1999) 509–512.
- [7] B. Bollobás, *Random Graphs*, (73) Cambridge University Press, 2001.
- [8] L. Lovász, *Large Networks and Graph Limits*, vol. 60, American Mathematical Society, 2012.
- [9] R. Albert, A.-L. Barabási, Statistical mechanics of complex networks, *Rev. Modern Phys.* 74 (1) (2002) 47.
- [10] G. Cimini, T. Squartini, F. Saracco, D. Garlaschelli, A. Gabrielli, G. Caldarelli, The statistical physics of real-world networks, *Nat. Rev. Phys.* 1 (1) (2019) 58–71.
- [11] S.N. Dorogovtsev, J.F.F. Mendes, Evolution of networks, *Adv. Phys.* 51 (4) (2002) 1079–1187.
- [12] M.E.J. Newman, The structure and function of complex networks, *SIAM Rev.* 45 (2003) 167–256.
- [13] S. Boccaletti, V. Latora, Y. Moreno, M. Chavez, D.-U. Hwang, Complex networks: Structure and dynamics, *Phys. Rep.* 424 (4–5) (Fevrier 2006) 175–308.
- [14] G. Caldarelli, Scale-Free Networks: Complex Webs in Nature and Technology, in: *Oxford Finance Series*, OUP Oxford, 2007.
- [15] A. Barrat, M. Barthélemy, A. Vespignani, *Dynamical Processes on Complex Networks*, Cambridge University Press, 2008.
- [16] M.E.J. Newman, *Networks: An Introduction*, Oxford University Press, Oxford; New York, 2010.
- [17] E. Estrada, *The Structure of Complex Networks: Theory and Applications*, Oxford University Press, Inc., New York, NY, USA, 2011.
- [18] A.-L. Barabási, M. Pósfai, *Network science*, Cambridge University Press, Cambridge, 2016.
- [19] V. Latora, V. Nicosia, G. Russo, *Complex Networks: Principles, Methods and Applications*, Cambridge University Press, 2017.
- [20] F. Menczer, S. Fortunato, C. Davis, *A First Course in Network Science*, Cambridge University Press, 2020.
- [21] C.T. Butts, Revisiting the foundations of network analysis, *Science* 325 (5939) (2009) 414–416.
- [22] P. Holme, J. Saramäki, Temporal networks, *Phys. Rep.* 519 (3) (2012) 97–125.
- [23] S. Boccaletti, G. Bianconi, R. Criado, C.I. Del Genio, J. Gómez-Gardeñes, M. Romance, I. Sendina-Nadal, Z. Wang, M. Zanin, The structure and dynamics of multilayer networks, *Phys. Rep.* 544 (1) (2014) 1–122.
- [24] A.R. Benson, D.F. Gleich, J. Leskovec, Higher-order organization of complex networks, *Science* 353 (6295) (2016) 163–166.
- [25] G. Petri, P. Expert, F. Turkheimer, R. Carhart-Harris, D. Nutt, P.J. Hellyer, F. Vaccarino, Homological scaffolds of brain functional networks, *J. R. Soc. Interface* 11 (101) (2014) 20140873.
- [26] A.E. Sizemore, C. Giusti, A. Kahn, J.M. Vettel, R.F. Betzel, D.S. Bassett, Cliques and cavities in the human connectome, *J. Comput. Neurosci.* 44 (1) (2018) 115–145.
- [27] J. Grilli, G. Barabás, M.J. Michalska-Smith, S. Allesina, Higher-order interactions stabilize dynamics in competitive network models, *Nature* 548 (7666) (2017) 210.
- [28] A. Sanchez-Gorostiaga, D. Bajić, M.L. Osborne, J.F. Poyatos, A. Sanchez, High-order interactions dominate the functional landscape of microbial consortia, *bioRxiv* (2018) 333534.
- [29] E. Ganmor, R. Segev, E. Schneidman, Sparse low-order interaction network underlies a highly correlated and learnable neural population code, *Proc. Natl. Acad. Sci. USA* 108 (23) (2011) 9679–9684.
- [30] J.M. Levine, J. Bascompte, P.B. Adler, S. Allesina, Beyond pairwise mechanisms of species coexistence in complex communities, *Nature* 546 (7656) (2017) 56.
- [31] A.R. Benson, R. Abebe, M.T. Schaub, A. Jadbabaie, J. Kleinberg, Simplicial closure and higher-order link prediction, *Proc. Natl. Acad. Sci. USA* 115 (48) (2018) E11221–E11230.
- [32] D. Centola, The spread of behavior in an online social network experiment, *Science* 329 (5996) (2010) 1194–1197.
- [33] M.E.J. Newman, S.H. Strogatz, D.J. Watts, Random graphs with arbitrary degree distributions and their applications, *Phys. Rev. E* 64 (2001) 026118.
- [34] R.H. Atkin, From cohomology in physics to Q-connectivity in social science, *Int. J. Man-Mach. Stud.* 4 (2) (1972) 139–167.
- [35] C. Berge, *Graphs and Hypergraphs*, North-Holland Pub. Co., 1973.
- [36] R. Atkin, *Mathematical Structure in Human Affairs*, Heinemann Educational Publishers, 1974.
- [37] M. Kivelä, A. Arenas, M. Barthélemy, J.P. Gleeson, Y. Moreno, M.A. Porter, Multilayer networks, *J. Comp. Netw.* 2 (3) (2014) 203–271.
- [38] M. De Domenico, C. Granell, M.A. Porter, A. Arenas, The physics of spreading processes in multilayer networks, *Nat. Phys.* 12 (10) (2016) 901–906.
- [39] F. Battiston, V. Nicosia, V. Latora, The new challenges of multiplex networks: Measures and models, *Eur. Phys. J. Spec. Top.* 226 (3) (2017) 401–416.
- [40] G. Bianconi, *Multilayer networks: Structure and function*, Oxford University Press, 2018.
- [41] A. Aleta, Y. Moreno, Multilayer networks in a nutshell, *Annu. Rev. Condens. Matter Phys.* 10 (2019) 45–62.
- [42] P. Holme, J. Saramäki, *Temporal Networks*, in: *Understanding Complex Systems*, Springer Berlin Heidelberg, 2013.
- [43] P. Holme, Modern temporal network theory: A colloquium, *Eur. Phys. J. B* 88 (9) (2015) 234.
- [44] R. Lambiotte, M. Rosvall, I. Scholtes, From networks to optimal higher-order models of complex systems, *Nat. Phys.* (2019) 1.
- [45] J.A. Bondy, U.S.R. Murty, *Graph Theory with Applications*, vol. 290, Macmillan London, 1976.
- [46] U. Alon, Biological networks: The tinkerer as an engineer, *Science* 301 (5641) (2003) 1866–1867.
- [47] N. Kashtan, U. Alon, Spontaneous evolution of modularity and network motifs, *Proc. Natl. Acad. Sci. USA* 102 (39) (2005) 13773–13778.
- [48] J.M. Montoya, S.L. Pimm, R.V. Solé, Ecological networks and their fragility, *Nature* 442 (7100) (2006) 259.
- [49] S.P. Borgatti, A. Mehra, D.J. Brass, G. Labianca, Network analysis in the social sciences, *Science* 323 (5916) (2009) 892–895.
- [50] M. McPherson, L. Smith-Lovin, J.M. Cook, Birds of a feather: Homophily in social networks, *Annu. Rev. Sociol.* 27 (1) (2001) 415–444.
- [51] J. Gao, S.V. Buldyrev, H.E. Stanley, S. Havlin, Networks formed from interdependent networks, *Nat. Phys.* 8 (1) (2012) 40.
- [52] S.V. Buldyrev, R. Parshani, G. Paul, H.E. Stanley, S. Havlin, Catastrophic cascade of failures in interdependent networks, *Nature* 464 (7291) (2010) 1025.

- [53] E. Bullmore, O. Sporns, Complex brain networks: Graph theoretical analysis of structural and functional systems, *Nat. Rev. Neurosci.* 10 (3) (2009) 186.
- [54] D.S. Bassett, O. Sporns, Network neuroscience, *Nat. Neurosci.* 20 (3) (2017) 353.
- [55] J.D. Medaglia, M.-E. Lynall, D.S. Bassett, Cognitive network neuroscience, *J. Cogn. Neurosci.* 27 (8) (2015) 1471–1491.
- [56] M. Boguñá, M. Kitsak, D. Krioukov, Cosmological networks, *New J. Phys.* 16 (9) (2014) 093031.
- [57] S. Fortunato, Community detection in graphs, *Phys. Rep.* 486 (3–5) (2010) 75–174.
- [58] G. Palla, I. Derényi, I. Farkas, T. Vicsek, Uncovering the overlapping community structure of complex networks in nature and society, *Nature* 435 (7043) (2005) 814.
- [59] B. Karrer, M.E.J. Newman, Stochastic blockmodels and community structure in networks, *Phys. Rev. E* 83 (1) (2011) 016107.
- [60] A. Lancichinetti, S. Fortunato, Limits of modularity maximization in community detection, *Phys. Rev. E* 84 (6) (2011) 066122.
- [61] E. Abbe, C. Sandon, Community detection in general stochastic block models: Fundamental limits and efficient algorithms for recovery, in: 2015 IEEE 56th Annual Symposium on Foundations of Computer Science, IEEE, 2015, pp. 670–688.
- [62] A. Lancichinetti, S. Fortunato, F. Radicchi, Benchmark graphs for testing community detection algorithms, *Phys. Rev. E* 78 (4) (2008) 046110.
- [63] J.-L. Guillaume, M. Latapy, Bipartite structure of all complex networks, *Inf. Process. Lett.* 90 (5) (2004) 215–221.
- [64] J.-L. Guillaume, M. Latapy, Bipartite graphs as models of complex networks, *Physica A* 371 (2) (2006) 795–813.
- [65] S. Wasserman, K. Faust, *Social Network Analysis: Methods and Applications (Structural Analysis in the Social Sciences)*, Cambridge University Press, 1994.
- [66] M.E.J. Newman, D.J. Watts, S.H. Strogatz, Random graph models of social networks, *Proc. Natl. Acad. Sci. USA* 99 (suppl 1) (2002) 2566–2572.
- [67] R. Guimerà, M. Sales-Pardo, L.A.N. Amaral, Module identification in bipartite and directed networks, *Phys. Rev. E* 76 (3) (2007) 036102.
- [68] T. Zhou, J. Ren, M. Medo, Y.-C. Zhang, Bipartite network projection and personal recommendation, *Phys. Rev. E* 76 (4) (2007) 046115.
- [69] K.A. Zweig, M. Kaufmann, A systematic approach to the one-mode projection of bipartite graphs, *Soc. Netw. Anal. Min.* 1 (3) (2011) 187–218.
- [70] M.T. Schaub, S. Segarra, Flow smoothing and denoising: Graph signal processing in the edge-space, in: 2018 IEEE Global Conference on Signal and Information Processing (GlobalSIP), IEEE, 2018, pp. 735–739.
- [71] R. Milo, S. Shen-Orr, S. Itzkovitz, N. Kashtan, D. Chklovskii, U. Alon, Network motifs: Simple building blocks of complex networks, *Science* 298 (5594) (2002) 824–827.
- [72] U. Alon, Network motifs: Theory and experimental approaches, *Nat. Rev. Genet.* 8 (6) (2007) 450.
- [73] S.E. Morgan, S. Achard, M. Termenon, E.T. Bullmore, P.E. Vértés, Low-dimensional morphospace of topological motifs in human fMRI brain networks, *Netw. Neurosci.* 2 (02) (2018) 285–302.
- [74] A. Avena-Koenigsberger, J. Goñi, R. Solé, O. Sporns, Network morphospace, *J. R. Soc. Interface* 12 (103) (2015) 20140881.
- [75] S.S. Shen-Orr, R. Milo, S. Mangan, U. Alon, Network motifs in the transcriptional regulation network of *Escherichia coli*, *Nat. Genet.* 31 (1) (2002) 64.
- [76] J.H. Fowler, C.T. Dawes, N.A. Christakis, Model of genetic variation in human social networks, *Proc. Natl. Acad. Sci. USA* 106 (6) (2009) 1720–1724.
- [77] A. Paranjape, A.R. Benson, J. Leskovec, Motifs in temporal networks, in: *Proceedings of the Tenth ACM International Conference on Web Search and Data Mining*, ACM, 2017, pp. 601–610.
- [78] L. Kovanen, M. Karsai, K. Kaski, J. Kertész, J. Saramäki, Temporal motifs in time-dependent networks, *J. Stat. Mech. Theory Exp.* 2011 (11) (2011) P11005.
- [79] P. Mahadevan, D. Krioukov, K. Fall, A. Vahdat, Systematic topology analysis and generation using degree correlations, in: *ACM SIGCOMM Comp. Rev.* vol. 36, (4) ACM, 2006, pp. 135–146.
- [80] C. Orsini, M.M. Dankulov, P. Colomer-de-Simón, A. Jamakovic, P. Mahadevan, A. Vahdat, K.E. Bassler, Z. Toroczka, M. Boguná, G. Caldarelli, Quantifying randomness in real networks, *Nature Commun.* 6 (2015) 8627.
- [81] I. Derényi, G. Palla, T. Vicsek, Clique percolation in random networks, *Phys. Rev. Lett.* 94 (16) (2005) 160202.
- [82] R.I. Dunbar, M. Spoors, Social networks, support cliques, and kinship, *Hum. Nat.* 6 (3) (1995) 273–290.
- [83] K.G. Provan, J.G. Sebastian, Networks within networks: Service link overlap, organizational cliques, and network effectiveness, *Acad. Manage. J.* 41 (4) (1998) 453–463.
- [84] A. Hatcher, *Algebraic Topology*, Cambridge University Press, 2002.
- [85] D. Horak, J. Jost, Spectra of combinatorial Laplace operators on simplicial complexes, *Adv. Math.* 244 (2013) 303–336.
- [86] A. Muhammad, M. Egerstedt, Control using higher order Laplacians in network topologies, in: *Proc. of 17th International Symposium on Mathematical Theory of Networks and Systems*, Citeseer, 2006, pp. 1024–1038.
- [87] A. Costa, M. Farber, *Random simplicial complexes*, in: *Configuration Spaces*, Springer, Berlin, 2016, pp. 129–153.
- [88] G. Bianconi, C. Rahmede, Network geometry with flavor: From complexity to quantum geometry, *Phys. Rev. E* 93 (3) (2016) 032315.
- [89] R. Ghrist, *Elementary Applied Topology*, CreateSpace Independent Publishing Platform, 2014.
- [90] G. Carlsson, Topology and data, *Bull. Amer. Math. Soc.* 46 (2) (2009) 255–308.
- [91] A. Patania, F. Vaccarino, G. Petri, Topological analysis of data, *EPJ Data Sci.* 6 (1) (2017) 7.
- [92] P. Expert, L.-D. Lord, M.L. Kringsbach, G. Petri, Editorial: Topological neuroscience, *Netw. Neurosci.* 3 (3) (2019) 653–655.
- [93] A. Higuchi, H. Miyoshi, T. Tsujishita, Higher dimensional hypercategories, 1999, arXiv:math/9907150.
- [94] A. Louis, Hypergraph Markov operators, eigenvalues and approximation algorithms, in: *Proceedings of the Forty-Seventh Annual ACM Symposium on Theory of Computing*, ACM, 2015, pp. 713–722.
- [95] T.-H.H. Chan, A. Louis, Z.G. Tang, C. Zhang, Spectral properties of hypergraph Laplacian and approximation algorithms, *J. ACM JACM* 65 (3) (2018) 15.
- [96] T.-H.H. Chan, Z. Liang, Generalizing the hypergraph Laplacian via a diffusion process with mediators, *Theoret. Comput. Sci.* (2019).
- [97] G. Ghoshal, V. Zlatić, G. Caldarelli, M. Newman, Random hypergraphs and their applications, *Phys. Rev. E* 79 (6) (2009) 066118.
- [98] T. Kumar, S. Vaidyanathan, H. Ananthapadmanabhan, S. Parthasarathy, B. Ravindran, Hypergraph clustering: A modularity maximization approach, 2018, arXiv:1812.10869.
- [99] P. Chodrow, A. Mellor, Annotated hypergraphs: Models and applications, *Appl. Netw. Sci.* 5 (1) (2020) 9.
- [100] L. Torres, A.S. Blevins, D.S. Bassett, T. Eliassi-Rad, The why, how, and when of representations for complex systems, 2020, arXiv:2006.02870.
- [101] E. Estrada, J.A. Rodríguez-Velázquez, Complex networks as hypergraphs, 2005, arXiv:physics/0505137.
- [102] B. Kamiński, V. Poulin, P. Prałat, P. Szufel, F. Theberge, Clustering via hypergraph modularity, *PLoS One* 14 (11) (2019).
- [103] D. Zhou, J. Huang, B. Schölkopf, Learning with hypergraphs: Clustering, classification, and embedding, in: *Advances in Neural Information Processing Systems*, 2007, pp. 1601–1608.
- [104] P.S. Chodrow, Configuration models of random hypergraphs and their applications, 2019, arXiv:1902.09302.
- [105] J.A. Rodríguez, On the Laplacian spectrum and walk-regular hypergraphs, *Linear Multilinear Algebra* 51 (3) (2003) 285–297.
- [106] A. Bellaachia, M. Al-Dhelaan, Random walks in hypergraph, in: *Proceedings of the 2013 International Conference on Applied Mathematics and Computational Methods*, Venice Italy, 2013, pp. 187–194.

- [107] C. Avin, Y. Lando, Z. Lotker, Radio cover time in hyper-graphs, in: *Proceedings of the 6th International Workshop on Foundations of Mobile Computing*, ACM, 2010, pp. 3–12.
- [108] J.-G. Young, G. Petri, F. Vaccarino, A. Patania, Construction of and efficient sampling from the simplicial configuration model, *Phys. Rev. E* 96 (3) (2017) 032312.
- [109] T.E. Goldberg, Combinatorial Laplacians of simplicial complexes, Sr. Thesis Bard Coll. (2002).
- [110] S. Maletić, M. Rajković, D. Vasiljević, Simplicial complexes of networks and their statistical properties, in: *International Conference on Computational Science*, Springer, 2008, pp. 568–575.
- [111] A. Duval, V. Reiner, Shifted simplicial complexes are Laplacian integral, *Trans. Amer. Math. Soc.* 354 (11) (2002) 4313–4344.
- [112] D.H. Serrano, D.S. Gómez, Higher order degree in simplicial complexes, multi combinatorial Laplacian and applications of TDA to complex networks, 2019, arXiv:1908.02583.
- [113] E. Estrada, G.J. Ross, Centralities in simplicial complexes. Applications to protein interaction networks, *J. Theoret. Biol.* 438 (2018) 46–60.
- [114] O.T. Courtney, G. Bianconi, Generalized network structures: The configuration model and the canonical ensemble of simplicial complexes, *Phys. Rev. E* 93 (6) (2016) 062311.
- [115] A. Patania, G. Petri, F. Vaccarino, The shape of collaborations, *EPJ Data Sci.* 6 (1) (2017) 18.
- [116] K. Kapoor, D. Sharma, J. Srivastava, Weighted node degree centrality for hypergraphs, in: *2013 IEEE 2nd Network Science Workshop (NSW)*, IEEE, 2013, pp. 152–155.
- [117] B. Jiang, I. Omer, Spatial topology and its structural analysis based on the concept of simplicial complex, *Trans. GIS* 11 (6) (2007) 943–960.
- [118] D.H. Serrano, D.S. Gómez, Centrality measures in simplicial complexes: Applications of TDA to network science, 2019, arXiv:1908.02967.
- [119] L. Lu, X. Peng, High-ordered random walks and generalized Laplacians on hypergraphs, in: *International Workshop on Algorithms and Models for the Web-Graph*, Springer, 2011, pp. 14–25.
- [120] E. Estrada, J.A. Rodríguez-Velázquez, Subgraph centrality and clustering in complex hyper-networks, *Physica A* 364 (2006) 581–594.
- [121] S.G. Aksoy, C. Joslyn, C. Ortiz Marrero, B. Praggastis, E. Purvine, Hypernetwork science via high-order hypergraph walks, *EPJ Data Science* 9 (2020) 1–34.
- [122] P. Bonacich, Factoring and weighting approaches to status scores and clique identification, *J. Math. Sociol.* 2 (1) (1972) 113–120.
- [123] M.E.J. Newman, Modularity and community structure in networks, *Proc. Natl. Acad. Sci. USA* 103 (23) (2006) 8577–8582.
- [124] A.N. Langville, C.D. Meyer, Deeper inside pagerank, *Internet Math.* 1 (3) (2004) 335–380.
- [125] J.M. Fletcher, T. Wennekers, From structure to activity: Using centrality measures to predict neuronal activity, *Int. J. Neural Syst.* 28 (02) (2018) 1750013.
- [126] P. Bonacich, Simultaneous group and individual centralities, *Soc. Netw.* 13 (2) (1991) 155–168.
- [127] P. Bonacich, A.C. Holdren, M. Johnston, Hyper-edges and multidimensional centrality, *Soc. Netw.* 26 (3) (2004) 189–203.
- [128] A.R. Benson, Three hypergraph eigenvector centralities, *SIAM J. Math. Data Sci.* 1 (2) (2019) 293–312.
- [129] L. Qi, Z. Luo, *Tensor Analysis: Spectral Theory and Special Tensors*, vol. 151, Siam, 2017.
- [130] M.S. Granovetter, The strength of weak ties, in: *Social Networks*, Elsevier, 1977, pp. 347–367.
- [131] T. Opsahl, Triadic closure in two-mode networks: Redefining the global and local clustering coefficients, *Soc. Netw.* 35 (2) (2013) 159–167.
- [132] S.P. Borgatti, M.G. Everett, Network analysis of 2-mode data, *Soc. Netw.* 19 (3) (1997) 243–269.
- [133] A.P. Kortun-Giles, G. Bianconi, Beyond the clustering coefficient: A topological analysis of node neighbourhoods in complex networks, *Chaos Solitons Fractals X* 1 (2019) 100004.
- [134] H. Yin, A.R. Benson, J. Leskovec, D.F. Gleich, Local higher-order graph clustering, in: *Proceedings of the 23rd ACM SIGKDD International Conference on Knowledge Discovery and Data Mining*, ACM, 2017, pp. 555–564.
- [135] H. Edelsbrunner, A Short Course in Computational Geometry and Topology, in: *SpringerBriefs in Applied Sciences and Technology*, Springer International Publishing, 2014.
- [136] R. Ghrist, Barcodes: The persistent topology of data, *Bull. Amer. Math. Soc.* 45 (1) (2008) 61–75.
- [137] A. Verri, C. Uras, P. Frosini, M. Ferri, On the use of size functions for shape analysis, *Biol. Cybernet.* 70 (2) (1993) 99–107.
- [138] F. Cagliari, M. Ferri, P. Pozzi, Size functions from a categorical viewpoint, *Acta Appl. Math.* 67 (3) (2001) 225–235.
- [139] H. Edelsbrunner, D. Letscher, A. Zomorodian, Topological persistence and simplification, in: *Proceedings 41st Annual Symposium on Foundations of Computer Science*, IEEE, 2000, pp. 454–463.
- [140] A. Zomorodian, G. Carlsson, Computing persistent homology, *Discrete Comput. Geom.* 33 (2) (2005) 249–274.
- [141] M. Feng, M.A. Porter, Persistent homology of geospatial data: A case study with voting, 2019, arXiv:1902.05911.
- [142] G. Carlsson, V. De Silva, Zigzag persistence, *Found. Comput. Math.* 10 (4) (2010) 367–405.
- [143] G. Carlsson, A. Zomorodian, The theory of multidimensional persistence, *Discrete Comput. Geom.* 42 (1) (2009) 71–93.
- [144] H. Edelsbrunner, D. Morozov, Persistent homology, in: *Handbook of Discrete and Computational Geometry*, Chapman and Hall/CRC, 2017, pp. 637–661.
- [145] N. Otter, M.A. Porter, U. Tillmann, P. Grindrod, H.A. Harrington, A roadmap for the computation of persistent homology, *EPJ Data Sci.* 6 (1) (2017) 17.
- [146] M. Muldoon, R. MacKay, J. Huke, D. Broomhead, Topology from time series, *Physica D* 65 (1–2) (1993) 1–16.
- [147] R.J. Adler, K. Bartz, S.C. Kou, A. Monod, Estimating thresholding levels for random fields via Euler characteristics, 2017, arXiv:1704.08562.
- [148] P. Pranav, R. Van de Weygaert, G. Vegter, B.J. Jones, R.J. Adler, J. Feldbrugge, C. Park, T. Buchert, M. Kerber, Topology and geometry of Gaussian random fields I: On Betti numbers, Euler characteristic, and Minkowski functionals, *Mon. Not. R. Astron. Soc.* 485 (3) (2019) 4167–4208.
- [149] S. Maletić, M. Rajković, Combinatorial Laplacian and entropy of simplicial complexes associated with complex networks, *Eur. Phys. J. ST* (1) (2012) 77–97.
- [150] L.-H. Lim, Hodge Laplacians on graphs, *Proc. Symp. Appl. Math.* (2015).
- [151] O. Parzanchevski, R. Rosenthal, Simplicial complexes: Spectrum, homology and random walks, *Random Struct. Algorithms* 50 (2) (2017) 225–261.
- [152] M.T. Schaub, A.R. Benson, P. Horn, G. Lippner, A. Jadbabaie, Random walks on simplicial complexes and the normalized Hodge Laplacian, *SIAM Rev.* 62 (2) (2020) 353–391.
- [153] J. Rodriguez, Laplacian eigenvalues and partition problems in hypergraphs, *Appl. Math. Lett.* 22 (6) (2009) 916–921.
- [154] F. Chung, The Laplacian of a hypergraph, *Expand. Graphs DIMACS Ser.* (1993) 21–36.
- [155] S. Saito, D.P. Mandic, H. Suzuki, Hypergraph p-Laplacian: A differential geometry view, in: *Thirty-Second AAAI Conference on Artificial Intelligence*, 2018.
- [156] J. Cooper, A. Dutle, Spectra of uniform hypergraphs, *Linear Algebra Appl.* 436 (9) (2012) 3268–3292.
- [157] S. Hu, L. Qi, The Laplacian of a uniform hypergraph, *J. Comb. Optim.* 29 (2) (2015) 331–366.
- [158] P. Li, O. Milenkovic, Submodular hypergraphs: P-Laplacians, cheeger inequalities and spectral clustering, in: *Proceedings of the 35th International Conference on Machine Learning*, 2018, pp. 3014–3023.
- [159] M. Lucas, G. Cencetti, F. Battiston, A multi-order Laplacian for synchronization in higher-order networks, 2020, arXiv:2003.09734.
- [160] D. Krioukov, M. Ostilli, Duality between equilibrium and growing networks, *Phys. Rev. E* 88 (2) (2013) 022808.

- [161] A.C. Coolen, A. Annibale, E. Roberts, *Generating Random Networks and Graphs*, Oxford University Press, 2017.
- [162] G. Bianconi, A. Capocci, Number of loops of size h in growing scale-free networks, *Phys. Rev. Lett.* 90 (7) (2003) 078701.
- [163] M.A. Serrano, M. Boguná, Tuning clustering in random networks with arbitrary degree distributions, *Phys. Rev. E* 72 (3) (2005) 036133.
- [164] B. Bollobás, P. Erdős, Cliques in random graphs, in: *Mathematical Proceedings of the Cambridge Philosophical Society*, vol. 80, (3) Cambridge University Press, 1976, pp. 419–427.
- [165] B.K. Fosdick, D.B. Larremore, J. Nishimura, J. Ugander, Configuring random graph models with fixed degree sequences, *SIAM Rev.* 60 (2) (2018) 315–355.
- [166] J.M. Diamond, Assembly of species communities, *Ecol. Evol. Commun.* (1975) 342–444.
- [167] E.F. Connor, D. Simberloff, The assembly of species communities: Chance or competition? *Ecology* 60 (6) (1979) 1132–1140.
- [168] M. Gail, N. Mantel, Counting the number of $r \times c$ contingency tables with fixed margins, *J. Am. Stat. Assoc.* 72 (360a) (1977) 859–862.
- [169] A. Verbeek, P.M. Kroonenberg, A survey of algorithms for exact distributions of test statistics in $r \times c$ contingency tables with fixed margins, *Comput. Statist. Data Anal.* 3 (1985) 159–185.
- [170] F. Saracco, R. Di Clemente, A. Gabrielli, T. Squartini, Randomizing bipartite networks: The case of the World Trade Web, *Sci. Rep.* 5 (2015) 10595.
- [171] C. Payrató-Borràs, L. Hernández, Y. Moreno, Breaking the spell of nestedness: The entropic origin of nestedness in mutualistic systems, *Phys. Rev. X* 9 (3) (2019) 031024.
- [172] M. Kitsak, D. Krioukov, Hidden variables in bipartite networks, *Phys. Rev. E* 84 (2) (2011) 026114.
- [173] A.A. Boroojeni, J. Dewar, T. Wu, J.M. Hyman, Generating bipartite networks with a prescribed joint degree distribution, *J. Complex Netw.* 5 (6) (2017) 839–857.
- [174] B. Söderberg, General formalism for inhomogeneous random graphs, *Phys. Rev. E* 66 (6) (2002) 066121.
- [175] A. Allard, P.-A. Noël, L.J. Dubé, B. Pourbohloul, Heterogeneous bond percolation on multitype networks with an application to epidemic dynamics, *Phys. Rev. E* 79 (3) (2009) 036113.
- [176] X. Fu, S. Yu, A.R. Benson, Modeling and analysis of tagging networks in stock exchange communities, *J. Complex Netw.* (2019).
- [177] S. Wasserman, P. Pattison, Logit models and logistic regressions for social networks: I. An introduction to Markov graphs and p, *Psychometrika* 61 (3) (1996) 401–425.
- [178] T.A. Snijders, P.E. Pattison, G.L. Robins, M.S. Handcock, New specifications for exponential random graph models, *Sociol. Methodol.* 36 (1) (2006) 99–153.
- [179] O. Frank, D. Strauss, Markov graphs, *J. Amer. Statist. Assoc.* 81 (395) (1986) 832–842.
- [180] P.W. Holland, S. Leinhardt, An exponential family of probability distributions for directed graphs, *J. Amer. Statist. Assoc.* 76 (373) (1981) 33–50.
- [181] M. Latapy, C. Magnien, N. Del Vecchio, Basic notions for the analysis of large two-mode networks, *Soc. Netw.* 30 (1) (2008) 31–48.
- [182] D. Iacubucci, S. Wasserman, Social networks with two sets of actors, *Psychometrika* 55 (4) (1990) 707–720.
- [183] J. Skvoretz, K. Faust, Logit models for affiliation networks, *Sociol. Methodol.* 29 (1) (1999) 253–280.
- [184] G. Robins, M. Alexander, Small worlds among interlocking directors: Network structure and distance in bipartite graphs, *Comput. Math. Organ. Theory* 10 (1) (2004) 69–94.
- [185] F. Agneessens, H. Roose, H. Waage, Choices of theatre events: P^* models for affiliation networks with attributes, *Metod. Zv.* 1 (2) (2004) 419.
- [186] D. Strauss, On a general class of models for interaction, *SIAM Rev.* 28 (4) (1986) 513–527.
- [187] M.S. Handcock, Statistical models for social networks: inference and degeneracy, in: R. Breiger, K. Carley, P. Pattison (Eds.), *Dynamic Social Network Modeling and Analysis*, National Academies Press, (Washington, DC), 2003, pp. 229–240.
- [188] R. Fischer, J.C. Leitão, T.P. Peixoto, E.G. Altmann, Sampling motif-constrained ensembles of networks, *Phys. Rev. Lett.* 115 (18) (2015) 188701.
- [189] P. Wang, K. Sharpe, G.L. Robins, P.E. Pattison, Exponential random graph (P^*) models for affiliation networks, *Soc. Netw.* 31 (1) (2009) 12–25.
- [190] P. Wang, P. Pattison, G. Robins, Exponential random graph model specifications for bipartite networks—A dependence hierarchy, *Soc. Netw.* 35 (2) (2013) 211–222.
- [191] G. Robins, P. Pattison, Y. Kalish, D. Lusher, An introduction to exponential random graph (P^*) models for social networks, *Soc. Netw.* 29 (2) (2007) 173–191.
- [192] J.A. Smith, Macrostructure from microstructure: Generating whole systems from ego networks, *Sociol. Methodol.* 42 (1) (2012) 155–205.
- [193] L. Jasny, Baseline models for two-mode social network data, *Policy Stud. J.* 40 (3) (2012) 458–491.
- [194] K. Faust, K.E. Willert, D.D. Rowlee, J. Skvoretz, Scaling and statistical models for affiliation networks: Patterns of participation among Soviet politicians during the Brezhnev era, *Soc. Netw.* 24 (3) (2002) 231–259.
- [195] T.A. Snijders, Markov chain Monte Carlo estimation of exponential random graph models, *J. Soc. Struct.* 3 (2) (2002) 1–40.
- [196] C.R. Shalizi, A. Rinaldo, Consistency under sampling of exponential random graph models, *Ann. Statist.* 41 (2) (2013) 508.
- [197] H. Crane, *Probabilistic Foundations of Statistical Network Analysis*, Chapman and Hall/CRC, 2018.
- [198] J.-G. Young, G. St-Onge, P. Desrosiers, L.J. Dubé, Universality of the stochastic block model, *Phys. Rev. E* 98 (3) (2018) 032309.
- [199] M.E.J. Newman, Communities, modules and large-scale structure in networks, *Nat. Phys.* 8 (1) (2012) 25–31.
- [200] M.E.J. Newman, Mixing patterns in networks, *Phys. Rev. E* 67 (2) (2003) 026126.
- [201] S.P. Borgatti, M.G. Everett, Models of core/periphery structures, *Soc. Netw.* 21 (4) (2000) 375–395.
- [202] P.W. Holland, K.B. Laskey, S. Leinhardt, Stochastic blockmodels: First steps, *Soc. Networks* 5 (2) (1983) 109–137.
- [203] P. Doreian, V. Batagelj, A. Ferligoj, Generalized blockmodeling of two-mode network data, *Soc. Netw.* 26 (1) (2004) 29–53.
- [204] K. Rohe, T. Qin, B. Yu, Co-clustering directed graphs to discover asymmetries and directional communities, *Proc. Natl. Acad. Sci. USA* 113 (45) (2016) 12679–12684.
- [205] D.B. Larremore, A. Clauset, A.Z. Jacobs, Efficiently inferring community structure in bipartite networks, *Phys. Rev. E* 90 (1) (2014) 012805.
- [206] S.C. Olhede, P.J. Wolfe, Network histograms and universality of blockmodel approximation, *Proc. Natl. Acad. Sci. USA* 111 (41) (2014) 14722–14727.
- [207] T.P. Peixoto, Entropy of stochastic blockmodel ensembles, *Phys. Rev. E* 85 (5) (2012) 056122.
- [208] R. Guimerà, A. Llorente, E. Moro, M. Sales-Pardo, Predicting human preferences using the block structure of complex social networks, *PLoS One* 7 (9) (2012) e44620.
- [209] B. Ball, B. Karrer, M.E.J. Newman, Efficient and principled method for detecting communities in networks, *Phys. Rev. E* 84 (3) (2011) 036103.
- [210] D. Hric, T.P. Peixoto, S. Fortunato, Network structure, metadata, and the prediction of missing nodes and annotations, *Phys. Rev. X* 6 (3) (2016) 031038.
- [211] M. Gerlach, T.P. Peixoto, E.G. Altmann, A network approach to topic models, *Sci. Adv.* 4 (7) (2018) eaaq1360.
- [212] D.M. Blei, A.Y. Ng, M.I. Jordan, Latent Dirichlet allocation, *J. Mach. Learn. Res.* 3 (Jan) (2003) 993–1022.
- [213] Q. Sheng, Y. Moreau, B. De Moor, Biclustering microarray data by Gibbs sampling, *Bioinformatics* 19 (suppl_2) (2003) ii196–ii205.
- [214] S.K. Iyer, D. Yogeshwaran, Percolation and connectivity in AB random geometric graphs, *Adv. Appl. Probab.* 44 (1) (2012) 21–41.
- [215] M. Penrose, *Random Geometric Graphs*, vol. 5, Oxford University Press, 2003.
- [216] B.M. Waxman, Routing of multipoint connections, *IEEE J. Sel. Areas Commun.* 6 (9) (1988) 1617–1622.
- [217] M.A. Serrano, D. Krioukov, M. Boguná, Self-similarity of complex networks and hidden metric spaces, *Phys. Rev. Lett.* 100 (7) (2008) 078701.

- [218] M. Kitsak, F. Papadopoulos, D. Krioukov, Latent geometry of bipartite networks, *Phys. Rev. E* 95 (3) (2017) 032309.
- [219] M. Mézard, A. Montanari, Uncovering the hidden geometry behind metabolic networks, *Mol. Biosyst.* 8 (3) (2012) 843–850.
- [220] D. Krioukov, Clustering implies geometry in networks, *Phys. Rev. Lett.* 116 (20) (2016) 208302.
- [221] M.E.J. Newman, Properties of highly clustered networks, *Phys. Rev. E* 68 (2) (2003) 026121.
- [222] J.A. Davis, S. Leinhardt, The Structure of Positive Interpersonal Relations in Small Groups, ERIC, 1967.
- [223] P.W. Holland, S. Leinhardt, Local structure in social networks, *Sociol. Methodol.* 7 (1976) 1–45.
- [224] J.P. Gleeson, S. Melnik, Analytical results for bond percolation and K-Core sizes on clustered networks, *Phys. Rev. E* 80 (4) (2009) 046121.
- [225] P. Trapman, On analytical approaches to epidemics on networks, *Theor. Popul. Biol.* 71 (2) (2007) 160–173.
- [226] M.E.J. Newman, Random graphs with clustering, *Phys. Rev. Lett.* 103 (5) (2009) 058701.
- [227] J.C. Miller, Percolation and epidemics in random clustered networks, *Phys. Rev. E* 80 (2) (2009) 020901.
- [228] J.P. Gleeson, Bond percolation on a class of clustered random networks, *Phys. Rev. E* 80 (3) (2009) 036107.
- [229] B. Karrer, M.E.J. Newman, Random graphs containing arbitrary distributions of subgraphs, *Phys. Rev. E* 82 (6) (2010) 066118.
- [230] A. Allard, L. Hébert-Dufresne, P.-A. Noël, V. Marceau, L.J. Dubé, Bond percolation on a class of correlated and clustered random graphs, *J. Phys. Math. Theor.* 45 (40) (2012) 405005.
- [231] A. Allard, L. Hébert-Dufresne, J.-G. Young, L.J. Dubé, General and exact approach to percolation on random graphs, *Phys. Rev. E* 92 (6) (2015) 062807.
- [232] M. Ritchie, L. Berthouze, I.Z. Kiss, Generation and analysis of networks with a prescribed degree sequence and subgraph family: Higher-order structure matters, *J. Complex Netw.* 5 (1) (2017) 1–31.
- [233] A.E. Wegner, Subgraph covers: An information-theoretic approach to motif analysis in networks, *Phys. Rev. X* 4 (4) (2014) 041026.
- [234] B. Bollobás, S. Janson, O. Riordan, Sparse random graphs with clustering, *Random Struct. Algorithms* 38 (3) (2011) 269–323.
- [235] M.E.J. Newman, T.P. Peixoto, Generalized communities in networks, *Phys. Rev. Lett.* 115 (8) (2015) 088701.
- [236] W. Devanny, D. Eppstein, B. Tillman, The computational hardness of Dk-series, in: *NetSci 2016*, 2016.
- [237] P. Pattison, G. Robins, Neighborhood-based models for social networks, *Sociol. Methodol.* 32 (1) (2002) 301–337.
- [238] D.J. Watts, P.S. Dodds, M.E.J. Newman, Identity and search in social networks, *Science* 296 (5571) (2002) 1302–1305.
- [239] J. Yang, J. Leskovec, Community-affiliation graph model for overlapping network community detection, in: *2012 IEEE 12th International Conference on Data Mining, IEEE, 2012*, pp. 1170–1175.
- [240] L. Hébert-Dufresne, P.-A. Noël, V. Marceau, A. Allard, L.J. Dubé, Propagation dynamics on networks featuring complex topologies, *Phys. Rev. E* 82 (3) (2010) 036115.
- [241] C. Seshadhri, T.G. Kolda, A. Pinar, Community structure and scale-free collections of Erdős-Rényi graphs, *Phys. Rev. E* 85 (5) (2012) 056109.
- [242] M. Karoński, E.R. Scheinerman, K.B. Singer-Cohen, On random intersection graphs: The subgraph problem, *Combin. Probab. Comput.* 8 (1–2) (1999) 131–159.
- [243] P. Erdős, A.W. Goodman, L. Pósa, The representation of a graph by set intersections, *Canad. J. Math.* 18 (1966) 106–112.
- [244] A. Frieze, M. Karoński, *Introduction to Random Graphs*, Cambridge University Press, 2016.
- [245] S. Nikolettseas, C. Raptopoulos, P. Spirakis, Large independent sets in general random intersection graphs, *Theoret. Comput. Sci.* 406 (3) (2008) 215–224.
- [246] M. Deijfen, W. Kets, Random intersection graphs with tunable degree distribution and clustering, *Probab. Engrg. Inform. Sci.* 23 (4) (2009) 661–674.
- [247] E. Godehardt, J. Jaworski, Two models of random intersection graphs for classification, in: *Exploratory Data Analysis in Empirical Research*, Springer, 2003, pp. 67–81.
- [248] G.B. Davis, K.M. Carley, Clearing the FOG: Fuzzy, overlapping groups for social networks, *Soc. Netw.* 30 (3) (2008) 201–212.
- [249] D. Barber, Clique matrices for statistical graph decomposition and parameterising restricted positive definite matrices, *Uncertain. Artif. Intell.* (2008) 26–33.
- [250] S.A. Williamson, M. Tec, Random clique covers for graphs with local density and global sparsity, in: *Proceedings of the 2019 Conference on Uncertainty in Artificial Intelligence*, 2018.
- [251] F.G. Ball, D.J. Sirl, P. Trapman, Epidemics on random intersection graphs, *Ann. Appl. Probab.* 24 (3) (2014) 1081–1128.
- [252] J. Xie, S. Kelley, B.K. Szymanski, Overlapping community detection in networks: The state-of-the-art and comparative study, *Acm Comput. Surv.* 45 (4) (2013) 43.
- [253] P. Erdős, On random graphs I, *Publ. Math.* 6 (1959) 290–297.
- [254] E.N. Gilbert, Random graphs, *Ann. Math. Stat.* 30 (4) (1959) 1141–1144, <http://www.jstor.org/stable/2237458>.
- [255] P. Erdős, A. Rényi, On the evolution of random graphs, *Publ. Math. Inst. Hung. Acad. Sci.* 5 (1) (1960) 17–60.
- [256] W.F. De La Vega, Sur La Cardinalité Maximum Des Couplages d'hypergraphes Aléatoires Uniformes, *Discrete Math.* 40 (2–3) (1982) 315–318.
- [257] J. Schmidt-Puzan, E. Shamir, Component structure in the evolution of random hypergraphs, *Combinatorica* 5 (1) (1985) 81–94.
- [258] G.F. de Arruda, G. Petri, Y. Moreno, Social contagion models on hypergraphs, *Phys. Rev. Res.* 2 (2) (2020) 023032.
- [259] R.W. Darling, J.R. Norris, Structure of large random hypergraphs, *Ann. Appl. Probab.* 15 (1A) (2005) 125–152.
- [260] M. Mézard, M. Mézard, A. Montanari, *Information, Physics, and Computation*, Oxford University Press, 2009.
- [261] A. Dembo, A. Montanari, Finite size scaling for the core of large random hypergraphs, *Ann. Appl. Probab.* 18 (5) (2008) 1993–2040.
- [262] J. Schmidt, E. Shamir, A threshold for perfect matchings in random D-pure hypergraphs, *Discrete Math.* 45 (2–3) (1983) 287–295.
- [263] H. Chen, A. Frieze, Coloring bipartite hypergraphs, in: *International Conference on Integer Programming and Combinatorial Optimization*, Springer, 1996, pp. 345–358.
- [264] J. Demetrotics, G.O. Katona, D. Miklós, O. Seleznev, B. Thalheim, Asymptotic properties of keys and functional dependencies in random databases, *Theoret. Comput. Sci.* 190 (2) (1998) 151–166.
- [265] S. Braddé, G. Bianconi, The percolation transition in correlated hypergraphs, *J. Stat. Mech. Theory Exp.* 2009 (07) (2009) P07028.
- [266] M. Girvan, M.E.J. Newman, Community structure in social and biological networks, *Proc. Natl. Acad. Sci. USA* 99 (12) (2002) 7821–7826.
- [267] M.E. Newman, M. Girvan, Finding and evaluating community structure in networks, *Phys. Rev. E* 69 (2) (2004) 026113.
- [268] F. Chung, L. Lu, Connected components in random graphs with given expected degree sequences, *Ann. Comb.* 6 (2) (2002) 125–145.
- [269] D. Stasi, K. Sadeghi, A. Rinaldo, S. Petrović, S.E. Fienberg, β models for random hypergraphs with a given degree sequence, 2014, [arXiv:1407.1004](https://arxiv.org/abs/1407.1004).
- [270] D. Ghoshdastidar, A. Dukkipati, Consistency of spectral partitioning of uniform hypergraphs under planted partition model, in: *Advances in Neural Information Processing Systems*, 2014, pp. 397–405.
- [271] Z.T. Ke, F. Shi, D. Xia, Community detection for hypergraph networks via regularized tensor power iteration, 2019, [arXiv:1909.06503](https://arxiv.org/abs/1909.06503).
- [272] K. Ahn, K. Lee, C. Suh, Hypergraph spectral clustering in the weighted stochastic block model, *IEEE J. Sel. Top. Signal Process.* 12 (5) (2018) 959–974.
- [273] S. Paul, O. Milenkovic, Y. Chen, Higher-order spectral clustering under superimposed stochastic block model, 2018, [arXiv:1812.06515](https://arxiv.org/abs/1812.06515).
- [274] K. Turnbull, S. Lunagómez, C. Nemeth, E. Airolidi, Latent space representations of hypergraphs, 2019, [arXiv:1909.00472](https://arxiv.org/abs/1909.00472).

- [275] J. Leskovec, D. Chakrabarti, J. Kleinberg, C. Faloutsos, Realistic, mathematically tractable graph generation and evolution, using Kronecker multiplication, in: European Conference on Principles of Data Mining and Knowledge Discovery, Springer, 2005, pp. 133–145.
- [276] N. Eikmeier, A. Ramani, D. Gleich, The HyperKron Graph Model for higher-order features, in: 2018 IEEE International Conference on Data Mining (ICDM), IEEE, 2018, pp. 941–946.
- [277] M. Kahle, Random geometric complexes, *Discrete Comput. Geom.* 45 (3) (2011) 553–573.
- [278] N. Linial, R. Meshulam, Homological connectivity of random 2-complexes, *Combinatorica* 26 (4) (2006) 475–487.
- [279] M. Kahle, Topology of random simplicial complexes: A survey, *AMS Contemp. Math.* 620 (2014) 201–222.
- [280] R. Meshulam, N. Wallach, Homological connectivity of random K-dimensional complexes, *Random Struct. Algorithms* 34 (3) (2009) 408–417.
- [281] M. Kahle, Topology of random clique complexes, *Discrete Math.* 309 (6) (2009) 1658–1671.
- [282] C.F. Fowler, Generalized random simplicial complexes, 2015, arXiv:1503.01831.
- [283] I. Iacopini, G. Petri, A. Barrat, V. Latora, Simplicial models of social contagion, *Nature Commun.* 10 (1) (2019) 2485.
- [284] D. Alberici, P. Contucci, E. Mingione, M. Molari, Aggregation models on hypergraphs, *Ann. Phys.* 376 (2017) 412–424.
- [285] K. Zuev, O. Eisenberg, D. Krioukov, Exponential random simplicial complexes, *J. Phys. A* 48 (46) (2015) 465002.
- [286] F. Chazal, B. Michel, An introduction to Topological Data Analysis: Fundamental and practical aspects for data scientists, 2017, arXiv:1710.04019.
- [287] M. Kahle, E. Meckes, Limit theorems for Betti numbers of random simplicial complexes, *Homol. Homotopy Appl.* 15 (1) (2013) 343–374.
- [288] O. Bobrowski, M. Kahle, Topology of random geometric complexes: A survey, *J. Appl. Comput. Topol.* 1 (3–4) (2018) 331–364.
- [289] B.T. Fasy, F. Lecci, A. Rinaldo, L. Wasserman, S. Balakrishnan, A. Singh, Confidence sets for persistence diagrams, *Ann. Statist.* 42 (6) (2014) 2301–2339.
- [290] G. Bianconi, R.M. Ziff, Topological percolation on hyperbolic simplicial complexes, *Phys. Rev. E* 98 (5) (2018) 052308.
- [291] G. Bianconi, I. Kryven, R.M. Ziff, Percolation on branching simplicial and cell complexes and its relation to interdependent percolation, *Phys. Rev. E* 100 (6) (2019) 062311.
- [292] J. Overgoor, A. Benson, J. Ugander, Choosing to grow a graph: Modeling network formation as discrete choice, in: The World Wide Web Conference, ACM, 2019, pp. 1409–1420.
- [293] G. Petri, A. Barrat, Simplicial activity driven model, *Phys. Rev. Lett.* 121 (22) (2018) 228301.
- [294] G. Ergün, Human sexual contact network as a bipartite graph, *Physica A* 308 (1–4) (2002) 483–488.
- [295] J.J. Ramasco, S.N. Dorogovtsev, R. Pastor-Satorras, Self-organization of collaboration networks, *Phys. Rev. E* 70 (3) (2004) 036106.
- [296] M. Beguerisse Díaz, M.A. Porter, J.-P. Onnela, Competition for popularity in bipartite networks, *Chaos* 20 (4) (2010) 043101.
- [297] K. Sneppen, M. Rosvall, A. Trusina, P. Minnhagen, A simple model for self-organization of bipartite networks, *Europhys. Lett.* 67 (3) (2004) 349.
- [298] P. Bak, C. Tang, K. Wiesenfeld, Self-organized criticality: An explanation of the 1/f noise, *Phys. Rev. Lett.* 59 (4) (1987) 381.
- [299] N. Friel, R. Rastelli, J. Wyse, A.E. Raftery, Interlocking directorates in Irish companies using a latent space model for bipartite networks, *Proc. Natl. Acad. Sci. USA* 113 (24) (2016) 6629–6634.
- [300] T. Evans, Exact solutions for network rewiring models, *Eur. Phys. J. B* 56 (1) (2007) 65–69.
- [301] T. Evans, A. Plato, Exact solution for the time evolution of network rewiring models, *Phys. Rev. E* 75 (5) (2007) 056101.
- [302] Z. Wu, G. Menichetti, C. Rahmede, G. Bianconi, Emergent complex network geometry, *Sci. Rep.* 5 (2015) 10073.
- [303] P. Pollner, G. Palla, T. Vicsek, Preferential attachment of communities: The same principle, but a higher level, *Europhys. Lett.* 73 (3) (2005) 478.
- [304] X. Zhou, L. Xiang, W. Xiao-Fan, Weighted evolving networks with self-organized communities, *Commun. Theor. Phys.* 50 (1) (2008) 261.
- [305] L. Hébert-Dufresne, A. Allard, V. Marceau, P.-A. Noël, L.J. Dubé, Structural preferential attachment: Network organization beyond the link, *Phys. Rev. Lett.* 107 (15) (2011) 158702.
- [306] L. Hébert-Dufresne, A. Allard, V. Marceau, P.-A. Noël, L.J. Dubé, Structural preferential attachment: Stochastic process for the growth of scale-free, modular, and self-similar systems, *Phys. Rev. E* 85 (2) (2012) 026108.
- [307] J.-G. Young, L. Hébert-Dufresne, A. Allard, L.J. Dubé, Growing networks of overlapping communities with internal structure, *Phys. Rev. E* 94 (2) (2016) 022317.
- [308] L. Hébert-Dufresne, E. Laurence, A. Allard, J.-G. Young, L.J. Dubé, Complex networks as an emerging property of hierarchical preferential attachment, *Phys. Rev. E* 92 (6) (2015) 062809.
- [309] D.J. Aldous, Exchangeability and related topics, in: *École d'Été de Probabilités de Saint-Flour XIII—1983*, Springer, 1985, pp. 1–198.
- [310] T.L. Griffiths, Z. Ghahramani, The Indian buffet process: An introduction and review, *J. Mach. Learn. Res.* 12 (Apr) (2011) 1185–1224.
- [311] Z.-K. Zhang, C. Liu, A hypergraph model of social tagging networks, *J. Stat. Mech. Theory Exp.* 2010 (10) (2010) P10005.
- [312] J.-W. Wang, L.-L. Rong, Q.-H. Deng, J.-Y. Zhang, Evolving hypernetwork model, *Eur. Phys. J. B* 77 (4) (2010) 493–498.
- [313] D. Liu, N. Blenn, P. Van Mieghem, A social network model exhibiting tunable overlapping community structure, *Procedia Comput. Sci.* 9 (2012) 1400–1409.
- [314] F. Hu, J.-L. Guo, F.-X. Li, H.-X. Zhao, Hypernetwork models based on random hypergraphs, *Int. J. Mod. Phys. C IJMP* 30 (08) (2019) 1–15.
- [315] Y. Guang-Yong, L. Jian-Guo, A local-world evolving hypernetwork model, *Chin. Phys. B* 23 (1) (2013) 018901.
- [316] Z. Wu, J. Duan, X. Fu, Synchronization of an evolving complex hyper-network, *Appl. Math. Model.* 38 (11–12) (2014) 2961–2968.
- [317] J.-L. Guo, X.-Y. Zhu, Q. Suo, J. Forrest, Non-uniform evolving hypergraphs and weighted evolving hypergraphs, *Sci. Rep.* 6 (2016) 36648.
- [318] P.L. Krapivsky, S. Redner, F. Leyvraz, Connectivity of growing random networks, *Phys. Rev. Lett.* 85 (21) (2000) 4629.
- [319] J.-L. Guo, Q. Suo, Brand effect versus competitiveness in hypernetworks, *Chaos* 25 (2) (2015) 023102.
- [320] G. Bianconi, Interdisciplinary and physics challenges of network theory, *Europhys. Lett.* 111 (5) (2015) 56001.
- [321] G. Bianconi, C. Rahmede, Complex quantum network manifolds in dimension $d > 2$ are scale-free, *Sci. Rep.* 5 (2015) 13979.
- [322] G. Bianconi, C. Rahmede, Z. Wu, Complex quantum network geometries: Evolution and phase transitions, *Phys. Rev. E* 92 (2) (2015) 022815.
- [323] O.T. Courtney, G. Bianconi, Weighted growing simplicial complexes, *Phys. Rev. E* 95 (6) (2017) 062301.
- [324] N. Fountoulakis, T. Iyer, C. Mailler, H. Sulzbach, Dynamical models for random simplicial complexes, 2019, arXiv:1910.12715.
- [325] A.E. Sizemore, E.A. Karuza, C. Giusti, D.S. Bassett, Knowledge gaps in the early growth of semantic feature networks, *Nat. Hum. Behav.* 2 (9) (2018) 682.
- [326] A.S. Blevins, D.S. Bassett, On the reorderability of node-filtered order complexes, *Phys. Rev. E* 101 (2020) 052311.
- [327] D.C. da Silva, G. Bianconi, R.A. da Costa, S.N. Dorogovtsev, J.F. Mendes, Complex network view of evolving manifolds, *Phys. Rev. E* 97 (3) (2018) 032316.
- [328] O.T. Courtney, G. Bianconi, Dense power-law networks and simplicial complexes, *Phys. Rev. E* 97 (5) (2018) 052303.
- [329] B. Kim, A. Schein, B.A. Desmarais, H. Wallach, The hyperedge event model, 2018, arXiv:1807.08225.
- [330] N. Masuda, M.A. Porter, R. Lambiotte, Random walks and diffusion on networks, *Phys. Rep.* (2017).
- [331] D. Aldous, J. Fill, Reversible Markov chains and random walks on graphs, *Unfinished Monograph* (2002).
- [332] A. Samukhin, S. Dorogovtsev, J. Mendes, Laplacian spectra of, and random walks on, complex networks: Are scale-free architectures really important? *Phys. Rev. E* 77 (3) (2008) 036115.

- [333] T. Hoffmann, M.A. Porter, R. Lambiotte, Generalized master equations for non-Poisson dynamics on networks, *Phys. Rev. E* 86 (4) (2012) 046102.
- [334] M.H. DeGroot, Reaching a consensus, *J. Amer. Statist. Assoc.* 69 (345) (1974) 118–121.
- [335] L. Boltzmann, *Lectures on gas theory*, English translation by S. Brush, University of California Press, Berkeley-Los Angeles, Calif, 1964.
- [336] R.C. Tolman, *The Principles of Statistical Mechanics*, Courier Corporation, 1979.
- [337] F.R. Chung, F.C. Graham, *Spectral Graph Theory*, (92) American Mathematical Soc., 1997.
- [338] L. Neuhäuser, A. Mellor, R. Lambiotte, Multibody interactions and nonlinear consensus dynamics on networked systems, *Phys. Rev. E* 101 (3) (2020) 032310.
- [339] J.J. Torres, G. Bianconi, Simplicial complexes: Higher-order spectral dimension and dynamics, *J. Phys.: Complex.* 1 (2020) 015002.
- [340] R. Burioni, D. Cassi, Universal properties of simplicial complexes and harmonics, *Random Struct. Algorithms* 76 (7) (1996) 1091.
- [341] A.P. Millán, J.J. Torres, G. Bianconi, Synchronization in network geometries with finite spectral dimension, *Phys. Rev. E* 99 (2) (2019) 022307.
- [342] J. Jia, M.T. Schaub, S. Segarra, A.R. Benson, Graph-based semi-supervised & active learning for edge flows, in: *Proceedings of the 25th ACM SIGKDD International Conference on Knowledge Discovery & Data Mining*, 2019, pp. 761–771.
- [343] S. Mukherjee, J. Steenbergen, Random walks on simplicial complexes and harmonics, *Random Struct. Algorithms* 49 (2) (2016) 379–405.
- [344] D. Dua, C. Graff, *UCI Machine Learning Repository*, University of California, Irvine, School of Information and Computer Sciences, 2017.
- [345] T. Carletti, F. Battiston, G. Cencetti, D. Fanelli, Random walks on hypergraphs, *Phys. Rev. E* 101 (2) (2020) 022308.
- [346] U. Chitra, B.J. Raphael, Random walks on hypergraphs with edge-dependent vertex weights, in: *Proceedings of the 36th International Conference on Machine Learning*, 2019, pp. 1172–1181.
- [347] S. Agarwal, K. Branson, S. Belongie, Higher order learning with graphs, in: *Proceedings of the 23rd International Conference on Machine Learning*, ACM, 2006, pp. 17–24.
- [348] P. Li, O. Milenkovic, Inhomogeneous hypergraph clustering with applications, in: *Advances in Neural Information Processing Systems*, 2017, pp. 2308–2318.
- [349] J. Li, J. He, Y. Zhu, E-tail product return prediction via hypergraph-based local graph cut, in: *Proceedings of the 24th ACM SIGKDD International Conference on Knowledge Discovery & Data Mining*, ACM, 2018, pp. 519–527.
- [350] L. Ding, A. Yilmaz, Interactive image segmentation using probabilistic hypergraphs, *Pattern Recognit.* 43 (5) (2010) 1863–1873.
- [351] Y. Huang, Q. Liu, S. Zhang, D.N. Metaxas, Image retrieval via probabilistic hypergraph ranking, in: *2010 IEEE Computer Society Conference on Computer Vision and Pattern Recognition*, IEEE, 2010, pp. 3376–3383.
- [352] A. Ducournau, A. Bretto, Random walks in directed hypergraphs and application to semi-supervised image segmentation, *Comput. Vis. Image Underst.* 120 (2014) 91–102.
- [353] K. Zeng, N. Wu, A. Sargolzaei, K. Yen, Learn to rank images: A unified probabilistic hypergraph model for visual search, *Math. Probl. Eng.* 2016 (2016).
- [354] Z. Zhang, H. Lin, Y. Gao, K. BNRist, Dynamic hypergraph structure learning, in: *IJCAI*, 2018, pp. 3162–3169.
- [355] T. Chan, Z.G. Tang, C. Zhang, Spectral properties of Laplacian and stochastic diffusion process for edge expansion in hypergraphs, 2015, [arXiv:1510.01520](https://arxiv.org/abs/1510.01520).
- [356] T.-H.H. Chan, Z.G. Tang, X. Wu, C. Zhang, Diffusion operator and spectral analysis for directed hypergraph Laplacian, *Theoret. Comput. Sci.* 784 (2019) 46–64.
- [357] J.C.W. Billings, M. Hu, G. Lerda, A.N. Medvedev, F. Mottes, A. Onicas, A. Santoro, G. Petri, Simplex2Vec embeddings for community detection in simplicial complexes, 2019, [arXiv:1906.09068](https://arxiv.org/abs/1906.09068).
- [358] V. Salnikov, D. Cassese, R. Lambiotte, Simplicial complexes and complex systems, *Eur. J. Phys.* 40 (1) (2018) 014001.
- [359] L.H. Tran, L.H. Tran, H. Trang, L. Hieu, Combinatorial and random walk hypergraph Laplacian eigenmaps, *Int. J. Mach. Learn. Comput.* 5 (6) (2015) 462.
- [360] S.N. Satchidanand, H. Ananthapadmanaban, B. Ravindran, Extended discriminative random walk: A hypergraph approach to multi-view multi-relational transductive learning, in: *Twenty-Fourth International Joint Conference on Artificial Intelligence*, 2015.
- [361] Y. Liu, J. Yuan, B. Duan, D. Li, Quantum walks on regular uniform hypergraphs, *Sci. Rep.* 8 (1) (2018) 9548.
- [362] C. Cooper, A. Frieze, T. Radzik, The cover times of random walks on hypergraphs, in: *International Colloquium on Structural Information and Communication Complexity*, Springer, 2011, pp. 210–221.
- [363] U. Harush, B. Barzel, Dynamic patterns of information flow in complex networks, *Nature Commun.* 8 (1) (2017) 2181.
- [364] A.M. Turing, The chemical basis of morphogenesis, *Philos. Trans. R. Soc. Lond. B Biol. Sci.* 237 (641) (1952) 37–72.
- [365] A. Arenas, A. Díaz-Guilera, C.J. Pérez, F. Vega-Redondo, Self-organized criticality in evolutionary systems with local interaction, *J. Econom. Dynam. Control* 26 (12) (2002) 2115–2142.
- [366] V. Colizza, R. Pastor-Satorras, A. Vespignani, Reaction–diffusion processes and metapopulation models in heterogeneous networks, *Nat. Phys.* 3 (4) (2007) 276–282.
- [367] H. Nakao, A.S. Mikhailov, Turing patterns in network-organized activator–inhibitor systems, *Nat. Phys.* 6 (7) (2010) 544–550.
- [368] M. Asllani, J.D. Challenger, F.S. Pavone, L. Sacconi, D. Fanelli, The theory of pattern formation on directed networks, *Nature Commun.* 5 (1) (2014) 1–9.
- [369] N.E. Kouvaris, M. Sebek, A. Iribarne, A. Díaz-Guilera, I.Z. Kiss, Stationary patterns in star networks of bistable units: Theory and application to chemical reactions, *Phys. Rev. E* 95 (4) (2017) 042203.
- [370] G. Cencetti, P. Clusella, D. Fanelli, Pattern invariance for reaction–diffusion systems on complex networks, *Sci. Rep.* 8 (1) (2018) 1–9.
- [371] T. Carletti, D. Fanelli, S. Nicoletti, Dynamical systems on hypergraphs., 2020, [arXiv:2006.01243](https://arxiv.org/abs/2006.01243).
- [372] C. Huygens, H. Oscillatorium, The pendulum clock, *Trans. RJ Blackwell Iowa State Univ. Press Ames.* (1986).
- [373] Z. Neda, E. Ravasz, Y. Brechet, T. Vicsek, A.-L. Barabási, The sound of many hands clapping, *Nature* 403 (6772) (2000) 849–850.
- [374] J. Buck, Synchronous rhythmic flashing of fireflies. II, *Q. Rev. Biol.* 63 (3) (1988) 265–289.
- [375] S. Boccaletti, J. Kurths, G. Osipov, D. Valladares, C. Zhou, The synchronization of chaotic systems, *Phys. Rep.* 366 (1) (2002) 1–101.
- [376] A. Pikovsky, M. Rosenblum, J. Kurths, *Synchronization: A Universal Concept in Nonlinear Sciences*, vol. 12, Cambridge University Press, Cambridge, 2003.
- [377] S.H. Strogatz, *Sync: The Emerging Science of Spontaneous Order*, Penguin UK, 2004.
- [378] S. Boccaletti, A.N. Pisarchik, C.I. Del Genio, A. Amann, *Synchronization: From Coupled Systems to Complex Networks*, Cambridge University Press, 2018.
- [379] Y. Kuramoto, *Chemical Oscillations, Waves, and Turbulence*, Springer-Verlag, Tokyo, 1984.
- [380] J.A. Acebrón, L.L. Bonilla, C.J.P. Vicente, F. Ritort, R. Spigler, The Kuramoto model: A simple paradigm for synchronization phenomena, *Rev. Modern Phys.* 77 (1) (2005) 137.
- [381] A. Arenas, A. Díaz-Guilera, J. Kurths, Y. Moreno, C. Zhou, Synchronization in complex networks, *Phys. Rep.* 469 (3) (2008) 93–153.
- [382] F.A. Rodrigues, T.K.D.M. Peron, P. Ji, J. Kurths, The Kuramoto model in complex networks, *Phys. Rep.* 610 (2016) 1–98.
- [383] M. Barahona, L.M. Pecora, Synchronization in small-world systems, *Phys. Rev. Lett.* 89 (5) (2002) 054101.

- [384] J. Gómez-Gardeñes, S. Gómez, A. Arenas, Y. Moreno, Explosive synchronization transitions in scale-free networks, *Phys. Rev. Lett.* 106 (12) (2011) 128701.
- [385] S. Boccaletti, J. Almendral, S. Guan, I. Leyva, Z. Liu, I. Sendiña-Nadal, Z. Wang, Y. Zou, Explosive transitions in complex networks' structure and dynamics: Percolation and synchronization, *Phys. Rep.* 660 (2016) 1–94.
- [386] V. Nicosia, M. Valencia, M. Chavez, A. Díaz-Guilera, V. Latora, Remote synchronization reveals network symmetries and functional modules, *Phys. Rev. Lett.* 110 (17) (2013) 174102.
- [387] L.M. Pecora, F. Sorrentino, A.M. Hagerstrom, T.E. Murphy, R. Roy, Cluster synchronization and isolated desynchronization in complex networks with symmetries, *Nature Commun.* 5 (1) (2014) 1–8.
- [388] D.M. Abrams, S.H. Strogatz, Chimera states for coupled oscillators, *Phys. Rev. Lett.* 93 (17) (2004) 174102.
- [389] H. Bi, X. Hu, S. Boccaletti, X. Wang, Y. Zou, Z. Liu, S. Guan, Coexistence of quantized, time dependent, clusters in globally coupled oscillators, *Phys. Rev. Lett.* 117 (20) (2016) 204101.
- [390] M.A. Aguiar, A.P. Dias, An overview of synchrony in coupled cell networks, in: *Modeling, Dynamics, Optimization and Bioeconomics III*, Springer, 2016, pp. 25–48.
- [391] E. Nijholt, B. Rink, J. Sanders, Center manifolds of coupled cell networks, *SIAM J. Math. Anal.* 49 (5) (2017) 4117–4148.
- [392] M. Golubitsky, I. Stewart, Nonlinear dynamics of networks: The groupoid formalism, *Bull. Am. Math. Soc.* 43 (3) (2006) 305–364.
- [393] I. Stewart, M. Golubitsky, M. Pivato, Symmetry groupoids and patterns of synchrony in coupled cell networks, *SIAM J. Appl. Dyn. Syst.* 2 (4) (2003) 609–646.
- [394] M. Golubitsky, I. Stewart, A. Török, Patterns of synchrony in coupled cell networks with multiple arrows, *SIAM J. Appl. Dyn. Syst.* 4 (1) (2005) 78–100.
- [395] S. Watanabe, S.H. Strogatz, Integrability of a globally coupled oscillator array, *Phys. Rev. Lett.* 70 (16) (1993) 2391.
- [396] S. Watanabe, S.H. Strogatz, Constants of motion for superconducting Josephson arrays, *Physica D* 74 (3–4) (1994) 197–253.
- [397] E. Ott, T.M. Antonsen, Low dimensional behavior of large systems of globally coupled oscillators, *Chaos* 18 (3) (2008) 037113.
- [398] C. Bick, M. Goodfellow, C.R. Laing, E.A. Martens, Understanding the dynamics of biological and neural oscillator networks through exact mean-field reductions: A review, *J. Math. Neurosci.* 10 (1) (2020) 1–43.
- [399] Y.M. Vega, M. Vázquez-Prada, A.F. Pacheco, Fitness for synchronization of network motifs, *Physica A* 343 (2004) 279–287.
- [400] O. D'Huys, R. Vicente, T. Erneux, J. Danckaert, I. Fischer, Synchronization properties of network motifs: Influence of coupling delay and symmetry, *Chaos* 18 (3) (2008) 037116.
- [401] P.S. Skardal, A. Arenas, Abrupt desynchronization and extensive multistability in globally coupled oscillator simplexes, *Phys. Rev. Lett.* 122 (24) (2019) 248301.
- [402] C. Xu, X. Wang, P.S. Skardal, Bifurcation analysis and structural stability of simplicial oscillator populations, *Phys. Rev. Research* 2 (2) (2020) 023281.
- [403] T. Tanaka, T. Aoyagi, Multistable attractors in a network of phase oscillators with three-body interactions, *Phys. Rev. Lett.* 106 (22) (2011) 224101.
- [404] P. Ashwin, A. Rodrigues, Hopf normal form with S_N symmetry and reduction to systems of nonlinearly coupled phase oscillators, *Physica D* 325 (2016) 14–24.
- [405] M. Komarov, A. Pikovsky, Finite-size-induced transitions to synchrony in oscillator ensembles with nonlinear global coupling, *Phys. Rev. E* 92 (2) (2015) 020901.
- [406] P.S. Skardal, A. Arenas, Higher-order interactions in complex networks of phase oscillators promote abrupt synchronization switching, 2019, arXiv:1909.08057.
- [407] D. Pazó, Thermodynamic limit of the first-order phase transition in the Kuramoto model, *Phys. Rev. E* 72 (4) (2005) 046211.
- [408] V. Nicosia, P.S. Skardal, A. Arenas, V. Latora, Collective phenomena emerging from the interactions between dynamical processes in multiplex networks, *Phys. Rev. Lett.* 118 (13) (2017) 138302.
- [409] R.M. D'Souza, J. Gómez-Gardeñes, J. Nagler, A. Arenas, Explosive phenomena in complex networks, *Adv. Phys.* 68 (3) (2019) 123–223.
- [410] V. Berec, Chimera state and route to explosive synchronization, *Chaos* 86 (2016) 75–81.
- [411] V. Berec, Explosive synchronization in clustered scale-free networks: Revealing the existence of chimera state, *Eur. Phys. J. Spec. Top.* 225 (1) (2016) 7–15.
- [412] C. Kuehn, C. Bick, A universal route to explosive phenomena, 2020, arXiv:2002.10714.
- [413] T. Stankovski, V. Ticineili, P.V. McClintock, A. Stefanovska, Coupling functions in networks of oscillators, *New J. Phys.* 17 (3) (2015) 035002.
- [414] I. León, D. Pazó, Phase reduction beyond the first order: The case of the mean-field complex Ginzburg-Landau equation, *Phys. Rev. E* 100 (1) (2019) 012211.
- [415] A.P. Millán, J.J. Torres, G. Bianconi, Explosive higher-order Kuramoto dynamics on simplicial complexes, *Phys. Rev. Lett.* 124 (2020) 218301.
- [416] A.P. Millán, J.J. Torres, G. Bianconi, Complex network geometry and frustrated synchronization, *Sci. Rep.* 8 (1) (2018) 9910.
- [417] C.C. Gong, A. Pikovsky, Low-dimensional dynamics for higher-order harmonic, globally coupled phase-oscillator ensembles, *Phys. Rev. E* 100 (6) (2019) 062210.
- [418] M. Rosenblum, A. Pikovsky, Self-organized quasiperiodicity in oscillator ensembles with global nonlinear coupling, *Phys. Rev. Lett.* 98 (6) (2007) 064101.
- [419] A. Pikovsky, M. Rosenblum, Self-organized partially synchronous dynamics in populations of nonlinearly coupled oscillators, *Physica D* 238 (1) (2009) 27–37.
- [420] O. Burylko, A. Pikovsky, Desynchronization transitions in nonlinearly coupled phase oscillators, *Physica D* 240 (17) (2011) 1352–1361.
- [421] H. Nakao, Phase reduction approach to synchronisation of nonlinear oscillators, *Contemp. Phys.* 57 (2) (2016) 188–214.
- [422] B. Pietras, A. Daffertshofer, Network dynamics of coupled oscillators and phase reduction techniques, *Phys. Rep.* (2019).
- [423] P. Ashwin, C. Bick, O. Burylko, Identical phase oscillator networks: Bifurcations, symmetry and reversibility for generalized coupling, *Front. Appl. Math. Stat.* 2 (2016) 7.
- [424] M.H. Matheny, J. Emenheiser, W. Fon, A. Chapman, A. Salova, M. Rohden, J. Li, M.H. de Bady, M. Pósai, L. Duenas-Ororio, Exotic states in a simple network of nanoelectromechanical oscillators, *Science* 363 (6431) (2019) eaav7932.
- [425] C. Bick, P. Ashwin, A. Rodrigues, Chaos in generically coupled phase oscillator networks with nonpairwise interactions, *Chaos* 26 (9) (2016) 094814.
- [426] C. Bick, Heteroclinic switching between chimeras, *Phys. Rev. E* 97 (5) (2018) 050201.
- [427] C. Bick, Heteroclinic dynamics of localized frequency synchrony: heteroclinic cycles for small populations, *J. Nonlin. Sci.* (2019).
- [428] C. Bick, A. Lohse, Heteroclinic dynamics of localized frequency synchrony: Stability of heteroclinic cycles and networks, *J. Nonlin. Sci.* (2019).
- [429] C. Bick, M. Timme, D. Paulikat, D. Rathlev, P. Ashwin, Chaos in symmetric phase oscillator networks, *Phys. Rev. Lett.* 107 (24) (2011) 244101.
- [430] M. Komarov, A. Pikovsky, Dynamics of multifrequency oscillator communities, *Phys. Rev. Lett.* 110 (13) (2013) 134101.
- [431] M. Rosenblum, A. Pikovsky, Numerical phase reduction beyond the first order approximation, *Chaos* 29 (1) (2019) 011105.
- [432] L.M. Pecora, T.L. Carroll, Synchronization in chaotic systems, *Phys. Rev. Lett.* 64 (8) (1990) 821.
- [433] M.G. Rosenblum, A.S. Pikovsky, J. Kurths, Phase synchronization of chaotic oscillators, *Phys. Rev. Lett.* 76 (11) (1996) 1804.

- [434] C.W. Wu, Synchronization in arrays of chaotic circuits coupled via hypergraphs: static and dynamic coupling, in: ISCAS'98. Proceedings of the 1998 IEEE International Symposium on Circuits and Systems (Cat. No. 98CH36187), vol. 3, IEEE, 1998, pp. 287–290.
- [435] A. Krawiecki, Chaotic synchronization on complex hypergraphs, *Chaos Solitons Fractals* 65 (2014) 44–50.
- [436] L. Gambuzza, F. Di Patti, L. Gallo, S. Lepri, M. Romance, R. Criado, M. Frasca, V. Latora, S. Boccaletti, The master stability function for synchronization in simplicial complexes, 2020, arXiv:2004.03913.
- [437] I. Lodato, S. Boccaletti, V. Latora, Synchronization properties of network motifs, *Europhys. Lett.* 78 (2) (2007) 28001.
- [438] M.C. Soriano, G. Van der Sande, I. Fischer, C.R. Mirasso, Synchronization in simple network motifs with negligible correlation and mutual information measures, *Phys. Rev. Lett.* 108 (13) (2012) 134101.
- [439] S. Krishnagopal, J. Lehnert, W. Poel, A. Zakharova, E. Schöll, Synchronization patterns: From network motifs to hierarchical networks, *Phil. Trans. R. Soc. A* 375 (2088) (2017) 20160216.
- [440] R. Amritkar, S. Jalan, C.-K. Hu, Synchronized clusters in coupled map networks. II. Stability analysis, *Phys. Rev. E* 72 (1) (2005) 016212.
- [441] L.M. Pecora, T.L. Carroll, Master stability functions for synchronized coupled systems, *Phys. Rev. Lett.* 80 (10) (1998) 2109.
- [442] A. Englert, S. Heiligenthal, W. Kinzel, I. Kanter, Synchronization of chaotic networks with time-delayed couplings: an analytic study, *Phys. Rev. E* 83 (4) (2011) 046222.
- [443] F. Sorrentino, E. Ott, Network synchronization of groups, *Phys. Rev. E* 76 (5) (2007) 056114.
- [444] A. Koseska, E. Volkov, J. Kurths, Oscillation quenching mechanisms: amplitude vs. oscillation death, *Phys. Rep.* 531 (4) (2013) 173–199.
- [445] R. Mulas, C. Kuehn, J. Jost, Coupled dynamics on hypergraphs: master stability of steady states and synchronization, 2020, arXiv:2003.13775.
- [446] P. Dayan, L.F. Abbott, L. Abbott, *Theoretical Neuroscience: Computational and Mathematical Modeling of Neural Systems*, MIT press Cambridge, MA, 2001.
- [447] W. Gerstner, W.M. Kistler, *Spiking Neuron Models: Single Neurons, Populations, Plasticity*, Cambridge University Press, 2002.
- [448] Q. Bian, H. Yao, Adaptive synchronization of bipartite dynamical networks with distributed delays and nonlinear derivative coupling, *Commun. Nonlinear Sci. Numer. Simul.* 16 (10) (2011) 4089–4098.
- [449] A. Shilnikov, R. Gordon, I. Belykh, Polyrhythmic synchronization in bursting networking motifs, *Chaos* 18 (3) (2008) 037120.
- [450] F.S. Matias, P.V. Carelli, C.R. Mirasso, M. Copelli, Anticipated synchronization in a biologically plausible model of neuronal motifs, *Phys. Rev. E* 84 (2) (2011) 021922.
- [451] L.L. Gollo, C. Mirasso, O. Sporns, M. Breakspear, Mechanisms of zero-lag synchronization in cortical motifs, *PLOS Comput. Biol.* 10 (4) (2014) e1003548.
- [452] J. Wojcik, J. Schwabedal, R. Clewley, A.L. Shilnikov, Key bifurcations of bursting polyrhythms in 3-cell central pattern generators, *PLoS one* 9 (4) (2014).
- [453] J. Collens, K. Pusiluri, A. Kelly, D. Knapper, T. Xing, D. Basodi, A. Shilnikov, Dynamics and bifurcations in multistable 3-cell neural networks, 2020, arXiv:2005.04278.
- [454] D.A. Smirnov, R.G. Andrzejak, Detection of weak directional coupling: phase-dynamics approach versus state-space approach, *Phys. Rev. E* 71 (3) (2005) 036207.
- [455] S. Frenzel, B. Pompe, Partial mutual information for coupling analysis of multivariate time series, *Phys. Rev. Lett.* 99 (20) (2007) 204101.
- [456] M.G. Rosenblum, A.S. Pikovsky, Detecting direction of coupling in interacting oscillators, *Phys. Rev. E* 64 (4) (2001) 045202.
- [457] B. Kralemann, A. Pikovsky, M. Rosenblum, Reconstructing phase dynamics of oscillator networks, *Chaos* 21 (2) (2011) 025104.
- [458] B. Kralemann, A. Pikovsky, M. Rosenblum, Reconstructing effective phase connectivity of oscillator networks from observations, *New J. Phys.* 16 (8) (2014) 085013.
- [459] B. Kralemann, L. Cimponeriu, M. Rosenblum, A. Pikovsky, R. Mrowka, Phase dynamics of coupled oscillators reconstructed from data, *Phys. Rev. E* 77 (6) (2008) 066205.
- [460] P. Tass, M.G. Rosenblum, J. Weule, J. Kurths, A. Pikovsky, J. Volkmann, A. Schnitzler, H.-J. Freund, Detection of n:m phase locking from noisy data: application to magnetoencephalography, *Phys. Rev. Lett.* 81 (15) (1998) 3291–3294.
- [461] B. Kralemann, A. Pikovsky, M. Rosenblum, Detecting triplet locking by triplet synchronization indices, *Phys. Rev. E* 87 (5) (2013) 052904.
- [462] J. Jia, Z. Song, W. Liu, J. Kurths, J. Xiao, Experimental study of the triplet synchronization of coupled nonidentical mechanical metronomes, *Sci. Rep.* 5 (2015) 17008.
- [463] A. Duggento, T. Stankovski, P.V. McClintock, A. Stefanovska, Dynamical Bayesian inference of time-evolving interactions: from a pair of coupled oscillators to networks of oscillators, *Phys. Rev. E* 86 (6) (2012) 061126.
- [464] R. Pastor-Satorras, A. Vespignani, Epidemic spreading in scale-free networks, *Phys. Rev. Lett.* 86 (14) (2001) 3200.
- [465] M.J. Keeling, P. Rohani, *Modeling Infectious Diseases in Humans and Animals*, Princeton University Press, 2011.
- [466] R. Pastor-Satorras, C. Castellano, P. Van Mieghem, A. Vespignani, Epidemic processes in complex networks, *Rev. Modern Phys.* 87 (3) (2015) 925.
- [467] G.F. de Arruda, F.A. Rodrigues, Y. Moreno, Fundamentals of spreading processes in single and multilayer complex networks, *Phys. Rep.* 756 (2018) 1–59.
- [468] W. Goffman, V.A. Newell, Generalization of epidemic theory: An application to the transmission of ideas, *Nature* 204 (4955) (1964) 225–228.
- [469] D. Centola, How behavior spreads: The science of complex contagions, vol. 3, Princeton University Press, 2018.
- [470] A. Nowak, J. Szamrej, B. Latané, From private attitude to public opinion: A dynamic theory of social impact, *Psychol. Rev.* 97 (3) (1990) 362.
- [471] R. Axelrod, The complexity of cooperation: Agent-based models of competition and collaboration, vol. 3, Princeton University Press, 1997.
- [472] P. Sen, B.K. Chakrabarti, *Sociophysics: An Introduction*, Oxford University Press, 2014.
- [473] C. Castellano, S. Fortunato, V. Loreto, Statistical physics of social dynamics, *Rev. Modern Phys.* 81 (2) (2009) 591.
- [474] A. Baronchelli, The emergence of consensus: A primer, *R. Soc. Open Sci.* 5 (2) (2018) 172189.
- [475] W.O. Kermack, A.G. McKendrick, A contribution to the mathematical theory of epidemics, *Proc. R. Soc. Lond. Ser. A Math. Phys. Eng. Sci.* 115 (772) (1927) 700–721.
- [476] R.M. Anderson, R.M. May, *Infectious Diseases of Humans: Dynamics and Control*, Oxford University Press, 1992.
- [477] H.W. Hethcote, The mathematics of infectious diseases, *SIAM Rev.* 42 (4) (2000) 599–653.
- [478] L. Hufnagel, D. Brockmann, T. Geisel, Forecast and control of epidemics in a globalized world, *Proc. Natl. Acad. Sci. USA* 101 (42) (2004) 15124–15129.
- [479] V. Colizza, A. Barrat, M. Barthélemy, A. Vespignani, The role of the airline transportation network in the prediction and predictability of global epidemics, *Proc. Natl. Acad. Sci. USA* 103 (7) (2006) 2015–2020.
- [480] Q. Zhang, K. Sun, M. Chinazzi, A.P. y Piontti, N.E. Dean, D.P. Rojas, S. Merler, D. Mistry, P. Poletti, L. Rossi, Spread of zika virus in the americas, *Proc. Natl. Acad. Sci. USA* 114 (22) (2017) E4334–E4343.
- [481] A.P. y Piontti, N. Perra, L. Rossi, N. Samay, A. Vespignani, *Charting the next Pandemic: Modeling Infectious Disease Spreading in the Data Science Age*, Springer, 2018.
- [482] C. Viboud, A. Vespignani, The future of influenza forecasts, *Proc. Natl. Acad. Sci. USA* 116 (8) (2019) 2802–2804.
- [483] A.J. Kucharski, T.W. Russell, C. Diamond, Y. Liu, J. Edmunds, S. Funk, R.M. Eggo, F. Sun, M. Jit, J.D. Munday, Early dynamics of transmission and control of COVID-19: A mathematical modelling study, *Lancet Infect. Dis.* (2020).

- [484] M.U.G. Kraemer, C.-H. Yang, B. Gutierrez, C.-H. Wu, B. Klein, D.M. Pigott, L. du Plessis, N.R. Faria, R. Li, W.P. Hanage, J.S. Brownstein, M. Layan, A. Vespignani, H. Tian, C. Dye, O.G. Pybus, S.V. Scarpino, The effect of human mobility and control measures on the COVID-19 epidemic in China, *Science* (2020).
- [485] A. Vazquez, B. Rácz, A. Lukács, A.-L. Barabási, Impact of non-Poissonian activity patterns on spreading processes, *Phys. Rev. Lett.* 98 (15) (2007) 158702.
- [486] S. Bansal, J. Read, B. Pourbohloul, L.A. Meyers, The dynamic nature of contact networks in infectious disease epidemiology, *J. Biol. Dyn.* 4 (5) (2010) 478–489.
- [487] M. Karsai, M. Kivela, R.K. Pan, K. Kaski, J. Kertész, A.-L. Barabási, J. Saramäki, Small but slow world: How network topology and burstiness slow down spreading, *Phys. Rev. E* 83 (2) (2011) 025102.
- [488] L.E. Rocha, F. Liljeros, P. Holme, Simulated epidemics in an empirical spatiotemporal network of 50,185 sexual contacts, *PLOS Comput. Biol.* 7 (3) (2011).
- [489] W. Wang, Q.-H. Liu, J. Liang, Y. Hu, T. Zhou, Coevolution spreading in complex networks, *Phys. Rep.* (2019).
- [490] J.P. Gleeson, High-accuracy approximation of binary-state dynamics on networks, *Phys. Rev. Lett.* 107 (6) (2011) 068701.
- [491] J.P. Gleeson, Binary-state dynamics on complex networks: pair approximation and beyond, *Phys. Rev. X* 3 (2) (2013) 021004.
- [492] E. Cozzo, R.A. Banos, S. Meloni, Y. Moreno, Contact-based social contagion in multiplex networks, *Phys. Rev. E* 88 (5) (2013) 050801.
- [493] W. Wang, M. Tang, H.E. Stanley, L.A. Braunstein, Unification of theoretical approaches for epidemic spreading on complex networks, *Rep. Progr. Phys.* 80 (3) (2017) 036603.
- [494] I.Z. Kiss, J.C. Miller, P.L. Simon, et al., *Mathematics of Epidemics on Networks*, Cham Springer, 2017.
- [495] D.J. Daley, D.G. Kendall, Epidemics and rumours, *Nature* 204 (4963) (1964) 1118–1118.
- [496] F.M. Bass, A new product growth for model consumer durables, *Manag. Sci.* 15 (5) (1969) 215–227.
- [497] S. Bikhchandani, D. Hirshleifer, I. Welch, A theory of fads, fashion, custom, and cultural change as informational cascades, *J. Polit. Econ.* 100 (5) (1992) 992–1026.
- [498] Y. Moreno, M. Nekovee, A.F. Pacheco, Dynamics of rumor spreading in complex networks, *Phys. Rev. E* 69 (6) (2004) 066130.
- [499] E.M. Rogers, *Diffusion of Innovations*, Simon and Schuster, 2010.
- [500] D. Centola, M. Macy, Complex contagions and the weakness of long ties, *Am. J. Sociol.* 113 (3) (2007) 702–734.
- [501] D. Guilbeault, J. Becker, D. Centola, Complex contagions: a decade in review, in: *Complex Spreading Phenomena in Social Systems*, Springer, 2018, pp. 3–25.
- [502] K.F. Kee, L. Sparks, D.C. Struppa, M. Mannucci, Social groups, social media, and higher dimensional social structures: a simplicial model of social aggregation for computational communication research, *Commun. Q.* 61 (1) (2013) 35–58.
- [503] SocioPatterns Collaboration, <http://www.sociopatterns.org/>.
- [504] P. Cisneros-Velarde, F. Bullo, Multi-group SIS epidemics with simplicial and higher-order interactions, 2020, arXiv:2005.11404.
- [505] S. Gómez, A. Arenas, J. Borge-Holthoefer, S. Meloni, Y. Moreno, Discrete-time Markov chain approach to contact-based disease spreading in complex networks, *Europhys. Lett.* 89 (3) (2010) 38009.
- [506] J.T. Matamalas, A. Arenas, S. Gómez, Effective approach to epidemic containment using link equations in complex networks, *Sci. Adv.* 4 (12) (2018) eaau4212.
- [507] J.T. Matamalas, S. Gómez, A. Arenas, Abrupt phase transition of epidemic spreading in simplicial complexes, *Phys. Rev. Research* 2 (1) (2020) 012049.
- [508] M.E.J. Newman, J. Park, Why social networks are different from other types of networks, *Phys. Rev. E* 68 (3) (2003) 036122.
- [509] J.C. Miller, Spread of infectious disease through clustered populations, *J. R. Soc. Interface* 6 (41) (2009) 1121–1134.
- [510] M. Ritchie, L. Berthouze, T. House, I.Z. Kiss, Higher-order structure and epidemic dynamics in clustered networks, *J. Theoret. Biol.* 348 (2014) 21–32.
- [511] D.J. O'Sullivan, G.J. O'Keeffe, P.G. Fennell, J.P. Gleeson, Mathematical modeling of complex contagion on clustered networks, *Front. Phys.* 3 (2015) 71.
- [512] L. Hébert-Dufresne, B.M. Althouse, Complex dynamics of synergistic coinfections on realistically clustered networks, *Proc. Natl. Acad. Sci. USA* 112 (33) (2015) 10551–10556.
- [513] G. St-Onge, V. Thibeault, A. Allard, L.J. Dubé, L. Hébert-Dufresne, Master equation analysis of mesoscopic localization in contagion dynamics on higher-order networks, 2020, arXiv:2004.10203.
- [514] L. Hébert-Dufresne, D. Mistry, B.M. Althouse, Spread of infectious disease and social awareness as parasitic contagions on clustered networks, 2020, arXiv:2003.10604.
- [515] G.-Y. Yang, Z.-L. Hu, J.-G. Liu, Knowledge diffusion in the collaboration hypernetwork, *Physica A* 419 (2015) 429–436.
- [516] J.-P. Wang, Q. Guo, G.-Y. Yang, J.-G. Liu, Improved knowledge diffusion model based on the collaboration hypernetwork, *Physica A* 428 (2015) 250–256.
- [517] G. Peng, H. Wang, H. Zhang, K. Huang, A hypernetwork-based approach to collaborative retrieval and reasoning of engineering design knowledge, *Adv. Eng. Softw.* 42 (2019) 100956.
- [518] Á. Bodó, G.Y. Katona, P.L. Simon, SIS epidemic propagation on hypergraphs, *Bull. Math. Biol.* 78 (4) (2016) 713–735.
- [519] G. Ghoshal, L. Sander, I. Sokolov, SIS Epidemics with household structure: the self-consistent field method, *Math. Biol.* 190 (1) (2004) 71–85.
- [520] T. House, M.J. Keeling, Deterministic epidemic models with explicit household structure, *Math. Biosci.* 213 (1) (2008) 29–39.
- [521] F. Ball, T. Britton, T. House, V. Isham, D. Mollison, L. Pellis, G.S. Tomba, Seven challenges for metapopulation models of epidemics, including households models, *Epidemics* 10 (2015) 63–67.
- [522] M. Granovetter, Threshold models of collective behavior, *Am. J. Sociol.* 83 (6) (1978) 1420–1443.
- [523] M. Karsai, G. Iniguez, K. Kaski, J. Kertész, Complex contagion process in spreading of online innovation, *J. R. Soc. Interface* 11 (101) (2014) 20140694.
- [524] Q. Suo, J.-L. Guo, A.-Z. Shen, Information spreading dynamics in hypernetworks, *Phys. A* 495 (2018) 475–487.
- [525] B. Jhun, M. Jo, B. Kahng, Simplicial SIS model in scale-free uniform hypergraph, *J. Stat. Mech. Theory Exp.* 2019 (12) (2019) 123207.
- [526] S. Lübeck, Universal scaling behavior of non-equilibrium phase transitions, *Internat. J. Modern Phys. B* 18 (31n32) (2004) 3977–4118.
- [527] S.C. Ferreira, C. Castellano, R. Pastor-Satorras, Epidemic thresholds of the susceptible-infected-susceptible model on networks: a comparison of numerical and theoretical results, *Phys. Rev. E* 86 (4) (2012) 041125.
- [528] G.F. de Arruda, M. Tizzani, Y. Moreno, Phase transitions and stability of dynamical processes on hypergraphs, 2020, arXiv:2005.10891.
- [529] D. Dahlerup, From a small to a large minority: Women in scandinavian politics, *Scand. Polit. Stud.* 11 (4) (1988) 275–298.
- [530] S. Grey, Numbers and beyond: the relevance of critical mass in gender research, *Polit. Gend.* 2 (4) (2006) 492–502.
- [531] D. Centola, J. Becker, D. Brackbill, A. Baronchelli, Experimental evidence for tipping points in social convention, *Science* 360 (6393) (2018) 1116–1119.
- [532] T. Ma, J. Guo, Study on information transmission model of enterprise informal organizations based on the hypernetwork, *Chin. J. Phys.* 56 (5) (2018) 2424–2438.
- [533] K. Dietz, Epidemics and rumours: a survey, *J. R. Stat. Soc.* 130 (4) (1967) 505–528.

- [534] S. Galam, Sociophysics: a review of galam models, *Internat. J. Modern Phys. C* 19 (03) (2008) 409–440.
- [535] D. Lazer, A. Pentland, L. Adamic, S. Aral, A.-L. Barabási, D. Brewer, N. Christakis, N. Contractor, J. Fowler, M. Gutmann, et al., Computational social science, *Science* 323 (5915) (2009) 721–723.
- [536] S. Galam, What is sociophysics about? in: *Sociophysics*, Springer, 2012, pp. 3–19.
- [537] R. Conte, N. Gilbert, G. Bonelli, C. Cioffi-Revilla, G. Deffuant, J. Kertesz, V. Loreto, S. Moat, J.-P. Nadal, A. Sanchez, Manifesto of computational social science, *Eur. Phys. J. Spec. Top.* 214 (1) (2012) 325–346.
- [538] T.M. Liggett, *Interacting Particle Systems*, vol. 276, Springer Science & Business Media, 2012.
- [539] J. Shao, S. Havlin, H. Stanley, Dynamic opinion model and invasion percolation, *Phys. Rev. Lett.* 103 (1) (2009) 018701.
- [540] K. Suchecki, V.M. Eguíluz, M. San Miguel, Conservation laws for the voter model in complex networks, *Europhys. Lett.* 69 (2) (2004) 228.
- [541] K. Suchecki, V.M. Eguíluz, M. San Miguel, Voter model dynamics in complex networks: role of dimensionality, disorder, and degree distribution, *Phys. Rev. E* 72 (3) (2005) 036132.
- [542] M. Diakonova, V. Nicosia, V. Latora, M. San Miguel, Irreducibility of multilayer network dynamics: The case of the voter model, *New J. Phys.* 18 (2) (2016) 023010.
- [543] J. Fernández-Gracia, K. Suchecki, J.J. Ramasco, M. San Miguel, V.M. Eguíluz, Is the voter model a model for voters? *Phys. Rev. Lett.* 112 (15) (2014) 158701.
- [544] M. Kearns, S. Suri, N. Montfort, An experimental study of the coloring problem on human subject networks, *Science* 313 (5788) (2006) 824–827.
- [545] S. Judd, M. Kearns, Y. Vorobeychik, Behavioral dynamics and influence in networked coloring and consensus, *Proc. Natl. Acad. Sci. USA* 107 (34) (2010) 14978–14982.
- [546] F. Chung, A. Tsiatas, Hypergraph coloring games and voter models, *Internet Math.* 10 (1–2) (2014) 66–86.
- [547] S. Redner, Reality-inspired voter models: A mini-review, *C. R. Phys.* (2019).
- [548] F. Vazquez, V.M. Eguíluz, M. San Miguel, Generic absorbing transition in coevolution dynamics, *Phys. Rev. Lett.* 100 (10) (2008) 108702.
- [549] L. Horstmeyer, C. Kuehn, Adaptive voter model on simplicial complexes, *Phys. Rev. E* 101 (2) (2020) 022305.
- [550] S. Galam, Minority opinion spreading in random geometry, *Eur. Phys. J. B* 25 (4) (2002) 403–406.
- [551] D.J. Watts, A simple model of global cascades on random networks, *Proc. Natl. Acad. Sci. USA* 99 (9) (2002) 5766–5771.
- [552] N. Lanchier, J. Neuffer, Stochastic dynamics on hypergraphs and the spatial majority rule model, *J. Stat. Phys.* 151 (1–2) (2013) 21–45.
- [553] M.J. de Oliveira, Isotropic majority-vote model on a square lattice, *J. Stat. Phys.* 66 (1–2) (1992) 273–281.
- [554] L.F. Pereira, F. Moreira, Majority-vote model on random graphs, *Phys. Rev. E* 71 (1) (2005) 016123.
- [555] V. Latora, M. Marchiori, Efficient behavior of small-world networks, *Phys. Rev. Lett.* 87 (19) (2001) 198701.
- [556] P.R. Campos, V.M. de Oliveira, F. Moreira, Small-world effects in the majority-vote model, *Phys. Rev. E* 67 (2) (2003) 026104.
- [557] E.M. Luz, F. Lima, Majority-vote on directed small-world networks, *Internat. J. Modern Phys. C* 18 (08) (2007) 1251–1261.
- [558] F. Lima, Majority-vote on directed Barabási–Albert networks, *Internat. J. Modern Phys. C* 17 (09) (2006) 1257–1265.
- [559] F. Lima, Majority-vote on undirected Barabási–Albert networks, *Commun. Comput. Phys.* 2 (2) (2007) 358–366.
- [560] T. Gradowski, A. Krawiecki, Majority-vote model on scale-free hypergraphs, *Acta. Phys. Polon.* 127 (3A) (2015) 1–4.
- [561] H. Hong, M. Ha, H. Park, Finite-size scaling in complex networks, *Phys. Rev. Lett.* 98 (25) (2007) 258701.
- [562] G. Deffuant, D. Neau, F. Amblard, G. Weisbuch, Mixing beliefs among interacting agents, *Adv. Complex Syst.* 3 (01n04) (2000) 87–98.
- [563] J. Lorenz, Continuous opinion dynamics under bounded confidence: A survey, *Internat. J. Modern Phys. C* 18 (12) (2007) 1819–1838.
- [564] S.E. Asch, H. Guetzkow, Effects of group pressure upon the modification and distortion of judgments, *Doc. Gestalt Psychol.* (1951) 222–236.
- [565] R. Axelrod, The dissemination of culture: a model with local convergence and global polarization, *J. Confl. Resolut.* 41 (2) (1997) 203–226.
- [566] C. Castellano, M. Marsili, A. Vespignani, Nonequilibrium phase transition in a model for social influence, *Phys. Rev. Lett.* 85 (16) (2000) 3536.
- [567] K. Klemm, V.M. Eguíluz, R. Toral, M. San Miguel, Nonequilibrium transitions in complex networks: A model of social interaction, *Phys. Rev. E* 67 (2) (2003) 026120.
- [568] K. Klemm, V.M. Eguíluz, R. Toral, M. San Miguel, Global culture: A noise-induced transition in finite systems, *Phys. Rev. E* 67 (4) (2003) 045101.
- [569] F. Battiston, V. Nicosia, V. Latora, M. San Miguel, Layered social influence promotes multiculturalism in the Axelrod model, *Sci. Rep.* 7 (1) (2017) 1809.
- [570] S. Maletić, M. Rajković, Consensus formation on a simplicial complex of opinions, *Phys. A* 397 (2014) 111–120.
- [571] S. Maletić, Y. Zhao, Hidden multidimensional social structure modeling applied to biased social perception, *Phys. A* 492 (2018) 1419–1430.
- [572] C.P. Roca, J.A. Cuesta, A. Sánchez, Evolutionary game theory: Temporal and spatial effects beyond replicator dynamics, *Phys. Life Rev.* 6 (4) (2009) 208–249.
- [573] G. Szabó, A. Szolnoki, R. Izsák, Rock-scissors-paper game on regular small-world networks, *J. Phys. Math. Gen.* 37 (7) (2004) 2599.
- [574] A. Szolnoki, M. Mobilia, L.-L. Jiang, B. Szczesny, A.M. Rucklidge, M. Perc, Cyclic dominance in evolutionary games: a review, *J. R. Soc. Interface* 11 (100) (2014) 20140735.
- [575] R. Axelrod, The evolution of cooperation, in: *Basic Books*, Basic Books, 1984.
- [576] A. Rapoport, M. Guyer, A taxonomy of 2 x 2 games, by anatol rapoport and melvin guyer, in: *Bobbs-Merrill Reprint Series in the Social Sciences*, S617, 1966.
- [577] J.-J. Rousseau, The discourses and other political writings, Volume 1 of Cambridge Texts in the History of Political Thought, , edited by Victor Gourevitch, Cambridge University Press, 1997.
- [578] R. Luce, H. Raiffa, *Games and Decisions: Introduction and Critical Survey*, 2012 Ed, Dover Publications, Mineola, NY, 1957.
- [579] B. Gui, R. Sugden, *Economics and Social Interaction: Accounting for Interpersonal Relations*, Cambridge University Press, 2005.
- [580] J.M. Smith, *Evolution and the Theory of Games*, Cambridge University Press, 1982.
- [581] J.M. Smith, G.A. Parker, The logic of asymmetric contests, *Anim. Behav.* 24 (1) (1976) 159–175.
- [582] R. Cressman, Evolutionary stability for two-stage Hawk-Dove games, *Rocky Mountain J. Math.* (1995) 145–155.
- [583] J. Smith, Game theory and the evolution of fighting, *Evol.* (1972) 8–28.
- [584] S. Diederich, M. Opper, Replicators with random interactions: A solvable model, *Phys. Rev. A* 39 (8) (1989) 4333.
- [585] J. Hofbauer, K. Sigmund, *Evolutionary Games and Population Dynamics*, Cambridge University Press, 1998.
- [586] M. Opper, S. Diederich, Replicator dynamics, *Comput. Phys. Comm.* 121 (1999) 141–144.
- [587] T. Chawanya, K. Tokita, Large-dimensional replicator equations with antisymmetric random interactions, *J. Phys. Soc. Japan* 71 (2) (2002) 429–431.
- [588] M. Perc, A. Szolnoki, Coevolutionary games—a mini review, *BioSystems* 99 (2) (2010) 109–125.
- [589] G. Hardin, The tragedy of the commons, *Science* 162 (3859) (1968) 1243–1248.
- [590] M.A. Nowak, R.M. May, Evolutionary games and spatial chaos, *Nature* 359 (6398) (1992) 826–829.
- [591] F.C. Santos, J.M. Pacheco, Scale-free networks provide a unifying framework for the emergence of cooperation, *Phys. Rev. Lett.* 95 (9) (2005) 098104.

- [592] J. Gómez-Gardeñes, M. Campillo, L. Floría, Y. Moreno, Dynamical organization of cooperation in complex topologies, *Phys. Rev. Lett.* 98 (10) (2007) 108103.
- [593] S. Assenza, J. Gómez-Gardeñes, V. Latora, Enhancement of cooperation in highly clustered scale-free networks, *Phys. Rev. E* 78 (1) (2008) 017101.
- [594] A. Cassar, Coordination and cooperation in local, random and small world networks: experimental evidence, *Games Econom. Behav.* 58 (2) (2007) 209–230.
- [595] O. Kirchkamp, R. Nagel, Naive learning and cooperation in network experiments, *Games Econom. Behav.* 58 (2) (2007) 269–292.
- [596] J. Grujić, C. Fosco, L. Araujo, J.A. Cuesta, A. Sánchez, Social experiments in the mesoscale: Humans playing a spatial prisoner's dilemma, *PLOS One* 5 (11) (2010).
- [597] A. Traulsen, D. Semmann, R.D. Sommerfeld, H.-J. Krambeck, M. Milinski, Human strategy updating in evolutionary games, *Proc. Natl. Acad. Sci. USA* 107 (7) (2010) 2962–2966.
- [598] C. Gracia-Lázaro, A. Ferrer, G. Ruiz, A. Tarancón, J.A. Cuesta, A. Sánchez, Y. Moreno, Heterogeneous networks do not promote cooperation when humans play a prisoner's dilemma, *Proc. Natl. Acad. Sci. USA* 109 (32) (2012) 12922–12926.
- [599] J. Grujić, C. Gracia-Lázaro, M. Milinski, D. Semmann, A. Traulsen, J.A. Cuesta, Y. Moreno, A. Sánchez, A comparative analysis of spatial prisoner's dilemma experiments: conditional cooperation and payoff irrelevance, *Sci. Rep.* 4 (2014) 4615.
- [600] D.G. Rand, M.A. Nowak, J.H. Fowler, N.A. Christakis, Static network structure can stabilize human cooperation, *Proc. Natl. Acad. Sci. USA* 111 (48) (2014) 17093–17098.
- [601] A. Sánchez, Physics of human cooperation: experimental evidence and theoretical models, *J. Stat. Mech. Theory Exp.* 2018 (2) (2018) 024001.
- [602] C. Hauert, M. Doebeli, Spatial structure often inhibits the evolution of cooperation in the snowdrift game, *Nature* 428 (6983) (2004) 643–646.
- [603] M.A. Nowak, Five rules for the evolution of cooperation, *Science* 314 (5805) (2006) 1560–1563.
- [604] G. Szabó, G. Fath, Evolutionary games on graphs, *Phys. Rep.* 446 (4–6) (2007) 97–216.
- [605] Z. Wang, L. Wang, A. Szolnoki, M. Perc, Evolutionary games on multilayer networks: a colloquium, *Eur. Phys. J. B* 88 (5) (2015) 124.
- [606] K. Sigmund, *The Calculus of Selfishness*, vol. 6, Princeton University Press, 2010.
- [607] M. Archetti, I. Scheuring, Review: evolution of cooperation in one-shot social dilemmas without assortment, *J. Theoret. Biol.* 299 (2012) 9–20.
- [608] M. Perc, J. Gómez-Gardeñes, A. Szolnoki, L.M. Floría, Y. Moreno, Evolutionary dynamics of group interactions on structured populations: A review, *J. R. Soc. Interface* 10 (80) (2013) 20120997.
- [609] M. Perc, J.J. Jordan, D.G. Rand, Z. Wang, S. Boccaletti, A. Szolnoki, Statistical physics of human cooperation, *Phys. Rev.* 687 (2017) 1–51.
- [610] J. Peña, B. Wu, J. Arranz, A. Traulsen, Evolutionary games of multiplayer cooperation on graphs, *PLOS Comput. Biol.* 12 (8) (2016).
- [611] G. Szabó, C. Hauert, Phase transitions and volunteering in spatial public goods games, *Phys. Rev. Lett.* 89 (11) (2002) 118101.
- [612] H. Brandt, C. Hauert, K. Sigmund, Punishment and reputation in spatial public goods games, *Proc. R. Soc. London B* 270 (1519) (2003) 1099–1104.
- [613] F.C. Santos, M.D. Santos, J.M. Pacheco, Social diversity promotes the emergence of cooperation in public goods games, *Nature* 454 (7201) (2008) 213–216.
- [614] Z. Rong, Z.-X. Wu, Effect of the degree correlation in public goods game on scale-free networks, *Europhys. Lett.* 87 (3) (2009) 30001.
- [615] Z. Rong, H.-X. Yang, W.-X. Wang, Feedback reciprocity mechanism promotes the cooperation of highly clustered scale-free networks, *Phys. Rev. E* 82 (4) (2010) 047101.
- [616] J. Gao, Z. Li, T. Wu, L. Wang, Diversity of contribution promotes cooperation in public goods games, *Phys. A* 389 (16) (2010) 3166–3171.
- [617] J. Vukov, F.C. Santos, J.M. Pacheco, Escaping the tragedy of the commons via directed investments, *J. Theoret. Biol.* 287 (2011) 37–41.
- [618] A. Szolnoki, M. Perc, Group-size effects on the evolution of cooperation in the spatial public goods game, *Phys. Rev. E* 84 (4) (2011) 047102.
- [619] M. Perc, P. Grigolini, Collective behavior and evolutionary games – an introduction, *Chaos Solitons Fractals* 56 (2013) 1–5, *Collective Behavior and Evolutionary Games*.
- [620] A. Szolnoki, M. Perc, G. Szabó, Topology-independent impact of noise on cooperation in spatial public goods games, *Phys. Rev. E* 80 (2009) 056109.
- [621] A. Szolnoki, M. Perc, Correlation of positive and negative reciprocity fails to confer an evolutionary advantage: Phase transitions to elementary strategies, *Phys. Rev. X* 3 (2013) 041021.
- [622] D. Helbing, A. Szolnoki, M. Perc, G. Szabó, Evolutionary establishment of moral and double moral standards through spatial interactions, *PLOS Comput. Biol.* 6 (2010) e1000758.
- [623] Z. Wang, A. Szolnoki, M. Perc, Evolution of public cooperation on interdependent networks: the impact of biased utility functions, *Europhys. Lett.* 97 (4) (2012) 48001.
- [624] Z. Wang, A. Szolnoki, M. Perc, Interdependent network reciprocity in evolutionary games, *Sci. Rep.* 3 (2013) 1183.
- [625] F. Battiston, V. Nicosia, V. Latora, Structural measures for multiplex networks, *Phys. Rev. E* 89 (3) (2014) 032804.
- [626] F. Battiston, M. Perc, V. Latora, Determinants of public cooperation in multiplex networks, *New J. Phys.* 19 (7) (2017) 073017.
- [627] C.P. Roca, D. Helbing, Emergence of social cohesion in a model society of greedy, mobile individuals, *Proc. Natl. Acad. Sci. USA* 108 (28) (2011) 11370–11374.
- [628] E. Pichler, A.M. Shapiro, Public goods games on adaptive coevolutionary networks, *Chaos* 27 (7) (2017) 073107.
- [629] G. Ren, L. Liu, M. Feng, Y. He, Coevolution of public goods game and networks based on survival of the fittest, *PLOS One* 13 (9) (2018).
- [630] C. Shen, C. Chu, L. Shi, M. Jusup, M. Perc, Z. Wang, Coevolutionary resolution of the public goods dilemma in interdependent structured populations, *Europhys. Lett.* 124 (4) (2018) 48003.
- [631] M. Perc, Stability of subsystem solutions in agent-based models, *Eur. J. Phys.* 39 (2018) 014001.
- [632] M.A. Javarone, F. Battiston, The role of noise in the spatial public goods game, *J. Stat. Mech. Theory Exp.* 2016 (7) (2016) 073404.
- [633] D.-F. Zheng, H. Yin, C.-H. Chan, P. Hui, Cooperative behavior in a model of evolutionary snowdrift games with N-person interactions, *Europhys. Lett.* 80 (1) (2007) 18002.
- [634] M.D. Santos, F.L. Pinheiro, F.C. Santos, J.M. Pacheco, Dynamics of N-Person snowdrift games in structured populations, *J. Theoret. Biol.* 315 (2012) 81–86.
- [635] K.H. Ji, J.-I. Kim, H.Y. Jung, S.Y. Park, R. Choi, U.K. Kim, C.S. Hwang, D. Lee, H. Hwang, J.K. Jeong, Effect of high-pressure oxygen annealing on negative bias illumination stress-induced instability of InGaZnO thin film transistors, *Appl. Phys. Lett.* 98 (10) (2011) 103509.
- [636] J.M. Pacheco, F.C. Santos, M.O. Souza, B. Skyrms, Evolutionary dynamics of collective action in N-Person stag hunt dilemmas, *Proc. R. Soc. B Biol. Sci.* 276 (1655) (2009) 315–321.
- [637] M.O. Souza, J.M. Pacheco, F.C. Santos, Evolution of cooperation under N-Person snowdrift games, *J. Theoret. Biol.* 260 (4) (2009) 581–588.
- [638] F.C. Santos, J.M. Pacheco, Risk of collective failure provides an escape from the tragedy of the commons, *Proc. Natl. Acad. Sci. USA* 108 (26) (2011) 10421–10425.
- [639] W. Chen, C. Gracia-Lázaro, Z. Li, L. Wang, Y. Moreno, Evolutionary dynamics of N-Person Hawk-Dove games, *Sci. Rep.* 7 (1) (2017) 1–10.
- [640] W. Güth, R. Schmittberger, B. Schwarze, An experimental analysis of ultimatum bargaining, *J. Econ. Behav. Organiz.* 3 (4) (1982) 367–388.
- [641] R. Sinatra, J. Iranzo, J. Gomez-Gardeñes, L.M. Floría, V. Latora, Y. Moreno, The ultimatum game in complex networks, *J. Stat. Mech. Theory Exp.* 2009 (09) (2009) P09012.

- [642] F.P. Santos, F.C. Santos, A. Paiva, J.M. Pacheco, Evolutionary dynamics of group fairness, *J. Theoret. Biol.* 378 (2015) 96–102.
- [643] J. Gomez-Gardeñes, M. Romance, R. Criado, D. Vilone, A. Sánchez, Evolutionary games defined at the network mesoscale: the public goods game, *Chaos Interdiscip. J. Nonlinear Sci.* 21 (1) (2011) 016113.
- [644] J. Gómez-Gardeñes, D. Vilone, A. Sánchez, Disentangling social and group heterogeneities: public goods games on complex networks, *Europhys. Lett.* 95 (6) (2011) 68003.
- [645] J. Peña, Y. Rochat, Bipartite graphs as models of population structures in evolutionary multiplayer games, *PLOS ONE* 7 (9) (2012).
- [646] C. Gracia-Lazaro, J. Gomez-Gardeñes, L.M. Floria, Y. Moreno, Intergroup information exchange drives cooperation in the public goods game, *Phys. Rev. E* 90 (4) (2014) 042808.
- [647] U. Alvarez-Rodriguez, F. Battiston, G.F. de Arruda, Y. Moreno, M. Perc, V. Latora, Evolutionary dynamics of higher-order interactions in social networks, 2020, arXiv:2001.10313.
- [648] A. Baronchelli, M. Felici, V. Loreto, E. Caglioti, L. Steels, Sharp transition towards shared vocabularies in multi-agent systems, *J. Stat. Mech. Theory Exp.* 2006 (06) (2006) P06014.
- [649] A. Baronchelli, L. Dall'Asta, A. Barrat, V. Loreto, Topology-induced coarsening in language games, *Phys. Rev. E* 73 (1) (2006) 015102.
- [650] U. Gneezy, Deception: The role of consequences, *Amer. Econ. Rev.* 95 (1) (2005) 384–394.
- [651] V. Capraro, M. Perc, D. Vilone, The evolution of lying in well-mixed populations, *J. R. Soc. Interface* 16 (2019) 20190211.
- [652] V. Capraro, M. Perc, D. Vilone, Lying on networks: The role of structure and topology in promoting honesty, *Phys. Rev. E* 101 (2020) 032305.
- [653] M. Milinski, R.D. Sommerfeld, H.-J. Krambeck, F.A. Reed, J. Marotzke, The collective-risk social dilemma and the prevention of simulated dangerous climate change, *Proc. Natl. Acad. Sci. USA* 105 (7) (2008) 2291–2294.
- [654] L.C. Freeman, Q-analysis and the structure of friendship networks, *Int. J. Man-Mach. Stud.* 12 (4) (1980) 367–378.
- [655] M. Andjelković, B. Tadić, S. Maletić, M. Rajković, Hierarchical sequencing of online social graphs, *Phys. A* 436 (2015) 582–595.
- [656] V. Sekara, A. Stopczynski, S. Lehmann, Fundamental structures of dynamic social networks, *Proc. Natl. Acad. Sci. USA* 113 (36) (2016) 9977–9982.
- [657] S. Mangan, U. Alon, Structure and function of the feed-forward loop network motif, *Proc. Natl. Acad. Sci. USA* 100 (21) (2003) 11980–11985.
- [658] E. Kuzmin, B. VanderSluis, W. Wang, G. Tan, R. Deshpande, Y. Chen, M. Usaj, A. Balint, M. Mattiazzi Usaj, J. van Leeuwen, E.N. Koch, C. Pons, A.J. Dagilis, M. Prysizlak, J.Z.Y. Wang, J. Hanchard, M. Riggi, K. Xu, H. Heydari, B.-J. San Luis, E. Shuteriqi, H. Zhu, N. Van Dyk, S. Sharifpoor, M. Costanzo, R. Loewith, A. Caudy, D. Bolnick, G.W. Brown, B.J. Andrews, C. Boone, C.L. Myers, Systematic analysis of complex genetic interactions, *Science* 360 (6386) (2018).
- [659] E. Schneidman, S. Still, M.J. Berry, W. Bialek, Network information and connected correlations, *Phys. Rev. Lett.* 91 (23) (2003) 238701.
- [660] E. Ibáñez-Marcelo, L. Campioni, A. Phinyomark, G. Petri, E.L. Santarcangelo, Topology highlights mesoscopic functional equivalence between imagery and perception: the case of hypnotizability, *NeuroImage* 200 (2019) 437–449.
- [661] J. McPherson, Hypernetwork sampling: duality and differentiation among voluntary organizations, *Soc. Netw.* 3 (4) (1982) 225–249.
- [662] B. Foster, S. Seidman, Urban structures derived from collections of overlapping subsets, *Urban Anthropol.* 11 (1982) 177–192.
- [663] B. Foster, S. Seidman, Overlap structure of ceremonial events in two Thai villages, *Thail. J. Dev. Adm.* 24 (1984) 143–157.
- [664] K. Faust, Centrality in affiliation networks, *Soc. Netw.* 19 (2) (1997) 157–191.
- [665] P. Bonacich, Power and centrality: A family of measures, *Am. J. Sociol.* 92 (5) (1987) 1170–1182.
- [666] S. Wylie, Mathematical structure in human affairs, by R. H. Atkin, *Math. Gaz.* 60 (411) (1976) 69–70.
- [667] P. Doreian, On the evolution of group and network structure, *Soc. Netw.* 2 (3) (1979) 235–252.
- [668] S. Lehmann, Fundamental structures in dynamic communication networks, 2019, arXiv:1907.09966.
- [669] M. Karsai, H. Jo, K. Kaski, Bursty human dynamics, *SpringerBriefs in Complexity*, Springer International Publishing, 2017.
- [670] P. Gould, A. Gatrell, A structural analysis of a game: The Liverpool v Manchester united cup final of 1977, *Soc. Netw.* 2 (3) (1979) 253–273.
- [671] L. Pappalardo, P. Cintia, A. Rossi, E. Massucco, P. Ferragina, D. Pedreschi, F. Giannotti, A public data set of spatio-temporal match events in soccer competitions, *Sci. Data* 6 (1) (2019) 236.
- [672] T. Gao, F. Li, Studying the utility preservation in social network anonymization via persistent homology, *Comput. Secur.* 77 (2018) 49–64.
- [673] J. Greening, N. Pinter-Wollman, N.H. Fefferman, Higher-order interactions: understanding the knowledge capacity of social groups using simplicial sets, *Current Zoology* 61 (1) (2015) 114–127.
- [674] C. Catutto, C. Schmitz, A. Baldassarri, V.D.P. Servedio, V. Loreto, a.A. Hotho, M. Grahl, G. Stumme, Network properties of folksonomies, in: S. Hoche, A. Nürnberger, J. Flach (Eds.), *AI Commun. J. Spec. Issue Netw. Anal. Nat. Sci. Eng.* (2007).
- [675] V. Latora, V. Nicosia, P. Panzarasa, Social cohesion, structural holes, and a tale of two measures, *J. Stat. Phys.* (151) (2013) 745–764.
- [676] S. Milojević, Principles of scientific research team formation and evolution, *Proc. Natl. Acad. Sci. USA* 111 (11) (2014) 3984–3989.
- [677] Q. Xiao, Node importance measure for scientific research collaboration from hypernetwork perspective, *Teh. Vjesn.* 23 (2) (2016) 397–404.
- [678] M.E.J. Newman, Scientific collaboration networks. I. Network construction and fundamental results, *Phys. Rev. E* 64 (1) (2001) 016131.
- [679] M.E.J. Newman, Scientific collaboration networks. II. Shortest paths, weighted networks, and centrality, *Phys. Rev. E* 64 (1) (2001) 016132.
- [680] M.E.J. Newman, The structure of scientific collaboration networks, *Proc. Natl. Acad. Sci. USA* 98 (2) (2001) 404–409.
- [681] G. Bianconi, R.K. Darst, J. Iacovacci, S. Fortunato, Triadic closure as a basic generating mechanism of communities in complex networks, *Phys. Rev. E* 90 (4) (2014) 042806.
- [682] E. Schneidman, M.J. Berry II, R. Segev, W. Bialek, Weak pairwise correlations imply strongly correlated network states in a neural population, *Nature* 440 (7087) (2006) 1007.
- [683] S. Yu, H. Yang, H. Nakahara, G.S. Santos, D. Nikolić, D. Plen, Higher-order interactions characterized in cortical activity, *J. Neurosci.* 31 (48) (2011) 17514–17526.
- [684] H. Shimazaki, S.-i. Amari, E.N. Brown, S. Grün, State-space analysis of time-varying higher-order spike correlation for multiple neural spike train data, *PLOS Comput. Biol.* 8 (3) (2012) e1002385.
- [685] U. Köster, J. Sohl-Dickstein, C.M. Gray, B.A. Olshausen, Modeling higher-order correlations within cortical microcolumns, *PLOS Comput. Biol.* 10 (7) (2014) e1003684.
- [686] H. Shimazaki, K. Sadeghi, T. Ishikawa, Y. Ikegaya, T. Toyozumi, Simultaneous silence organizes structured higher-order interactions in neural populations, *Sci. Rep.* 5 (2015) 9821.
- [687] N.A. Cayco-Gajic, J. Zylberberg, E. Shea-Brown, Triplet correlations among similarly tuned cells impact population coding, *Front. Comput. Neurosci.* 9 (2015) 57.
- [688] J.J. Arenzon, R.M. De Almeida, Neural networks with high-order connections, *Phys. Rev. E* 48 (5) (1993) 4060.
- [689] N. Lemke, J.J. Arenzon, F.A. Tamarit, Chaotic dynamics of high-order neural networks, *J. Stat. Phys.* 79 (1–2) (1995) 415–427.
- [690] T. Ezaki, T. Watanabe, M. Ohzeki, N. Masuda, Energy landscape analysis of neuroimaging data, *Phil. Trans. R. Soc. A* 375 (2017) 20160287.
- [691] T. Watanabe, S. Hirose, H. Wada, Y. Imai, T. Machida, I. Shirouzu, S. Konishi, Y. Miyashita, N. Masuda, Energy landscapes of resting-state brain networks, *Front. Neuroinform.* 8 (2014) 12.
- [692] C. Giusti, E. Pastalkova, C. Curto, V. Itskov, Clique topology reveals intrinsic geometric structure in neural correlations, *Proc. Natl. Acad. Sci. USA* 112 (44) (2015) 13455–13460.

- [693] Y. Dabaghian, F. Mémoli, L. Frank, G. Carlsson, A topological paradigm for hippocampal spatial map formation using persistent homology, *PLOS Comput. Biol.* 8 (8) (2012) e1002581.
- [694] Y. Dabaghian, V.L. Brandt, L.M. Frank, Reconciling the hippocampal map as a topological template, *Elife* 3 (2014) e03476.
- [695] A. Babichev, D. Morozov, Y. Dabaghian, Robust spatial memory maps encoded by networks with transient connections, *PLOS Comput. Biol.* 14 (9) (2018) e1006433.
- [696] M.W. Reimann, M. Nolte, M. Scolamiero, K. Turner, R. Perin, G. Chindemi, P. Dłotko, R. Levi, K. Hess, H. Markram, Cliques of neurons bound into cavities provide a missing link between structure and function, *Front. Comput. Neurosci.* 11 (2017) 48.
- [697] F. de Vico Fallani, J. Richiardi, M. Chavez, S. Achard, Graph analysis of functional brain networks: practical issues in translational neuroscience, *Philos. Trans. R. Soc. B* 369 (1653) (2014) 20130521.
- [698] X. Huang, K. Xu, C. Chu, T. Jiang, S. Yu, Weak higher-order interactions in macroscopic functional networks of the resting brain, *J. Neurosci.* 37 (43) (2017) 10481–10497.
- [699] H. Zhang, X. Chen, Y. Zhang, D. Shen, Test-retest reliability of “high-order” functional connectivity in Young healthy adults, *Front. Neurosci.* 11 (2017) 439.
- [700] S.M. Plis, J. Sui, T. Lane, S. Roy, V.P. Clark, V.K. Potluru, R.J. Huster, A. Michael, S.R. Sponheim, M.P. Weisend, V. Calhoun, High-order interactions observed in multi-task intrinsic networks are dominant indicators of aberrant brain function in schizophrenia, *Neuroimage* 102 (2014) 35–48.
- [701] H. Zhang, X. Chen, F. Shi, G. Li, M. Kim, P. Giannakopoulos, S. Haller, D. Shen, Topographical information-based high-order functional connectivity and its application in abnormality detection for mild cognitive impairment, *J. Alzheimers Dis.* 54 (3) (2016) 1095–1112.
- [702] H. Lee, H. Kang, M.K. Chung, S. Lim, B.-N. Kim, D.S. Lee, Integrated multimodal network approach to PET and MRI based on multidimensional persistent homology, *Hum. Brain Mapp.* 38 (3) (2017) 1387–1402.
- [703] H. Lee, M.K. Chung, H. Kang, D.S. Lee, Hole detection in metabolic connectivity of Alzheimer's disease using k- Laplacian, in: *International Conference on Medical Image Computing and Computer-Assisted Intervention*, Springer, 2014, pp. 297–304.
- [704] P. Bendich, J.S. Marron, E. Miller, A. Pieloch, S. Skwerer, Persistent homology analysis of brain artery trees, *Ann. Appl. Stat.* 10 (1) (2016) 198.
- [705] H. Lee, H. Kang, M.K. Chung, B.-N. Kim, D.S. Lee, Persistent brain network homology from the perspective of dendrogram, *IEEE Trans. Med. Imaging* 31 (12) (2012) 2267–2277.
- [706] H. Lee, M.K. Chung, H. Kang, B.-N. Kim, D.S. Lee, Discriminative persistent homology of brain networks, in: *2011 IEEE International Symposium on Biomedical Imaging: from Nano to Macro*, IEEE, 2011, pp. 841–844.
- [707] F.A. Santos, E.P. Raposo, M.D. Coutinho-Filho, M. Copelli, C.J. Stam, L. Douw, Topological phase transitions in functional brain networks, *Physical Review E* 100 (3) (2019) 032414.
- [708] M.K. Chung, V. Villalta-Gil, H. Lee, P.J. Rathouz, B.B. Lahey, D.H. Zald, Exact topological inference for paired brain networks via persistent homology, in: *International Conference on Information Processing in Medical Imaging*, Springer, 2017, pp. 299–310.
- [709] E. Rybakken, N. Baas, B. Dunn, Decoding of neural data using cohomological feature extraction, *Neural Comput.* 31 (1) (2019) 68–93.
- [710] L.-D. Lord, P. Expert, H.M. Fernandes, G. Petri, T.J. Van Hartevelt, F. Vaccarino, G. Deco, F. Turkheimer, M.L. Kringelbach, Insights into brain architectures from the homological scaffolds of functional connectivity networks, *Front. Syst. Neurosci.* 10 (2016) 85.
- [711] H. Lee, M.K. Chung, H. Choi, H. Kang, S. Ha, Y.K. Kim, D.S. Lee, Harmonic holes as the submodules of brain network and network dissimilarity, in: *International Workshop on Computational Topology in Image Context*, Springer, 2019, pp. 110–122.
- [712] M.K. Chung, H. Lee, A. DiChristofano, H. Ombao, V. Solo, Exact topological inference of the resting-state brain networks in twins, *Netw. Neurosci.* 3 (3) (2019) 674–694.
- [713] E. Ibáñez-Marcelo, L. Campioni, D. Manzoni, E.L. Santarcangelo, G. Petri, Spectral and topological analyses of the cortical representation of the head position: Does hypnotizability matter? *Brain Behav.* 9 (6) (2019) e01277.
- [714] M. Saggat, O. Sporns, J. Gonzalez-Castillo, P.A. Bandettini, G. Carlsson, G. Glover, A.L. Reiss, Towards a new approach to reveal dynamical organization of the brain using topological data analysis, *Nature Commun.* 9 (1) (2018) 1–14.
- [715] C.T. Ellis, M. Lesnick, G. Henselman-Petrusek, B. Keller, J.D. Cohen, Feasibility of topological data analysis for event-related fMRI, *Netw. Neurosci.* 3 (3) (2019) 695–706.
- [716] C. Giusti, R. Ghrist, D.S. Bassett, Two's company, three (or more) is a simplex, *J. Comput. Neurosci.* 41 (1) (2016) 1–14.
- [717] A.E. Sizemore, J.E. Phillips-Cremins, R. Ghrist, D.S. Bassett, The importance of the whole: Topological data analysis for the network neuroscientist, *Netw. Neurosci.* 3 (3) (2019) 656–673.
- [718] T.J. Case, E.A. Bender, Testing for higher order interactions, *Am. Nat.* 118 (6) (1981) 920–929.
- [719] P.A. Abrams, Arguments in favor of higher order interactions, *Am. Nat.* 121 (6) (1983) 887–891.
- [720] P. Kareiva, Special feature: higher order interactions as a foil to reductionist ecology, *Ecology* 75 (6) (1994).
- [721] I. Billick, T.J. Case, Higher order interactions in ecological communities: What are they and how can they be detected? *Ecology* 75 (6) (1994) 1529–1543.
- [722] J. Wootton, Indirect effects and habitat use in an intertidal community: Interaction chains and interaction modifications, *Am. Nat.* 141 (1) (1993) 71–89.
- [723] E. Bairey, E.D. Kelsic, R. Kishony, High-order species interactions shape ecosystem diversity, *Nature Commun.* 7 (1) (2017) 12285.
- [724] E.D. Kelsic, J. Zhao, K. Vetsigian, R. Kishony, Counteraction of antibiotic production and degradation stabilizes microbial communities, *Nature* 521 (7553) (2015) 516.
- [725] M.H. Perlin, D.R. Clark, C. McKenzie, H. Patel, N. Jackson, C. Kormanik, C. Powell, A. Bajorek, D.A. Myers, L.A. Dugatkin, Protection of *Salmonella* by ampicillin-resistant *Escherichia coli* in the presence of otherwise lethal drug concentrations, *Proc. R. Soc. B Biol. Sci.* 276 (1674) (2009) 3759–3768.
- [726] M.I. Abrudan, F. Smakman, A.J. Grimbergen, S. Westhoff, E.L. Miller, G.P. Van Wezel, D.E. Rozen, Socially mediated induction and suppression of antibiosis during bacterial coexistence, *Proc. Natl. Acad. Sci. USA* 112 (35) (2015) 11054–11059.
- [727] M. Koen-Alonso, A process-oriented approach to the multispecies functional response, in: *From Energetics To Ecosystems: The Dynamics and Structure of Ecological Systems*, Springer, 2007, pp. 1–36.
- [728] V.M. de Oliveira, J.F. Fontanari, Random replicators with high-order interactions, *Phys. Rev. Lett.* 85 (23) (2000) 4984–4987.
- [729] Y. Yoshino, T. Galla, K. Tokita, Rank abundance relations in evolutionary dynamics of random replicators, *Phys. Rev. E* 78 (3) (2008) 031924.
- [730] M. Sonntag, H.-M. Teichert, Competition hypergraphs, *Discrete Appl. Math.* 143 (1) (2004) 324–329.
- [731] A.J. Golubski, E.E. Westlund, J. Vandermeer, M. Pascual, Ecological networks over the edge: Hypergraph trait-mediated indirect interaction (TMII) structure, *Trends Ecol. Evol.* 31 (5) (2016) 344–354.
- [732] R.M. May, Will a large complex system be stable? *Nature* 436 (1972) 413–414.
- [733] J.H. Vandermeer, The competitive structure of communities: An experimental approach with protozoa, *Ecology* 50 (3) (1969) 362–371.
- [734] W.E. Neill, The community matrix and interdependence of the competition coefficients, *Am. Nat.* 108 (962) (1974) 399–408.
- [735] C.F. Dormann, S.H. Roxburgh, Experimental evidence rejects pairwise modelling approach to coexistence in plant communities, *Proc. Biol. Sci.* 272 (1569) (2005) 1279–1285.
- [736] A. Weigelt, J. Schumacher, T. Walther, M. Bartelheimer, T. Steinlein, W. Beyschlag, Identifying mechanisms of competition in multi-species communities, *J. Ecol.* 95 (1) (2007) 53–64.

- [737] S. Allesina, J.M. Levine, A competitive network theory of species diversity, *Proc. Natl. Acad. Sci. USA* 108 (14) (2011) 5638–5642.
- [738] B. Kerr, M.A. Riley, M.W. Feldman, B.J. Bohannan, Local dispersal promotes biodiversity in a real-life game of rock-paper-scissors, *Nature* 418 (6894) (2002) 171.
- [739] J. Hofbauer, K. Sigmund, Evolutionary game dynamics, *Bull. Amer. Math. Soc.* 40 (4) (2003) 479–519.
- [740] M.A. Nowak, K. Sigmund, Evolutionary dynamics of biological games, *Science* 303 (5659) (2004) 793–799.
- [741] P.D. Taylor, L.B. Jonker, Evolutionary stable strategies and game dynamics, *Math. Biosci.* 40 (1–2) (1978) 145–156.
- [742] J. Hofbauer, P. Schuster, K. Sigmund, A note on evolutionary stable strategies and game dynamics, 2010, Levine's Working Paper Archive 441.
- [743] M.M. Mayfield, D.B. Stouffer, Higher-order interactions capture unexplained complexity in diverse communities, *Nat. Ecol. Evol.* 1 (3) (2017) 0062.
- [744] S. Valverde, B. Vidiella, R. Montañez, A. Fraile, S. Sacristán, F. García-Arenal, Coexistence of nestedness and modularity in host-pathogen infection networks, *Nat. Ecol. Evol.* (2020) 1–10.
- [745] M.S. Mariani, Z.-M. Ren, J. Bascompte, C.J. Tessone, Nestedness in complex networks: Observation, emergence, and implications, *Phys. Rev.* (2019).
- [746] Z.N. Oltvai, A.-L. Barabási, Life's complexity pyramid, *Science* 298 (5594) (2002) 763–764.
- [747] T. Aittokallio, B. Schwikowski, Graph-based methods for analysing networks in cell biology, *Brief. Bioinform.* 7 (3) (2006) 243–255.
- [748] R. Vermeulen, E.L. Schymanski, A.-L. Barabási, G.W. Miller, The exposome and health: where chemistry meets biology, *Science* 367 (6476) (2020) 392–396.
- [749] A. Ruepp, B. Waegle, M. Lechner, B. Brauner, I. Dunger-Kaltenbach, G. Fobo, G. Frishman, C. Montrone, H.-W. Mewes, CORUM: The comprehensive resource of mammalian protein complexes—2009, *Nucl. Acids Res.* 38 (suppl_1) (2010) D497–D501.
- [750] P. Wong, S. Althammer, A. Hildebrand, A. Kirschner, P. Pagel, B. Geissler, P. Smialowski, F. Blöchl, M. Oesterheld, T. Schmidt, An evolutionary and structural characterization of mammalian protein complex organization, *BMC Genomics* 9 (1) (2008) 629.
- [751] S. Klamt, U.-U. Haus, F. Theis, Hypergraphs and cellular networks, *PLOS Comput. Biol.* 5 (2009) e1000385.
- [752] A. Ritz, A.N. Tegge, H. Kim, C.L. Poirel, T. Murali, Signaling hypergraphs, *Trends Biotechnol.* 32 (7) (2014) 356–362.
- [753] T. Gaudelet, N. Malod-Dognin, N. Pržulj, Higher-order molecular organization as a source of biological function, *Bioinformatics* 34 (17) (2018) i944–i953.
- [754] N. Pržulj, D.G. Corneil, I. Jurisica, Modeling interactome: scale-free or geometric? *Bioinformatics* 20 (18) (2004) 3508–3515.
- [755] N. Franzese, A. Groce, T. Murali, A. Ritz, Hypergraph-based connectivity measures for signaling pathway topologies, *PLOS Comput. Biol.* 15 (10) (2019).
- [756] F. Klimm, C.M. Deane, G. Reinert, Hypergraphs for predicting essential genes using multiprotein complex data, *bioRxiv* (2020).
- [757] N. Percy, N. Chuzhanova, J.J. Crofts, Complexity and robustness in hypernetwork models of metabolism, *J. Theoret. Biol.* 406 (2016) 99–104.
- [758] T. Shen, Z. Zhang, Z. Chen, D. Gu, S. Liang, Y. Xu, R. Li, Y. Wei, Z. Liu, Y. Yi, X. Xie, A genome-scale metabolic network alignment method within a hypergraph-based framework using a rotational tensor-vector product, *Sci. Rep.* 8 (1) (2018) 1–16.
- [759] J. Jost, R. Mulas, Hypergraph Laplace operators for chemical reaction networks, *Adv. Math.* 351 (2019) 870–896.
- [760] Z. Tian, T. Hwang, R. Kuang, A hypergraph-based learning algorithm for classifying gene expression and arrayCGH data with prior knowledge, *Bioinformatics* 25 (21) (2009) 2831–2838.
- [761] A. Battle, M.C. Jonikas, P. Walter, J.S. Weissman, D. Koller, Automated identification of pathways from quantitative genetic interaction data, *Mol. Syst. Biol.* 6 (1) (2010).
- [762] P. Sumazin, X. Yang, H.-S. Chiu, W.-J. Chung, A. Iyer, D. Llobet-Navas, P. Rajbhandari, M. Bansal, P. Guarnieri, J. Silva, A. Califano, An extensive microRNA-mediated network of RNA-RNA interactions regulates established oncogenic pathways in glioblastoma, *Cell* 147 (2) (2011) 370–381.
- [763] A. Rahman, C.L. Poirel, D.J. Badger, C. Estep, T. Murali, Reverse engineering molecular hypergraphs, *IEEE/ACM Trans. Comput. Biol. Bioinform.* 10 (5) (2013) 1113–1124.
- [764] M. Marques-Pita, L.M. Rocha, Canalization and control in automata networks: body segmentation in drosophila melanogaster, *PLOS ONE* 8 (3) (2013).
- [765] Y. Kong, T. Yu, A hypergraph-based method for large-scale dynamic correlation study at the transcriptomic scale, *BMC Genomics* 20 (1) (2019) 397.
- [766] A. Zimmer, I. Katzir, E. Dekel, A.E. Mayo, U. Alon, Prediction of multidimensional drug dose responses based on measurements of drug pairs, *Proc. Natl. Acad. Sci. USA* 113 (37) (2016) 10442–10447.
- [767] I. Katzir, M. Cokol, B.B. Aldridge, U. Alon, Prediction of ultra-high-order antibiotic combinations based on pairwise interactions, *PLOS Comput. Biol.* 15 (1) (2019) e1006774.
- [768] A. Tendler, A. Zimmer, A. Mayo, U. Alon, Noise-precision tradeoff in predicting combinations of mutations and drugs, *PLOS Comput. Biol.* 15 (5) (2019) e1006956.
- [769] A. Zimmer, A. Tendler, I. Katzir, A. Mayo, U. Alon, Prediction of drug cocktail effects when the number of measurements is limited, *PLoS Biol.* 15 (10) (2017) e2002518.
- [770] J. Otwinowski, J.B. Plotkin, Inferring fitness landscapes by regression produces biased estimates of epistasis, *Proc. Natl. Acad. Sci. USA* 111 (22) (2014) E2301–E2309.
- [771] K. Crona, A. Gavryushkin, D. Greene, N. Beerenwinkel, Inferring genetic interactions from comparative fitness data, *Elife* 6 (2017) e28629.
- [772] D.M. Weinreich, Y. Lan, C.S. Wylie, R.B. Heckendorn, Should evolutionary geneticists worry about higher-order epistasis? *Curr. Opin. Genet. Dev.* 23 (6) (2013) 700–707.
- [773] T.F. Mackay, J.H. Moore, Why epistasis is important for tackling complex human disease genetics, *Genome Med.* 6 (6) (2014) 42.
- [774] A. Sanchez, Defining higher-order interactions in synthetic ecology: lessons from physics and quantitative genetics, *Cell Syst.* 9 (6) (2019) 519–520.
- [775] R.F. Guerrero, S.V. Scarpino, J.V. Rodrigues, D.L. Hartl, C.B. Ogbunugafor, Proteostasis environment shapes higher-order epistasis operating on antibiotic resistance, *Genetics* 212 (2) (2019) 565–575.
- [776] S. Yitbarek, J.L. Guitart, S.A. Knutie, C.B. Ogbunugafor, Deconstructing higher-order interactions in the microbiota: A theoretical examination, *bioRxiv* (2019) 647156.
- [777] H. Mickalide, S. Kuehn, Higher-order interaction between species inhibits bacterial invasion of a phototroph-predator microbial community, *Cell Syst.* 9 (6) (2019) 521–533.
- [778] Y. Niu, G. Wang, C. Qu, G. Yan, RWHMDA: random walk on hypergraph for microbe-disease association prediction, *Front. Microbiol.* 10 (2019) 1578.
- [779] G. St-Onge, V. Thibeault, A. Allard, L.J. Dubé, L. Hébert-Dufresne, School closures, event cancellations, and the mesoscopic localization of epidemics in networks with higher-order structure, 2020, *arXiv:2003.05924*.
- [780] F.T. Pokorný, M. Hawasly, S. Ramamoorthy, Topological trajectory classification with filtrations of simplicial complexes and persistent homology, *Int. J. Robot. Res.* 35 (1–3) (2016) 204–223.
- [781] M. Herlihy, D. Kozlov, S. Rajsbaum, Distributed computing through combinatorial topology, Newnes, 2013.

- [782] É. Goubault, J. Ledent, S. Rajsbaum, A simplicial complex model for dynamic epistemic logic to study distributed task computability, in: *Proceedings Ninth International Symposium on Games, Automata, Logics, and Formal Verification*, 2018.
- [783] H. van Ditmarsch, E. Goubault, J. Ledent, S. Rajsbaum, Knowledge and simplicial complexes, 2020, [arXiv:2002.08863](https://arxiv.org/abs/2002.08863).
- [784] M. Reitz, G. Bianconi, The higher-order spectrum of simplicial complexes: A renormalization group approach, 2020, [arXiv:200309143](https://arxiv.org/abs/200309143).
- [785] S. Kališnik, V. Kurlin, D. Lešnik, A higher-dimensional homologically persistent skeleton, *Adv. Appl. Math.* 102 (2019) 113–142.
- [786] M. Guerra, A.D. Gregorio, U. Fugacci, G. Petri, F. Vaccarino, Homological scaffold via minimal homology bases, 2020, [arXiv:2004.11606](https://arxiv.org/abs/2004.11606).
- [787] G. Karypis, R. Aggarwal, V. Kumar, S. Shekhar, Multilevel hypergraph partitioning: Applications in VLSI domain, *IEEE Trans. Very Large Scale Integr. VLSI Syst.* 7 (1) (1999) 69–79.
- [788] N. Neubauer, K. Obermayer, Towards community detection in k-partite k-uniform hypergraphs, in: *Proceedings of the NIPS 2009 Workshop on Analyzing Networks and Learning with Graphs*, 2009, pp. 1–9.
- [789] M. Marietti, D. Testa, Cores of simplicial complexes, *Discrete Comput. Geom.* 40 (3) (2008) 444–468.
- [790] A.M. Duval, C.J. Klivans, J.L. Martin, Critical groups of simplicial complexes, *Ann. Comb.* 17 (1) (2013) 53–70.
- [791] J. Steenbergen, C. Klivans, S. Mukherjee, A Cheeger-type inequality on simplicial complexes, *Adv. Appl. Math.* 56 (2014) 56–77.
- [792] O. Parzanchevski, Mixing in high-dimensional expanders, *Combin. Probab. Comput.* 26 (5) (2017) 746–761.
- [793] A. Sizemore, C. Giusti, D.S. Bassett, Classification of weighted networks through mesoscale homological features, *J. Complex Netw.* 5 (2) (2017) 245–273.
- [794] G. Petri, M. Scolamiero, I. Donato, F. Vaccarino, Topological strata of weighted complex networks, *PLOS ONE* 8 (6) (2013).
- [795] O. Bobrowski, P. Skraba, Homological percolation and the euler characteristic, *Phys. Rev. E* 101 (3) (2020) 032304.
- [796] I. Brugere, B. Gallagher, T.Y. Berger-Wolf, Network structure inference, a survey: Motivations, methods, and applications, *ACM Comput. Surv.* 51 (2018) 24:1–24:39.
- [797] T.P. Peixoto, Network reconstruction and community detection from dynamics, *Phys. Rev. Lett.* 123 (12) (2019) 128301.
- [798] T. Squartini, G. Caldarelli, G. Cimini, A. Gabrielli, D. Garlaschelli, Reconstruction methods for networks: the case of economic and financial systems, *Phys. Rep.* 757 (2018) 1–47.
- [799] A. Phinyomark, E. Ibanez-Marcelo, G. Petri, Resting-state fmri functional connectivity: Big data preprocessing pipelines and topological data analysis, *IEEE Trans. Big Data* 3 (4) (2017) 415–428.
- [800] S. Battiston, J.B. Glattfelder, D. Garlaschelli, F. Lillo, G. Caldarelli, The structure of financial networks, in: *Network Science*, Springer, 2010, pp. 131–163.
- [801] L. Faes, D. Kugiumtzis, G. Nollo, F. Jurysta, D. Marinazzo, Estimating the decomposition of predictive information in multivariate systems, *Phys. Rev. E* 91 (3) (2015) 032904.
- [802] L. Faes, D. Marinazzo, S. Stramaglia, Multiscale information decomposition: Exact computation for multivariate Gaussian processes, *Entropy* 19 (8) (2017) 408.
- [803] F.E. Rosas, P.A. Mediano, M. Gastpar, H.J. Jensen, Quantifying high-order interdependencies via multivariate extensions of the mutual information, *Phys. Rev. E* 100 (3) (2019) 032305.
- [804] L. Hébert-Dufresne, S.V. Scarpino, J.-G. Young, Macroscopic patterns of interacting contagions are indistinguishable from social reinforcement, *Nat. Phys.* (2020) 1–6.